Report 4/99

Long-Range Transport of Selected Persistent Organic Pollutants

Development of Transport Models for Polychlorinated Biphenyls, Benzo[a]pyrene, Dioxins/Furans and Lindane

Joint report of EMEP Centres: MSC-E and CCC

MSC-E

Margarita Pekar, Natalia Pavlova, Alexey Gusev, Viktor Shatalov, Nadezhda Vulikh, Daria Ioannisian, Sergey Dutchak

CCC

Torunn Berg, Anne-Gunn Hjellbrekke

METEOROLOGICAL SYNTHESIZING CENTRE - EAST

Kedrova str.8-1, Moscow, 117 292, Russia

Tel.: 007 095 124 47 58

Fax: 007 095 310 70 93

e-mail: msce@glasnet.ru

Acknowledgements

A large number of anonymous co-workers in participating countries have been involved in this work. A list of participating institutes can be seen below. The staff at CCC wishes to express their gratitude and appreciation for continued good co-operation and efforts.

Czech Republic	Czech Hydrometeorological Institute
Finland	Finnish Meteorological Institute
Germany	Umweltbundesamt
Iceland	The Icelandic Meteorological Office
Ireland	Environmental Protection Agency (EPA)
Norway	Norwegian Institute for Air Research (NILU)
Sweden	Swedish Water and Air Pollution Research Institute (IVL)

The authors express their gratitude to specialists of MSC-E for valuable advises and recommendations. The authors are grateful to European Centre of Medium Range Weather Forecast (ECMWF) for providing the data on surface roughness. The authors express their gratitude to Dr. A.Bulgakov for considerable contribution to the description of physical-chemical properties of POPs.

A great contribution to the translation and technical preparation of the report is made by Larissa Zayavlina, Irina Strizhkina, Olga Rozovskaya, and Svetlana Yevdokimova.

Summary

This report was prepared in accordance with the EMEP (Co-operative Programme for Monitoring and Evaluation of Long-Range Transmission of Air Pollutants in Europe) working plan for 1999 [ECE/EB.AIR/59, annex III]. The main objective was further development of long-range transport multi-compartment model for persistent organic pollutants (POPs).

In the report approaches to modelling of selected POPs (PCBs, PAHs, PCDD/Fs, and lindane) are considered. The model comprises the description of exchange processes between atmosphere and underlying surface including atmosphere/vegetation exchange. The investigations of physical-chemical properties of selected POPs affecting their long-range transport were continued. On the basis of these investigations the parameterizations of the model for PCB-28, 52, 101, 118, 138, 153, 180, B[a]P, 2,3,4,7,8-PeCDF, and lindane were prepared.

For modelling the official emission data submitted by MSC-W were used. In addition to official data available expert estimates of POP emissions for European region were used. These data and their analysis are presented in the report.

Measurement data were analyzed and prepared for the comparison with modeling results by CCC.

Tentative calculations made on the basis of the model developed allowed to estimate the contribution of different processes to the long-range transport of the above mentioned POPs and determine physical-chemical parameters and processes crucial for modelling. Results of calculations were compared with available measurement data.

On the basis of the results obtained conclusions and recommendations for subsequent work were made.

Contents

Introduction

Problems of the environment pollution by persistent organic pollutants (POPs) more and more attract attention on national and international levels. A number of international organizations such as UNEP, WMO, HELCOM, OSPAR, AMAP, EUROTRAC and others incorporated POPs to their working programmes.

Essential progress in this field was achieved within the framework of the Convention on Long-Range Transboundary Air Pollution (LTRAP). In June 1998 in Arhus (Denmark) 36 Parties to the Convention signed the Protocol on POPs. In addition to the fulfillment of the basic obligations on the control of POP emissions, production and use Parties to the Protocol shall develop and maintain emission inventories and report emission data to the UN ECE Secretariat, encourage research, monitoring and co-operation, in particular, in the fields of: emissions, long-range transport, deposition levels, etc. In accordance with Protocol Article 9 EMEP shall provide Executive Body with information on the long-range transport and deposition of POPs.

EMEP results should promote further evaluating international abatement strategies and reviewing the implementation of the Protocol on POPs and compliance with Parties obligations. Strategic and operational tasks in the field of research and evaluation of POP transport have been formulated in "Vision for the EMEP work by 2005/2010. Seven-phase programme (1999-2001)" [EB.AIR/GE.1/1998/3/Rev.1]. The preparation of this document was based on the scientific results of the workshops held within the framework of LTRAP (Durham, USA, 1992; Beekbergen, the Netherlands, 1994; Moscow, Russia, 1996).

The twenty second session of the Steering Body to EMEP took a decision [EB.AIR/GE.1/1998/2] to change its emphasis from a compartmentalized approach focusing on reports and analysis from an individual Centres' work to a more integrated approach addressing subjects and issues of importance to the Convention. In compliance with this decision and the work-plan element "Persistent organic pollutants (modelling and measurements)" two EMEP Centres: CCC and MSC-E have prepared subject-oriented report.

The main objective of EMEP in the field of POP activity for 1999 is defined in the report of the sixteenth session of the Executive Body [ECE/EB.AIR/59, annex III]. "Increase the provision of monitoring and modelling data on transboundary fluxes, concentrations and depositions of selected POPs (PAH, PCB, HCB, chlordane, lindane, α-HCH, DDT/DDE) over Europe. Develop the modelling bases of selected POPs (PCBs, B[a]P, dioxins/furans) and verify the functioning of the models. Study further the physical-chemical processes of POPs in different environmental compartments, taking also into account their global transport".

The progress in accomplishing of EMEP tasks is determined to a certain degree by close cooperation between countries and EMEP Centres in such fields as emissions, monitoring and modelling.

Emissions

Meteorological Synthesizing Centre West (MSC-W) is a responsible centre for EMEP emission database. Evaluating emission data available for POP modelling it can be mentioned that compared to the previous years the situation is becoming better. The number of countries, which submitted data to MSC-W emission database increased. It is possible to distinguish a group of countries: Bulgaria, Great Britain, Hungary, Germany, the Netherlands, Poland, Slovakia, Finland, which contributed more actively. At the same time it can be mentioned that data on spatial distribution, source heights, temporal variations and uncertainty values are absent. For the majority of countries total annual emissions and spatial distribution are estimated on the expert bases. For several countries neither official data nor expert estimates are available. For modelling emissions of these countries were put to zero.

Another important objective is updating and complementing EMEP/CORINAIR Atmospheric Emission Inventory Guidebook providing countries with a unified methodology for POP emission inventories. This activity is carried out by the UN ECE Task Force on Emission Inventories (TFEI) with the support of countries and EMEP Centres. In particular, MSC-E in collaboration with Belarus and the Russian Federation make efforts in adaptation and use of the Guidebook for emission inventories in interested eastern European countries. For this purpose MSC-E initiated the second training workshop (Pushkin, Russia, April 1999). Experts from twelve countries took part in the workshop. The outcome of the meeting was presented at the recent session of the TFEI in Denmark in June 1999.

Measurements

Chemical Coordinating Centre (CCC) summarizes, analyzes and makes their quality assurance, reports data and compiles the monitoring database. Observations of POPs have not been a part of the EMEP monitoring programme before 1999. As a first step the Steering Body of EMEP requested CCC to collect available data on POPs from national and international programmes (HELCOM, AMAP, OSPAR). In this stage measurement data on

PCBs and B[a]P were collected from eight stations located in the following countries: Germany, Ireland, Iceland, Norway, Finland, the Czech Republic, and Sweden.

Measurement data were analyzed and prepared for comparison with modelling results. Description of the POP monitoring activity in 1996-1997 was prepared by CCC (Section 4.1 of this report). Practically all stations are located in the northern region of Europe. It is really necessary to have some measurement data in South and Eastern Europe. In addition to atmospheric measurements for model validation it is necessary to measure POP content in different environmental compartments.

Modelling

Meteorological Synthesizing Centre East (MSC-E) is responsible for the evaluation and modelling of the POP transport. At this stage a special attention is paid to the refinement of physical-chemical properties of selected PCBs, selected PAHs, lindane, selected PCDD/Fs. Detailed information on the congeners is included in Annexes A, B, C to the report.

The next important point is the investigations of exchange processes between environmental compartments. The main attention was concentrated on the development of atmosphere/ vegetation exchange module. Refining of POP atmosphere/sea exchange module with emphases on the effect of sea currents on POP transboundary transport is underway. Results of POP modelling were presented at the EUROTRAC/MEPOP workshop (February 1999) and AMAP workshop (June 1999).

In parallel with the development of the regional model a preparatory work for hemispherical modelling is going on. This activity is aimed at the evaluation of POP transport between Europe and other continents (North America, Asia, Africa, the Arctic).

Thus the objective of this stage is the study of POP properties and processes affecting their fate in different environmental compartments, the development of a multi-compartment model, tentative calculations of POP transport, comparison of modelling results against measurements.

The results of investigation of POP transboundary transport will be presented at the WMO/EMEP/UNEP/EUROTRAC Workshop on modelling of atmospheric transport and deposition of POPs and HMs (Geneva, 16-19 November 1999).

It is necessary to stress that the work in the field of modelling is carried out in close co-operation with experts from the Netherlands, Germany, Great Britain, Bulgaria, Belarus, Russia, and others.

The outline of the report is as follows:

In Chapter 1 we present the review of the present stage of the development of the multi-compartment POP long-range transport model focusing on changes made in the current year. The model assumptions and parameterization for POPs selected for modelling are given.

Chapter 2 is aimed at the description of the emission data used for the modelling. Here we present the official data and expert estimates of POP emissions as well as their spatial distribution.

In Chapter 3 we present the calculation results for selected PCB congeners, B[a]P, 2,3,4,7,8-PeCDF, and lindane. Here we discuss the influence of different processes on the POP long-range transport modelling results. The assessment of deposition of selected POPs on regional seas is presented as well.

Chapter 4 contains the analysis of the measurement data available and the comparison of calculation results with measurements within the EMEP grid.

Chapter 5 presents the conclusions and directions of further investigations resulting from the analysis of the modelling results obtained.

The report is supplied with five annexes (Annex A – Annex E) where the physical-chemical properties of the selected compounds are considered. The last annex (Annex E) contains the measurement data on some POPs obtained from CCC database.

Chapter 1

Progress in the development of POP transboundary transport model

This chapter contains the description of three-dimensional POP transport model being under development in Meteorological Synthesizing Centre-East.

It is well-known that evaluation of contamination of the environment by POPs requires a multi-compartment approach. For this reason exchange between air and underlying surface (soil, sea water) was described in the model at previous stages of its development. At this stage the attention was paid to the description of atmosphere/vegetation exchange for selected POPs and of gas/particle partitioning.

Compared to the previous version of the POP long-range transport model described in [*Pekar et al.,* 1998], the following changes were made:

- The description of the atmosphere/vegetation exchange for POP gaseous is made (section 1.2).

- On the basis of literature data on PCB physical-chemical properties model parameterization for seven congeners (PCB-28, 52, 101, 118, 138, 153, and 180) was prepared (Annex B).

- In PCB modelling both gas and aerosol phases of a pollutant in the air are taken into account (section 1.1).

- In B[a]P transport modelling the exchange with the underlying surface (soil and sea water) is taken into account (section 3.2).

- Investigations of physical-chemical properties of PAHs and preparation of appropriate model parameterization is being continued (Annex C).

- On the basis of the analysis of literature data on sources of dioxins/furans emission into the atmosphere and on their physical-chemical properties the model parameterization for 2,3,4,7,8-PeCDF was prepared (Annex D).

- The work on the block describing the transport of POPs with sea currents is started (at present this block is not included into model).

The present version of the model with the modifications listed above was used for the simulation of the long-range transport of seven PCB congeners, B[a]P, 2,3,4,7,8-PeCDF, and lindane. Modelling results were compared with measurement data and with the earlier obtained results. In addition the investigation of the influence of the processes discussed on the POP long-range transport modelling was performed.

Note that a detailed description of POP transport model ASIMD without the above listed changes has been given in the MSC-E report [*Pekar et al.,* 1998], and we restrict ourselves by a general description of the model but stand in detail at the description of the atmosphere/vegetation exchange block.

1.1. *General description of the model*

Figure 1.1 shows the scheme of processes introduced to the model up to the moment.

The atmospheric transport model ASIMD includes the following processes:

- horizontal advection;
- vertical turbulent diffusion;
- gas/particle partitioning based on the Junge model;
- gas phase degradation in air;
- deposition on the underlying surface of three types (soil, sea water, vegetation), including dry deposition of the gas phase (gaseous exchange) and aerosol phase, washout of the gas and aerosol phases.

The model considers gaseous and aerosol state of the substance in the atmosphere. It is assumed that the equilibrium between the gas and aerosol phases is set up instantaneously in air as described by the *Junge* model [*Junge*, 1977; *Pankow*, 1987]. The process of gas phase dry deposition is considered as the process of POP exchange between the atmosphere and the underlying surface. Transport processes, wet scavenging and dry deposition of the aerosol phase are described in MSC-E report [*Pekar et al.,* 1998].

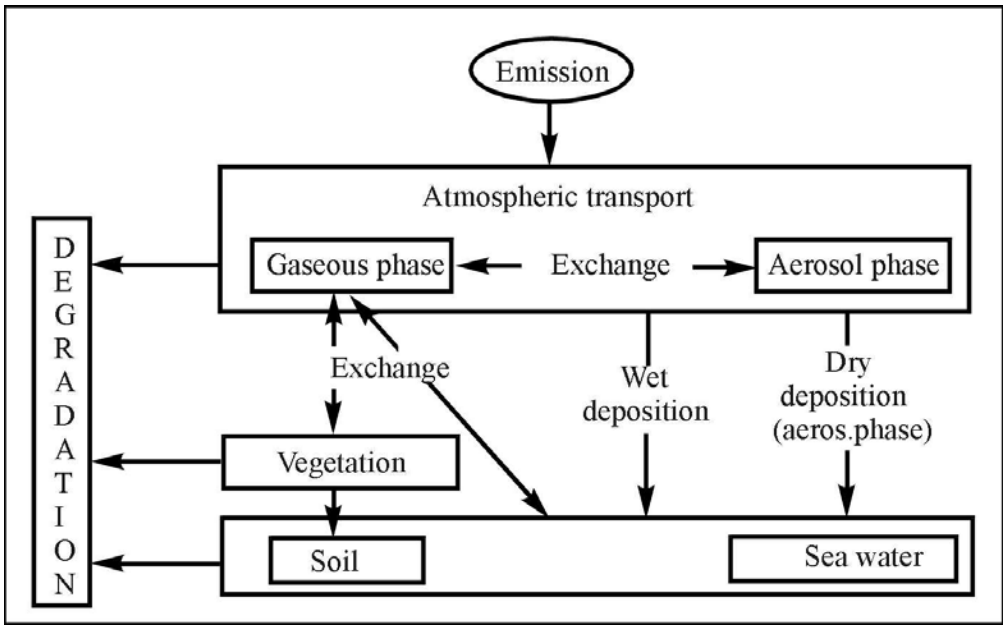

Figure 1.1. Scheme of basic processes considered in the regional ASIMD model

The soil model described in [*Jacobs and van Pul*, 1996] is used as the soil block. The appropriate program unit has been developed in RIVM and made available to MSC-E together with parameterization and initial data to be integrated into the ASIMD model. The model considers the soil surface layer of 15 cm split into 5 layers which thickness increases with depth. It is supposed that POPs are present in soil in three phases: gaseous, dissolved and sorbed on particles and the equilibrium between phases is set up instantaneously. The volatilization from the soil surface (re-emission) is possible.

The soil model considers the following processes:

- POP vertical diffusion;
- convective water flows which can be directed both upwards and downwards;
- volatilization (re-emission);
- POP degradation.

The sea model described in [*Jacobs and van Pul*, 1996] is used as the sea block. The appropriate program unit has been developed in RIVM and made available to MSC-E. The model considers the water surface layer of 25 m depth. Mechanisms of POP input to water are the same as to soil: dry and wet deposition of gas and aerosol phases. Due to hydrophobic character of some POPs their volatilization fluxes from the sea and lake surfaces can be very high.

The sea model considers the following processes:

- volatilization (re-emission);
- POP degradation in sea water;

At this stage some processes occurring with POPs in sea water are not considered namely:

- vertical and horizontal transport by large-scale currents;
- adsorption on suspended particulate matter containing organic carbon;
- sorption on dissolved organic carbon;
- sedimentation;
- re-suspension from sediments in coastal and shallow water.

At the next stages these processes are planned to be included into the model.

It is presumed that POP in the gas phase entering sea water due to gaseous exchange or washout with precipitation participate in further gaseous exchange with the atmosphere. At the same time POPs in the aerosol phase are not dissolved in water and do not take part in the gaseous exchange with the atmosphere remaining to be associated with particles.

The description of atmosphere/vegetation exchange is done on the basis of one-chamber leaf model described in [*Duyzer and van Oss*, 1997; *Hauk et al.,* 1994; *Paterson et al*., 1994]. The uptake of a pollutant by vegetation is described with the help of resistance analogy. The resistance is calculated distinctly for cases of deciduous and coniferous forests and grass cover. The model considers the defoliation of vegetation. Further decay of plant material and its transfer to soil is studied insufficiently and is described in the model as a first-order process as a preliminary rough hypothesis.

Degradation processes in all the media are described as first-order processes with degradation rates different for different compartments and pollutants. The importance of taking into account the degradation in vegetation was already pointed out in the literature [*MacCrady and Maggard,* 1993; *Chrostowski and Foster,* 1996].

1.2. *General description of the atmosphere/vegetation exchange module*

As known from papers [*Hauk et al*., 1994; *Horstmann and McLachlan,* 1998] gaseous exchange plays a predominating role in the uptake of semi-volatile pollutants by vegetation. Therefore at this stage of investigations we restricted ourselves with consideration of atmospheric pollutant gas phase exchange with vegetation.

Apart from physical-chemical properties of the atmospheric pollutant, for the description of the atmosphere/vegetation exchange the following data are used:

- spatial distribution of vegetation types over the computational grid;
- spatial distribution of the leaf area index for all vegetation types.

Leaf area index means the ratio of the total area of leaves within a given grid cell to the area of the grid cell itself.

1.2.1. Atmosphere/vegetation exchange module

Up to the moment two types of different models of exchange of atmosphere/vegetation are described in the literature: one-chamber leaf model assuming that the exchange between air and leaf volume takes place during "one time step" and two-chamber leaf model in which it is supposed that except for the interaction through the leaf surface the exchange between surface layer of a leaf and its inner reservoir takes place. Let us consider the peculiarities of the two models.

- *Two-chamber model*. In this model described in [*Hauk et al*., 1994; *McLachlan et al*., 1995] vegetation is considered as some "internal reservoir" surrounded by a cuticle layer. Consequently the exchange between the atmosphere and vegetation takes place in two steps: at first a pollutant penetrates from air to the cuticle layer and then from it into the internal reservoir. Model results agree well with experimental data indicating two characteristic time scales of the interaction. The exchange with a leaf is fast with time scale about one hour, it is slow when interacting with leaf reservoir - time scale is several days or even weeks. In [*Hauk et al.,* 1994] it is indicated that this model results are in a good consistency with observations. At the same time, however, it is indicated that numerical realization of this model appeared to be unstable. On the other hand, in modelling of a sufficiently long process (such as long-range transport) the presence of two time scales become insignificant since all processes can be correctly described by the choice of effective values of kinetic parameters.

- *One-chamber model*. In this model vegetation is represented by a single reservoir with which the exchange takes place. Two ways of pollutant penetration to a plant are considered: through cuticle and stomata (the second way is open only during the day-time and vegetative period). The exchange process is described by the resistance analogy: the resistance of air turbulent and laminar layers and the resistances of cuticle and stomata (the last two are obviously connected "in parallel").

  Therefore for the description of long-range transport processes the application of the one-chamber model seems to be more appropriate.

  As mentioned above the degradation process in vegetation can play an essential role in air/vegetation exchange. This process is described as a first order process. Let us consider a method of evaluating the degradation rate.

- *Degradation in vegetation*. The degradation rate in vegetation is one of the least investigated parameters. The only experimental data available in the literature deal with

dioxins/furans [*MacCrady and Maggard,* 1993]. In the model it is suggested to estimate degradation in vegetation by measured ratios of equilibrium concentrations in vegetation and air. Such data are available, for example, for a number of PCB congeners [*Thomas et al,* 1998], some polyaromatic hydrocarbons [*Simonich and Hites,* 1994] etc. The method for evaluation of degradation rate based on the ratio of equilibrium concentrations is described in the next section. Clearly, this method provides only a rough estimation of the degradation rate and does not eliminate the necessity of the experimental determination of this constant.

1.2.2. Description of vegetation types

Available information on vegetation in the grid cells is of two types. First, data indicating per cent of the cell area covered by:

- deciduous forests;
- coniferous forests;
- arable land;
- land covered by grain crops;
- land covered by grass;
- inland water;
- urban areas;
- other land.

These data are taken from European Land Use Data Base provided by RIVM. Calculations were made for three types of vegetation: coniferous forest, deciduous forest, and grass.

Second, monthly data on leaf index in each grid cell. This information was taken from the archive "Global Data Set for Land-Atmosphere Models" (ISLSCP) [*ECMWF*, 1994].

1.3. *Mathematical model of atmosphere/vegetation exchange*

1.3.1. Processes and methods of their description

The model used is a one-chamber one. As in the majority of models [*Bacci et al*., 1990a,b; *MacCrady and Maggard*, 1993; *Paterson et al.,* 1994; *McLachlan et al*., 1995] (models of the earlier period see in the review by [*Paterson et al.*, 1990]) here we represent leaves (vegetation) by a single block and the POP atmosphere-leaf exchange is considered as a reversible first order process. POP concentration variations in a leaf are described by the following equation [*Bacci et al*., 1990a,b]:

$$\frac{dC_V}{dt} = k_1 C_A - k_2 C_V , \qquad (1.1)$$

where C_V and C_A are POP concentrations in a vegetation and air, mol/m^3
k_1 and k_2 are uptake and clearance rates, respectively, s^{-1}.

Clearance rate is in turn determined by volatilization rate and degradation rate, so that:

$$k_2 = k_v + k_d \qquad (1.2)$$

where k_v and k_d are being volatilization and degradation rates, respectively.

The influence of the degradation process in vegetation is at present under discussion.

Neglecting for the present the degradation process, one can rewrite eq.(1.1) in the form:

$$\frac{dC_V}{dt} = \frac{S_L}{R_T}\left(C_A - C_V / K_{VA}\right), \qquad (1.3)$$

where S_L is the leaf area per its volume, m^2/m^3
R_T is the total resistance, s/m;
K_{VA} is the bioconcentration factor, i.e. the ratio of equilibrium concentrations of a pollutant in vegetation and air.

Thus this model is completely determined by two parameters: K_{VA} (bioconcentration factor) and ratio S_L/R_T (sorption rate). The first parameter is static, the second one is dynamic.

With allowance for degradation in vegetation, eq.(1.1) can be rewritten in the form:

$$\frac{dC_V}{dt} = \frac{S_L}{R_T}\left(C_A - C_V / K_{VA}\right) - k_d C_V . \qquad (1.4)$$

In this case the degradation rate k_d is to be added to the two parameters listed above.

To illustrate exchange process features let us consider its simplified version assuming that air concentration and all the parameters in question are constant. Then the solution of eq.(1.1) is:

$$C_V = \frac{k_1}{k_2} C_A + \left(C_V^0 - \frac{k_1}{k_2} C_A \right) exp\left(- k_2 t\right), \qquad (1.5)$$

where C_V^0 is the pollutant initial concentration in vegetation.

Eq.(1.5) shows that:

- Equilibrium concentrations in the atmosphere and vegetation satisfy the relation:

$$C_V = \frac{k_1}{k_2} C_A \qquad (1.6)$$

so that the ratio k_1/k_2 can be considered as a modified (reduced) bioconcentration factor K^*_{VA} (cf. [*Chrostowski and Foster,* 1996]). The latter can be expressed via the above parameters as:

$$K^*_{VA} = \frac{k_1}{k_2} = \frac{S_L / R_T}{S_L /(R_T K_{VA}) + k_d} = \frac{K_{VA}}{1 + \frac{R_T K_{VA}}{S_L} k_d} . \qquad (1.7)$$

It is clear that the right-hand part of the latter expression decreases with k_d increase. Eq.(1.7) can be used for the evaluation of degradation rate if the rest of its parameters including equilibrium concentration ratio have been already determined.

- Clearance rate k_2 equals to:

$$k_2 = \frac{S_L}{R_T K_{VA}} + k_d , \qquad (1.8)$$

hence the dynamic equilibrium between pollutant gas phase and vegetation is reached more rapidly the higher the degradation rate is. For example, in [*Thomas et al*., 1998] it is shown experimentally that for PCBs the equilibrium is set up during the period shorter than two weeks. Degradation in vegetation can explain this fact. In [*MacCrady and Maggard*, 1993; *Chrostowski and Foster,* 1996] it is mentioned that degradation constant can appear to be more important than re-emission constant. The above considerations indicate that it is important to study further atmosphere/vegetation exchange and in particular to determine experimentally the degradation rate values.

1.3.2. Evaluation of model parameters

Static parameters. The leaf-air partition coefficient is called differently by different authors: bioconcentration factor BCF, BCF_v or K_{BA} [*Bacci et al*., 1990a,b.; *Paterson et al*., 1991; *Müller et al*., 1994], grass-air partition coefficient K_{GA} [*McLachlan et al*., 1995], plant-atmosphere partition coefficient K_v [*Simonich and Hites*, 1994] or plant-air partition coefficient K_{PA} [*Kömp and McLachlan,* 1997a,b]. Here we use the notation K_{VA}.

The equilibrium in the leaf-air system is determined by parameters of POP partitioning between leaf components and air and relative volume of each component:

$$K_{VA} = \sum v_i K_{iA} , \qquad (1.9)$$

where v_i is leaf volume fraction accounted for component *i*,
K_{iA} is partition coefficient in the system (component *i*)/air.

Let us describe existing model assumptions on the leaf structure (these assumptions can be used both in one-chamber and two-chamber exchange models). In literature several leaf models are being discussed. The most sophisticated *six-component model* was suggested by [*Müller at al*., 1994]. The v_i values obtained in this study (on the basis of literature data) for the three vegetation types are listed in table 1.1.

Table 1.1. Leaf composition

Leaf type	Leaf fraction accounted for component *i*, %					
	Water (v_W)	Cell lipids (v_L)	Cuticle (v_C)	Carbohydrates (v_F)	Protein (v_P)	Air* (v_A)
Spruce needles	58	3.7	2.7	21.6	2.4	11.6
Azalea leaf	62	1.3	1.9	9.0	4.2	21.6
Grass leaf	65	0.3	0.4	7.8	3.9	22.6

* Calculated as the difference of 100% and the sum of fractions of the remained components.

Using published correlations with octanol-water partition coefficient (K_{OW}) [*Müller et al.*, 1994] calculated leaf-water partition coefficients (K_{iW}). They were converted to coefficients K_{iA} by multiplication by the inverse value of dimensionless Henry's law constant ($K_{WA}= RT/H$). As a result the following empirical expression was obtained:

$$K_{VA} = \left(\frac{RT}{H}\right)\cdot[v_C(1.11K_{OW}{}^{0.97}) + v_w + v_l K_{OW} + v_f(0.0372K_{OW}{}^{0.95}) + v_P(86.2K_{OW}{}^{-1} + 3.70)] \qquad (1.10)$$

Correlations of K_{iW} with K_{OW} for the last two terms of expression (1.10) were obtained in [*Müller et al.*, 1994] for a set of 6-11 organic substances with relatively narrow range of K_{OW} values and their accuracy and universality are doubtful. Therefore for practical use of the discussed model additional experimental data are required.

Five-component model of a broad-leaved tree was suggested by [*Riederer*, 1990] for azalea leaf. According to this model such a leaf consists of 30% of air, 64.5% of water, 4.7% of polar components, 0.1% glycolipids, and cuticle which is accounted for 0.7% of the volume.

A simpler *three-component model* was suggested in [*Paterson et al.,* 1991] for azalea leaf. The following correlation relation was obtained for calculations of K_{VA} value in the air-azalea system. The coefficients on the right correspond to air, water and lipid fractions of model leaf volume; octanol is assumed to be the surrogate of lipids:

$$K_{VA} = 0.19 + 0.7K_{WA} + 0.05K_{OA} \qquad (1.11)$$

where K_{WA} is water-air partition coefficient equal to the inverse value of dimensionless Henry's law constant,

K_{OA} is octanol-air partition coefficient.

Finally in [*Bacci et al.*, 1990a,b] the following expression for K_{VA} is suggested:

$$K_{VA} = L \times K_{OA,} \tag{1.12}$$

where L is a volumetric fraction of lipids in a leaf.

Eq.(1.12) represents the simplest *one-component* leaf model consisting of the lipid component and all other components, which do not take part in POP uptake. This model seems to be quite efficient for hydrophobic compounds with high values of K_{OA}. For example, for PCB values of K_{OA} (10^7 - 10^{11}) are so much higher than K_{WA} (10^1 - 10^2) and unity that clearly all terms but the last on the right in (1.11) can be neglected for any plant without considerable loss in the calculation accuracy.

The value of L depends on a plant species. From the viewpoints of different authors lipid volumetric fraction in azalea leaves is 2.2% [*Bacci et al*., 1990a], 3.2% [*Müller et al*., 1994] and 5% [*Paterson et al.*, 1991]. The estimate by [*Müller et al*., 1994] obtained on the basis of direct measurements seems to be most reliable. The other two estimates [*Bacci et al*., 1990a; *Paterson et al.*, 1991] were obtained by correlation of (1.11) and (1.12) types and they depend on a set of used compounds and the accuracy of K_{OA} value.

J.Tolls and M.S.McLachlan [1994] estimated mean volumetric lipid content for grass as 1% (L = 0.01). This value is in agreement with the estimate 0.7% obtained by [*Müller et al.*, 1994]. Lipids in a model leaf of a broad-leaved tree have approximately the same fraction of the volume (0.8%) [*Riederer,* 1990]. For spruce needles total lipid content is estimated as 6.4% [*Müller et al*., 1994].

Thus the optimum representation of K_{VA} dependence on physical-chemical properties of organic pollutants with high values of K_{OA} is (1.12). The above mentioned L values (1% for grass cover, 0.8% for deciduous forest, and 6.4% for coniferous forest) can be recommended for herbaceous plants, deciduous and coniferous forests respectively.

Kinetic parameters. Eq.(1.3) can be also written as follows:

$$\frac{dC_L}{dt} = k_1(C_A - C_L / K_{VA}) . \tag{1.13}$$

The uptake rate k_1 of POP is often represented as a function of S_L (see eq.(1.3) above):

$$k_1 = \frac{S_L}{R_T} = S_L k_{AV} , \tag{1.14}$$

where R_T is total resistance to the exchange through leaf-air interface, s/m,
k_{AV} is the mass transfer coefficient through leaf-air interface, m/s.

Value R_T (and k_{AV} since $k_{AV} = R_T^{-1}$) is calculated by formula:

$$R_T = R_b + R_L, \quad (1.15)$$

where R_b is the sum of resistances of laminar and turbulent atmospheric layers, s/m;
R_L is leaf surface resistance, s/m.

In its turn, R_L is calculated as [*Riederer,* 1990; *Duyzer and van Oss,* 1997]:

$$R_L^{-1} = R_C^{-1} + R_S^{-1}, \quad (1.16)$$

where R_C is cuticle resistance, s/m;
R_S is stomatal resistance.

The last term is added to the leaf resistance in the daytime (about 15 hours during the vegetative period).

Resistance R_S is estimated as a product of stomatal resistance for water vapor by a square root of the ratio of molecular mass to POP water molecular mass [*Baldocchi et al.*, 1987], i.e.

$$R_S = R(\mathrm{H_2O})\left(\frac{M}{M_{\mathrm{H_2O}}}\right)^{1/2}, \quad (1.17)$$

where $R(\mathrm{H_2O})$ is stomatal resistance to water vapor 2×10^3 s/m,
M and $M_{\mathrm{H_2O}}$ are molar masses of pollutant and vapor, respectively.

Experimental tests of this method of R_S calculations for hydrophobic substances were not carried out, but it is the only one commonly accepted.

Cuticle resistance R_C is experimentally determined for a specific plant and substance or it is calculated using correlation relations obtained with experimental values of R_C for other species. By now several groups of experimental data are published. These data are obtained by two ways for various species and plants. There are data on two species of spruce, one species of bush (*Azalea indica*), grass (*Lolium multiflorum*) and orange tree (*Citrus aurantium*).

Assessment of cuticle resistance for deciduous forests. Data for *Citrus aurantium* were obtained by the procedure developed earlier in investigations of the penetration velocity of agricultural chemicals to a leaf in case of their application as water aerosol [*Kerler and Schönherr,* 1988]. Leaf cuticle is separated from its remained part and is set between two reservoirs. The upper reservoir contacting with the external cuticle surface contains the solution of the substance in question, the lower one contains water. The so-called permeability coefficient P of cuticle (traditionally measured in cm/s) is then calculated via the velocity of substance penetration from the upper to the lower reservoir. P is a proportionality coefficient between substance fluxes from the upper reservoir to the lower one and the difference in concentrations between them [*Price*, 1983]:

$$J = P(C_1 - C_2), \quad (1.18)$$

where J is substance flux from the upper reservoir to the lower one, mol/cm^2/s;
C_1 and C_2 are substance concentrations in the upper and lower reservoirs, mol/cm^3, respectively.

Cuticle permeability coefficient is parametrized via diffusion coefficient in cuticle D (cm^2/s), cuticle-water partition coefficient K_{CW}, cuticle thickness Δx (cm) and tortuosity factor l [*Price*, 1983]:

$$P = DK_{CW}/(\Delta x\, l) \quad (1.19)$$

The diffusion coefficient is, in turn, inversely proportional to the molar volume V_m of the compound in question. Leaf cuticle thickness depends on a plant type and varies from fractions of μm to more than 10 μm [*Price*, 1983]. For the model leaf of a broad-leaved tree it is accepted that Δx = 1μm [*Riederer*, 1990].

On the basis of P values experimentally determined for 8 species with K_{OW} from 2 to 7.9 [*Kerler and Schönherr*, 1988] linear correlations of log$P$ with logK_{OW}, logK_{CW} and molar volume V_m, cm^3/mol, were calculated. The correlation coefficient log$P$ and logK_{OW}, was equal to 0.91 and the difference between measured and calculated values of P was as much as the order of magnitude. Somewhat better correlation was obtained with logK_{CW}:

$$\log P = 0.734 \cdot \log K_{CW} - 11.26; \qquad r = 0.95, \quad (1.20)$$

where r is the correlation coefficient.

In full agreement with expression (1.19) the correlation was improved with the introduction of molar volume (in addition to K_{CW}) which is functionally connected with diffusion coefficient:

$$\log P = (238/V_m) \cdot \log K_{CW} - 12.48; \quad r = 0.98 \quad (1.21)$$

Permeability coefficient in the water-cuticle-water system is transformed to permeability coefficient in the air-cuticle-air system by division by K_{WA}. The reverse value can serve as a certain estimate of R_C [*Riederer*, 1990]:

$$R_C \approx \frac{K_{AW}}{P},$$

though strictly speaking R_C^{-1} is equal to the permeability coefficient in the air-cuticle-water system. Similarly, correlations (1.20) and (1.21) can be re-written for logR_C:

$$\log R_C = \log K_{AW} - 0.734 \cdot \log K_{CW} + 11.26, \quad (1.22)$$

$$\log R_C = \log K_{AW} - (238/V_m) \cdot \log K_{CW} + 12.48, \quad (1.23)$$

where $K_{AW} = H/RT$ is the dimensionless Henry's law constant.

It seems that the preference should be given to expression (1.23) due to better statistical factors and better consistency with the theoretical dependence. Value $\log K_{CW}$ can be estimated by its correlation with $\log K_{OW}$ obtained by the same authors but for a larger set of substances [*Kerler and Schönherr*, 1988]:

$$\log K_{CW} = 0.97 \cdot \log K_{OW} + 0.057 \quad (1.24)$$

The other set of experimental data on the uptake of 14 substances by azalea leaves is presented in papers [*Bacci et al*., 1990a,b; *Bacci et al*., 1992]. In these experiments the plants were contained in continuously illuminated glass chamber where a certain concentration of substance was kept (uptake stage). After 360 hours clean air was injected to the chamber (clearance stage) and during about 500 hours, desorption kinetics of leaves was studied. Using data on substance concentrations in leaves at different time, rates of the direct and inverse processes which are functions of R_b and R_L were calculated. Later on, by the least-squares technique the following relation:

$$1/k_2 = \tau_O + \tau_A \cdot K_{VA} \quad (1.25)$$

was obtained [*Paterson et al.*, 1991].

Here τ_O and τ_A are characteristic times of the transport in cuticle and air boundary layer, respectively, $\tau_O = 126$ hours, $\tau_A = 5 \times 10^{-6}$ hours.

Taking into account that $k_1/k_2 = K_{OA}$ we obtain:

$$\frac{1}{k_1} = \frac{R_T}{S_L} = \frac{\tau_O}{K_{VA}} + \tau_A \quad (1.26)$$

Then:

$$R_T = S_L \tau_O / K_{VA} + S_L \tau_A \quad (1.27)$$

Since eq.(1.27) is quite similar to (1.15), we have:

$$R_L = S_L \cdot \tau_O / K_{VA} = 126\, S_L / K_{VA} \quad (1.28)$$

The essential problem in using the latter formula is the lack of experimentally measured values of S_L. Assuming that azalea leaf thickness is the same as that of a model leaf of a broad-leaved tree, i.e. 0.3 mm [*Riederer,* 1990] and neglecting lateral leaf areas and considering it to be flat we obtain $S_L = 6700$ m^2/m^3. Clearly the accuracy of this estimate is not high since according to the data of table 1.1 and in the text below, features of azalea leaves and of broad-leaved tree are essentially different. For the same reason the application of obtained R_C to other foliage plants seems problematic. Besides, parameter τ_0 obtained for azalea is assumed to be independent of substance characteristics though in physical sense it is inversely proportional to diffusion coefficient in cuticle.

Hence, eq.(1.23) was chosen for model calculations of cuticle resistance for deciduous forests.

Assessment of cuticle resistance for grass cover. The only grass species for which kinetic parameters of POP uptake were determined is *Lolium multiflorum* [*Tolls and McLachlan,* 1994]. The procedure was approximately the same as in the case of azalea. The obtained results were interpreted in terms of two-chamber fugacity model. On obvious assumptions that cuticle makes the main contribution to the resistance of POP transport to the internal leaf reservoir, the authors obtained the following relation:

$$d_{SR} = k_{SR} \cdot S_L \cdot Z_L, \qquad (1.29)$$

where d_{SR} is fugitive conduction between the leaf surface layer and internal leaf reservoir normalized to fresh leaf area, mol/Pa/h/m^3;

Z_L is fugitive capacity of leaf lipid component, mol/Pa/m^3, $Z_A = (RT)^{-1} \cdot a_{SR}$,

α_{SR} is interface area between the surface layer and internal leaf reservoir normalized to its volume, m^2/m^3, $\alpha_{SR} \approx S_L$,

k_{SR} is mass transfer coefficient between the surface layer and internal reservoir of a leaf, m/s.

Mass transfer coefficient k_{SR} can be calculated as follows:

$$k_{SR} = d_{SR}/a_{SR}Z_L = d_{SR}/a_{SR}(Z_L/Z_A)Z_A = d_{SR}RTL/a_{SR}K_{VA}, \qquad (1.30)$$

where Z_A is fugitive capacity of air, mol/Pa/m^3, $Z_A = RT^{-1}$, $Z_L/Z_A = K_{VA}$.

Values of parameters d_{SR} and K_{VA} for *Lolium multiflorum* and for a number of compounds were determined by model adjustment using experimental data, L was taken to be 0.01 and value α_{SR} was measured experimentally (α_{SR} = 7200 m^2/m^3) [*Tolls and McLachlan*, 1994]. Using these data and eq.(1.30) we calculated values of mass transfer coefficient k_{SR} for all pollutants in question. For hexachlorobenzene negative logarithm k_{SR}(m/s) is equal to 10.84 for α-HCH - 11.37, γ-HCH - 11.57, PCB-28 - 11.19, PCB-52 - 11.44, PCB-101 - 11.63, phenanthrene - 11.39, anthracene - 10.74, 1-chloroanthracene - 11.05, 1,2,3,4-tetrachloronaphtalane - 11.06.

In the framework of one-chamber model obtained by the simplification of the two-chamber one, the product $k_{SR} K_{OA}$ is treated as the mass transfer coefficient of POP from the leaf area to its volume [*McLachlan et al.*, 1995] or, in other words, as an inverse value of R_L. Consequently, we have:

$$\log R_L = -\log k_{SR} - \log K_{OA}. \qquad (1.31)$$

Values $\log k_{SR}$ required for calculations of a number of POPs are presented above. For the rest of substances they can be estimated by the obtained correlation with molar volume. Mass transfer coefficient in its physical sense is completely identical to permeability coefficient P divided by partition coefficient K_{OW}, i.e. it is directly proportional to substance diffusion coefficient in cuticle. In its turn, diffusion coefficient is inversely proportional to the molar

volume (V_m, cm^3/mol) of a substance raised to some power. Therefore the required dependence is presented in form $\log k_{SR} = A \log V_m + B$. The molar volume of all substances listed above but phenanthrene can be calculated by LeBass method. For the whole set of species (without phenanthrene) the following correlation is obtained:

$$\log k_{SR} = -5.61 \log V_m + 2.11, \quad n = 9, \quad r = 0.91, \tag{1.32}$$

where n is the number of substances used for calculations of correlations;
r is the correlation coefficient.

The greatest deviation from the regression line is observed for γ-HCH. The difference is 0.3 of logarithmic units, which is quite satisfactory by itself. However, the fact that two isomers of HCH of equal molar volume and different only in spatial configuration of molecules differ almost in two times shows that LeBass method is not quite sufficient for them. Leaving alone these two substances and operating only with aromatic species we have:

$$\log k_{SR} = -5.29 \log V_m + 1.43, \quad n = 7, \quad r = 0.98 \tag{1.33}$$

The deviation from the regression line (1.33) does not exceed 0.1 of logarithmic unit.

In model calculations of grass cuticle resistance eq.(1.31) and eq.(1.33) were used.

Assessment of cuticle resistance for coniferous forests. Similarly, using parameters of the two-chamber model determined by results of experiments with needles of two spruce species (*Picea omorica and Picea abies*) [*Hauk et al*., 1994] and by experimentally measured $\alpha_{SR} = 7080$ m^2/m^3 it is possible to calculate mass transfer coefficients of DDE in needles. For *Picea omorica* $k_{SR} = 1.37 \times 10^{-11}$ m/s, for *Picea abies* - 0.68×10^{-11} m/s. Experimental data for other coniferous trees are not available. Therefore optimum estimate of k_{SR} for coniferous trees is the mean of the two above values: $k_{SR} = 10^{-11}$ m/s. The accuracy of this value seems to be not better than a factor of an order of magnitude since k_{SR} values for two close species differ two times. The only possibility to calculate k_{SR} for other POPs is the formula $\log k_{SR} = A \cdot \log V_m + B$ where A is the same as in (1.33) and B is calculated on the basis of known values V_m and k_{SR} for DDE; $V_m^{DDE} = 305.2$ cm^3/mol, $k_{SR} = 10^{-11}$ m/s:

$$\log k_{SR} = -5.61 \log V_m + 2.94. \tag{1.34}$$

In model calculations cuticle resistance for coniferous forests eq.(1.31) and eq.(1.34) were used.

1.4. *Model assumptions and parameterization*

1.4.1. Model assumptions

1. POP initial concentrations in all compartments are equal to zero.

2. All POPs (but lindane) are present in the atmosphere in the gas and aerosol phase. Partitioning between these phases is described by the *Junge* model.

3. It is assumed that POPs in the aerosol phase are not dissolved in water and do not take part in the gaseous exchange with the atmosphere remaining to be associated with particles.

4. In the description of the atmosphere/vegetation gas exchange the one-chamber leaf model is used.

1.4.2. Parameterization for seven PCB congeners (PCB-28, 52, 101, 118, 138, 153, 180)

1. *Henry constants*

The temperature dependence of Henry constant on temperature is given in the form:

$$\log H \text{ (Pa m}^3\text{/mol)} = -A/T(K) + B,$$

The values of the coefficients *A* and *B* for seven PCB congeners are given in table 1.2 (calculated on the basis of data from [*Burkhard et al.,* 1985; *ten Hulscher et al.,* 1992], see Annex B):

Table 1.2. Coefficients of Henry constant temperature dependence for seven PCB congeners

IUPAC number	*A*	*B*
28	3227	12.28
52	3379	12.84
101	3510	13.17
118	3510	12.88
138	3625	13.27
153	3625	13.38
180	3724	13.53

2. *Saturated vapor pressure over subcooled liquid*

The temperature dependence of the saturated vapor pressure over subcooled liquid is given in the form:

$$\log p^0_L \text{ (Pa)} = -A/T(K) + B$$

The coefficients A and B of this dependence for seven PCB congeners are presented in table 1.3 (calculated with the help of data from [*Falconer and Bidleman*, 1994], see Annex B):

Table 1.3. Coefficients of temperature dependence of the saturated vapor pressure for seven PCB congeners

IUPAC number	*A*	*B*
28	4075	12.20
52	4220	12.36
101	4514	12.67
118	4664	12.72
138	4800	12.81
153	4775	12.85
180	5042	13.03

3. *Washout ratio for the aerosol phase*

$W_p = 4 \times 10^4$ [*Franz and Eisenreich,* 1998].

4. *Dry deposition velocities for the aerosol phase, cm/s*

$$V_d^{land} = (0.02 \cdot u_*^2 + 0.01) \cdot \left(z_0 / 10^{-3}\right)^{0.33},$$

$V_d^{sea} = 0.15 \cdot u_*^2 + 0.013.$ [*Pekar,* 1996]

5. *Degradation rates*

Air:

Table 1.4. Degradation rates k_{dA} in air, s^{-1}

IUPAC number	With seasonal variation [*Kwok et* al., 1995]			Recommended in [*Mackay et al,* 1992]
	Winter	Autumn/Spring	Summer	
28	1.4×10^{-7}	1.3×10^{-6}	3.2×10^{-6}	3.5×10^{-7}
52	9.0×10^{-8}	8.0×10^{-7}	2.0×10^{-6}	1.13×10^{-7}
101	5.4×10^{-8}	4.8×10^{-7}	1.2×10^{-6}	1.13×10^{-7}
118	5.4×10^{-8}	4.8×10^{-7}	1.2×10^{-6}	1.13×10^{-7}
138	2.7×10^{-8}	2.4×10^{-7}	6.0×10^{-7}	3.5×10^{-8}
153	2.7×10^{-8}	2.4×10^{-7}	6.0×10^{-7}	3.5×10^{-8}
180	–	–	–	3.5×10^{-8}

Values recommended by [*Mackay et al,* 1992] are adopted as basic ones. For PCB-153 the calculation of degradation rate with consideration for seasonal variation is also performed and the comparison the obtained results is made.

Soil: $k_{dS} = 3.5 \times 10^{-9}$, s^{-1}.

Water:

Table 1.5. Degradation rates in water [*Mackay et al*., 1992]

IUPAC number	28	52	101	118	138	153	180
k_{dW}, s^{-1}	1.13×10^{-8}	3.5×10^{-9}	3.5×10^{-9}	3.5×10^{-9}	3.5×10^{-9}	3.5×10^{-9}	3.5×10^{-9}

Vegetation:

Table 1.6. Degradation rates in vegetation

IUPAC number	28	52	101	118	138	153	180
k_{dV}, s^{-1}	9.7×10^{-7}	1.7×10^{-6}	2.8×10^{-6}	4.2×10^{-6}	2.6×10^{-6}	4.2×10^{-6}	2.3×10^{-6}

Computed by the method described in section 1.3.1 on the basis of data from [*Thomas et al.,* 1998]. In the basic model version degradation in vegetation is not taken into account but for PCB-153 the calculations with degradation in vegetation are carried out and the calculation results of both calculation series are compared.

6. *Octanol-water partition coefficient*

Table 1.7. Octanol-water partition coefficient [*Mackay et al*., 1992; *Hawker and Connel*, 1988]

IUPAC number	28	52	101	118	138	153	180
K_{OW}	6.31×10^{5}	1.26×10^{6}	2.51×10^{6}	5.5×10^{6}	6.76×10^{6}	7.94×10^{6}	2.29×10^{7}

7. *Organic carbon-water partition coefficient*

Table 1.8. Organic carbon-water partition coefficient

IUPAC number	28	52	101	118	138	153	180
K_{OC}, m^3/kg	259	516	1030	2253	2772	3257	9393

8. *Octanol-air partition coefficient*

In the model, we use the temperature dependence of the form:

$$\log K_{OA} = A/T(K) - B.$$

The coefficients for this formula are presented in table 1.9:

Table 1.9. Coefficients of temperature dependence for octanol-water partition coefficients for seven PCB congeners

IUPAC number	*A*	*B*
28	3792	4.63
52	3981	5.02
101	3841	3.82
118	4693	5.92
138	4584	5.57
153	4695	6.02
180	4535	4.70

9. *Molecular diffusion coefficients*

Air:

Table 1.10. Molecular diffusion coefficients in air

IUPAC number	28	52	101	118	138	153	180
D_A, m^2/s	5.42×10^{-6}	5.09×10^{-6}	4.82×10^{-6}	4.82×10^{-6}	4.58×10^{-6}	4.58×10^{-6}	4.38×10^{-6}

Water:

Table 1.11. Molecular diffusion coefficients in water [*Schwarzenbach et al*, 1993]

IUPAC number	28	52	101	118	138	153	180
D_W, m^2/s	6.09×10^{-10}	5.71×10^{-10}	5.40×10^{-10}	5.40×10^{-10}	5.14×10^{-10}	5.14×10^{-10}	4.91×10^{-10}

1.4.3. B[a]P parameterization

1. *Henry constants*

The temperature dependence of the Henry constant for fresh water is:

$$\log H \text{ (Pa m}^3\text{/mol)} = 9.61 - 3263/T,$$

(calculated by *A.Bulgakov* on the basis of papers [*Mackay et al.,* 1992; *Hincley et al*., 1990; *May et al*., 1983]). Using data on other polyaromatic hydrocarbons the constants included in this dependence have been refined compared to the previous MSC-E report.

The temperature dependence of Henry constant for sea water:

$$\log H \text{ (Pa m}^3\text{/mol)} = 12.13 - 3964/T,$$ [*Vozhzennikov et al*., 1997]

In calculations the dependence for marine water is used.

2. *Saturated vapor pressure for subcooled liquid*

The temperature dependence of the saturated vapor pressure over subcooled liquid is given in the form:

$\log p^0_L$ (Pa) = 11.59 - 4989/T, [*Hincley et al*., 1990]

3. *Washout ratio for the aerosol phase*

$W_p = 5 \times 10^5$ [*Baart et al*., 1995],

$W_p = 2.4 \times 10^4$ [*Franz and Eisenreich,* 1998].

The last value is used in the model as a basic one. However, for PCB-153 calculations with both values were carried out and the comparison was made.

4. *Dry deposition velocities for the particulate phase, cm/s*

$$V_d^{land} = (0.04 \cdot u_*^2 + 0.02) \cdot \left(z_0 / 10^{-3}\right)^{0.30},$$

$V_d^{sea} = 0.15 \cdot u_*^2 + 0.023$, [*Pekar*, 1996].

5. *Degradation rates*

Air:

Table 1.12. Degradation rates in air

	Winter	Autumn/Spring	Summer
k_{dA}, s^{-1}	7.716×10^{-7}	1.157×10^{-6}	2.315×10^{-6}

(the mean value is taken from [*Mackay et al*, 1992] and a natural seasonal variation is introduced).

Soil: $k_{dS} = 1.13 \times 10^{-8}$, s^{-1}.

Water: $k_{dW} = 1.13 \times 10^{-7}$, s^{-1} [*Mackay et al*., 1992].

6. *Octanol-water partition coefficient*:

$K_{OW} = 1 \times 10^6$ [*Mackay et al*., 1992].

7. *Organic carbon-water partition coefficient*

K_{OC} = 500, m^3/kg calculated using data of [*Mackay et al*., 1992].

8. *Octanol-air partition coefficient*

The temperature dependence of the octanol/air partition coefficient is:

$$\log K_{OA} = 4989/T - 5.97,$$

(calculated by *A.Bulgakov* on the basis of the paper [*Mackay et al*., 1992]).

9. *Molecular diffusion coefficients*

Air: $D_A = 1 \times 10^{-6}$, m^2/s,

Water: $D_W = 5 \times 10^{-10}$, m^2/s, [*Schwarzenbach et al,* 1993].

1.4.4. Parameterization for 2,3,4,7,8-PeCDF

1. *Henry constant*

$\log H$ (Pa m^3/mol) = 14.69- 4468 /T [*Bulgakov and Ioannisian,* 1998]

2. *Saturated vapor pressure over subcooled liquid*

$\log p^0_L$ (Pa)= -4607 /T + 11.70, [*Bulgakov and Ioannisian,* 1998]

3. *Washout ratio for the aerosol phase*

$W_p = 1.8 \times 10^4$ [*Eitzer and Hites*, 1989b]

4. *Dry deposition velocity of the aerosol phase, cm/s*

$$V_d^{land} = (0.04 \cdot u_*^2 + 0.02) \cdot \left(z_0 / 10^{-3}\right)^{0.30},$$

$$V_d^{sea} = 0.15 \cdot u_*^2 + 0.023$$ [*Pekar*, 1996].

5. *Organic carbon-water partition coefficient*

K_{OC} = 1297, m^3/kg calculated using the data of [*Mackay et al*., 1992]

6. *Degradation constants* [*Mackay et al*., 1992].

Air: $k_{dA} = 1/\tau_a = 3.5 \times 10^{-7}$, s^{-1}

Soil: $k_{dS} = 1/\tau_s = 1.13 \times 10^{-8}$, s^{-1}

Sea surface layer: $k_{dW} = 1/\tau_w = 3.5 \times 10^{-7}$, s^{-1}.

1.4.5. Lindane parameterization

Similar to the previous report parameterization for the lindane model is made on the basis of the parameterization described in [*Jacobs and van Pul*, 1996]. It is assumed that lindane is present in the atmosphere in the gas phase only.

1. *Henry constant*

   $\log H$ (Pa m^3/mol) = 10.10 - 3183/T

2. *Organic carbon-water partition coefficient*

   K_{OC} = 1.3, m^3/kg

3. *Degradation rate* [*Strand and Hov*, 1996]

   Air: $k_{dA} = 2.5 \times 10^{-7}$, s^{-1}

   Soil: $k_{dS} = 3.0 \times 10^{-8}$, s^{-1}

   Sea surface layer: $k_{dW} = 4.66 \times 10^{-9}$, s^{-1}

4. *Molecular diffusion coefficients*

   Air: $D_A = 5.0 \times 10^{-6}$, m^2/s

   Water: $D_W = 5.0 \times 10^{-10}$, m^2/s.

Chapter 2

Emissions

This chapter deals with a concise description of available official data and expert estimates of emissions of selected POPs such as PCBs, PAHs, PCDD/Fs and lindane. Spatial distribution of emissions, estimates of temporal variability and distributions with height used in modelling of transboundary transport of the listed POPs are discussed.

2.1. *Emission data*

Official data on emissions for 1997 and previous years submitted by EMEP countries before April 1999 were provided by MSC-W and included in this section.

2.1.1 Polychlorinated biphenyls

The bulk of PCB emissions (about 90% [*Berdowski et al*., 1997]) is due to a leakage of various technical mixtures used in electrical equipment. Official emission data on polychlorinated biphenyls submitted from 1990 to 1997 are presented in table 2.1. Column "Estimates for 1990" contains expert estimates of total emission in 1990 taken from [*Berdowsky et al.*, 1997].

In model calculations official data available are used. For countries which have not submitted official data available PCB emission estimates [*Berdowski et al*., 1997] for 1990 were used. Total PCB emission within the EMEP grid was about 112 tonnes.

Spatial distribution of PCB emissions with resolution 150×150 km^2 over EMEP cells (figure 2.1.) was made on the basis of data contained in [*Berdowski et al*., 1997].

Table 2.1. PCB emission data, t/yr.

Country	Emission used in calculation [a]	UN/ECE reported official emission data (data provided by MSC-W in April 1999)							
		1990	1991	1992	1993	1994	1995	1996	1997
Albania	0.034								
Austria	1.32								
Belarus	0.6								
Belgium	5.2								
Bosnia&Herzegovina	0.128								
Bulgaria	0.25844	0.25844					0.38219	0.26173	0.2810
Croatia	0.132								
Cyprus	0.044								
Czech Republic	1.99								
Denmark	0.987								
Estonia	0.179								
Finland	15.8				5.3	1.1	15.8		
France	13	13							
Germany	44	44							
Greece	0.251								
Hungary	0.135	0.135	0.120	0.108	0.106	0.105	0.101	0.098	
Iceland	0.047								
Ireland	0.063								
Italy	5.83								
Latvia	0.162								
Lithuania	0.221								0.013
Luxembourg	0.119								
Netherlands	0	0	0	1.45E-05	2.88E-05	2.83E-05	1.53E-05		
Norway	0.384								
Poland	2.373	2.373					2.338	2.342	
Portugal	0.523								
Republic of Moldova	0.269								
Romania	0.515								
Russian Federation	7.25								
Slovakia	1.33	0.1614[b]					0.1389		0.1367
Slovenia	0.071								
Spain	8.53								
Sweden	1.93								
Switzerland	1.64								
The FYR of Macedonia	0.083								
Ukraine	3.74								
United Kingdom	5.708	6.9758[b]	6.4	5.901	5.4069	4.8452	4.2905	3.7495	3.247
Yugoslavia	0.435								

[a] Emission estimates for 1990 according to [*Berdowski et al.*, 1997], in dashed cells official data used in calculation

[b] official data provided when model calculations were finished

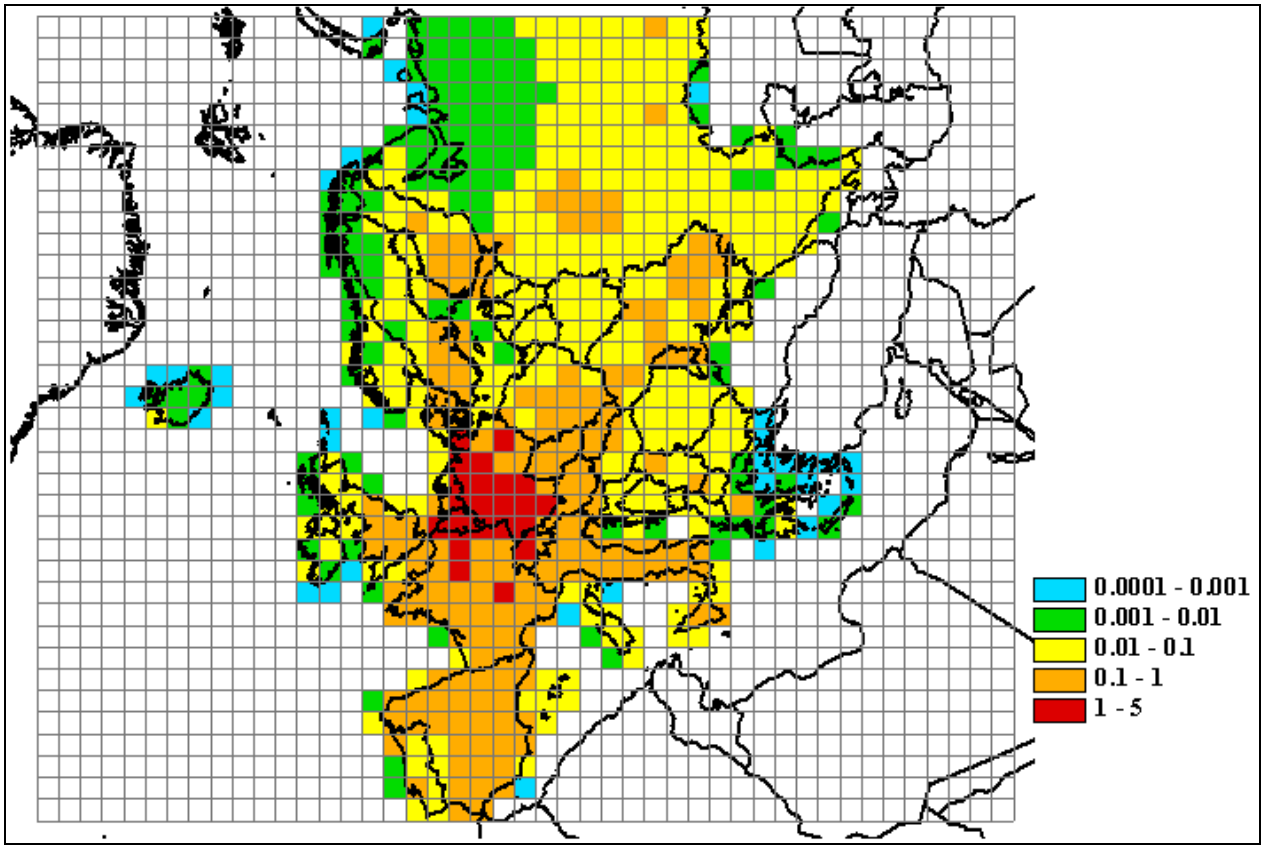

Figure 2.1. PCB emission spatial distribution in 1990, t/yr.

PCBs as a group of substances includes 209 congeners. At this stage, from these 209 the following 7 congeners: PCB 28, 52, 101, 118, 138, 153 and 180 were chosen for modelling. They cover wide range of physical-chemical properties of whole group (see *Annex B*). Model calculations were performed for the above 7 congeners. For these very isomers the greatest amount of measurement data are available for model verification.

The analysis of technical mixtures containing PCBs Aroclors 1016, 1242, 1254, 1260 and Clophens A30, A40, A50, A60 showed that on the average for these mixtures the input (in weighted %) of these isomers is: 3,5, 3.8, 3.8, 3.0, 2.9, 4.1, 1.6 [*Schulz et al*., 1989]. The total contribution of these seven isomers to the composition of the technical mixtures in question is on the average 23 weighted per cent (range 13 - 33). It is consistent with data of *A.Baart et al*. [1995] who estimated this value as 25% (range 10 - 40) as well as with estimates provided in [*Boström and Tuija,* 1997].

These reasons allowed to work out different scenarios for calculations and comparison with measurements. The calculations was made both with total PCB emission as well as for distinct PCB congeners in accordance to their contributions to the total emissions (see Chapter 3 for details).

2.1.2 Polycyclic aromatic hydrocarbons

Official emission data on polycyclic aromatic hydrocarbons (PAHs) at least for one year during the period 1990-97 were submitted by 19 countries. These data are presented in table 2.2. Denmark, Hungary, the Netherlands and Poland submitted emissions of Borneff 6 PAHs. The rest of countries submitted the total PAH emission without indication which species were included to the inventory.

Table 2.2. PAH emission data, t/yr.

Country	UN/ECE reported official emission data (data provided by MSC-W in April 1999)							
	1990	1991	1992	1993	1994	1995	1996	1997
Austria					477.4	518	539	519
Belgium [a]	350.733			291.777		308.141		
Bulgaria	677.32 B[a]P=17					521.43	487.51	364.3
Croatia							25.542	25.185
Denmark [b]					37.202			33.237
Finland						556		
France	3480							
Germany	420							
Hungary [b]	132.33	121.62	86.87	80.71	72.34	67.62	63.25	
Lithuania								71.283
Luxembourg					1093	638	732	
Moldova			0.120	0.052	0.073	0.179	0.062	0.220
Netherlands [b]	172	163	156	149	139	128	109	
Norway						172	167	
Poland [b]	372					536	523	
Russian Federation	14.7	13.5	12.5	12.4	12.7	12.8	12.5	12.5
Slovakia	77.8					30.1		29.4
Sweden	182		153			153		
United Kingdom	1072.19	1063.82	983.29	909.79	820.67	764.98	730.24	

[a] Figures for 1995 are totals for Flanders and Wallonia; figures for other years are totals for Flanders only

[b] 6 Borneff PAHs (fluoranthene, benzo[a]pyrene, benzo[b]fluoranthene, benzo[k]fluoranthene, benzo[ghi]perylene, indeno[1,2,3-cd]pyrene)

According to the protocol on persistent organic pollutants for PAH emission inventory four indicative compounds are used: benzo[a]pyrene, benzo[b]fluorantene, benzo[k]fluorantene and indeno[1,2,3-cd]pyrene.

Model calculations of PAH transboundary transport were made on the example of benzo[a]pyrene. At this stage, emission expert estimates 6 Borneff PAHs for 1990 were used [*Berdowski et al.*, 1997]. To estimate the fraction of B[a] emission we used the approach taken from *A.Baart et al.* [1995]. On the average for Europe this contribution is 8%. For countries which submitted the official data on 6 Borneff PAHs for 1990 official data were

used, for the rest of countries - 6 Borneff PAH emission estimates [*Berdowski et al.,* 1997]. In this case the total emission of benzo[a]pyrene within the EMEP grid was about 1250 tonnes. The results obtained are presented in table 2.3.

Table 2.3. Benzo[a]pyrene emissions in 1990, t/yr.

Country	Emission of 6 Borneff PAH in 1990 [a]	Official PAH emission data for 1990	B[a]P, % of 6 Borneff PAH [b]	B[a]P emission in 1990 used in calculations
Albania	35.8		6	2
Austria	243		10	24
Belarus	191		9	17
Belgium	818		8	65
Bosnia & Herzegovina	47.8		8	4
Bulgaria	54.9	17 (B[a]P)		17
Croatia	54		8	4
Cyprus	0.182		8	0
Czech Republic	259		10	26
Denmark	76.7		6	5
Estonia	28		9	3
Finland	104		8	8
France	3479		9	313
Germany	420		8	34
Greece	153		7	11
Hungary	192	132.33 [c]	8	11
Iceland	6.35		8	0.5
Ireland	73.7		8	6
Italy	694		7	49
Latvia	38.4		9	3
Lithuania	52.3		9	5
Luxembourg	6.24		8	0.5
Netherlands	184	172 [c]	8	14
Norway	140		8	11
Poland	372	372 [c]	10	37
Portugal	138		7	10
Republic of Moldova	58		9	5
Romania	723		10	72
Russian Federation	1938		9	174
Slovakia	310		10	31
Slovenia	50.5		8	4
Spain	521		6	31
Sweden	282		7	20
Switzerland	96.1		12	12
The FYR of Macedonia	21.7		8	2
Ukraine	1137		9	102
United Kingdom	1437		7	101
Yugoslavia	172		8	14

[a] [*Berdowski et al*., 1997] [b] [*Baart et al*., 1995] [c] 6 Borneff PAHs

Gridded emissions of benzo[a]pyrene with spatial resolution 150×150 km^2 are presented in figure 2.2.

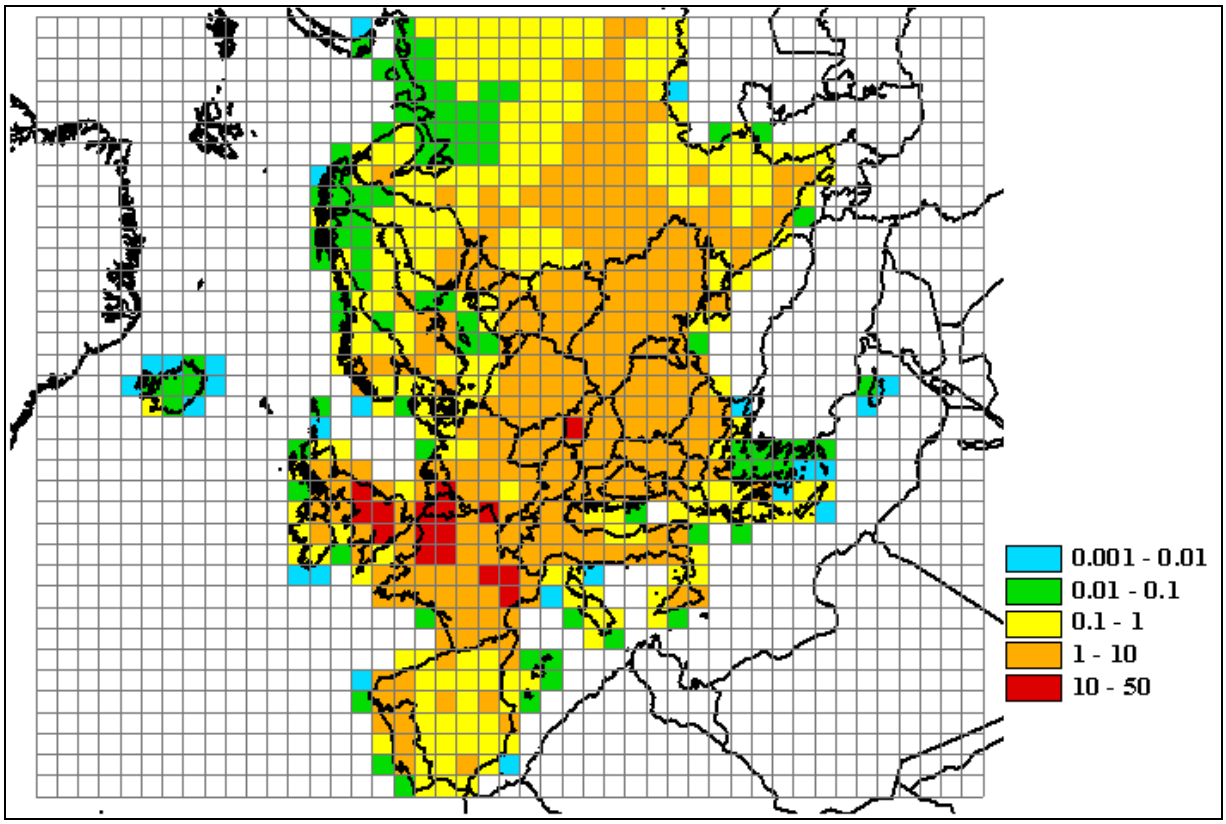

Figure 2.2. Spatial distribution of benzo[a]pyrene emissions in 1990, t/yr.

2.1.3. Dioxins/furans

Official data on dioxins/furans emissions at least for one year during the period 1990-97 were submitted by 21 countries. These data are presented in table 2.4.

In model calculations official emission data for 1996 or official data for previous years were used. For countries for which no official data were available estimates on dioxins/furans emission for 1990 [*Berdowski et al.*, 1997] were used. Total dioxins/furans emission within the EMEP grid was about 9 kg I-Teq.

Spatial distribution of dioxins/furans emissions over the EMEP grid with gridsize 150×150 km^2 is presented in figure 2.3.

In this report three main types of sources of dioxins and furans emissions to the atmosphere are considered: organic fuel combustion, waste incineration, and secondary non-ferrous treatment. These sources amount to 60% of the total input of PCDD/Fs.

Emissions from these source categories were studied in view of their contribution to the total toxicity of a mixture of individual compounds from PCDD/F family.

Table 2.4. Emission data on dioxins/furans, g I-Teq /yr.

Country	Emission used in calculation [a]	UN/ECE reported official emission data (data provided by MSC-W in April 1999)							
		1990	1991	1992	1993	1994	1995	1996	1997
Albania	12.1								
Austria	28.7					28.6 [c]	30.9 [c]	30.8[c]	30.7
Belarus	106								
Belgium [b]	426	441					426		
Bosnia&Herzegovina	7.13								
Bulgaria	340.935	554.196					456	340.935	309.576
Croatia	97	95						97	95.04
Cyprus	1.02								
Czech Republic	224								
Denmark	15					15			20
Estonia	17.7								
Finland	155						155		
France	1640	1640							
Germany	307	1196					307		
Greece	25.4								
Hungary	105.22	180.58	159.67	121.77	120.98	114.9	113.51	105.22	
Iceland	0.553								
Ireland	43.9								
Italy	772	772							
Latvia	13.5								
Lithuania	23.0								5.805
Luxembourg	16					23	16	16	
Netherlands	60.7	618	537	515	384	143	74.2	60.7	
Norway	125						125	0.105[c]	
Poland	351	359					368	351	
Portugal	17.4								
Republic of Moldova	22.7								
Romania	1500								
Russian Federation	1019	1200 [c]							
Slovakia	43	495.9 [c]					653.4[c]		464.5
Slovenia	5.99								
Spain	133.8	133.8							
Sweden	33	58-127			19-46				
Switzerland	172	242	230	217	203	192	181	172	161.6
The FYR of Macedonia	4.90								
Ukraine	877								
United Kingdom	427.31	960	943.39	922.12	884.19	786.87	660.02	412.47[c]	218.13
Yugoslavia	112								

[a] Emission estimates for 1990 according to [*Berdowski et al.*, 1997], in dashed cells official data used in calculation

[b] Figures are totals for Flanders; totals for Wallonia are included only in 1995

[c] official data provided when model calculations were finished

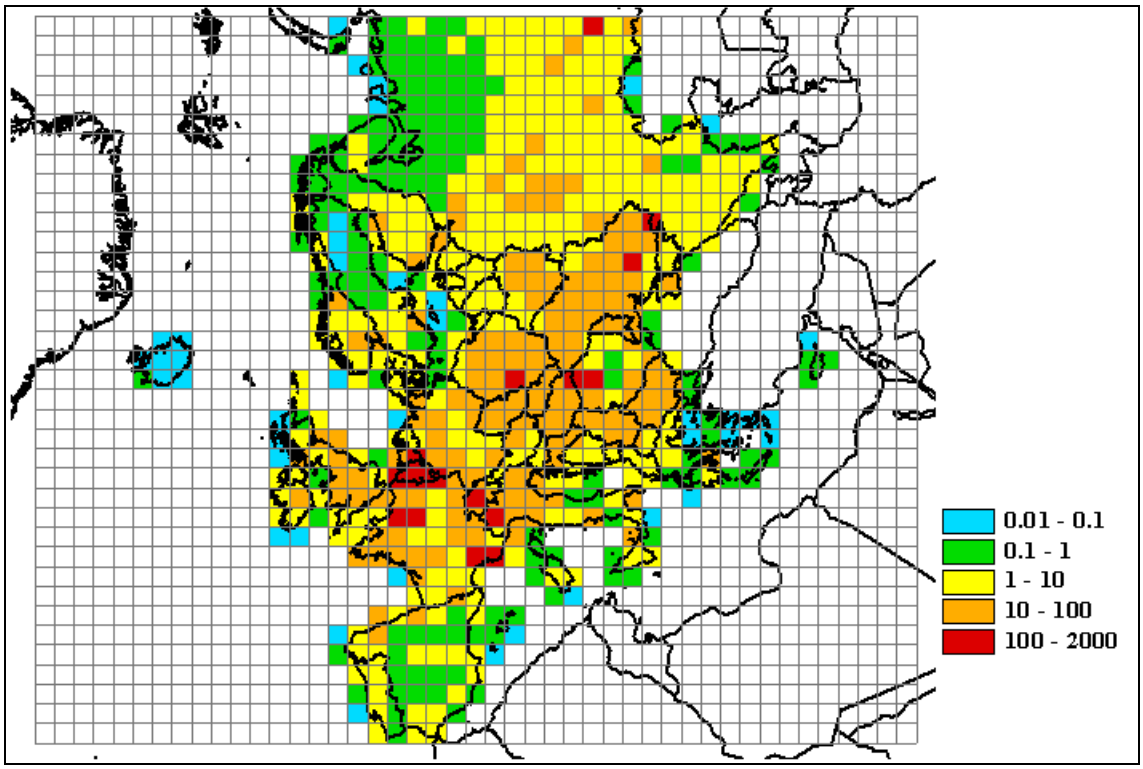

Figure 2.3. Spatial distribution of dioxins/furans emissions, g I-Teq /yr.

On the basis of literature data averaged profiles of homologous group for each source category were formed, most significant homologous groups in view of their input to total toxicity were determined, and 2,3,7,8-substituted congeners were selected because of their role in the formation of the toxicity of this group. The investigation results are planned to be published as a separate report.

The priority homologous groups were PeCDF, HxCDF and PeCDD. Their total contribution to PCDD/F mixture toxicity at the source outlet is 75% for organic fuel combustion, 75% for waste incineration and about 90% for secondary non-ferrous metal treatment.

In the selected groups seven compounds with substitutions in positions 2,3,7,8 are toxic Toxic congeners in the selected group and their toxicity coefficients in the international system of toxicity coefficients are presented in table 2.5.

PCDD/F toxicity distribution with homologous groups and toxicity inside a homologous group is illustrated in figure 2.4.

Table 2.5. Toxicity coefficients of 7 congeners of PeCDF, HeCDF and PeCDD

Homologue group	Congeners, determining toxicity	Toxicity coefficient
PeCDF	1,2,3,7,8 – PeCDF	0.05
	2,3,4,7,8 – PeCDF	0.5
HeCDF	1,2,3,4,7,8 –HeCDF	0.1
	1,2,3,6,7,8 – HeCDF	0.1
	1,2,3,7,8,9 – HeCDF	0.1
	2,3,4,6,7,8 – HeCDF	0.1
PeCDD	1,2,3,7,8 – PeCDD	0.5

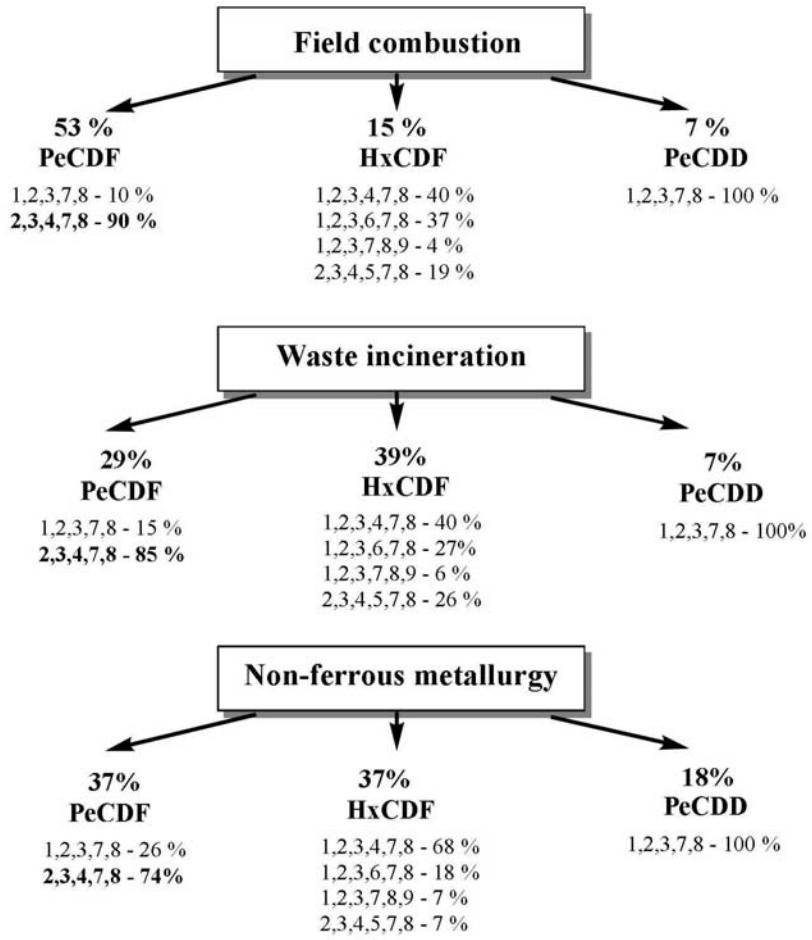

Figure 2.4 PCDD/F toxicity distribution with homologous groups and toxicity inside a homologous group

PeCDF group contributes half of toxicity of emissions from "Fuel combustion" sources and one third from other two types of sources. The main cogener forming the toxicity of this group is 2,3,4,7,8-PeCDF. Therefore it was chosen for provisional modelling of the transboundary transport. The calculations were made on the basis of total PCDD/F emission and physical-chemical properties of 2,3,4,7,8-PeCDF.

2.1.4 Lindane

In calculations of lindane transboundary transport expert emission estimates made under UBA project [*Berdowski et al.,* 1997] were used (table 2.6). In figure 2.5 spatial distribution of lindane emissions over the EMEP grid with spatial resolution 150×150 km^2 for 1990 is shown. Total lindane emission within the EMEP grid for 1990 was 1307 tonnes.

Table 2.6 Lindane emission estimates for 1990 [*Berdowski et al*., 1997]. Units: t/yr.

Country	Emissions	Country	Emissions	Country	Emissions
Albania	3.50	Germany	---	Poland	0
Austria	13.3	Greece	19.4	Portugal	4.40
Belarus	47.2	Hungary	0.300	Romania	51.4
Belgium	54.3	Iceland	0	Russian Federation*	348
Bosnia&Herzegovina	6.23	Ireland	0.900	Slovakia	0.090
Bulgaria	0	Italy	44.9	Slovenia	1.23
Croatia	11.0	Latvia	13.6	Spain	0
Cyprus	---	Lithuania	25.1	Sweden	0
Czech Republic	0.210	Luxembourg	0	Switzerland	0.800
Denmark	3.80	The FYR of Macedonia	0.760	Ukraine	265
Estonia	7.45	Republic of Moldova	13.2	United Kingdom	114
Finland	8.80	Netherlands	15.0	Yugoslavia	18.6
France	211	Norway	4.10	TOTAL:	1307

* within the EMEP grid

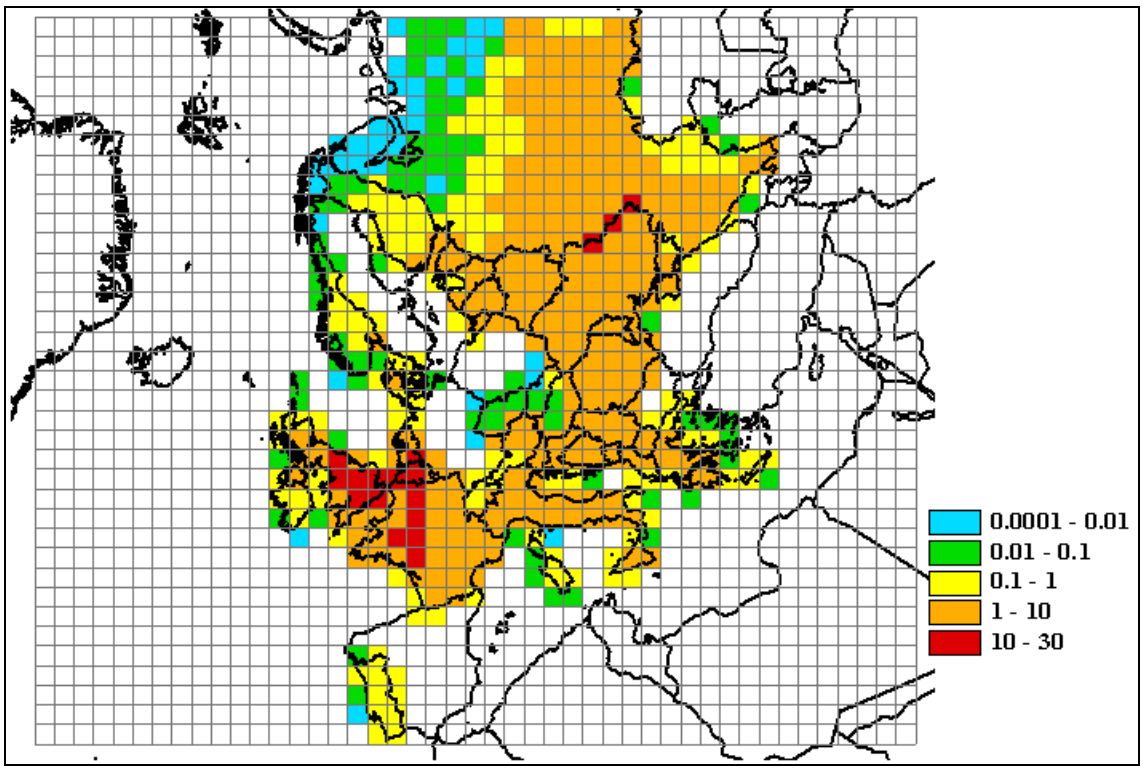

Figure 2.5. Spatial distribution of lindane emissions in 1990. Units: t/yr.

2.2. *Emission distribution with height*

At present no official information on emission distribution with height (below 100 m and above 100 m) is available. It is possible, however, to make certain assumption on the height distribution using per cent contribution to the total emission of different source categories:

2.2.1 Polychlorinated biphenyls

About 90 % of PCB emissions are due to the leakage of various mixtures containing PCBs from electrical installations. Therefore it can be assumed that 100% of PCB emission enters the atmosphere below 100 m.

2.2.2 Polycyclic aromatic hydrocarbons

According to *J.J.M.Berdowski et al*. [1997] the per cent input of different sources to total 6 Borneff PAH emissions on the average in Europe is: fuel combustion for heat generation by small stationary sources - 42%, wood preservation - 31%, mobile sources - 11%, ferrous metal production - 4%, non-ferrous metal industry - 6%, other sources - 6% [*Berdowski et al.,* 1997]. Reasoning from these data it was assumed that about 90% of emission enters the atmosphere below 100 m.

2.2.3 Dioxins/furans

Per cent contribution of various sources to the total emission of dioxins and furans in Europe on the average is: fuel combustion by stationary sources for electricity and heat generation - 38% (category SNAP 01 - 5%, category SNAP 02 - 22 %, category SNAP 03 - 11 %), ferrous metal production - 17%, non-ferrous metal industry - 14%, waste incineration - 24%, other sources - 7% [*Berdowski et al*., 1997]. On the basis of these data it can be assumed that about 30% of the emission enters the atmosphere above 100 m and 70% - below 100 m.

2.2.4 Lindane

Taking into account the character of lindane application it was assumed in calculations that 100% of lindane emissions enters the atmosphere below 100 m.

2.3. *Temporal variability of emissions*

2.3.1 Polychlorinated biphenyls

It was assumed that PCB emissions due to the leakage from electrical equipment take place uniformly round the year. Since it is the main source of the direct emission to the atmosphere it was assumed that it is independent of a season.

2.3.2 Polycyclic aromatic hydrocarbons

Temporal variation of B[a]P emissions to the atmosphere in model calculations was taken as in the work of *A.Baart et al*. [1995] during heating period (from October to March) - 60% of the total emissions and from April to September - 40% (variation amplitude - 20%).

2.3.3 Dioxins/furans

For a simplified estimate of seasonal variations of dioxins/furans emissions we used temporal factors of LOTOS [*EMEP/CORINAIR,* 1996] and the input of different source categories to total European emission [*Berdowski et al*., 1997]. The variation amplitude is about 10% with maximum emissions in winter.

2.3.4 Lindane

Temporal variation of lindane input to the atmosphere was presumed to be the same as in [*Jacobs and van Pul,* 1996]. It was taken that 10% of lindane was emitted in February, 15% - in March and by 25% - in April-June each.

2.4. *Uncertainties of emission estimates*

The uncertainties of PCB, PAH, dioxins/furans emissions is conditioned by a number of factors: limited number of emission factors, uncertainty of data on kinds of activity, scarce information on emission composition etc.

According to *J.J.M.Berdowski et al*. [1997] uncertainty PCB and PAH emission factors is within the range of 2-5. The uncertainty of dioxins/furans emission factors is greatest and lies in the range 5-20.

Chapter 3

Modelling results

The Centre has made a series of provisional calculations for selected POPs. The calculation results allowed us to assess the input of individual processes of POP transport and accumulation in different environmental compartments, to make provisional evaluation of their depositions and concentrations using available emissions of these species. Below in this chapter, calculation results of selected POPs (PCBs, B[a]P, 2,3,4,7,8-PeCDF and lindane) and their analysis are discussed.

3.1. *PCB modelling*

Provisional results of PCB modelling presented in the last year report were performed on the basis of properties of PCB-153 as an indicative congener. The refinement of properties of individual PCBs made it possible to select model parameters for 7 congeners - 28, 53, 101, 118, 138, 153, 180. In this section modelling results for the selected PCB congeners are discussed.

The description of physical-chemical properties of these congeners is presented in Annex B. Data on emissions for 1990 with their spatial distribution within the EMEP grid are considered in chapter 2. The calculation results for 7 congeners and PCB-153 as an indicator compound are presented below.

3.1.1. Modelling of transport of selected PCBs with allowance for gas/particle partitioning

For convenience of the comparison the same emission equal to a seventh of total emission for 1990 were prescribed for each congener. For initial conditions it was assumed that original concentrations in all compartments were equal to zero. Degradation in air is assumed to be constant in time for each congener. Degradation coefficients for individual congeners are taken from the handbook [*Mackay et al.,* 1992].

Figure 3.1 shows mass balance diagrams for each congener and for seven congeners after one year. Mass balance is calculated for the whole calculation grid 45×37 cells. The mass balance contains: the mass in soil (accumulated and degraded); the mass in sea (accumulated and degraded); the mass degraded in air; the mass transported outside the grid (through lateral and upper boundaries) and the mass remained in air by the end of integration.

As evident from the diagrams different PCB congeners have different degradation rates in air and different depositions velocities on the underlying surface. For instance, PCB-28 has the highest degradation rate in air and the least velocity of deposition on the underlying surface whereas PCB-180 has the least rate of degradation in air and the highest velocity of deposition on the underlying surface.

It should be mentioned that degradation rate of different PCB congeners in air is mainly determined by half-life of the gas phase. For example, half-life of PCB-28 is 71 day, PCB-180 - 229 days. Besides a substantial fraction of PCB-180 is present in the atmosphere in the aerosol phase and its degradation is not calculated whereas PCB-28 occurs in the atmosphere mainly in the gas phase. This is the reason for the difference in degraded masses in air for these congeners.

Deposition velocity on the underlying surface depends both upon physical-chemical properties of PCB-congeners and on gas/particle partitioning.

The degree of solubility in precipitation of the gas phase of all PCB congeners is very weak due to their hydrophoby. Washout ratio of the aerosol phase taken in calculations to be 4×10^4 is so significant that wet scavenging of the aerosol phase makes an appreciable contribution to total deposition on the underlying surface. In the same way dry deposition velocity of the gas phase on soil (gas-exchange) is very low for all PCB congeners whereas the aerosol phase deposition velocity determined by particle deposition velocity is sufficiently high. Therefore the aerosol phase makes an appreciable contribution to total PCB depositions on soil. For example, total depositions of PCB-28 on soil after 1 year was 2% of annual emissions, PCB-180 - 29%.

Thus, the calculation results indicated that the difference in physical-chemical properties of PCB congeners appreciably affect the total mass balance.

Each element of total mass balance (balance of the sum of 7 congeners) in figure 3.1 is the integrated mass of 7 congeners for a given element relative to total annual emissions of the 7 PCB congeners. Obviously individual congeners makes different contribution to each element of the total mass balance.

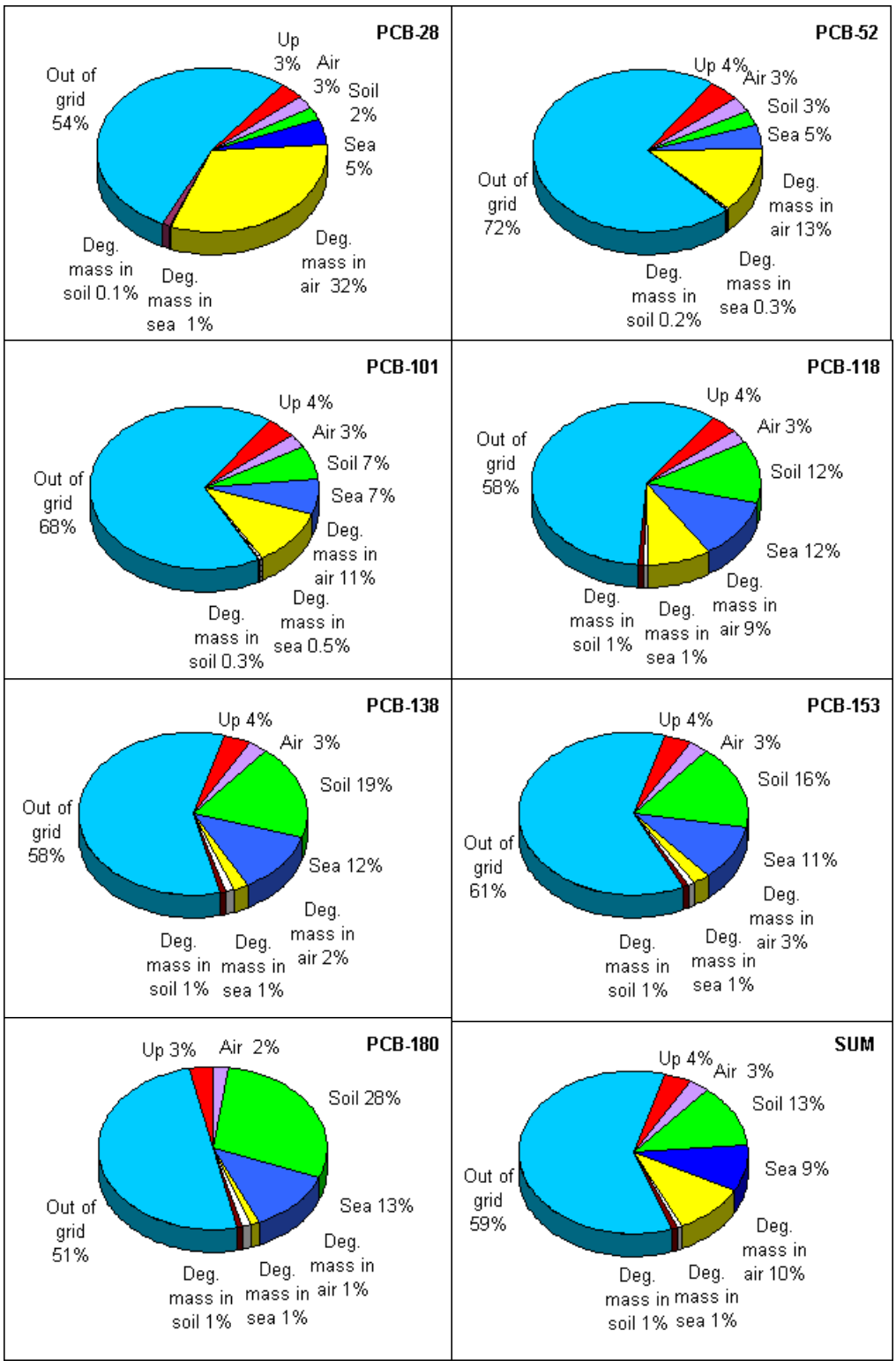

Figure 3.1. Mass balance of each congener and of all seven congeners for 1996

Figure 3.2 shows relative contributions of each PCB congener in these elements, namely to masses accumulated in compartments, degraded in them or transported outside the grid under the condition of equal emissions for all congeners.

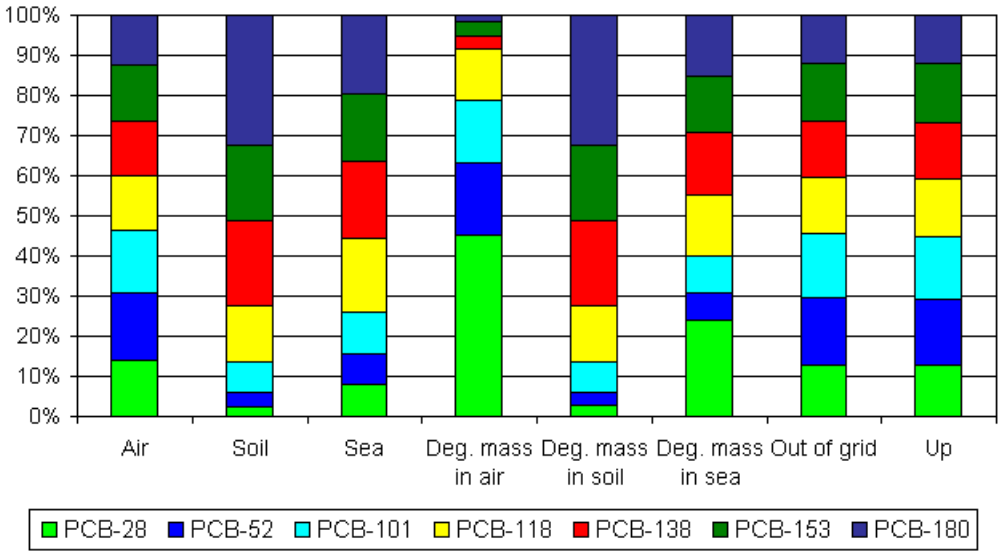

Figure 3.2. Contribution of individual PCB congeners to mass balance elements for 1996

As seen from figure 3.2 contributions to some elements of the total mass balance for diagram of seven congeners is actually the same. Such elements are the transport outside the grid through lateral and upper bounds and the remained matter in the atmosphere by the end of integration. The input of different congeners to other mass balance elements is essentially different. These elements are: the mass in soil and sea and the mass degraded in the atmosphere, soil and sea.

The main contribution to the mass in soil makes PCB-180 whereas the contribution of PCB-28 and PCB-52 is very small.

Contributions of PCB congeners to the mass in sea differ to a less extent. It is connected with the fact that over land dry and wet depositions of the aerosol phase predominate, whereas over sea dry deposition flux of the gas phase is more significant.

Contributions of different congeners to degradation in air differ drastically. The principal contribution makes PCB-28 whereas contribution of PCB-138, 153 and 180 is very low.

In figure 3.2 the contribution of each PCB congener to elements of the total mass balance is presented. Except for degradation in air the input of different congeners to soil and sea are the most important diagram elements. The input to sea takes place due to four processes: gas phase dry deposition, aerosol phase dry deposition, gas phase wet deposition and wet deposition of the aerosol phase. Figure 3.1 presents data on the input of the congeners to soil and sea (namely, sum of mass in soil/sea and degradation in soil/sea). However, neither figure 3.1 nor 3.2 contain information on the processes responsible for this input. This information manifested in figure 3.3.

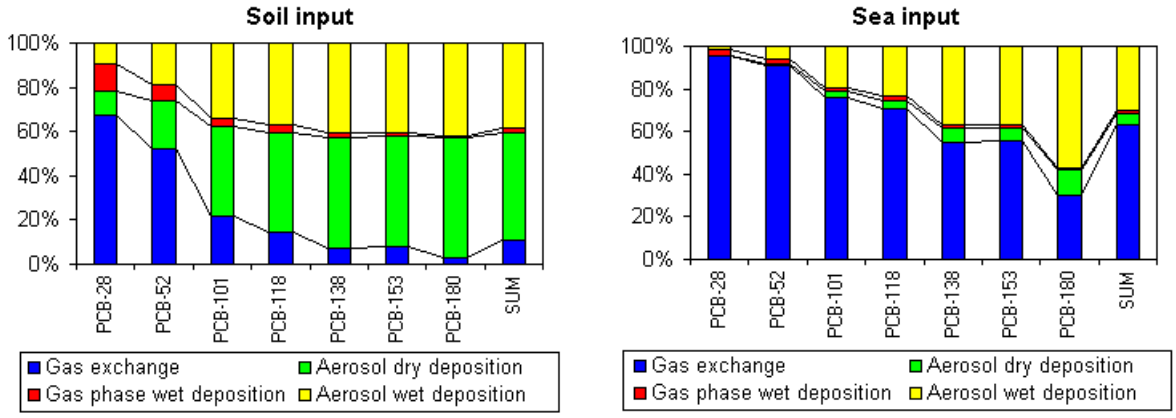

a **b**

Figure 3.3. Input of dry deposition of the gaseous and aerosol phase and wet deposition of the gaseous and aerosol phase to total deposition over land (a) and over sea (b) for 1996

Figure 3.3 depicts fractions of inputs to soil (a) and sea (b) due to gas phase dry deposition, aerosol phase dry deposition, gas phase wet deposition and aerosol phase wet deposition for each congener and for seven congeners.

As seen from figure 3.3 each of four mechanisms mentioned makes different contributions of different congeners to depositions on sea and land.

For low chlorinated PCB (for example, PCB-28) maximum contribution to total depositions on land makes the process of gas phase dry deposition (gas exchange between the atmosphere and soil) as to high chlorinated PCB (for example, PCB-180) the maximum contribution results from dry and wet deposition of aerosol.

In regard to total depositions on sea gas phase dry deposition (gas exchange between the atmosphere and sea) is essential for all the congeners. For high chlorinated PCB the fraction of dry and wet depositions of the aerosol phase increases over sea.

Analysing figure 3.3 the following conclusions can be drawn:

- The fraction of gas phase wet deposition of all the congeners both over sea and land is negligible compared to other processes of deposition on the surface due to poor solubility of PCB gas phase in precipitation.

- Gas exchange flux over sea makes more essential contribution than the gas exchange flux over soil for all the congeners.

- Dry deposition flux of the aerosol phase for all the congeners over land makes a substantial contribution to total depositions whereas its contribution to total depositions on sea is insignificant.
- In the input to soil of PCB-28 and PCB-52 the flux of gas phase dry deposition predominates. For other congeners the input to soil is defined by dry and wet deposition

of the aerosol phase. It is worth mentioning that the higher is PCB chlorination degree the less is the contribution of the gas phase to total depositions over soil.

- Maximum input of PCB congeners (but PCB-180) to sea makes dry deposition of the gas phase. With the increase of PCB chlorination degree the contribution of the aerosol phase (in particular their wet deposition) increases.

Figure 3.4 shows the contribution of each PCB congener to dry and wet depositions of the gas and aerosol phase over land (a) and over sea (b). Separate averaging for all sea and soil cells is made. The deposition of all seven congeners are taken for 100%.

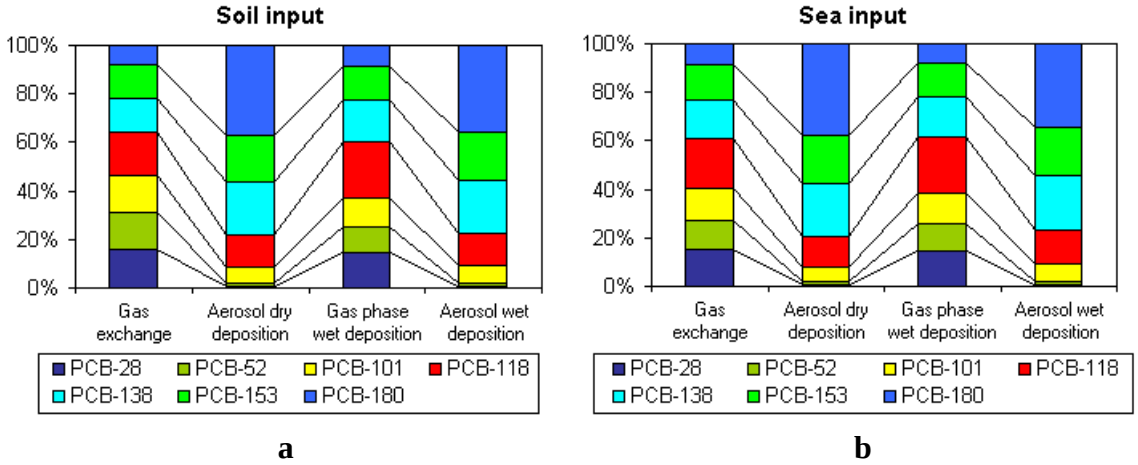

a **b**

Figure 3.4. Contribution of individual PCB congeners to dry deposition of the gas and aerosol phases and wet deposition of gas and aerosol phase over land (a) and over sea (b) for 1996

As evident from figure 3.4 each congener contributes from 8 to 20% to the total dry deposition of the gas phase both over sea and over land (gas exchange in the figure) (dry deposition of the gas phase is meant as the net gas flux with allowance for re-emission). This difference is explained both by different gas phase fractions of different PCB and their different physical-chemical properties.

As it follows from calculation results the maximum input to dry deposition of the gas phase makes PCB-118 (18% over land and 20% over sea) and minimum - PCB-180 (8% over land and 9% over sea). The contribution to gas phase wet deposition varies from 8% for PCB-180 to 23% for PCB-118 both over land and over sea.

The fact that dry and wet deposition of PCB-118 gas phase appeared to be maximum, even higher than dry and wet deposition of such congeners as PCB-28, 52, 101, can be explained by the competition of two phenomena: the content of the PCB gas phase in the atmosphere and the ability of the gas phase to be deposited on the underlying surface due to dry and wet deposition. For example, at the essential content of PCB-118 gas phase in the atmosphere it is better dissolved and has better sorption capability in soil than PCB-28, 52, 101.

Inputs of dry deposition of the aerosol phase differ greatly for different PCB congeners. This difference is conditioned mainly by gas/particle partitioning since aerosol phase dry deposition velocities are taken to be equal for all the congeners and they depend only on ambient conditions (wind speed, roughness, length). The input of PCB-28 is minimum amounting to about 0.5%. The contribution of PCB-180 is maximum amounting to about 37%.

Contributions of the aerosol phase wet deposition is also defined only by gas/particle partitioning since the parameter of aerosol phase washout is assumed to be constant for all the congeners and it is equal to 4×10^4. The fraction of PCB-28 in wet depositions of the aerosol phase is minimum and it equals 0.6% (over land and sea) and the fraction of PCB-180 is maximum and it is about 35% over land and over sea.

Figure 3.5 presents gas exchange fluxes over land (a) and over sea (b) for all seven congeners. Separate averaging for all sea and soil cells is made.

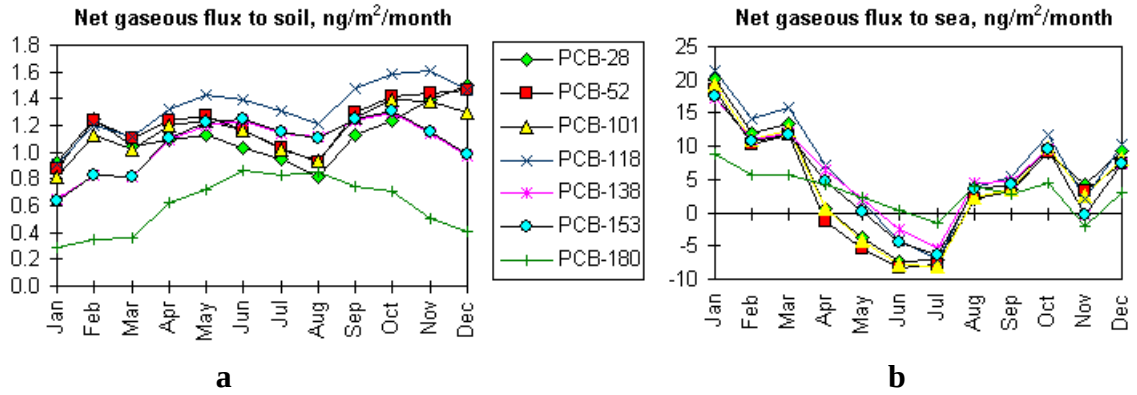

a **b**

Figure 3.5. Gas exchange flux over land (a) and over sea (b) for different congeners PCB for 1996, ng/m^2/month

As seen from figure 3.5 the gas exchange flux over sea appreciably exceeds the flux over land for all congeners in spite of the fact that the concentration over sea is considerably less than over soil due to remoteness from emission sources.

During the year the flux over soil is positive (it is directed from the atmosphere to soil) for all congeners. Gas exchange flux variation over land is slightly pronounced due to two competing processes: the decrease of gas exchange flux with temperature increase in summer months and the increase of the gas phase in the atmosphere during summer.

The gas exchange flux over sea is positive and directed from the atmosphere to sea during cold months and it is negative and directed from sea to the atmosphere during warm months. Re-emission flux of PCB-28, 52 and 101 is maximum from May to August. Re-emission flux of PCB-118, 138 and 153 is 2-3 times lower and it is observed from June to August. PCB-180 re-emission flux is minimum because of a small content of the gas phase.

Figure 3.6 presents seasonal variations of the aerosol phase dry deposition flux over land (a) and over sea (b) for 7 congeners considered.

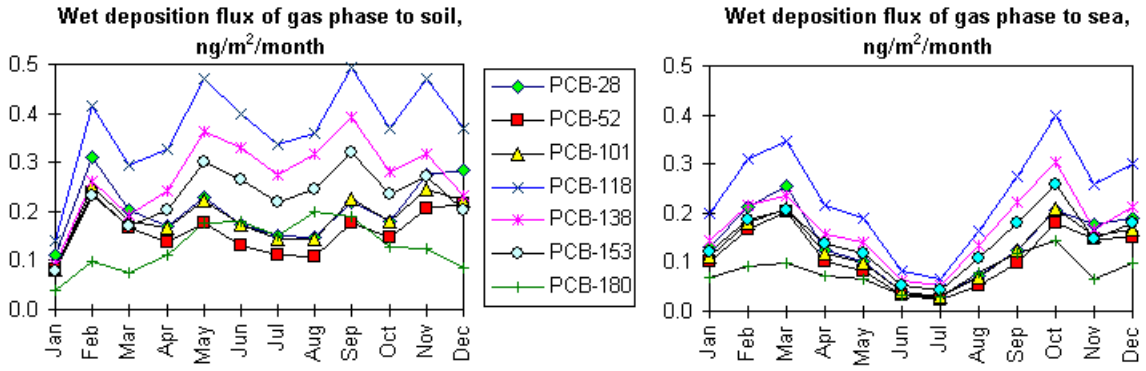

Figure 3.6. Dry deposition flux of the aerosol phase over land (a) and over sea (b) for different PCB congeners for 1996, ng/m^2/month

For PCB congeners, which appreciable part is associated with particles, the deposition flux of the aerosol phase exceeds considerably the flux of gas exchange between air and soil (for example, aerosol phase dry deposition flux of PCB-180 is higher then as much as 10 times that of the gas flux).

Dry deposition flux of the aerosol phase is essentially less over sea, than over land at the same time it is appreciably lower than the flux of gas exchange between the atmosphere and sea.

Figures 3.7 and 3.8 demonstrate wet deposition fluxes of the gas phase (figure 3.7) and of the aerosol phase (figure 3.8) over land (a) and over sea (b).

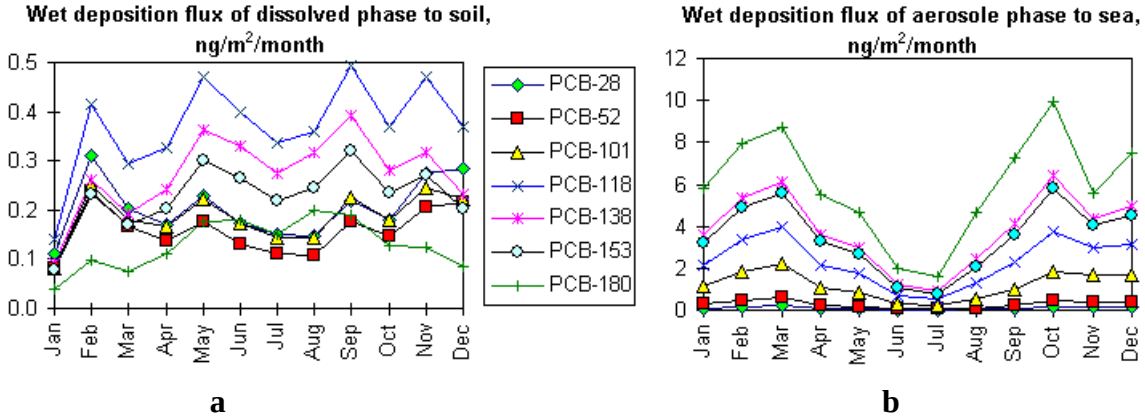

Figure 3.7. Gas phase wet deposition flux over land (a) and over sea (b) of different PCB congeners for 1996, ng/m^2/month

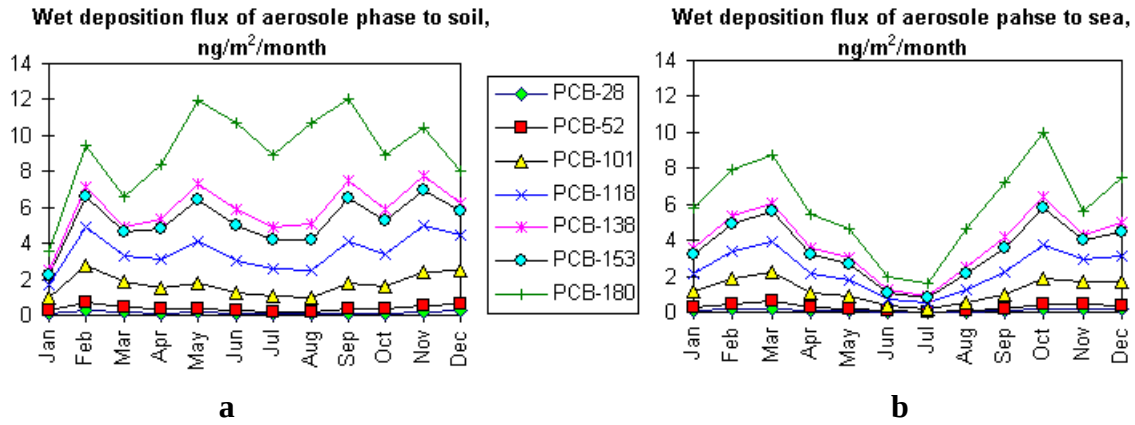

Figure 3.8. Wet deposition flux of the aerosol phase over land (a) and over sea (b) for different PCB congeners for 1996, ng/m^2/month

For the majority of congeners wet deposition fluxes of the aerosol phase both over land and sea are appreciably higher than wet deposition fluxes of the gas phase due to poor solubility of gaseous PCBs in precipitation. For PCB-28 and PCB-52, which occur in the atmosphere mainly in gas phase, these fluxes are comparable.

Modelling results of PCB with the consideration of the atmosphere/vegetation exchange will be described in the following sections.

3.1.2. Modelling of transport of selected PCBs with allowance for atmosphere/vegetation exchange

In order to assess the influence of physical-chemical properties of individual congeners on the atmosphere/vegetation exchange calculations for seven congeners for 1996 were carried out. Seasonal variations of air concentrations, dry and wet depositions caused by the integration of the exchange process with vegetation were evaluated.

Calculations were carried out without allowance for degradation in vegetation. It was assumed that emission of each congener was 4% of the total PCB emission within the EMEP grid in 1990 (see Section 2.1 *Emission data*). As it was mentioned in section 2.1 total emission over the EMEP area was 112 tonnes for 1990.

The calculated mass balance is shown in figure 3.9. It follows from the figure that the input of the exchange with vegetation is more important for high chlorinated PCB (PCB-118, 138, 153, 180) and less significant for low chlorinated PCBs (PCB-28, 52).

Here and below the "forest floor" means PCB mass in the defoliated plant material (leaves, needles, grass).

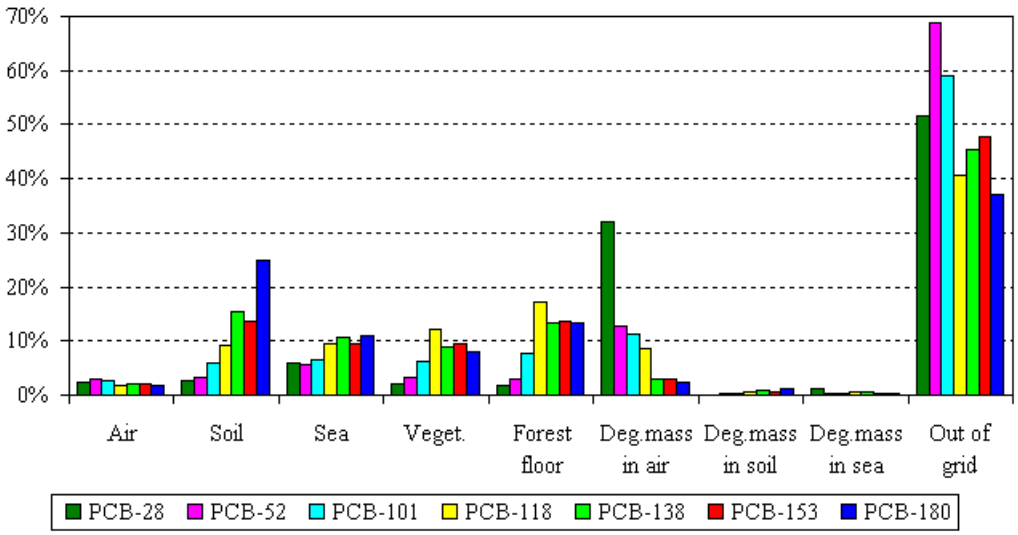

Figure 3.9. Mass balances obtained by modelling of the long-range transport of seven selected PCB congeners

For the fraction of substance accumulated in vegetation (including forest floor) a pronounced maximum is observed for PCB-118 with the decrease of accumulated substance both to the direction of lighter congeners and to heavier congeners. This dependence is explained by two factors at once: the fraction of a substance in the gas phase decreasing with the increase of congener chlorination degree (note that the model considers only interaction of pollutant gas phase with vegetation) and so-called bioconcentration coefficient, i.e. the ratio of concentrations of substance in air and vegetation. The smaller is coefficient the higher volatility of a substance, therefore the uptake by vegetation increases with chlorination degree.

Plots of PCB concentrations in vegetation and their content in the forest floor are demonstrated in figures 3.10 and 3.11.

These plots also confirm conclusions drawn from the consideration of mass balance: the exchange with vegetation is the most essential for PCB-118. It is worth noting that just PCB-118 is most toxic among selected seven congeners.

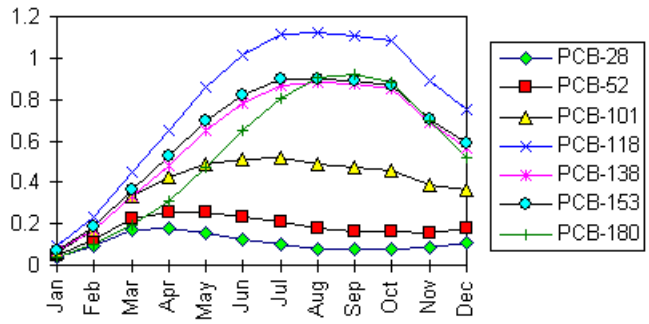

Figure 3.10. Concentration in vegetation, ng/g d.w.

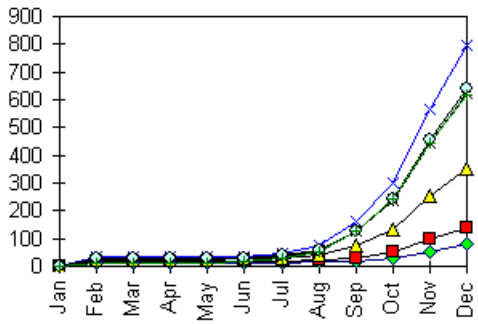

Figure 3.11. Content in the forest floor, kg

Consider dynamics of the flux to vegetation during modelling (see figure 3.12).

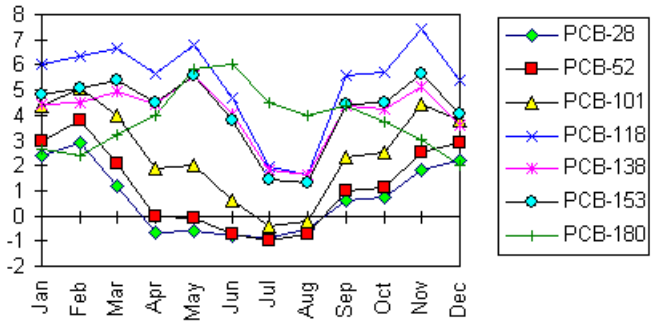

Figure 3.12. Flux to vegetation, ng/m^2/month

The plots show that vegetation can be a re-emission source of PCB-28, 52 and 110 during a year. The flux of other congeners remains positive during a year, decreasing in summer due to the increase of concentration in vegetation and decrease of bioaccumulation coefficient with temperature increase.

3.1.3. The evaluation of possibility of PCB transboundary transport modelling based on PCB-153 properties

Calculations for seven PCB congeners allowed us to evaluate possibilities to calculate the long-range transport of the total PCB mass using properties of PCB-153. For this purpose calculated values of concentrations and depositions obtained for PCB-153 were compared with means of corresponding values of seven congeners considered.

Figure 3.13 present PCB-153 seasonal air concentrations and mean value for seven selected congeners. As seen from the figure PCB-153 air concentration seasonal variations in principal repeat seasonal variations of mean concentrations of seven congeners and the maximum difference (in March) is 12%.

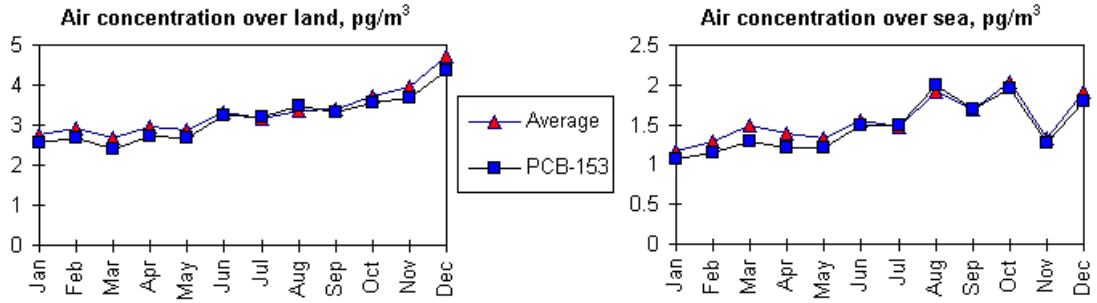

Figure 3.13. Air concentrations: mean for congeners and PCB-153, pg/m^3

Somewhat greater difference is observed for wet and dry depositions, concentrations in vegetation and the content in forest floor (see figures 3.14, 3.15 и 3.16).

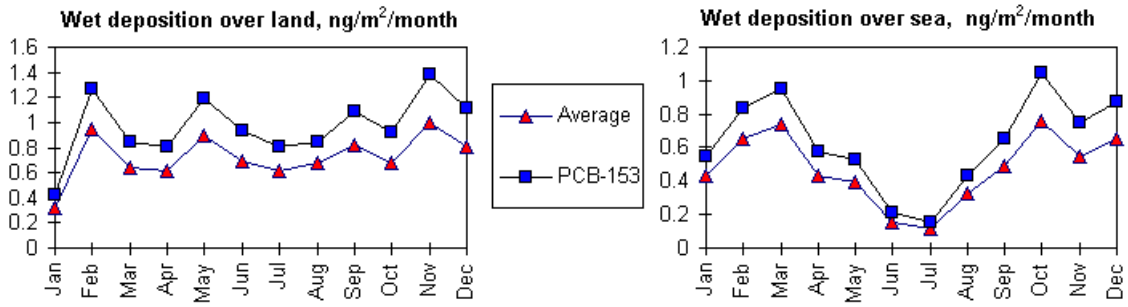

Figure 3.14. Wet deposition: mean for the congeners and PCB-153, ng/m^2/month

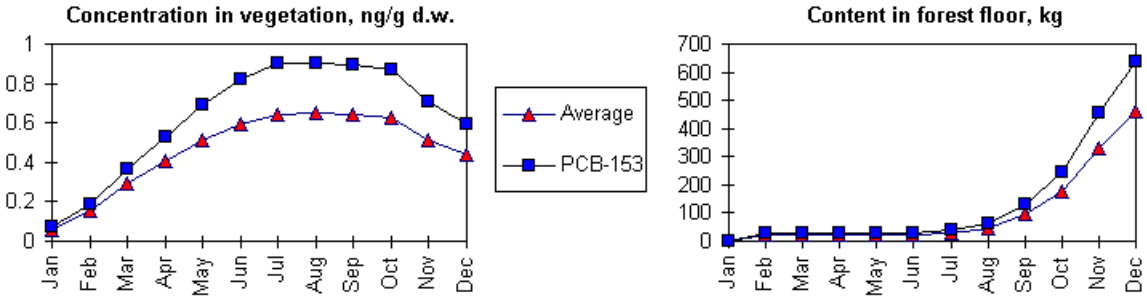

Figure 3.15. Dry deposition: mean for the congeners and PCB-153, ng/m^2/month

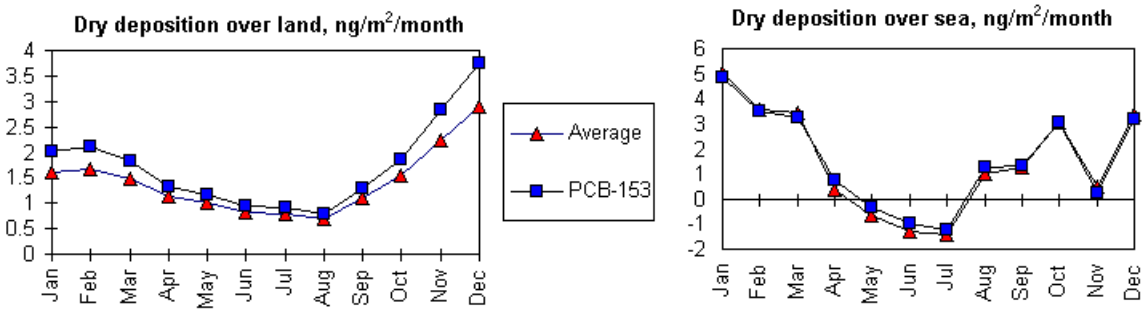

Figure 3.16. Concentration in vegetation (ng/g d.w.) and the content in forest floor (kg): mean for the congeners and PCB-153

In this case the difference is 30% - 40% for wet deposition and concentrations in vegetation and forest floor. Dry depositions differ within 25% - 30%.

At the same time like for atmospheric concentrations, seasonal variations of all the values considered for the sum of seven congeners are in a good agreement with seasonal variations of the same values for PCB-153.

The arguments set forth above manifest the limits within which it is possible to estimate the transport of PCB mixture using parameters of PCB-153.

3.1.4. Effect of the atmosphere/vegetation exchange on the example of PCB-153

In order to evaluate the impact of atmosphere/vegetation exchange process three variants of calculations of PCB-153 transport for 1996 were performed: without consideration of exchange with vegetation (variant 1), with consideration of the exchange with vegetation but neglecting the degradation in vegetation (variant 2) and with consideration of degradation process in vegetation (variant 3). The contribution of this process to the total mass balance was evaluated on the example of PCB-153. In these three variations it was supposed that PCB-153 emission was 4% of the total PCB emission in 1990. As it was mentioned in section 2.1 total emission of PCB was 112 tonnes in 1990. The mass balance for three variants is shown in figure 3.17.

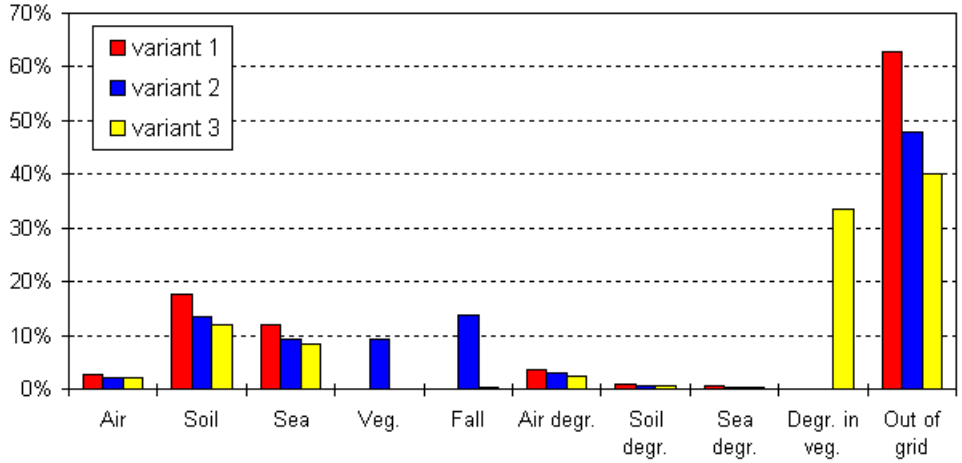

Figure 3.17. Atmosphere/vegetation exchange effect: PCB-153 mass balance

The figure indicates that the consideration of the atmosphere/vegetation exchange processes results in noticeable variations of the mass balance. The export outside the grid decreases substantially (about 60% in the first variant, about 50% - in the second one and about 40% - in the third variant). Vegetation, being an additional medium in the model, accumulates (possibly with the subsequent degradation) a large quantity of pollutant (about 25% of total emission for the variant without degradation and about 30% - with degradation). Another values affected noticeably by the atmosphere/vegetation exchange is pollutant content in soil and ocean water (with the consideration of the exchange process including degradation of pollutant content in soil decreases from 18% to 12% and in sea from 12% to 8%). Thus the exchange with vegetation can play an essential role in PCB long-range transport and parameters of this process need to be refined.

In order to see how the atmosphere/vegetation affects other parameters of the long-range transport let us consider the plot of air concentration seasonal variations and wet and dry deposition. The plots of air concentration seasonal variations are presented in figure 3.18.

It is evident that the character of the plot describing seasonal variations remained the same, air concentrations decreases by a factor of 1.5-1.6 when the atmosphere/vegetation exchange process is taken into account. The same is true for wet and dry deposition over sea and land presented in figures 3.19 and 3.20.

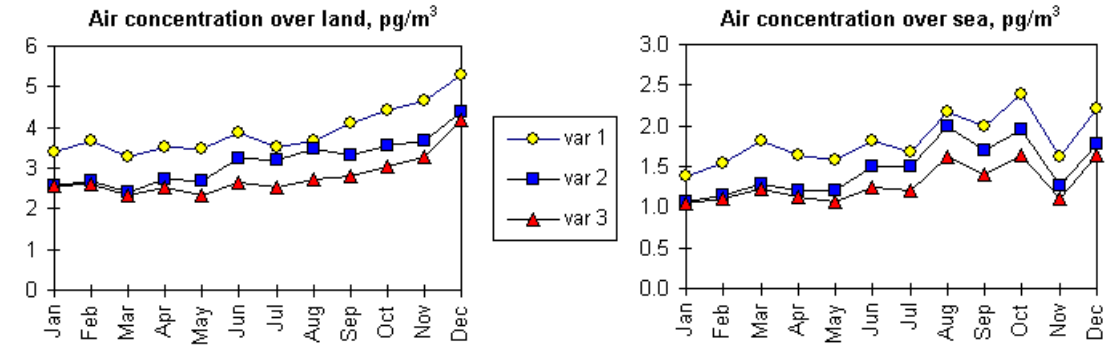

Figure 3.18. Effect of the atmosphere/vegetation exchange: PCB-153 air concentrations, pg/m^3

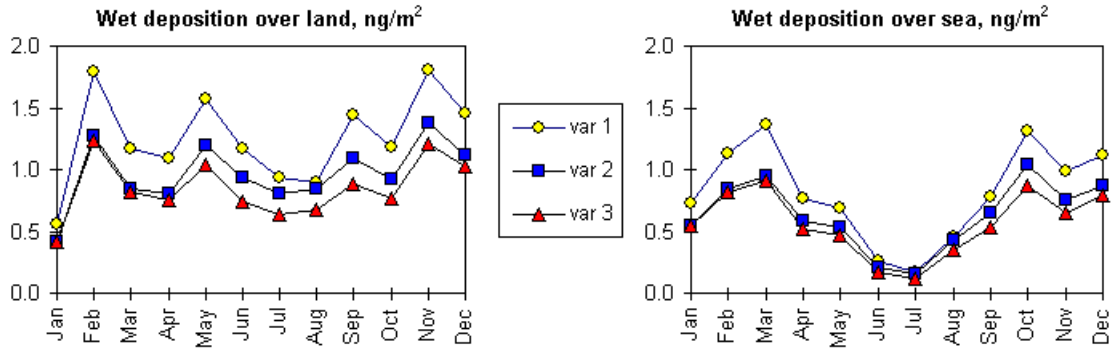

Figure 3.19. Effect of the atmosphere/vegetation exchange: PCB-153 wet deposition, ng/m^2

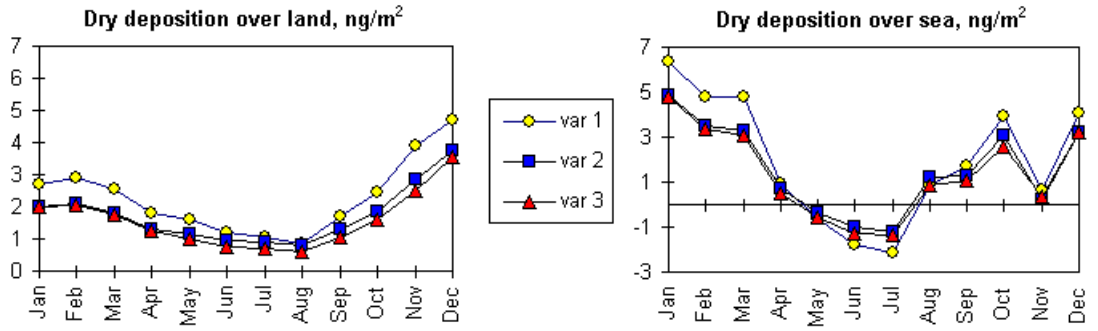

Figure 3.20. Effect of the atmosphere/vegetation exchange: dry deposition of PCB-153, ng/m^2

The comparison of seasonal variations of concentrations in vegetation and in forest floor with and without consideration of degradation in vegetation (see figures 3.21 and 3.22) indicated the significance of this process for the long-range transport modelling. These figures present calculation results for two variants: with (right axis) and without (left axis) degradation in vegetation. It is evident that with consideration of degradation concentrations in vegetation decreases in 40-60 times and in the forest floor - in 10-40 times.

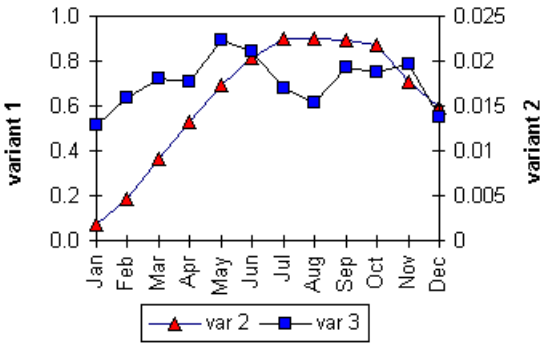

Figure 3.21. Concentration in vegetation; effect of degradation in vegetation, ng/g d.w.

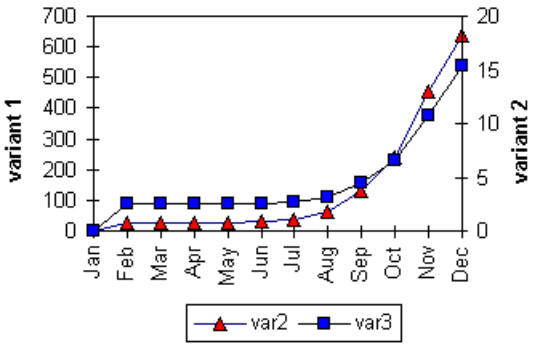

Figure 3.22. Content in forest floor; effect of degradation in vegetation, kg

3.1.5. Modelling of the transport and accumulation of PCB for 11-year period

To evaluate the trends of PCB accumulation in different compartments the simulation of PCB for the period of 11 years (from 1987 to 1997). The selection of this period was conditioned by the availability of meteorological information. The process of exchange with vegetation was taken into account. Degradation in vegetation was not considered. These calculations were based on total PCB emission and chemical-physical properties of PCB-153 as an indicator congener. On the basis of studies described in section 3.1.3 this assumption can lead to the error within a factor of 1.5 which is acceptable for provisional calculations. As it is mentioned in section 2.1 PCB total emission within the EMEP grid is 112 tonnes. Figure 3.23 demonstrates mass balance of PCB within the EMEP grid relative to total emissions of the same period.

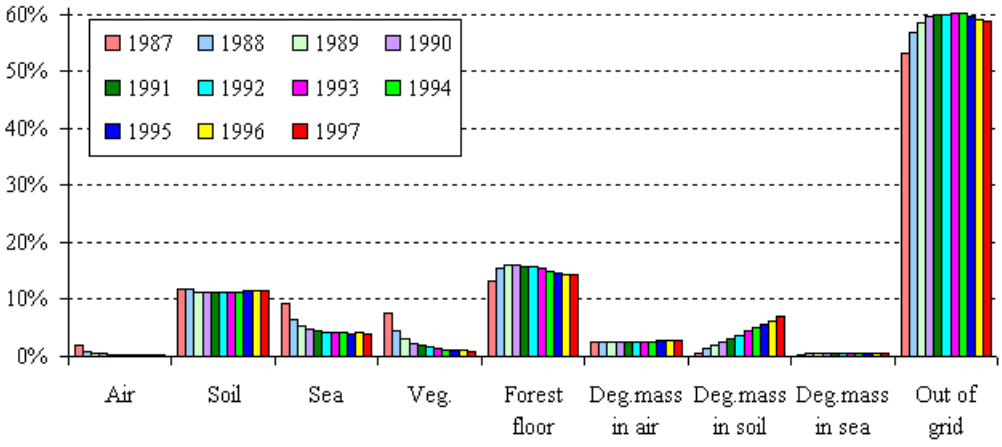

Figure 3.23. PCB mass balance within the EMEP grid for 11 years

On the basis of data presented in figure 3.23 it is possible to analyse processes of the input and accumulation of PCB in soil, sea water and vegetation.

Content in soil

The fraction of PCB content in soil relative to total emission is nearly constant being about 12% for the whole 11-year period. It points out to the fact that by the end of the period the accumulation in soil is far from "saturation" and the input is kept at the same rate during the period. Degradation increases with PCB accumulation in soil from 1% to 7%. Figure 3.24 demonstrates dynamics of PCB inflow to soil due to dry deposition and wet scavenging (gaseous and aerosol phase together) and accumulation and degradation of the pollutant in soil. As evident from the figure dry deposition is more important than wet scavenging. The contribution of each process separately for each phase is considered in section 3.1.1. As it was indicated dry deposition of the aerosol phase on soil substantially exceeds gas exchange especially in winter when the fraction of PCB adsorbed on particles increases. Dry deposition flux has a pronounced seasonal variation. With pollutant accumulation in soil the value of dry deposition flux decreases. It is possible that in calculations for a longer period the re-emission from soil will take place.

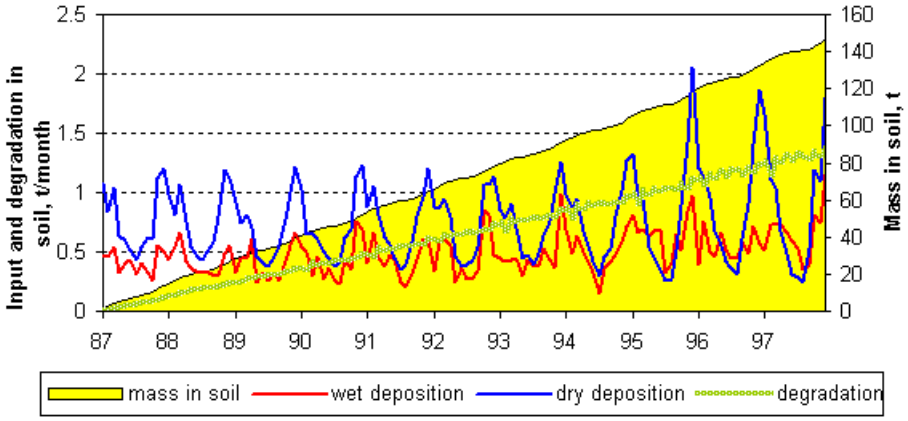

Figure 3.24. PCB input, accumulation and degradation in soil

Content in sea water

The character of PCB input to sea varies distinctly during 11 years. During the first year it is about 9% of total emission. During subsequent years the input rate decreases to about 4% keeping on this level to the end of the period. Figure 3.25 presents dynamics of PCB input to sea due to dry deposition and wet scavenging (by gaseous and aerosol phase together) as well as accumulation and degradation of the pollutant in marine water. In view of the model assumption that PCB aerosol phase is not dissolved in water and it does not participate in gas exchange, the figure manifests accumulation dynamics both for total PCB mass and separately for the gas phase. As seen from the figure in 2 years the gas phase mass in sea stops growing remaining on the level of about 7 tonnes and undergoing only seasonal variations.

Degradation in sea except for the first year is nearly constant being about 0.5% of the emission entered up to the moment. Like in the case of soil dry deposition process is more important then wet scavenging. At the same time the contribution of gas exchange flux becomes more essential than over the land (see section 3.1.1). As follows from the figure beginning with the first year in summer the gas exchange flux becomes negative, i.e., re-emission from the sea surface to the atmosphere takes place.

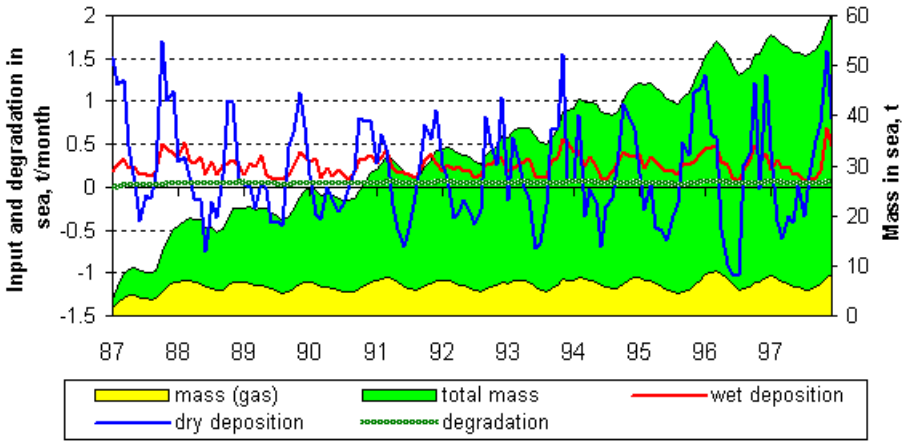

Figure 3.25. Input, accumulation and degradation of PCBs in sea water

Content in vegetation

The input to vegetation (figure 3.26) relative to total emission decreases from 21% to 15% (including the mass in the forest floor) during 11-year period. In the forest floor PCB mass is about 14% and it varies insignificantly from year to year. Fig.3.26 shows the plot of PCB mass variation in vegetation and forest floor for 11-year period.

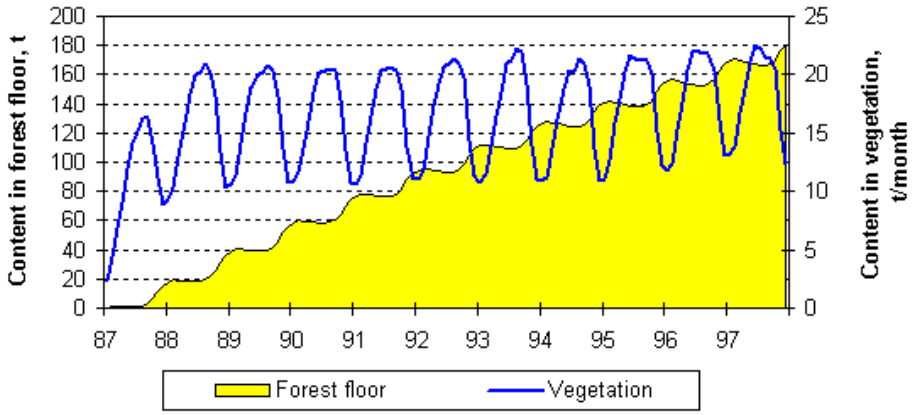

Figure 3.26. Input and accumulation of PCBs in vegetation and forest floor

As seen from the plot the gas exchange process with vegetation reaches quasi-stationary state in two years with a pronounced seasonal variation. The uptake of PCB by vegetation is about 20 tonnes in summer months and about 10 tonnes in winter. Contrary to the content in vegetation the content in the forest floor increases approximately linearly.

Concentrations in air and export outside the grid

Dynamics of PCB content within the EMEP grid in air during the modelling period is shown in figure 3.27. Air content has a pronounced seasonal variation from 2 tonnes in winter to 4-5 tonnes in summer. Degradation in air and export outside the grid vary insignificantly amounting to 3% and 55% of the total emission, respectively.

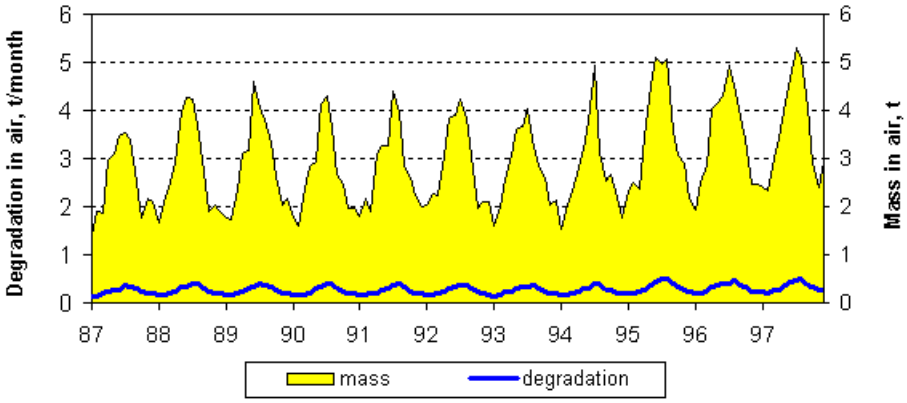

Figure 3.27. Dynamics of PCB content in air for 11-year period

Figure 3.28 displays PCB total mean annual concentrations in the lower air layer for 1996 (the 10th year of simulation). The region of maximum concentrations of PCB (0.5-2 ng/m^3) coincides with the region of maximum emissions. In the majority of European countries PCB concentrations exceed 0.1 ng/m^3. Minimum concentrations from 0.025 to 0.05 ng/m^3 are characteristic of remote regions such as Ireland, Iceland, Sweden, Norway and Finland.

The comparison of calculated PCB air concentrations with observations at the EMEP network is given below (see section 4.3 *Comparison of calculation and measurement data on PCB-153*). The comparison revealed that PCB mean concentrations are underestimated as much as 3 times by calculations. According to other measurements carried out in 1991-92 PCB mean annual concentrations in urban air of Great Britain were 1.3 ng/m^3 for London, 0.36 ng/m^3 for Stevenage, 0.56 ng/m^3 for Cardiff, 0.44 ng/m^3 for Manchester [*Halsall et al.*, 1995].

Figure 3.29 demonstrates PCB mean annual concentrations in vegetation for 1996 (the 10th year). Maximum concentrations from 6 to 12 ng/g d.w. are characteristic for regions with maximum emissions. High concentrations from 1 to 6 ng/g d.w. are obtained for the northern part of Russia, Finland, Sweden, France, Germany and Great Britain.

Figure 3.30 shows the map of PCB deposition densities for 1996 (the 10th year) The maximum deposition densities (8-15 μg/m^2) corresponds to the region of maximum emissions, namely Belgium, the Netherlands, Luxembourg, and the western part of Germany. Deposition density exceeding 2 μg/m^2 is observed over Germany, part of France, Austria, part of Italy Switzerland, the Czech Republic. Deposition densities more than 0.5 μg/m^2 are characteristic of the majority of European countries except Portugal and part of Greece.

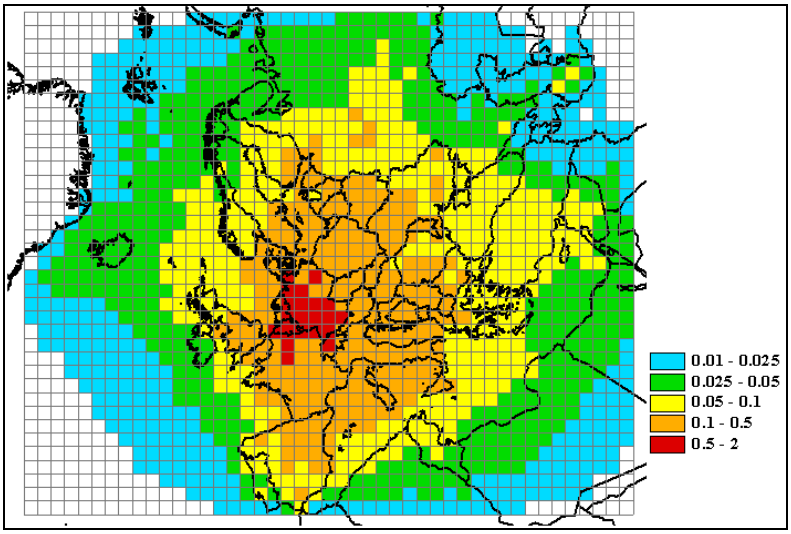

Figure 3.28. Total mean annual concentration of PCBs in air, ng/m^3

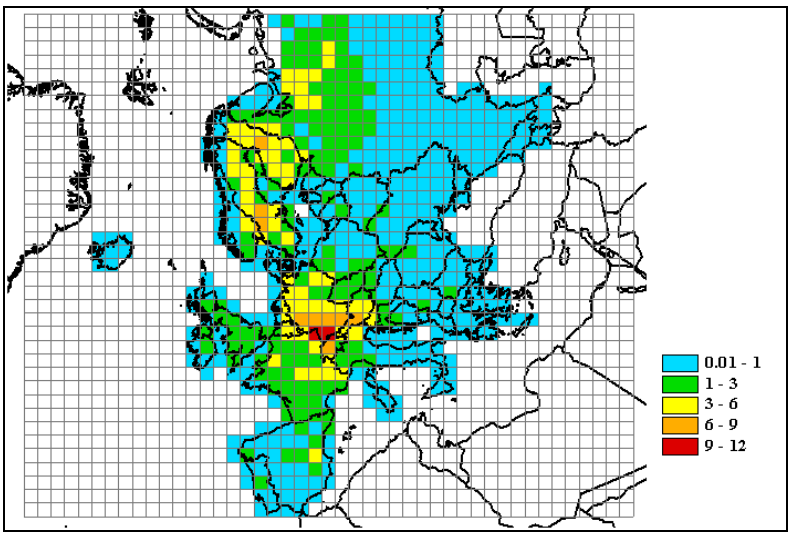

Figure 3.29. Total mean annual concentration of PCBs in vegetation, ng/g d.w.

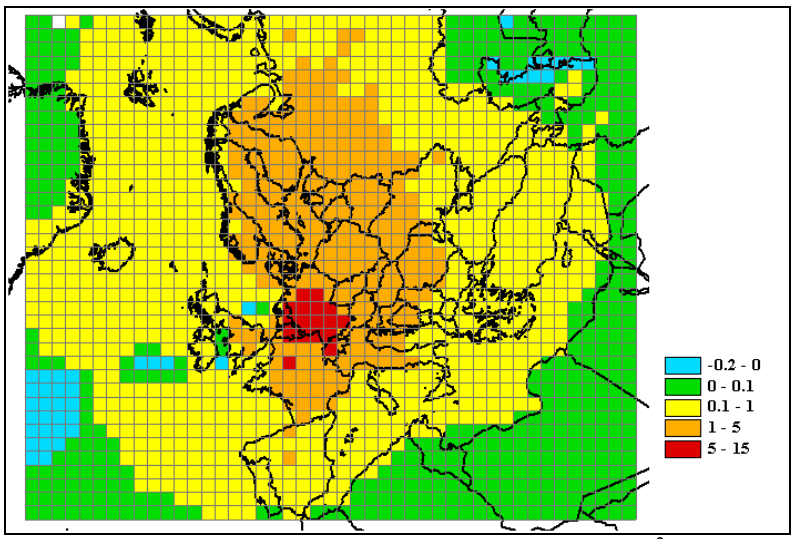

Figure 3.30. Total deposition of PCBs, µg/m^2/yr.

3.1.6. Conclusions

1. Comparing modelling results for congener PCB-153 with the results of the previous report it can be noted that introduction of degradation in compartments and gas/particles partitioning results in the increase of the fraction of the pollutant absorbed by soil from 5% to 17% in the total mass balance. At the same time the transport outside the grid decreases from 78% to 65%.

2. The most important processes affecting PCB transboundary transport are degradation in air and interaction with the underlying surface. Contributions of these processes are rather different for different congeners. In the behaviour of different PCB congeners in the environment similarities and dissimilarities are observed.

Similarities

- The fraction of gas phase wet deposition of all PCB congeners is negligible compared to other processes of deposition onto the surface due to poor solubility of the gas phase of all PCB in precipitation.

- Gas exchange flux over sea exceeds that over soil for all PCBs.

- During the first year gas exchange flux over sea for all congeners is of re-emission character in summer.

- The transport outside the grid is essential and equal to 76% for all congeners.

- Degradation in soil and sea is not high for all congeners and during the first year it is about 1% for soil and 1% for sea (life-time of almost all congeners in soil and sea is 9 years and only the life-time of PCB-28 in sea is about 3 years).

Dissimilarities

- Degradation in air is very different for different congeners. For PCB-28 it is maximum (27%) due to its relatively short life-time in the atmosphere (33 days) and a large fraction of its gaseous fraction in the atmosphere. For other congeners degradation in air ranges from 1 to 10%.

- Input to soil due to dry and wet scavenging is essentially different for different congeners. The maximum input is observed for PCB-180 (27%) mainly due to high content of its aerosol phase. The minimum input is observed for PCB-28 (2%) due to low content of its aerosol phase.

- The input to sea is essentially different for different congeners. It is maximum for PCB-118, PCB-138 and PCB-180 (12%) and it is minimum for PCB-52 (5%).

- In the input to soil of PCB-28 and PCB-52 the gas phase dry deposition flux predominates. For other congeners the input to soil is mainly due to dry and wet

deposition of the aerosol phase. At the same time the higher is congener chlorination the less is its gas phase contribution to total deposition on soil.

- Gas phase dry deposition of all PCB congeners makes maximum input to sea (except PCB-180). The contribution of the aerosol phase (in particular wet deposition) increases for all congeners with the increase of PCB chlorination degree.

3. The atmosphere/vegetation exchange process can appreciably affect transboundary transport of PCBs. According to preliminary calculations the uptake of PCBs by vegetation amounts to 25-30%. The parameters describing PCB uptake by vegetation and degradation in it need further refinement and analysis.

4. The fraction of a substance accumulated by vegetation is maximum for PCB-118. Note that PCB-118 is most toxic of the seven congeners.

5. At a given parameterization, vegetation can become a source of re-emission for PCB-28, 52, and 101 in summer months.

6. The consideration of the degradation process can lead to the reduction of concentrations and depositions by a factor of 1.5.

7. The analysis of calculation results for selected seven PCB congeners shows that PCB-153 can be used as an indicator congener for a development of approaches to modelling of PCBs (with possible deviation within the factor of 1.5).

8. The calculation results of PCB transport and accumulation for 11-year period show that the accumulation process in soil and sea water does not reach saturation. At the same time gas exchange between air and sea water reaches quasi-stationary state during the second year.

9. The calculations indicate the re-emission from the sea surface is observed during the first year. No re-emission from soil was observed during the whole period.

3.2. *Benzo[a]pyrene modelling*

Compared with 1998 calculations (see MSC-E report [*Pekar et al*., 1998]) a description of exchange processes with the underlying surface (land, sea and vegetation) was added to the B[a]P model. Preliminary calculations with integration of the air/vegetation exchange block showed that inclusion of this block for B[a]P leads to accumulation in vegetation not more than 3% of the total emission and changes the rest balance values by at most 2 – 3% which is within the model accuracy. Besides, the estimates of the air/vegetation exchange parameters (and, in particular, degradation rates in vegetation) are of a preliminary character and need further refinement. Hence, at this stage of investigations it was decided to carry out simulations without taking into account the air/vegetation exchange process. In future, however, these issues are assumed to be a topic for the discussion on the Workshop on POP and HM (November 1999).

The following calculations were performed using the model described in Chapter 1:

- simulation of B[a]P transport for estimating the affect of different processes on its long-range transport and investigation of seasonal variations of B[a]P concentrations and depositions;

- simulation of B[a]P transport within the period from 1987 to 1997 (11 years) for the investigation of accumulation processes in different environmental compartments;

- simulations of B[a]P transport with different wet deposition velocities for investigating the affect of wet deposition process on the long-range transport of B[a]P.

3.2.1. Modelling of B[a]P transport: effect of different processes and seasonal variations

Figure 3.31 presents the mass balance for B[a]P within the EMEP grid obtained for 1996; total emission for this year within the EMEP grid is about 1250 tonnes. The analysis of the obtained results shows that the uptake of B[a]P by soil within the EMEP grid amounts to 37% of the annual emission. The uptake by the sea compartment amounts to about 7%. A considerable part of B[a]P (38%) degraded in air. The transport outside the calculation grid amounts to 17%. Considerable per cent of air degradation is due to rather intensive degradation rate of B[a]P in the atmosphere.

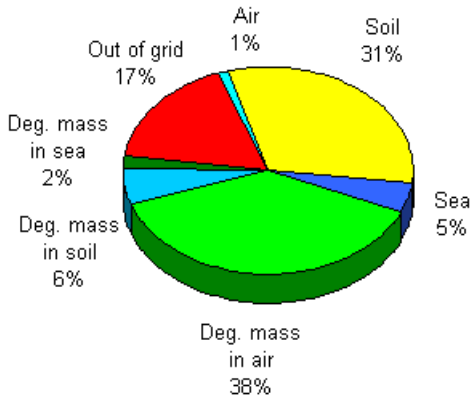

Figure 3.31. Balance mass B[a]P for 1996

Under a given parameterization, the half-life of B[a]P in the air is slightly more than 7 days.

Let us turn our attention to the analysis of seasonal variations of B[a]P air concentrations obtained during the simulation. Variations of total (gas and aerosol phase) concentration over land and sea are presented on figure 3.32.

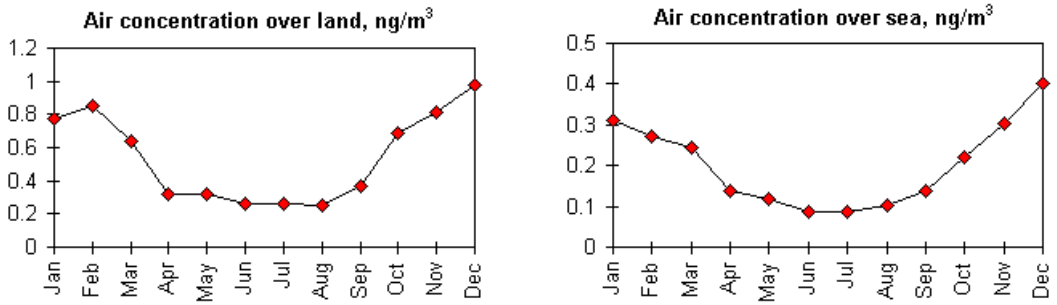

Figure 3.32. Total concentrations of B[a]P in the lower atmospheric layer over land and sea, ng/m^3

From the figure one can see that the total air concentration of benzo[a]pyrene decreases in summer and increases in winter. This phenomenon can be explained both by emission seasonal variations (see section 2.3 *Temporal variability of emission*) and by temperature dependence for gas/particles exchange parameters.

Seasonal variations of concentrations for B[a]P gaseous and aerosol phase (averaged over all vertical layers) are presented on figure 3.33. It is seen that the B[a]P gas phase concentration has the maximum in summer months whereas the aerosol phase concentration is maximum in winter months. The part of the gaseous phase increases in summer and decreases in winter. In particular, at temperatures close to zero the fraction of B[a]P gaseous phase amounts to 1–2%, at temperatures close to 20^0 C this fraction increases up to 13%, and at 30^0 C it reaches 35%.

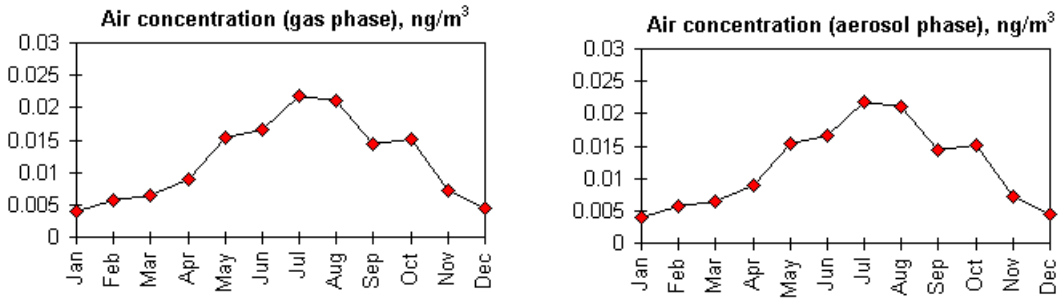

Figure 3.33. Monthly means of aerosol and gas phases of B[a]P air concentrations for 1996, ng/m^3

Figures 3.34, 3.35, and 3.36 present seasonal variations of dry and wet depositions and gaseous flux over land and sea.

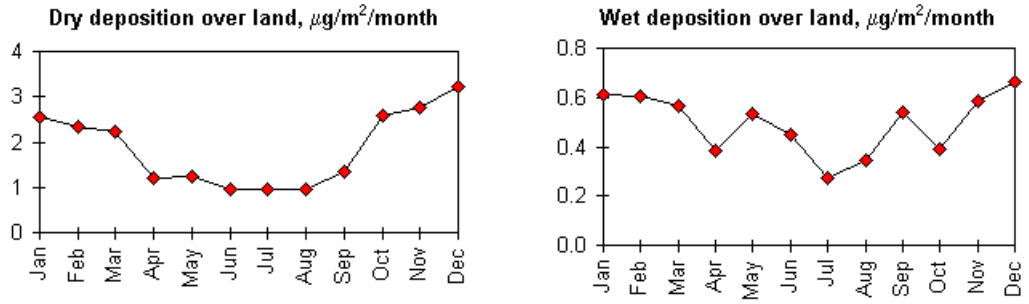

Figure 3.34. Dry and wet deposition of B[a]P over land in 1996, μg/m^2/month

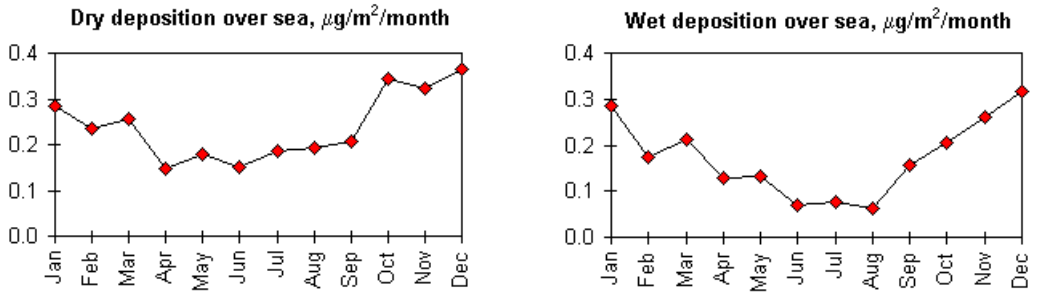

Figure 3.35. Dry and wet deposition B[a]P over sea in 1996, μg/m^2/month

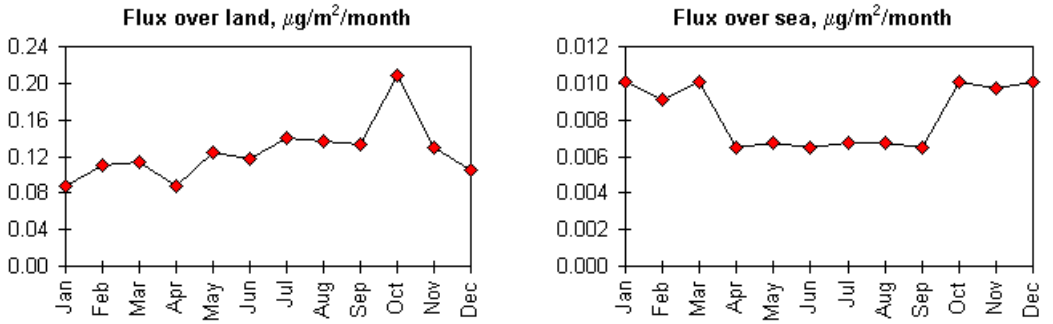

Figure 3.36. Gaseous flux of B[a]P over land and sea for 1996, μg/m^2/month

B[a]P dry deposition on land makes more essential contribution in the total deposition compared with wet deposition. Over the sea, situation is changed and contributions of dry and wet deposition are approximately equal. The contribution of gaseous flux over land and sea is inessential compared with that of aerosol phase deposition. Under the current parameterization, B[a]P re-emission is absent.

The distribution of the gas and aerosol phase concentrations with height in the atmosphere is also of interest. Figure 3.37 presents monthly mean gas and aerosol phase concentrations for different vertical layers of the calculation grid (the lower layer is 1st with height from 0 to 100 m, the upper is 4th with height from 1100 to 2100 m).

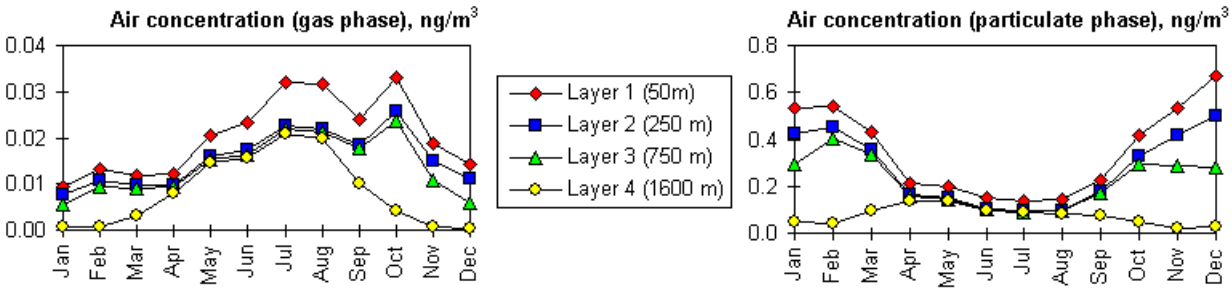

Figure 3.37. Vertical distribution of B[a]P air concentrations, ng/m^3

As seen from the figure both aerosol and gaseous phases are concentrated mainly in the lower layers in winter (from October to March; the ratio of concentration in the upper atmospheric layer to the mean concentration for these months ranges from 0.1 to 0.3). From April to September the tendency of concentration to increase in the upper layers takes place (the ratio of concentration in the upper layer to the average concentration ranges from 0.4 to 0.9). Due to this fact the increase of a number of vertical layers and the upper limit of the calculation grid is planned.

3.2.2. Modelling of transport and accumulation of B[a]P within 11-year period

Now let us consider the results of simulation of B[a]P for the 11-year period (from 1987 to 1997). Figure 3.38 presents the mass balance of B[a]P within the EMEP grid with respect to the emission accumulated within the period considered.

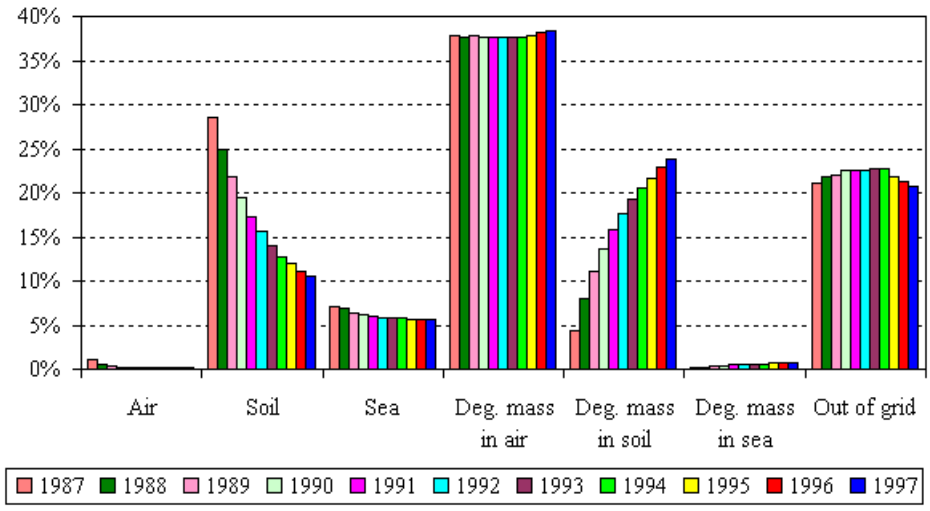

Figure 3.38. B[a]P mass balance within the EMEP grid

Data presented in this figure allows one to analyse the uptake and accumulation processes for B[a]P by soil and sea water.

Soil content

The part of accumulated emission uptaken by soil for the 11 years (mind that annual emission amounts to about 1250 tonnes) decreases from 28% for the first year to 11% by the last year. Consequently, the degraded mass increases with increase of B[a]P soil content from 4% to 24% of total emission. Figure 3.39 presents the variation of B[a]P soil content during 11 years. As seen from figures 3.38 and 3.39 the rates of accumulation in soil decrease a little by the end of 11-year period. This shows that during the considered period establishing of the quasi-stationary state is already noticeable but not yet finished. B[a]P dry deposition (total dry deposition flux for the gaseous and aerosol phase) over land plays more essential role than wet scavenging. The dry deposition flux shows considerable seasonal variations.

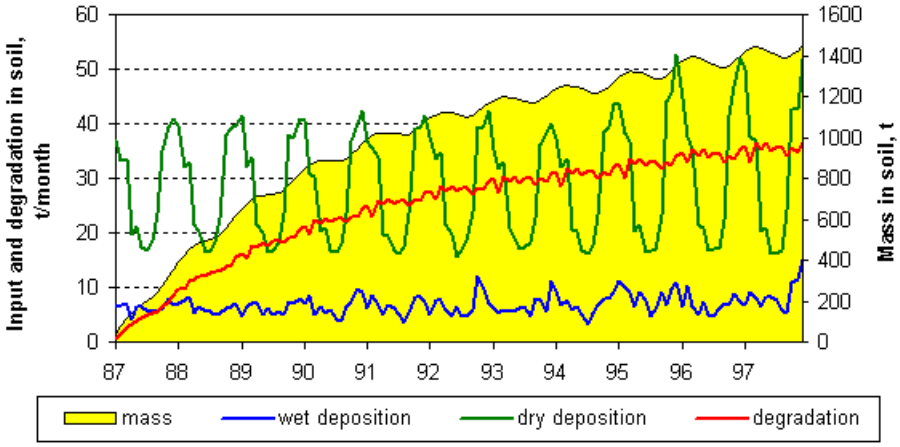

Figure 3.39. Soil uptake (dry and wet depositions), accumulation and degradation of B[a]P in soil within 11-year period

Sea content

Figure 3.40 presents variation of B[a]P uptake by sea water due to dry deposition and wet scavenging (total for gaseous and aerosol phase) as well as of B[a]P accumulation and degradation in sea water. According to the model assumption, the aerosol phase uptaken by water is not then dissolved and does not take part in the gas exchange. Therefore, the figure represents variations of the uptake both for the total mass and the gaseous phase separately. As seen from the figure the total mass accumulated in the sea increases almost linearly whereas the increase of the gaseous phase content in the sea becomes slower and the gaseous exchange tends to reach the quasi-stationary level. The figure presents also variations of dry and wet deposition and degradation processes. In contrast to the land case the fluxes of dry and wet deposition over land are comparable.

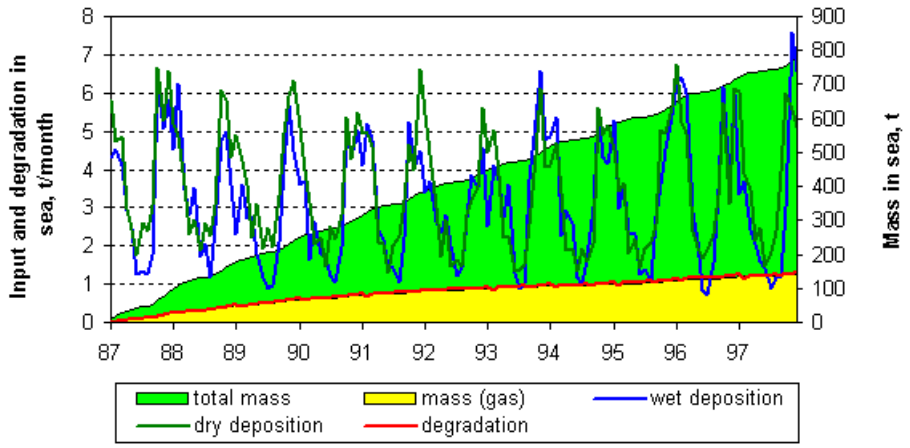

Figure 3.40. Sea uptake (dry and wet depositions), accumulation and degradation of B[a]P in sea water within 11-year period

Consideration of dry deposition graphs for land and sea for 11-year period confirms the above conclusion that under the current parameterization re-emission processes does not take place for B[a]P.

Air content

The variation of B[a]P air content within the EMEP grid for 11 year period is presented on figure 3.41. The air content ranges from about 8 tonnes in summer to 18 tonnes in winter. Seasonal variations of B[a]P mass in the air are explained both by emission seasonal variations and by temperature dependence of the gas/particle partitioning.

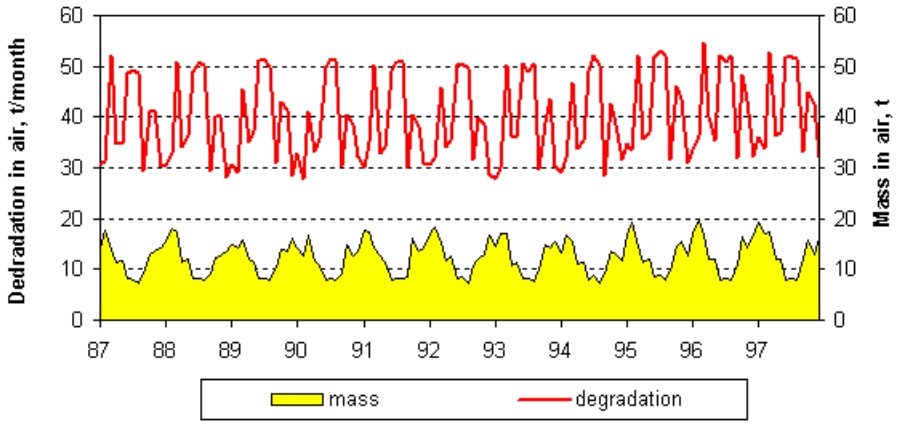

Figure 3.41. Variation of B[a]P air content within 11-year period

As follows from total mass balance presented in figure 3.38 air degradation process is one of the most essential under a given model parameterization. During the period considered the fraction of B[a]P mass degraded in the air is not changed essentially and equals about 38% of total emission.

Figure 3.42 presents annual means of B[a]P air concentrations in the surface layer for 1996 (10th year). The domain with maximum concentrations corresponds to that with maximum emission. The concentrations over 5 ng/m^3/yr. are typical of Belgium, the Netherlands and Luxembourg. The concentrations exceeding 1 ng/m^3/yr. are found over a part of Great Britain, Germany, Poland, and Italy as well as over France, Austria, Switzerland, the Czech Republic, Hungary, and Romania. For the rest of countries annual means of B[a]P concentrations range from 0.2 to 1 ng/m^3/yr.

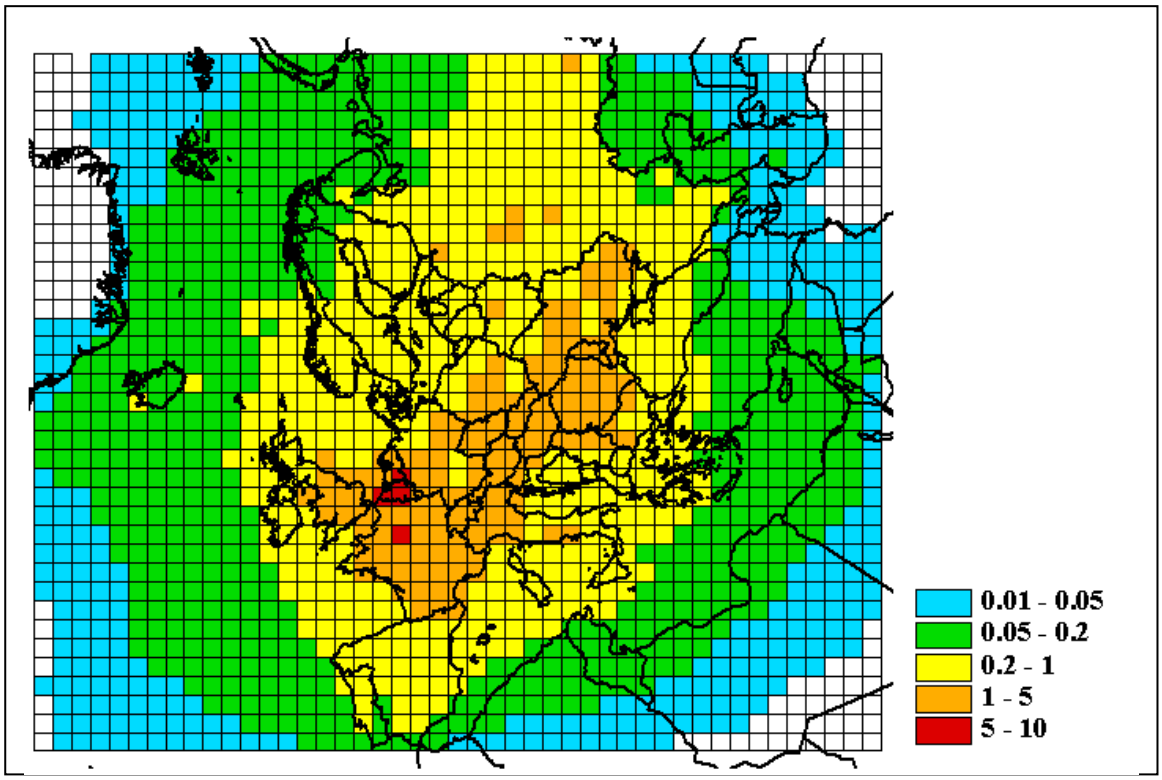

Figure 3.42. Annual mean air B[a]P concentrations in the surface layer, ng/m^3/yr.

The comparison of the calculated air concentrations of B[a]P with the measurements of the EMEP network is presented below (*4.4. Comparison of calculated and measured data of B[a]P*). The comparison results show that the calculated mean annual B[a]P concentrations overestimate the measured ones by a factor of 3.3.

Figure 3.43 presents the map of B[a]P deposition density for 1996 (10th). The maximum deposition density corresponds to the domains with maximum emissions, that is in Belgium, the Netherlands and Luxembourg as well as in the northern and southern parts of France. The densities more than 50 ng/m^2/yr. are found over part of Great Britain, Germany, Poland, and Italy as well as over France, Austria, Switzerland, the Czech Republic, Hungary, Romania, parts of Belarus and the Ukraine. For the rest of countries these densities range from 1 to 10 ng/m^2/yr. Note that the deposition density measured at site DE9 (Germany) in 1997 is 33 ng/m^2/yr.

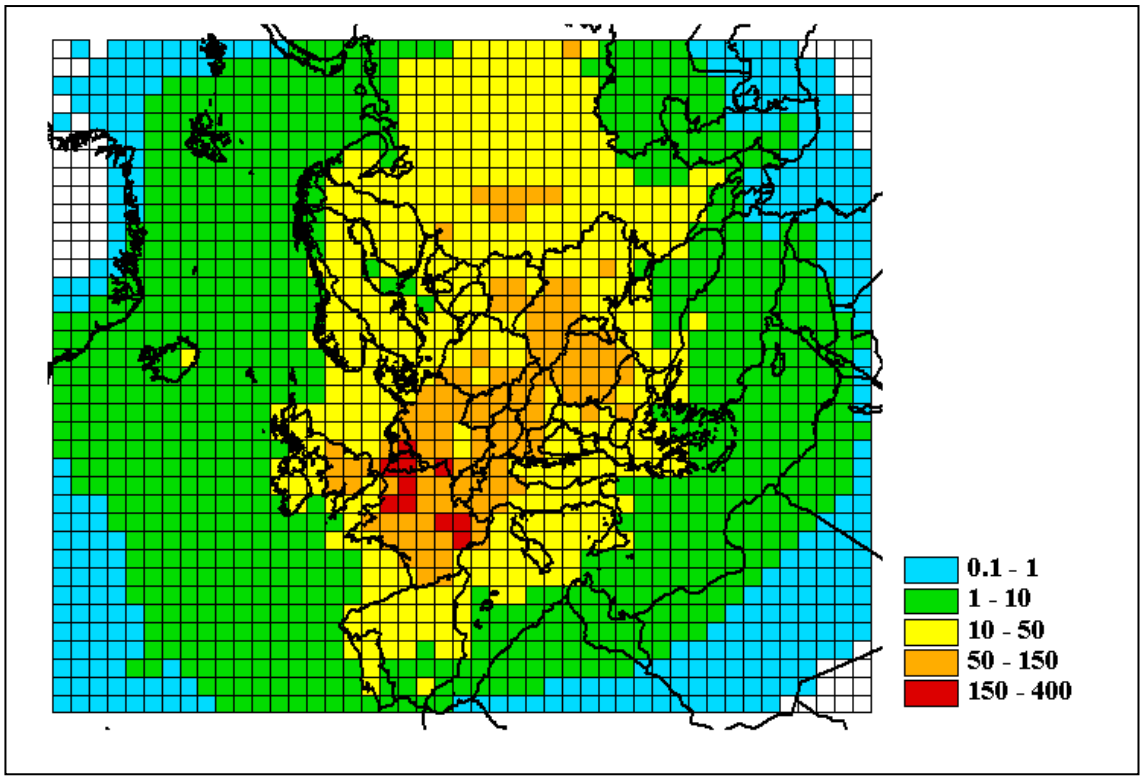

Figure 3.43. Densities of B[a]P total depositions for 1996, ng/m^2/yr.

3.2.3. Sensitivity analysis with respect to the wet deposition parameter

As it follows from the analysis of modelling results, one of the most essential processes affecting the long-range transport of B[a]P is the exchange with the underlying surface and, in particular, wet deposition. Here the affect of changing the wet deposition parameter for the aerosol phase will be considered.

To study this issue two variants of the simulations were made: first for $W_P = 2.4\times10^4$ [*Franz and Eisenreich,* 1998] and the second for $W_P = 5\times10^5$ [*Baart et al.*, 1995]. Figure 3.44 presents the comparison of the mass balance for these two cases.

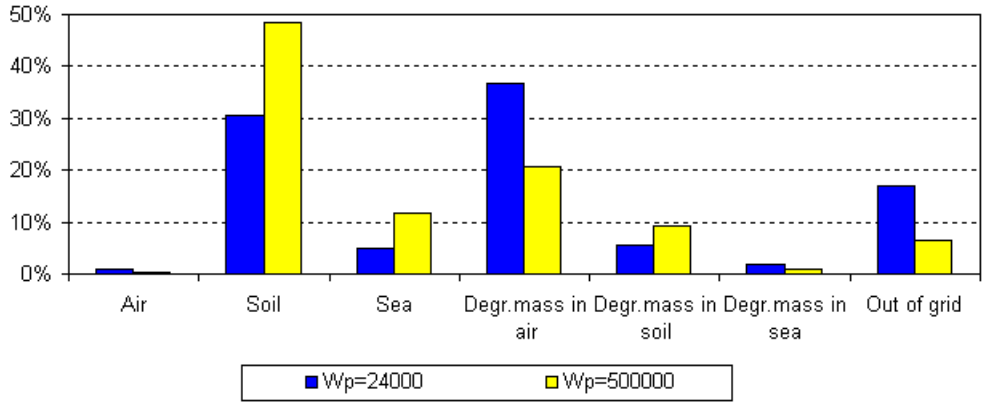

Figure 3.44. Comparison of the mass balance for two different values of scavenging ratio for the aerosol phase

The balance quantities for these two cases differ within a factor of two. The more detailed analysis shows that some characteristics can differ more than twice and for values of wet deposition the difference reaches a factor of 4. Hence, value W_P affects the long-range transport essentially and needs further refinement.

3.2.4. Conclusions

The obtained results and their analysis allow us to make the following conclusions:

- According to calculation results the most essential processes affecting B[a]P transboundary transport are degradation in air and dry and wet deposition of the aerosol phase.

- The fraction of gas phase varied from 1% in winter to 15% in summer.

- Dry deposition of B[a]P over land makes more essential contribution to total depositions compared with wet deposition. Over sea, contributions of dry and wet depositions are comparable. The contribution of the gaseous flux both over soil and sea is small.

- Strongly pronounced seasonal variation of air concentrations of B[a]P takes place. Namely, the concentrations in winter are less than in summer.

- Due to temperature dependence of the gas/particle partitioning seasonal variations of air concentrations of B[a]P gaseous phase are opposite to seasonal variations of total concentration. In summer air concentrations of B[a]P gaseous phase are 4 – 5 times higher than in winter.

- The investigation of height distribution of B[a]P concentrations is essential for the evaluation of its long-range transport. In this connection it is supposed to extend the total height of the calculation grid by inclusion of additional vertical layers.

- The calculation results of B[a]P transport for the period of 11 years showed that the accumulation process in soil and sea water does not reach quasi-stationarity during this period. No re-emission from sea and land surfaces is observed during 11-year period.

3.3. *Dioxins/furans modelling*

In this section calculation results of polychlorinated dibenzo-p-dioxins and dibenzofurans on the example of physical-chemical properties of 2,3,4,7,8-pentachlorodibenzofuran (2,3,4,7,8-PeCDF) are considered. The main problem was to study basic processes affecting transboundary transport of PCDD/Fs.

3.3.1. Description of modelling results

In calculations for 1996 official emission data and expert estimates of PCDD/F emissions for 1990 were used [*Berdowski et al.*, 1997]. Total PCDD/F emission within the EMEP grid was about 9 kg I-Teq.

Figure 3.45 presents the mass balance of 2,3,4,7,8-PeCDF with the EMEP grid for 1996.

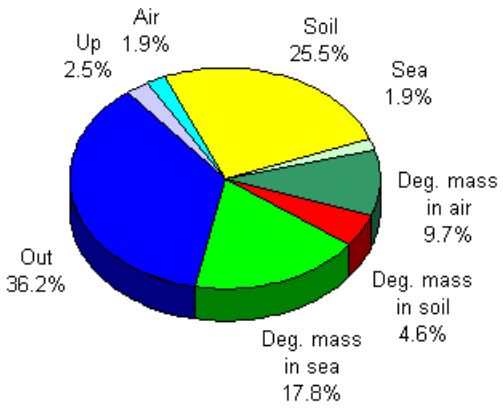

Figure 3.45. Mass balance of 2,3,4,7,8-PeCDF for 1996

The input to soil is 30% of the annual emission, the input to seas and oceans - 20%. The remained 50% was transported outside the grid and degraded in air (36% exported outside the grid, 10% degraded in air, 2% - remained in air by the end of integration period).

Degradation is as follows: in soil - 5% (of 30% input into it), in sea - 18 % (of 20% input to it). Thus degradation in the ocean surface layer is so high that almost all substance penetrating to it degrades there. According to the handbook [*Mackay et al.*, 1992] 2,3,4,7,8-PeCDF half-life in air and marine water is about 20 days, in soil - about 2 years. In spite of the fact that degradation rate in air of 2,3,4,7,8-PeCDF is the same as in the ocean surface layer, only 10% of the substance is degraded in air testifying to intensive depletion of its air concentration due to dry and wet deposition and to the fact that an essential part of the substance is present in the atmosphere in aerosol phase.

The fraction of 2,3,4,7,8-PeCDF aerosol phase at different temperatures is shown in table 3.1.

Table 3.1. The fraction of 2,3,4,7,8-PeCDF associated with particles at different temperatures

Temperature T, C	Vapour pressure p_L, Pa	Fraction on particles φ %
-20	3.09×10^{-7}	98.8
-10	1.52×10^{-6}	94.36
0	6.68×10^{-6}	79.25
+10	2.64×10^{-5}	49.18
+20	9.47×10^{-5}	21.21
+30	3.13×10^{-4}	7.54

Figure 3.46 demonstrates seasonal variation of emission of 2,3,4,7,8-PeCDF and it content in air.

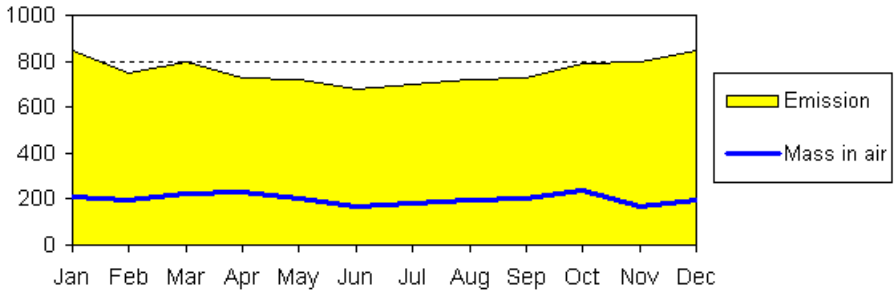

Figure 3.46. Emission (g I-Teq/month) and mass in air (g I-Teq)

Emission of dioxins and furans varies during a year with the maximum in winter and minimum in summer, the variation amplitude is 10%. This annual variation is distinctly pronounced in the plot. The mass content in air is approximately 4 times lower than emissions. It evidences to the fact that the loss of the substance from air due to deposition, degradation and export outside the grid is almost a constant value over the year being equal to $^3/_4$ of the rate due to emission.

Figure 3.47 shows plots of 2,3,4,7,8-PeCDF input to soil (a) and to sea (b) by four different mechanisms: gas phase dry deposition, gas phase wet deposition, aerosol phase dry deposition and aerosol phase wet deposition.

As seen from the figure monthly input of 2,3,4,7,8-PeCDF to soil is approximately 1.5 time higher than the input to sea. The contribution of aerosol phase is about 48% of the input to soil and the gas phase - 52%. Seasonal variation of the input to soil has a distinct minimum in summer months.

In figure 3.47(a) the solid line shows 2,3,4,7,8-PeCDF mass in soil. It grows uniformly over the year reaching 2300 g I-Teq (about 25% of annual emissions) by the end of the year allowing for degradation in soil (summing is made over all the grid cells). Degradation in soil amounts to about 400 g I-Teq.

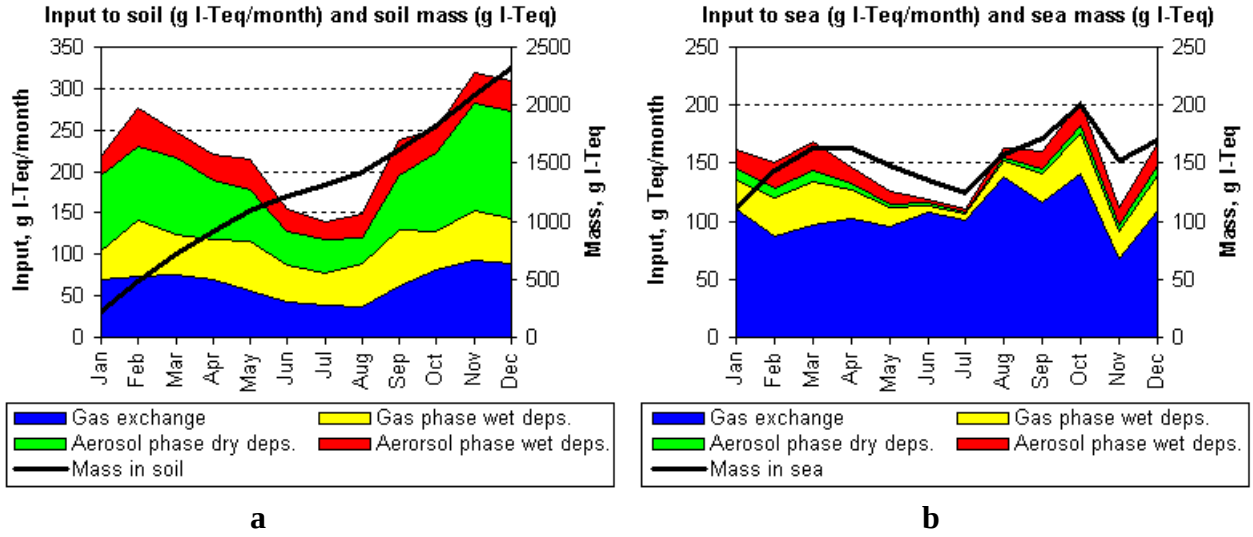

a **b**

Figure 3.47. Input of 2,3,4,7,8-PeCDF to soil (a) and to sea (b), g I-Teq/month. Contributions of dry and wet depositions of the gas and aerosol phase. Mass in soil (a) and in sea (b), g I-Teq

Figure 3.47(b) shows the input of 2,3,4,7,8-PeCDF to the upper sea layer and its mass there with allowance for degradation. As evident from the figure during the whole year the mass in sea is practically coincides with the input from the atmosphere due to dry and wet depositions of the gas and aerosol phase. It is connected with the fact that 2,3,4,7,8-PeCDF degradation rate in the ocean surface layer is so high that actually all the matter entering the layer is rapidly degraded. The gas phase dry deposition makes the main contribution to the input to sea (71%). Re-emission is not observed both over land and over sea.

Figure 3.48 manifests the map of total (dry and wet) deposition of 2,3,4,7,8-PeCDF for 1996.

The maximum deposition density (more than 1500 pg I-Teq /m^2/yr.) is observed over part of Romania and Hungary. Deposition density exceeding 500 pg I-Teq /m^2/yr. is observed in the majority of countries of Central Europe including Austria, Slovakia, Poland, the Ukraine, Italy, France, Belgium, Luxembourg, the Netherlands, Switzerland, Yugoslavia. Deposition density more than 250 pg I-Teq /m^2/yr. is characteristic of all the countries of Central Europe, part of the United Kingdom, part of Norway and Finland, all Baltic countries, the Ukraine, Belarus, Moldova and the east of European part of Russia. Deposition density more than 100 pg I-Teq/m^2/yr. covers Europe on the whole, the Mediterranean, North and Baltic Seas.

Deposition density on the sea surface is lower than on land. It is maximum (more than 500 pg I-Teq/m^2/yr.) along the coastal line of Italy, France, Belgium and the Netherlands. Deposition densities more than 250 pg I-Teq/m^2/yr. is observed over the Black and Azov Seas, Adriatic, Tyrrhenian and Ionic Seas as well as over the North and Baltic Seas.

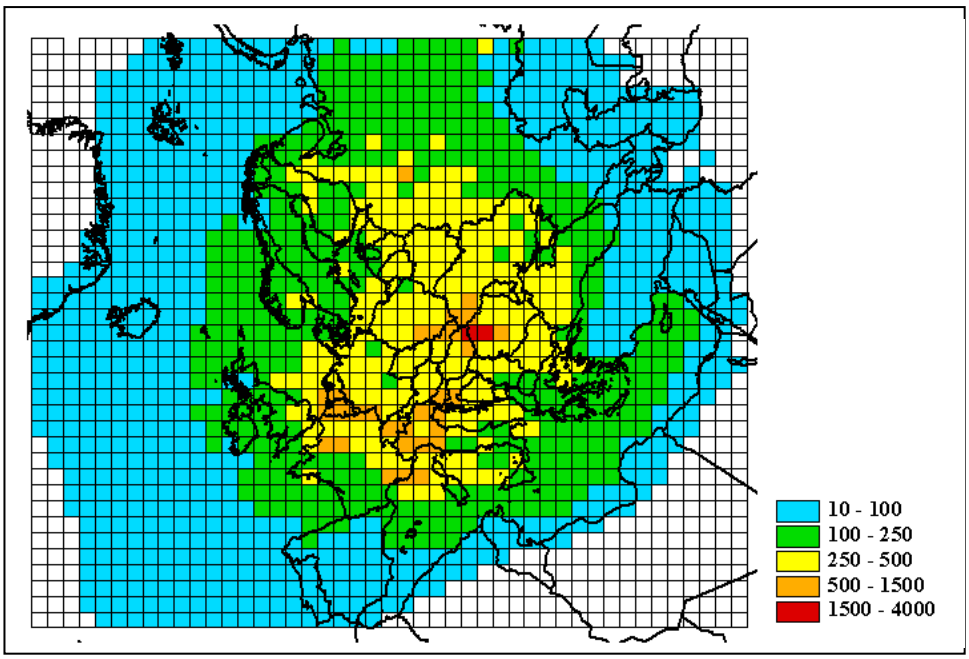

Figure 3.48. Density of 2,3,4,7,8-PeCDF total deposition, pg I-Teq/m^2/yr.

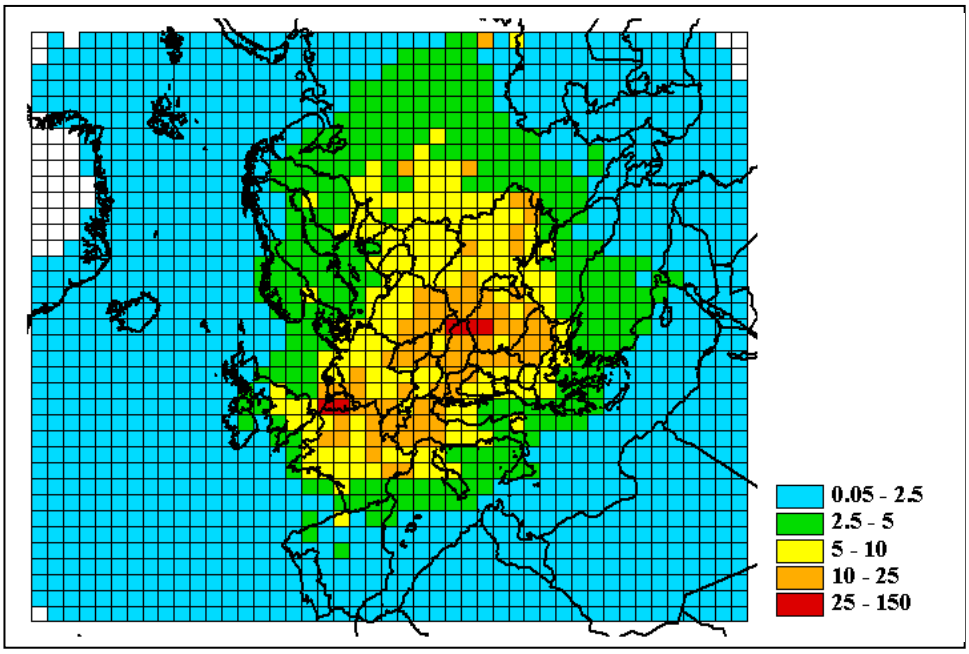

Figure 3.49. Mean annual concentrations of 2,3,4,7,8-PeCDF in air, fg I-Teq/m^3

Figure 3.49 shows mean annual concentrations of 2,3,4,7,8-PeCDF in surface layer of the atmosphere. In some countries (Romania, Slovakia, Hungry, Belgium) maximum mean annual concentrations can reach 25-140 fg I-Teq/m^3. In other countries of Central Europe these concentrations are 10-25 fg I-Teq/m^3. Concentrations 5-10 fg I-Teq/m^3 are observed in all European countries but Scandinavia, Spain and Portugal (such concentrations are observed only in a small part of Scandinavian countries and Spain). Mean annual concentrations as much as 2.5-5 fg I-Teq/m^3 are characteristic of Turkey, Scandinavia and European part of Russia.

The comparison of the calculated air concentrations of PCDD/Fs with available measurements is presented below (4.5. *Comparison of calculated and measured data of PCDD/Fs*). In view of preliminary character of calculations the comparison results indicate a reasonable agreement with measurements.

3.3.2. Conclusions

Based on the calculation data the following conclusions can be drawn:

- The main sources of emission of dioxins/furans to the atmosphere are organic fuel combustion, waste incineration and secondary non-ferrous treatment. The contribution of these sources to the total emission of PCDD/Fs amounts to 60%.

- The analysis of PCDD/F physical-chemical properties allowed to select the following homologue groups: PeCDF, HxCDF, and PeCDD. The PeCDF group makes a considerable contribution to the total toxicity. The main congener forming the toxicity of this group is 2,3,4,7,8-PeCDF. On the basis of the above-mentioned analysis the parameterization of the model was developed and the tentative calculation were made for 2,3,4,7,8-PeCDF.

- The main process in the modelling of the transboundary transport of PCDD/F is the exchange with the underlying surface. The input to soil in the framework of the EMEP region amounts to 30% of the annual emission, and the input to sea – to 20%. The degradation in sea plays the essential role in the air/sea exchange: from 20% of total emission accumulated in sea 18% have been degraded.

- The fraction of the 2,3,4,7,8-PeCDF bound to particles strongly depends on the temperature. This fraction amounts to more than 98% at -20^0 C and decreases to 8% at $+30^0$ C.

- The inputs from the atmosphere to soil due to dry and wet depositions of gas and aerosol phases are approximately the same whereas the input to sea takes place at most due to dry and wet deposition of the gaseous phase (about 70%). No re-emission from sea and land surfaces is observed during the calculation period.

3.4. *Lindane modelling*

This section deals with results of lindane transboundary transport modelling during the period of 1987-1997. Estimates of lindane emissions in Europe made by *J.Berdowski et al.* for 1990 [*Berdowski et al.,* 1997] were used. The total emission within the EMEP grid was 1307 tonnes. In calculations annual emission variations connected with seasonal application of this pesticide in spring and summer months were considered. It was assumed that 10% of lindane was emitted in February, 15% - in March and 25% - in April-June each. In calculations only the gas phase of lindane was considered. The process of atmosphere/vegetation exchange was not considered. As initial conditions it was assumed that lindane concentration in all the compartments was zero. Model parameterization is outlined in Chapter 1 (section 1.4.5 *Parameterization for lindane*).

3.4.1. Description of modelling results

Calculations are performed for the period of 11 years (1987-1997). This allows us to assess the rate of lindane accumulation in soil and sea, which can vary dependent on the amount of lindane stored in these two compartments.

Figure 3.50 presents the mass balance of lindane within the EMEP grid region after 11 years. The bulk of lindane input to soil is 23% (21% is degraded in soil and 2% - 270 tonnes is retained in soil after 11 years). A great part of lindane enters the sea (9% is degraded inside the sea and 8% - 1100 tonnes is retained in the sea after 11 years). 14% of lindane is degraded in the atmosphere due to rather rapid degradation in air (the half-life of lindane in air is about 46 days). 46% of lindane is transported outside the EMEP grid. These 46% is degraded in the atmosphere and deposited to the land and ocean outside the EMEP grid.

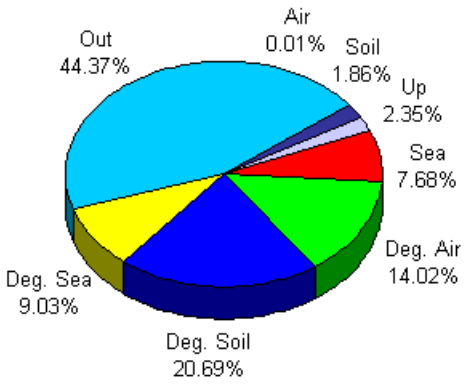

Figure 3.50. Mass balance of lindane after 11 years

Due to rather fast degradation of lindane in soil (the half-life is about 1 year), a small part of lindane remains in soil. Degradation in sea water is less intensive than in soil (the half-life in surface sea water is about 7 years). One can say that the ocean can serve as the main reservoir for lindane, which is capable to store and to re-emit it back to the atmosphere for a long time.

Soil and sea are the main sinks of lindane in our calculations (23% enters soil and 17% sea). The net mass in soil and in sea compartments is formed due to 4 mechanisms: dry deposition of the gaseous phase (input), wet deposition of the gaseous phase (input), re-volatilization (output), degradation (output). The last mechanism leads to a complete depletion of lindane due to its decomposition in soil and sea.

Wet deposition of lindane depends on the emission (and re-emission) intensity and precipitation amount only, while dry deposition and re-volatilization depend on the lindane amount accumulated in soil and sea. If the accumulation is sufficiently large compared with the concentration in air, re-emission can take place under appropriate meteorological conditions. Degradation also depends on the amount of lindane accumulated in soil or sea – the larger amount, the larger degradation (with constant degradation rate).

Figure 3.51 represents the input/output to/from soil and sea in the years 1-11 due to these 4 mechanisms. After 2 years of simulation the soil is "saturated" with lindane and the input becomes approximately equal to the output. The sea is far from "saturation" after 11 years: input prevails over output.

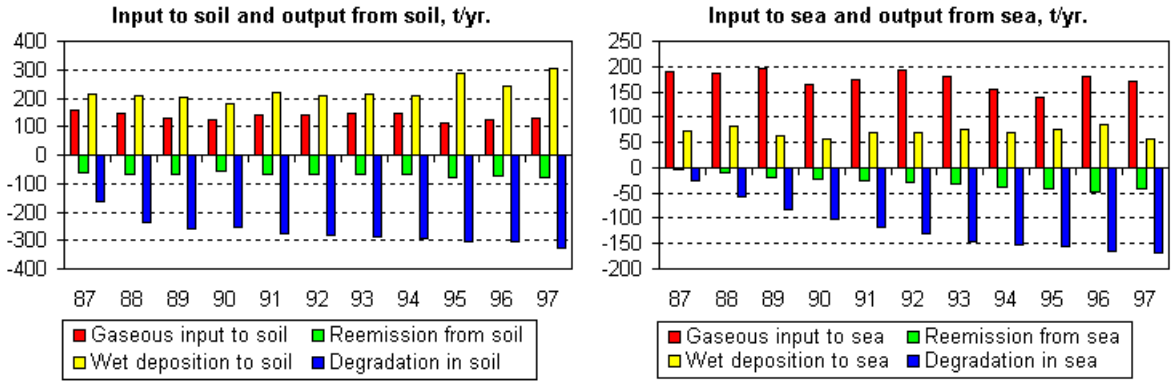

Figure 3.51. Input to soil and sea due to dry and wet deposition and output from soil (left) and sea (right) due to re-emission and degradation during 11 years, t/yr.

Figure 3.52 represents input to soil (a) and sea (b) in tonnes per month (left scale), and masses in the corresponding compartment in tonnes (grey region, right scale) after 11 years. Due to non-uniform emission intensity of lindane annual trend of input/output processes is strongly pronounced.

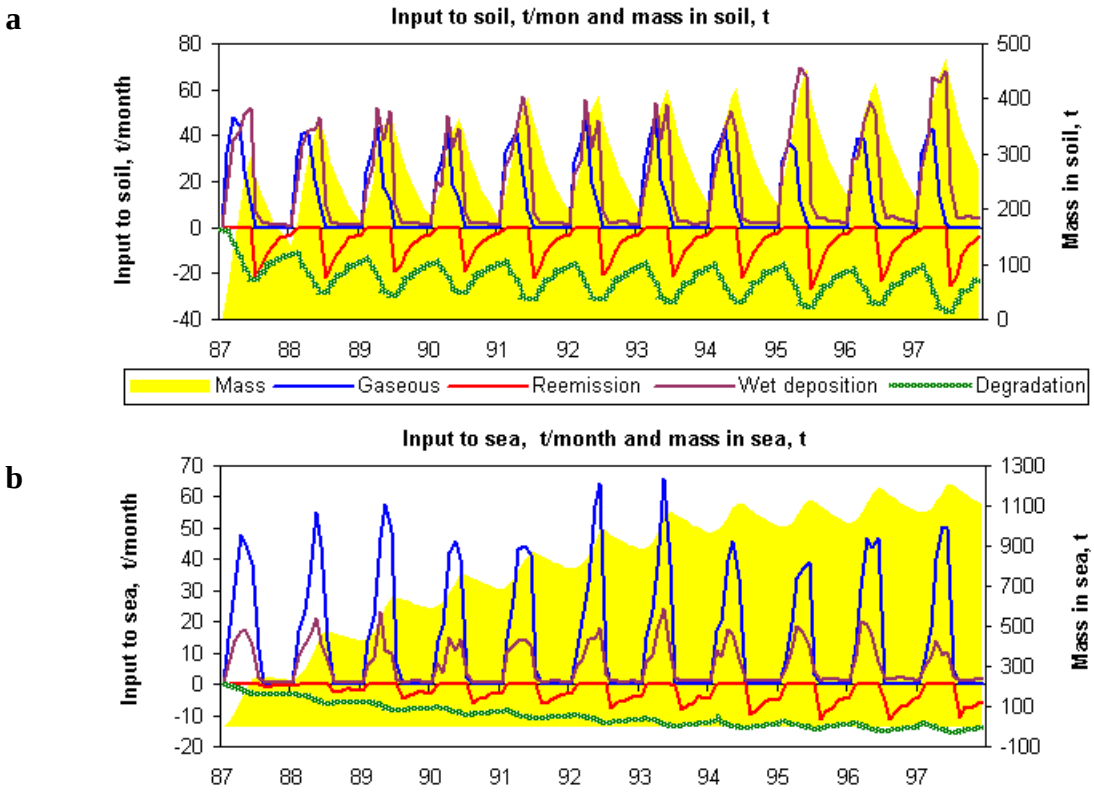

Figure 3.52. Lindane input to soil (a) and sea (b) due to dry and wet deposition and output from soil (a) and sea (b) due to re-emission and degradation during 11 years, tonnes per month

Soil. Dry deposition flux to soil is reduced by 25% after 3 years. In the first year input to soil due to dry deposition is about 150 tonnes (11% of annual emissions), and in the 4th – 11th year it is about 120 tonnes per year (9% of annual emissions). Wet deposition flux is approximately constant each year and equals 200-250 tonnes (15%-19% of annual emissions). The input to soil due to wet and dry deposition mainly takes place over February-June in the period of lindane application as pesticide (figure 3.52a).

Re-emission flux from soil is approximately the same over the 1st – 11th year and equals 60 tonnes per year (5% of annual emissions). Consequently the input from air to soil (~ 350 tonnes per year, 27% of annual emissions) is much greater than output from soil to air. Degradation in soil increases with lindane accumulation in soil - from 160 tonnes (in the 1st year) to 325 tonnes (in the 11th year).

Figure 3.52a also represents mass in soil during 11 years (grey region, right scale). Annual trend of mass in soil is strongly pronounced. This fact is connected with high re-emission from soil to air and relatively fast degradation (half-life is about 1 year).

Sea. Dry deposition flux to sea is almost the same from the first to the 11th year covered by calculations (~180 tonnes/year) and wet deposition flux is about 80 tonnes per year. Wet deposition flux over ocean is 3 times less than over land since average concentration over sea

is less than over land. Nevertheless dry deposition flux of lindane over sea is greater than over land. Therefore air-ocean exchange is much more intensive than air-soil exchange. The input to ocean due to wet and dry deposition mainly occurs during February-July.

Re-emission flux from ocean to air grows from 3 tonnes per year in the 1st year to 40 tonnes per year in the 11th year. Re-emission takes place in August-January when lindane is not applied. The value of lindane re-emission from sea surface correlates with the lindane amount accumulated in the sea surface layer. The input of lindane from air to sea (230 tonnes) prevails over its output from sea to air even in the 11th year (40 tonnes).

Degradation in the sea surface layer increases with lindane accumulation in sea - from 25 tonnes (in the 1st year) to 167 tonnes (in the 11th year).

Lindane mass in the sea surface layer during the period studied is also shown in figure 3.52b (grey region, right scale). Annual trend of the mass in sea is distinctly pronounced. Contrary to soil mass mean annual sea mass continuously increases over the period. This is connected with weaker (compared with soil) degradation rate in sea (life-time about 7 years).

Figure 3.53 shows mean annual concentrations of lindane in surface layer of the atmosphere (over EMEP grid). The distribution of air concentration over the EMEP region depends mainly on the emission distribution and also on meteorological conditions and deposition rates. The maximum concentration of 4 ng/m^3 is obtained over France and the Ukraine – the countries with the maximum emission density.

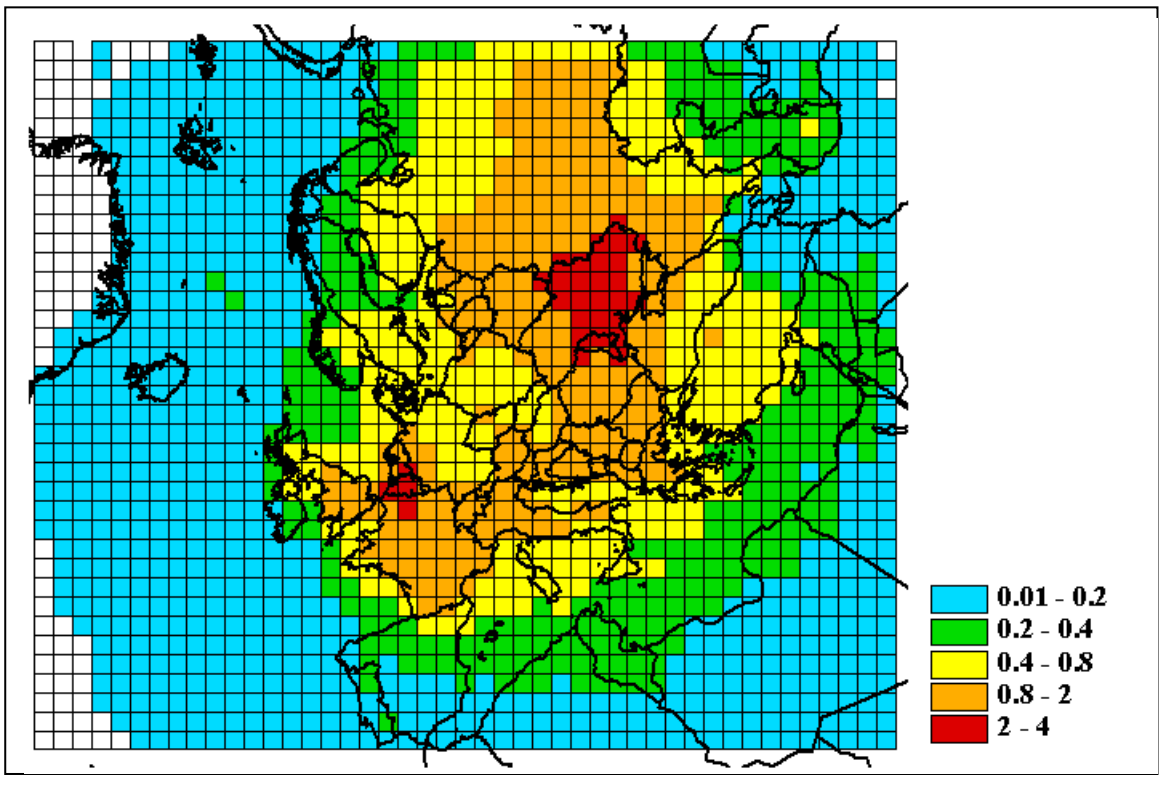

Figure 3.53. Mean annual lindane concentrations in air, ng/m^3

Figure 3.54 presents lindane total (wet plus dry) deposition densities per year (averaging is made over 11 years). The maximum deposition densities are 50-80 μg/m^2/yr.

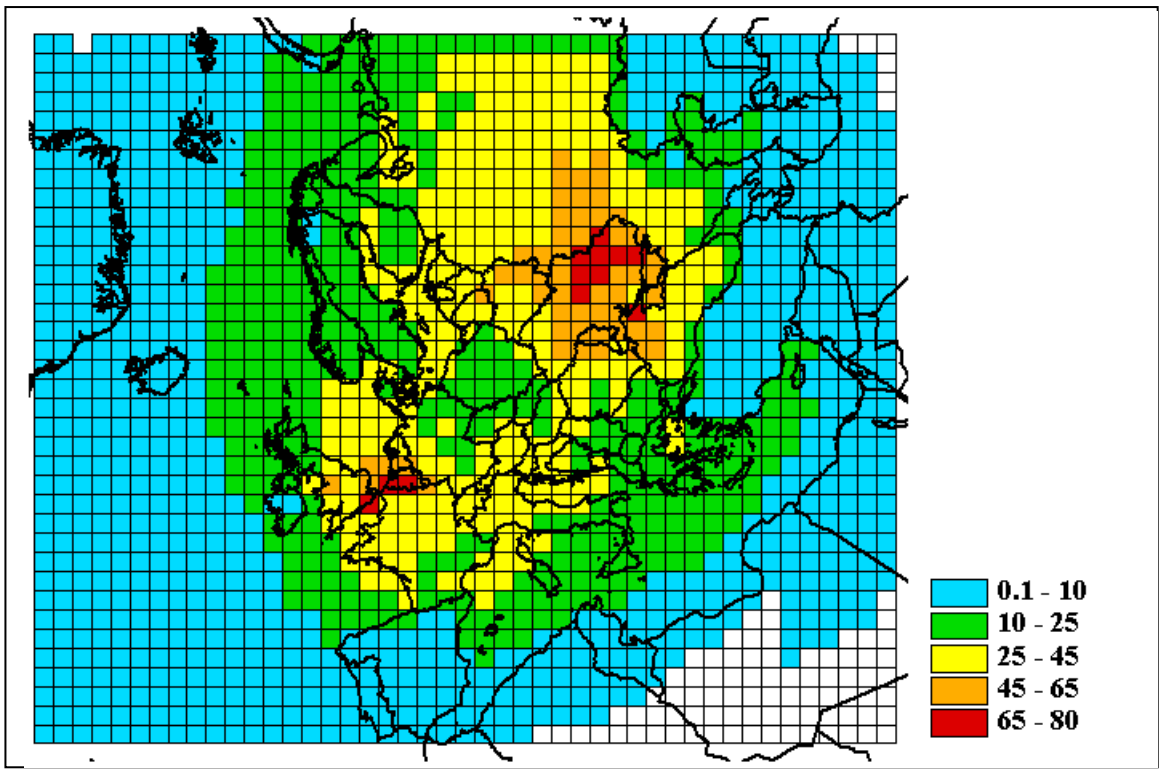

Figure 3.54. Total (wet and dry) depositions of lindane, μg/m^2/yr.

3.4.2. Conclusions

- Modelling results covering 11 year period indicated that an essential part of this substance enters soil and sea (23% and 17% respectable) or is degraded in air (half-life in air is 46 days) or transported outside the EMEP grid. The export outside the EMEP grid after 11 years was 46%, degradation in air 14%.

- Lindane accumulation in soil is very fast: during the first year it reached about 8% of annual emissions. The accumulation processes is retarded due to lindane degradation in soil (life-time in soil is about 1 year) and amounts to 15% of annual emissions.

- Lindane mass in soil has drastic seasonal variations due to seasonal variations of emissions, re-emission and degradation. In the second half of each year of 11 year period when emissions are ceased re-emission from soil predominates over the input to soil.

- Lindane accumulation in seas is most intensively during first 7 years. Then the accumulation is retarded due to degradation in the marine environment (half-life about 7 years).

- Lindane content in sea has severe seasonal variations, connected with annual emission variations and with processes of re-emission and degradation.

- Lindane input to soil due to washout with precipitation predominates over its input to soil due to gas phase dry deposition.

- Input to sea due to gas phase dry deposition predominates over wet depositions.

- Annual re-emission and annual degradation increases with the increase of lindane mass in sea. Degradation seas correlates with lindane mass in sea in the same way as degradation in soil correlates with lindane mass in soil.

- Maximum mean annual air concentration is 4 ng/m^3 and corresponds to regions of maximum emissions. Mean annual concentration over the North, Baltic and Mediterranean Seas are 0.2-0.8 ng/m^3.

- Maximum total deposition of lindane (dry and wet) is 80 μg/m^2/yr. and corresponds to the region of maximum concentrations. Total depositions over the North, Baltic and Mediterranean Seas are 10-20 μg/m^2/yr.

- At this stage of model development in calculations only the gas phase of lindane was considered. The process of atmosphere/vegetation exchange was not considered. At further stages it is planned to consider the gas and aerosol phase and the partitioning between them. It is also supposed to take into account the effect of vegetation on lindane airborne transport.

3.5. *Estimation of depositions on regional seas*

Total depositions and deposition densities of PCB, benzo[a]pyrene, 2,3,4,7,8-PeCDF, lindane were calculated for the North, Baltic and Mediterranean Seas. The calculation results are presented in tables 3.2 and 3.3

Table 3.2. Deposition densities of PCB, benzo[a]pyrene, 2,3,4,7,8-PeCDF and lindane for 1996

Compound	Unit	Mediterranean Sea	Baltic Sea	North Sea
PCB	ng/m^2/yr.	472	1843	886
B[a]P	μg/m^2/yr.	9	18	18
2,3,4,7,8 PeCDF	pg I-Teq/m^2/yr.	143	167	151
Lindane	μg/m^2/yr.	16	46	38

Table 3.3. Total depositions of PCB, benzo[a]pyrene, 2,3,4,7,8-PeCDF and lindane for 1996

Compound	Unit	Mediterranean Sea	Baltic Sea	North Sea
PCB	kg/yr.	1623	715	594
B[a]P	t/yr	30	7	12
2,3,4,7,8 PeCDF	g I-Teq/yr.	492	65	101
Lindane	t/yr.	56	18	26

According to calculation results the highest depositions of the pollutants considered fell on the Mediterranean Sea due to its area. If we consider mean deposition density on the sea basins, then the highest intensity is accounted for the Baltic Sea. Comparative diagrams of total depositions and their densities on the Mediterranean, Baltic and North Seas are presented in figures 3.55-3.58.

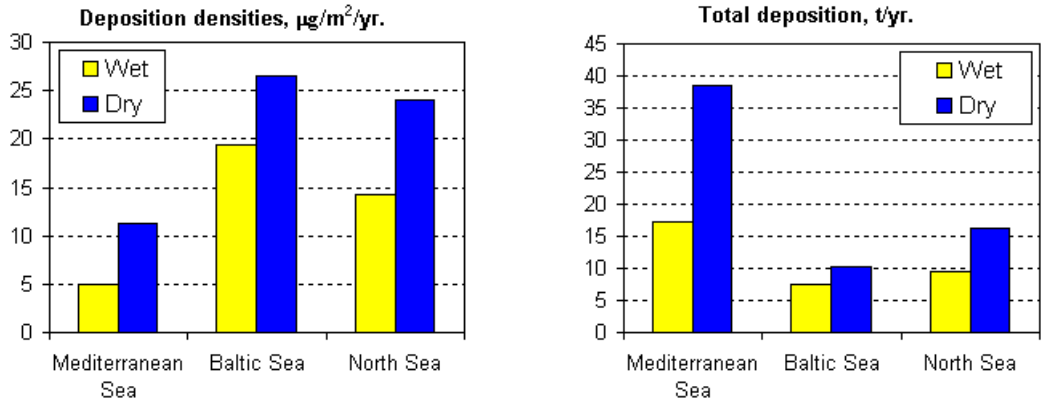

Figure 3.55. Total depositions (right) and deposition densities (left) of lindane on regional seas for 1996

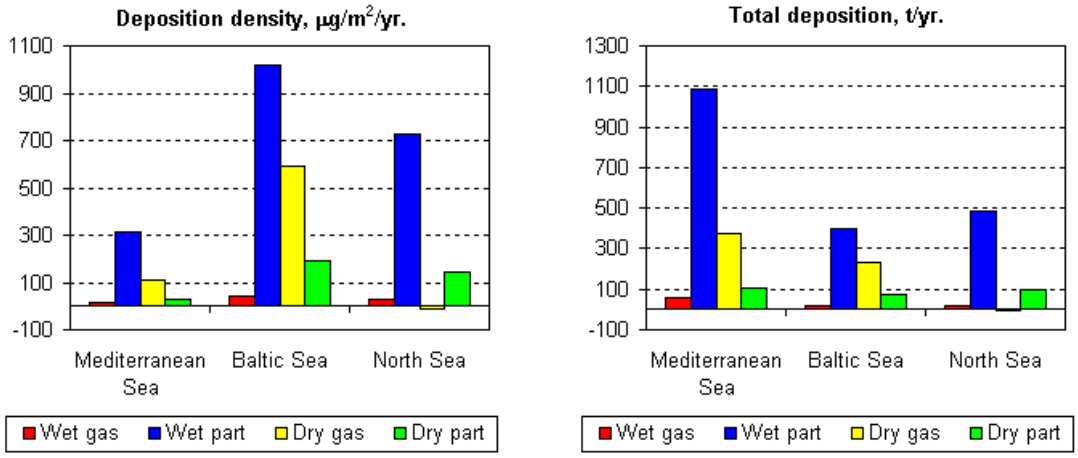

Figure 3.56. Total depositions (right) and deposition densities (left) of PCB on regional seas for 1996

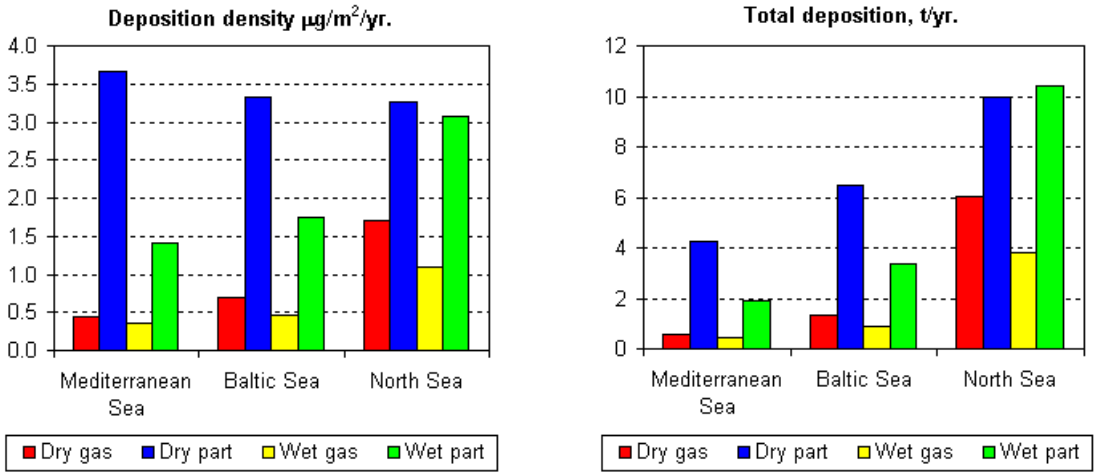

Figure 3.57. Total depositions (right) and deposition densities (left) of benzo[a]pyrene on regional seas for 1996

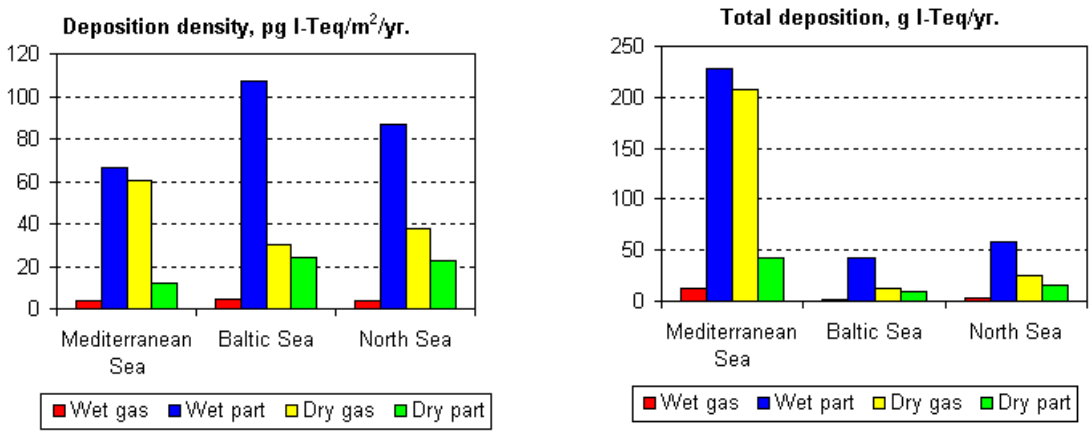

Figure 3.58. Total depositions (right) and deposition densities (left) of 2,3,4,7,8-PeCDF on regional seas for 1996

Chapter 4

Comparison of measurements with modelling results

In this chapter the measurement data obtained at EMEP monitoring stations are analysed and the comparison of modelling results for selected POPs (PCBs, B[a]P, 2,3,4,7,8-PeCDF, and lindane) with measurement data is presented.

4.1. *Analysis of available POP measurement data for 1996 and 1997*

4.1.1. Introduction

Persistent organic components (POPs) have not been a part of the EMEP's monitoring program before 1999. During the sixth phase of EMEP, co-operation concerning POPs between EMEP and other international programs was, however, extended. As a first step the Steering Body of EMEP requested EMEP/CCC to collect already available data on POPs among the participants. A number of stations have been reporting POPs within the EMEP-area in connection with different national and international programmes (HELCOM, AMAP, OSPARCOM). The following POPs are included in this report: PCBs and benzo[a]pyrene.

4.1.2. The measurement sites

The location of the measurement sites for which there are data reported are given in table 4.1.

Table 4.1. List of monitoring stations included in the POPs data base

Country	Station codes	Station name	Location		Height above sea, m
			Lat.	Long.	
Czech Republic	CZ3	Kosetice	49o35'N	15o05'E	633
Finland	FI96	Pallas	67o58'N	24o7'E	566
Germany	DE1	Westerland	54o55'N	8o18'E	12
	DE9	Zingst	54o26'N	12o44'E	1
Iceland	IS91	Stórhöfdi	63o24'N	20o17'W	118
Ireland	IE2	Turlough Hill	53o02'N	6o24'W	420
Norway	NO42	Spitsbergen, Zeppelinfjell	78o54'N	11o53'E	474
Sweden	SE2	Rörvik	57o25'N	11o56'E	10

The site codes used are the new EMEP codes introduced during 1992. Stations without standard EMEP codes have been coded with the country ISO code and numbers from 90 and higher.

4.1.3. Summaries of the data

Annual summaries of POPs in precipitation and air are given in table 2 and 3, respectively. The definitions are as follows:

W.Mean:	the precipitation weighted arithmetic mean value
Min:	the minimum value reported for a specific component
Max:	the maximum value reported for a specific component
Numbel:	the number of data below the detection limit
Num samples:	the number of samples for a specified component
Samp flag:	a flag which gives information on the resolution of the reported data. The code used in this report is: D: daily D1: one day each week D2: two days each week W: weekly WC: weekly with change the first day each month W1: one week each month W2: two-weekly W4: four-weekly M: monthly Y: yearly
QA:	a flag which gives information on the quality of the data (further details in section 4.1.4)
Arit mean:	the arithmetic mean value used for air components only
Arit sd:	the arithmetic standard deviation from the arithmetic mean value. It is computed for air components only
Geom mean:	the geometric mean value used for air components only
50%:	the 50 percentile

A more detailed description of the flags is given in *T.Berg and A.-G.Hjellbrekke* [1998].

Monthly averages of POPs are given in section E3 and E4 (Annex E). The monthly mean values of precipitation data are precipitation weighted arithmetic averages. Average air concentrations are arithmetic averages of the reported values.

The units used for the results in this report are given in table 4.2.

Table 4.2. Units used for the measured components

Components	Units
Amount of precipitation	Mm
POPs in precipitation	ng/l
Benzo[a]pyrene in air	ng/m^3
PCBs in air	pg/m^3

4.1.4. Quality of the monitoring data

To provide sufficiently accurate data for EMEP's needs, data with expected lower accuracy have been flagged (QA) in the tables with annual summaries and monthly means. The definitions of the quality flags are as follows:

1. High detection limit
2. Site location not regionally representative
3. Sampling problems
4. Analytical problems
5. Sampling site at high altitude
6. Concentration level low compared to stations in the neighbourhood
7. Extremely long sampling time
8. Sum of wet deposition + deposited particles on the funnel. Unit: ng/m^2 day
9. Estimated values
10. Extremely high single sample concentrations

The data have been checked for outliners. Extremely high values, outside four times standard deviation in a lognormal distribution, have been flagged in the EMEP database and are excluded from this report.

It is generally difficult to give full credit to the information content in the POP data. SE2 and FI96 have the same type of precipitation sampler with $1m^2$ collection area. The results are given as deposition rates, ng/m^2 day. The rationale is that this includes both wet deposition and some dry deposition on the exposed collector surface. The deposition rates of PCBs at FI96 are about half those at SE2, which is reasonable, considering that precipitation amount are about the same (~400 mm). German data for PCBs in precipitation are low, and most samples are below the detection limit. The concentrations are less than 20% of those reported from SE2. It is recommended to disregard these data. Values from Iceland are generally low, which is also reasonable, considering the geographical location in relation to known source areas.

NO42 has a serious contamination problem for PCBs in 1996. All these data are to be disregarded. The problem may persist in 1997, but these data are more consistent and may be

used with caution. Iceland has low concentrations, which is dominated by the low-chlorinated PCBs. CZ03 shows a more balanced composition of individual PCB congeners. There is a marked seasonal trend, with higher concentrations in the summer months than in fall and winter.

Benzo[a]pyrene (also other PAHs) is rapidly destroyed by UV. In the absence of local sources, therefore, a pronounced seasonal trend is to be expected. However, the low values at CZ3 relative to SE2 are difficult to explain, but may be partly explained by missing data for Sept - Dec 1996. CZ03 reports higher concentration values in 1997. The time series of annual mean concentrations for CZ03, are quite variable. Data reported prior to 1995s, appear to be of mixed quality. The first sample in January 1997 is very high with respect to benzo[a]pyrene in air and also influences the annual mean value. This is related to the meteorological conditions in January 1997 (low temperature, weak winds).

Intercomparisons on POPs still remain to be carried out in the framework of EMEP. As a first step, an Expert Meeting on measurements of POPs in air and precipitation was hold at Lillehammer (Norway) in November 1997. The Expert Meeting gave technical recommendations on measurements of POP in air and precipitation, and on the quality assurance of the POP measurements. A summary from this meeting is published in *A.Lükewille* [1998].

4.2. *General description of the comparison with measurement data*

Below we present the comparison of modelling results of selected POPs with measurements of EMEP monitoring network for 1989-97 [*Berg and Hjellbrekke*, 1998]. Data on concentrations in air and precipitation for PCB-153, B[a]P and lindane measured at the following EMEP stations: CZ3, DE1, DE9, DK31, F196, IE2, IS91, NO42, NO99 and SE2 were used in the comparison. Figure 4.1 shows the locations of these stations.

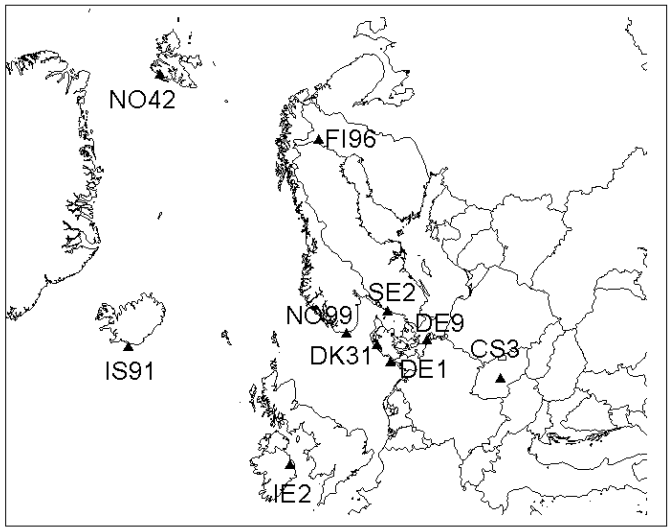

Figure 4.1. Locations of the stations monitoring PCB, B[a]P and lindane

For the comparison the following calculation results were chosen:

- Modelling results of PCB for 1987-97 with no allowance for degradation in vegetation. In the comparison the fraction of PCB-153 emissions in total PCB emissions was taken into account on the basis of above reasoning (chapter 2, section "*Polychlorinated biphenyls*").
- B[a]P modelling results for 1987-97 with no allowance for the atmosphere-vegetation exchange.
- Modelling results of lindane for 1987-97.
- Modelling results of PCDD/Fs for 1996.

Only mean annual concentrations in air and precipitation were used for the comparison. As recommended by CCC (see section 4.1 *Analysis of available POP measurement data for 1996 and 1997*) measurement data of stations NO42 for 1996 and IE2 for 1997 were not used as well as data of IE2 for 1997 since all values appeared to be below the detection limit.

4.3. *Comparison of calculated and measured data on PCB-153*

4.3.1. PCB-153 concentration in precipitation

In the comparison data on PCB-153 mean annual concentrations in precipitation observed at stations DE9, IE2 and IS91 were used. Measurement values and calculation results are presented in table 4.3.

Table 4.3. PCB-153 mean annual concentrations in precipitation, ng/l

Station	Year	Observed	Calculated	Obs/Calc
DE9	1996	0.1	0.091	1.1
DE9	1997	0.428	0.065	6.6
IS91	1995	0.037	0.011	3.4
IS91	1996	0.07	0.013	5.4
Mean		0.159	0.049	4.1

As seen from the data of table 4.3 measured and calculated concentrations in precipitation differ no more than by a factor of 7. For all stations on the average the calculation values are times lower than observations 4.

4.3.2 PCB-153 air concentration

PCB-153 air mean annual concentrations observed at stations CZ3,FI96, IS91, NO42, NO99 and SE2 were used in the comparison. Appropriate measurement values and calculation results are manifested in table 4.4.

Table 4.4. PCB-153 mean annual concentrations in the air, pg/m^3

Station	Year	Observed	Calculated	Obs/Calc
CZ3	1997	40.64	12.76	3.2
FI96	1996	1.52	1.76	0.9
IS91	1995	0.69	1.41	0.5
IS91	1996	1.77	1.90	0.9
IS91	1997	0.27	1.98	0.1
NO42	1993	0.73	0.68	1.1
NO42	1994	0.63	0.68	0.9
NO42	1995	0.32	0.59	0.5
NO42	1997	0.70	0.96	0.7
NO99	1992	48.95	2.85	17.2
NO99	1993	32.69	4.10	8.0
NO99	1994	28.91	4.60	6.3
SE2	1994	5.32	6.63	0.8
SE2	1995	4.45	7.15	0.6
SE2	1996	2.15	6.55	0.3
Mean		11.3	3.6	2.8
Correlation			0.49	

The data of table 4.4 indicate that except for noticeable discrepancies with measurements of station NO99 in 1992 all other values appeared to be within the limits of an order of magnitude. On the average calculated concentrations of PCB-153 are underestimated in 2.8 times compared to measurements. The correlation is 0.49.

4.4. *Comparison of calculated and measured data on B[a]P*

4.4.1. B[a]P concentration in precipitation

In the comparison B[a]P mean annual concentrations in precipitation observed at stations DE1, DE9 and SE2 were used. Measurement values and calculation results are presented in table 4.5.

The comparison results show that the discrepancy between measurements and calculation results for all stations is on the average 2.7 times. The correspondence between wet deposition densities for SE2 station is well enough.

Table 4.5. B[a]P mean annual concentrations in precipitation, ng/l
(for SE2 deposition densities, ng/m^2/day are presented)

Station	Year	Observed	Calculated	Obs/Calc
DE1	1996	3.88	12.96	0.30
DE9	1995	3.84	15.16	0.25
DE9	1996	8.4	17.66	0.47
DE9	1997	6.26	14.48	0.43
Mean		5.60	15.06	0.36
SE2	1996	10.58	11.44	0.93

4.4.2. B[a]P air concentration

B[a]P air mean annual concentrations observed at stations CZ3, SE2, NO42 and FI96 were compared with calculation results. Observed and calculated values are shown in table 4.6.

Table 4.6. B[a]P mean annual concentrations in air, ng/m^3

Station	Year	Observed	Calculated	Obs/Calc
CZ3	1989	2.80	1.20	2.34
CZ3	1990	0.83	1.07	0.78
CZ3	1991	0.02	1.17	0.02
CZ3	1992	0.84	1.10	0.77
CZ3	1993	0.03	1.11	0.03
CZ3	1994	0.03	1.15	0.03
CZ3	1995	0.04	1.69	0.02
CZ3	1996	0.06	1.74	0.03
CZ3	1997	0.64	1.60	0.40
SE2	1994	0.07	0.67	0.10
SE2	1995	0.10	0.69	0.15
SE2	1996	0.09	0.71	0.13
NO42	1997	0.02	0.04	0.45
FI96	1996	0.02	0.18	0.11
Mean		0.40	1.01	0.38

The comparison results manifest that except for station CZ3 the difference between values considered is not more than one order of magnitude. The calculated values overestimate observations at all stations on the average by a factor of 2.3.

In addition calculated values were compared with measurement data found in literature. For example, *P.J.Coleman et al*. [1997] give B[a]P air concentrations in urban regions of the United Kingdom equal 0.3-1.8 ng/m^3. According to [*Cotham and Bidleman*, 1995] mean annual concentration in urban regions is 14 ng/m^3 and in rural regions - 0.12 ng/m^3. The comparison of these data with the calculation results indicate a satisfactory agreement though in general the calculated concentrations are slightly overestimated.

4.5. *Comparison of calculated and measured data on PCDD/Fs*

Modelling results of PCDD/Fs were compared with available measurement data obtained in literature. Calculations were made with the total PCDD/Fs emission for 1996 using physical-chemical properties of 2,3,4,7,8-PeCDF (according to assumptions made for dioxins/furans in section 2.1 *Emission data*). Taking into account the preliminary character of calculations, mean annual concentrations of PCDD/Fs in air were used for the comparison.

Measured concentrations of PCDD/Fs at EMEP station CS3 Kosetice in 1994 were in the

range 2 to 156.3 fg I-TEQ/m^3 with average value 38.4 fg I-TEQ/m^3 [*Lükewille,* 1998]. The calculated value for this cell is 11.7 fg I-TEQ/m^3. According to [*Lohmann and Jones,* 1998] typical air concentrations of PCDD/Fs are less than 10 fg/m^3 I-TEQ at remote sites, from 20 to 50 fg/m^3 I-TEQ at rural ones, and from 100 to 400 fg/m^3 I-TEQ at urban/industrial sites. Calculated mean annual air concentration range approximately from 1 to 150 fg/m^3 I-TEQ which is in a reasonable agreement with measurements.

4.6. *Comparison of calculated and measured data on lindane*

4.6.1 Lindane concentration in precipitation

Calculation results of lindane concentrations in air and precipitation were compared with observational data at monitoring stations. Measured and calculated data of mean annual concentrations of lindane are presented in table 4.7. The comparison of measured and calculated concentrations of lindane in precipitation is shown in figure 4.2.

Table 4.7. Measured and calculated concentrations of lindane in precipitation and the correlation between these sets of data, ng/l

Station	Year	Observed	Calculated	Obs/Calc
DE1	1990	4.54	13.96	0.3
DE1	1992	18.22	11.26	1.6
DE1	1993	9.28	10.97	0.8
DE1	1995	6.32	17.91	0.4
DE1	1996	10.38	20.79	0.5
DK31	1990	16.98	14.32	1.2
DK31	1991	11.91	16.92	0.7
DK31	1992	15.82	10.71	1.5
NO99	1991	4.05	10.28	0.4
NO99	1992	5.02	5.6	0.9
NO99	1993	8.45	11.11	0.8
NO99	1994	9.98	12.87	0.8
NO99	1995	5.54	11.64	0.5
NO99	1996	8.01	24.31	0.3
NO99	1997	4.91	12.06	0.4
DE9	1995	6.52	36.16	0.2
DE9	1997	20.9	33.6	0.6
IE2	1994	1.43	8.36	0.2
IE2	1995	2.15	6.36	0.3
IE2	1996	2.04	9.51	0.2
IE2	1997	4.19	18.97	0.2
IS91	1995	0.44	3.12	0.1
IS91	1996	0.27	4.36	0.1
IS91	1997	0.43	3.89	0.1
Mean		7.4	13.7	0.5
Correlation			0.49	

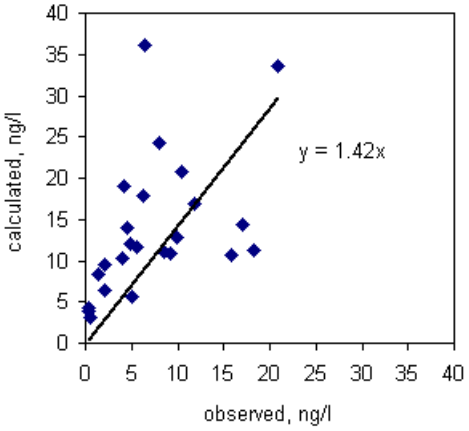

Figure 4.2. Lindane concentration in precipitation, ng/l (comparison of measured data with calculation results)

4.6.2. Lindane air concentration

Measured and calculated data of mean annual concentrations of lindane in air are presented in table 4.8. The comparison of measured and calculated concentrations is shown in figure 4.3.

Table 4.8. Measured and calculated values of lindane concentrations in air and correlation between these sets of data, pg/m^3

Station	Year	Observed	Calculated	Obs/Calc
IS91	1995	14.19	73.07	0.2
IS91	1997	6.42	140.0	0.05
NO42	1993	14.41	31.11	0.5
NO42	1994	16.06	31.61	0.5
NO42	1995	13.13	24.77	0.5
NO42	1996	12.85	42.52	0.3
NO42	1997	15.3	46.7	0.3
NO49	1992	86.25	243.2	0.4
NO99	1993	58.52	349.99	0.2
NO99	1994	122.89	316.11	0.4
NO99	1995	64.98	274.62	0.2
NO99	1996	60.72	369.05	0.2
NO99	1997	62.0	328.0	0.2
FI96	1996	10.67	213.09	0.1
SE2	1994	51.2	441.89	0.1
SE2	1995	26.82	367.61	0.1
SE2	1996	24.8	495.47	0.1
CS3	1997	35.3	591	0.1
Mean		38.7	243.3	0.2
Correlation			0.45	

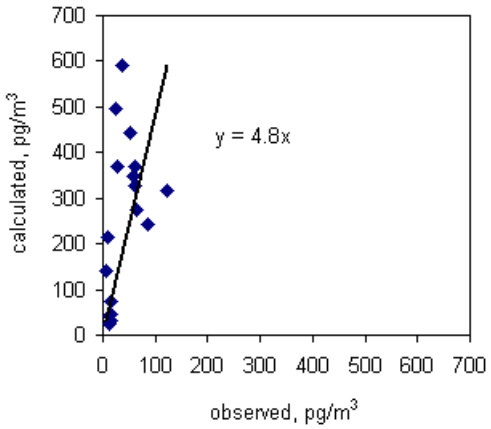

Figure 4.3. Lindane concentrations in air, pg/m^3 (comparison of measured data with calculation results)

As seen from tables 4.7-4.8 and figures 4.2-4.3 calculated mean annual concentrations in air exceed measured ones on the average 6 times and the calculated mean annual concentrations in precipitation exceed measured ones on the average by a factor of 2. The correlation coefficient between calculated and measured values is 0.49 for lindane concentrations in air and 0.45 for lindane concentrations in precipitation.

4.7. *Conclusions*

- The comparison of PCB-153 modelling results with observations manifested that measured mean annual concentrations in precipitation for all stations considered are underestimated on the average by a factor of 4. Measured mean annual concentrations of PCB-153 in air are also 2.8 times underestimated on the average.

- The comparison of calculation results of B[a]P with observations demonstrated that the difference between measured and calculated for concentrations in air and precipitation is 2.3 times on the average. Practically for all stations B[a]P calculated concentrations overestimate the monitoring data.

- Lindane modelling results showed that mean annual concentrations of lindane in air exceed measured ones on the average by a factor of 6. The correlation coefficient for air concentrations is 0.45.

- Calculated mean annual concentrations of lindane in precipitation exceed measured ones by a factor of 2. The correlation coefficient between measured and calculated concentrations in precipitation is 0.49.

Chapter 5

Conclusions

During this year the development of 3D eulerian POP model has been continued. Approaches to modelling of selected PCBs, PAHs, PCDD/Fs, and lindane were further investigated. For the majority of species both gas and aerosol phases in air were taken into account. Air/vegetation exchange was incorporated into the model and tentative calculations were performed. The analysis of available official emission data and emission estimates of POPs has been made. POP measurement data for 1996-97 have been analysed as well.

The results of tentative calculations for selected POPs show that the export outside the EMEP grid amounts to a considerable part of the emission. This indicates that assessment of POP contamination requires hemispheric or global scale modelling.

5.1. *PCB modelling*

- Developing approaches for estimating the pollution by PCBs, seven PCB congeners (PCB-28, 52, 101,118, 138, 153 and 180) have been selected for modelling representing a wide spectrum of properties inherent to this group. On the basis of their physical-chemical properties the parameterization of the model was made and tentative calculations were performed.

- The calculation results testify that due to the differences in physical-chemical properties the contributions of main processes such as degradation and dry/wet deposition to overall mass balance for selected congeners are essentially different. For low chlorinated congeners the gas phase predominates in the air whereas for high chlorinated congeners so does the aerosol phase.

- For low chlorinated PCB congeners the maximum contribution to the input to soil is due to dry deposition of the gas phase. The more chlorinated the congener is the less is the contribution of the gas phase to total deposition on soil.

- For all congeners except for PCB-180 dry deposition of the gas phase makes the maximum contribution to the input to sea. The contribution of the aerosol phase (especially for wet deposition) is increased for highly chlorinated congeners.
- The analysis of calculation results for selected seven PCB congeners shows that PCB-153 can be used as an indicator congener for a development of approaches to modelling of PCBs (with possible deviation within the factor of 1.5).
- The atmosphere/vegetation exchange process can appreciably affect transboundary transport of PCBs. According to preliminary calculations the uptake of PCBs by vegetation amounts to 25-30%.
- The calculation results of PCB transport for the period of 11 years with properties of PCB-153 manifest that the accumulation process in soil and sea water does not reach quasi-stationarity state during this period. The gaseous exchange between air and marine water reaches quasi-stationary state during the second year. The re-emission from the sea reservoir is observed as early as during the first year whereas re-emission from soil is not observed during the whole period.
- The comparison of PCB-153 modelling results with measurements showed that measured mean annual concentrations in precipitation are underestimated on the average by a factor of 4, measured mean annual concentrations in air - on the average by a factor of 3.

5.2. *B[a]P modelling*

- Developing approaches to evaluation of contamination by PAHs, physical-chemical properties of several compounds from this group were analyzed. B[a]P was chosen as an indicator compound for modelling. The model parameterization was refined and tentative calculations were made.
- According to calculation results the most essential processes affecting B[a]P transboundary transport are degradation in air and dry and wet deposition of the aerosol phase. The fraction of gas phase varied from 1% in winter to 15% in summer.
- Dry deposition of B[a]P over land makes more essential contribution to total depositions compared with wet deposition. Over sea, contributions of dry and wet depositions are comparable. The contribution of the gaseous flux both over soil and sea is small.
- Preliminary calculations with allowance of air/vegetation exchange showed that under the current model parameterization the influence of this process on the transboundary transport is inessential.
- The calculation results of B[a]P transport for the period of 11 years showed that the accumulation process in soil and sea water does not reach quasi-stationarity during this period. No re-emission from sea and land surfaces is observed during 11-year period.

- The comparison of B[a]P modelling results with measurements showed that measured concentrations in air and in precipitation are overestimated approximately by a factor of 3.

5.3. *Dioxins/furans modelling*

- The main sources of emission of dioxins/furans to the atmosphere are organic fuel combustion, waste incineration and secondary non-ferrous treatment. The contribution of these sources to the total emission of PCDD/Fs amounts to 60%.

- The analysis of PCDD/F physical-chemical properties allowed to select the following homologue groups: PeCDF, HxCDF, and PeCDD. The PeCDF group makes a considerable contribution to the total toxicity. The main congener forming the toxicity of this group is 2,3,4,7,8-PeCDF. On the basis of the above-mentioned analysis the parameterization of the model was developed and the tentative calculation were made for 2,3,4,7,8-PeCDF.

- The main process in the modelling of the transboundary transport of PCDD/F is the exchange with the underlying surface. The input to soil in the framework of the EMEP region amounts to 30% of the annual emission, and the input to sea – to 20%. The degradation in sea plays the essential role in the air/sea exchange: from 20% of total emission accumulated in sea 18% have been degraded.

- The fraction of the 2,3,4,7,8-PeCDF bound to particles strongly depends on the temperature. This fraction amounts to more than 98% at -20^0 C and decreases to 8% at $+30^0$ C.

- The inputs from the atmosphere to soil due to dry and wet depositions of gas and aerosol phases are approximately the same whereas the input to sea takes place at most due to dry and wet deposition of the gaseous phase (about 70%). No re-emission from sea and land surfaces is observed during the calculation period.

5.4. *Lindane modelling*

- Modelling results covering 11 year period indicated that an essential part of this substance enters soil and sea (23% and 17% respectable) or is degraded in air (half-life in air is 46 days) or transported outside the EMEP grid. The export outside the EMEP grid after 11 years was 46%, degradation in air 14%.

- Lindane accumulation in soil is very fast: during the first year it reached about 8% of annual emissions. The accumulation processes is retarded due to lindane degradation in soil (life-time in soil is about 1 year) and amounts to 15% of annual emissions.

- Lindane accumulation in seas is most intensively during first 7 years. Then the accumulation is retarded due to degradation in the marine environment (half-life about 7 years).

- Lindane input to soil due to wet deposition predominated over its input to soil due to gas phase dry deposition. Lindane input to sea due to gas phase dry deposition predominated over wet deposition.

- The comparison of calculation results against measurements showed that mean annual concentration of lindane in air exceeded observations on the average by a factor of 6. The calculated mean annual concentration in precipitation exceeded observations on the average by a factor of 2.

- For modelling of lindane transport it is planned to take into account both gas and aerosol phases in air. The influence of air/vegetation exchange is also planned to be considered.

5.5. *Directions of further research*

On the following stages of the development of modelling bases for selected POPs it is necessary:

- to refine expert estimates of POPs emissions.

- to study further PCB, PAH and dioxins/furans physical-chemical properties synthesizing scientific results obtained within the framework of MEPOP programme and other national and international programmes.

- to refine the description of the exchange with sea medium including the transport with sea currents, sedimentation process, and partitioning between dissolved and suspended phases.

- to refine further the description of the air/vegetation exchange process with refinement of kinetic parameters of the exchange (uptake and re-emission rates, degradation rate, etc.) for different types of vegetation.

- to develop model of POP transport models on the hemispherical and global scales to assess the transboundary transport in the European region.

- to refine data on different characteristics of the underline surface including data on land-use, leaf index, content of organic carbon in soil and ocean currents.

- to broaden co-operation with international and national programmes (MEPOP, PARCOM, HELCOM, AMAP etc.) for the investigation of all the problems since there are great uncertainties in emission data, physical-chemical parameters of the considered species, and in the description of processes influencing POP transport over long distances.

ANNEX A

Basic POP physical-chemical properties affecting their transport in the environment

As it was already mentioned POP transport in the environment in many respects depends on their physical-chemical properties. These first of all include saturated vapour pressure, solubility, Henry constant, octanol-water, octanol-air and organic carbon-water partition coefficients. In what follows a brief description of basic physical-chemical properties is given.

A.1. *Vapour pressure*

Saturated vapour pressure characterizes a capability of a substance to be transferred to the gaseous state (for liquid this process is called vaporization for solid substances - sublimation). According to the classification suggested by *F.Wania and D.Mackay* [1996] the efficiency of POP condensation with subcooled liquid pressure (p^0_L) at 25^0C above 1 Pa is very low. POPs with vapour pressure from 1 to 10^{-2} Pa are condensed at the temperature about -30^0C and they deposit mostly in the polar latitudes. Species with vapour pressure of subcooled liquid from 10^{-2} to 10^{-4} Pa are condensed at the temperature above 0^0C and the fall out mainly in the middle latitudes. Finally POPs of low volatility with vapour pressure of subcooled liquid below 10^{-4} Pa actually are not vaporized or this process goes on very slowly and these substances tend to deposit in the vicinity of a source.

Using vapour pressure of subcooled liquid it is possible to characterize POP partitioning between the gas phase and solid phase of atmospheric aerosol. According to the Junge-Pankow model [*Junge*, 1977; *Pankow,* 1987] POP fraction adsorbed on particle surfaces is:

$$\phi = c\theta / (p^0_L + c\theta), \qquad \text{(A1)}$$

where c is the constant dependent on thermodynamic parameters of the adsorption process and on properties of aerosol particle surface (c = 0.17 Pa×m [*Junge,* 1997];

θ is the specific surface of aerosol particles, m^2/m^3. ($\theta = 1.5\times10^{-4}$ for background aerosol).

Thus POP with lower vapour pressure are better sorbed on atmospheric aerosol particles thereby increasing the probability of their subsequent deposition and washout with precipitation.

A.2. *Henry constant*

Another important physical-chemical parameter of POP affecting their behaviour in the atmosphere is Henry constant (H, Pa m^3/mol).

Under natural conditions maximum possible values such as saturated vapour pressure in air and solubility in water are not as a rule achieved. However, according to Henry law the ratio of equilibrium values of substance partial pressure P_A to its concentration in water C_W equals the ratio of saturated vapour pressure p^0 and solubility S which is named for Henry constant H, i.e. the proportion

$$\frac{P_A}{C_W} = \frac{p^0}{S} = H \qquad \text{(A2)}$$

is fulfilled. Here H - Henry constant in this case measured in [Pa m^3/mol] on the assumption that species concentration in water is measured in mol/m^3. Expressing saturated vapour pressure of a substance in terms of its air molar concentration using Mendeleev-Clapeyron equation, one can represent the Henry constant in the dimensionless form K_H:

$$\frac{C_A}{C_W} = K_{AW} = K_H = \frac{H}{RT} \qquad \text{(A3)}$$

here K_{AW} is the dimensionless atmosphere-water partition coefficient;
R is the universal gas-constant;
T is the absolute temperature, K.

Henry constant value is used in the description of the following processes affecting POP long-range transport:

1. Gaseous exchange between atmosphere and soil.

2. Gaseous exchange between atmosphere and sea water.

3. Wet scavenging of the POP gaseous phase.

A.3. *Octanol-water partition coefficient*

Octanol-water partition coefficient (K_{OW}) is a measure of substance hydrophoby and characterizes its partitioning between water and lipid media substituted for octanol. It is

determined as a ratio of equilibrium concentrations in octanol C_O (mol/l) and in water C_W (mol/l):

$$K_{OW} = C_O / C_W \qquad \text{(A4)}$$

K_{OW} is used for estimation of partition coefficient in the organic carbon-water system (K_{OC}), of partition coefficient in the octanol-air system (K_{OA}), and of bioconcentration factor (BCF).

A.4. *Organic carbon-water partition coefficient*

For the description of POP sorption by soil and bottom sediments organic carbon-water partition coefficient (K_{OC}, dm^3/kg) is used. It is determined as:

$$K_{OC} = K_P / f_{OC}, \qquad \text{(A5)}$$

where K_P is the partition coefficient equal to the ratio of POP concentration in the solid state of soil (bottom sediments) to that in the water phase;
f_{OC} is the mass fraction of organic carbon in soil and bottom sediments.

K_{OC} value can be estimated by octanol-air partition coefficient (K_{OW}) using the following correlation relations:

$$\log K_{OC} = 1.00 \log K_{OW} - 0.21 \qquad \text{[}\textit{Karikhoff et al.}\text{, 1979]}$$

or

$$K_{OC} = 0.41 K_{OW}. \qquad \text{[}\textit{Karikhoff,}\text{ 1981].}$$

A.5. *Octanol-air partition coefficient*

Octanol-air partition coefficient (K_{OA}) characterizes partitioning between air and lipid film (cuticle) covering the plant surface. Besides in the literature of recent years [*Wania*, 1997 and references of this article; *Harner and Bidleman*, 1998] it is shown that the basic mechanism of POP sorption by atmospheric aerosol can be the absorption process by the organic film covering the particles. It is true for urban aerosol particles characterized by relatively high content of organic matter. For the description of POP partitioning between the gas phase and particle organic film coefficient K_{OA} is used [*Finizio et al.*, 1997].

Octanol-air partition coefficient is an equilibrium ratio of POP concentrations in octanol and air. Its value can be determined on the basis of octanol-air and air-water partition coefficients (see equation (A3)):

$$K_{OA} = K_{OW} / K_{AW} = K_{OW} \times RT / H. \qquad \text{(A6)}$$

This estimate, however, leads to a considerable error since K_{OW} characterizes POP partitioning between octanol saturated with water and water saturated with octanol whereas

Henry constant characterizes partitioning between pure water and air. Besides an inaccuracy in the determination of K_{OW} value and Henry constant also introduces an error to value K_{OA}. Therefore it is better to use value K_{OA} obtained by direct measurements, for example [*Harner et al*., 1995; *Harner and Bidleman*, 1996].

It should be mentioned that for POP modelling it is necessary to know temperature dependencies of physical-chemical characteristics (saturated vapour pressure, Henry constant, octanol-air partition coefficient), data on POP distribution with particle sizes in the atmosphere and degradation constants in environmental compartments. These characteristics for different groups of pollutants are presented in annexes B, C, and D.

ANNEX B

PCB physical-chemical properties

Polychlorinated biphenyls (PCBs) are toxic pollutants characterized by persistence in the atmosphere and other environmental compartments, by their ability to be transported over long distance and to be accumulated in food chains. PCBs are included in the Protocol on persistent organic pollutants under UN ECE Convention on Long-Range Transboundary Air Pollution of 1979.

B.1. *The selection of priority PCB congeners for modelling*

PCBs are derivatives of biphenyl in which from one to ten atoms of hydrogen are substituted for chlorine atoms. Among 209 of PCB possible congeners so-called "coplanar" compounds are most dangerous. They have not more than one chlorine atom in ortho-position (positions 2,2',6,6') allowing both rings to be approximately in one plane. In regard to toxicity these substances are similar to polychlorinated dibenzo-paradioxins (PCDDs) and polychlorinated dibenzofurans (PCDFs). Toxicity equivalents were designated to the following congeners (No. corresponds to IUPAC classification): 77, 81, 126, 169 (non-ortho congeners of PCB), and 105, 114, 118, 123, 156, 157, 167, 189 (mono-ortho congeners).

On the other hand, the greatest contribution of the overall emissions of PCBs to the atmosphere (indicative PCB see [*Baart et al.*, 1995]) make congeners with IUPAC Nos. 28, 52, 101, 118 (mono-ortho congeners), and 138, 153, and 180 representing a wide spectrum of PCBs with chlorine content from three (PCB-28) to seven (PCB-180) atoms.

Furthermore data on concentrations in the atmosphere and other natural compartments of these congeners are most frequent in the literature allowing to compare simulation results with measurement values. For further investigation and simulation we have chosen the congeners with IUPAC Nos. 28, 52, 101, 118, 138, 153, and 180 characterizing the behaviour of five homologous groups in the atmosphere and other media. At the next stage obviously a special attention should be paid to more toxic coplanar congeners.

The structur composition, and some properties of polychlorinated biphenyls listed are presented in table B1.

Table B1. Structure, composition and some properties of selected congeners PCB

IUPAC number	Compound	Structural formula	Brutto formula	Molec. mass	Toxicity
28	2,4,4'–Cl_3biphenyl	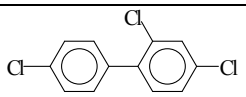	$C_{12}H_7Cl_3$	257.7	non toxic
52	2,2'5,5'-Cl_4 biphenyl	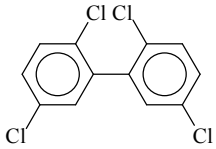	$C_{12}H_6Cl_4$	292	non toxic
101	2,2'4,5,5'-Cl_5 biphenyl	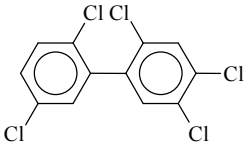	$C_{12}H_5Cl_5$	326.4	non toxic
118	2,3',4,4',5-Cl_5 biphenyl	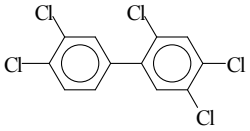	$C_{12}H_5Cl_5$	326.4	toxic*
138	2,2,3,4,4',5'-Cl_6 biphenyl	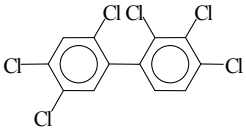	$C_{12}H_4Cl_6$	360.9	non toxic
153	2,2',4,4'5,5'–Cl_6 biphenyl	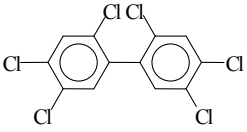	$C_{12}H_4Cl_6$	360.9	non toxic
180	2,2',3,4,4',5,5'-Cl_7 biphenyl	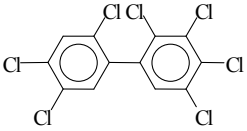	$C_{12}H_3Cl_7$	395.3	non toxic

* - Toxicity equivalent according to WHO international system is 0.0001

B.2. *Physical-chemical properties*

B.2.1. Dependence of saturated vapour pressure on temperature

The dependence of the saturated vapour pressure p^0_L of subcooled liquid on the temperature for 180 PCB congeners was determined by *R.L.Falconer and T.F.Bidleman* [1994] in the form of log p^0_L (Pa) = $-A/T(K) + B$. The coefficients of this dependence for seven PCB congeners are listed in table B2.

Table B2. Dependence of the saturated vapour pressure of subcooled liquid (Pa) on the temperature for seven PCB congeners: log p^0_L (Pa) = $-A/T$ (K) + B [*Falconer and Bidleman*, 1994]

IUPAC No.	Chlorine atoms positions	*A*	*B*
28	2,4,4’	4075	12.20
52	2,2’,5,5’	4220	12.36
101	2,2’,4,5,5’	4514	12.67
118	2,3’,4,4’,5	4664	12.72
138	2,2’,3,4,4’,5’	4800	12.81
153	2,2’,4,4’,5,5’	4775	12.85
180	2,2’,3,4,4’,5,5’	5042	13.03

The values of p^0_L (Pa) calculated by these dependencies for different ambient temperatures are given in table B3.

Table B3. Values of subcooled liquid vapour pressure (Pa) at different temperatures for seven PCB congeners

IUPAC No.	Chlorine atom position	p^0_L, Pa			
		-10^0C	0^0C	$+10^0$C	$+25^0$C
28	2,4,4’	5.1×10^{-4}	1.9×10^{-3}	6.3×10^{-3}	3.4×10^{-2}
52	2,2’,5,5’	2.0×10^{-4}	8.0×10^{-4}	2.8×10^{-3}	1.6×10^{-2}
101	2,2’,4,5,5’	3.2×10^{-5}	1.4×10^{-4}	5.2×10^{-4}	3.3×10^{-3}
118	2,3’,4,4’,5	9.7×10^{-6}	4.3×10^{-5}	1.7×10^{-4}	1.2×10^{-3}
138	2,2’,3,4,4’,5’	3.6×10^{-6}	1.7×10^{-5}	7.1×10^{-5}	5.0×10^{-4}
153	2,2’,4,4’,5,5’	4.9×10^{-6}	2.3×10^{-5}	9.5×10^{-5}	6.7×10^{-4}
180	2,2’,3,4,4’,5,5’	7.2×10^{-7}	3.6×10^{-6}	1.6×10^{-5}	1.3×10^{-4}

As evident from table B3 for all the congeners p^0_L values increase with temperature rise resulting in the reduction of their adsorption on particles (see eq. (B12) below).

B.2.2. Henry constant dependence on temperature

Henry constant values (H, Pa m^3/mol) at 25^0C for seven PCB congeners published in literature are given in table B4.

Table B4. Henry constants (Pa m^3/mol) at 25^0C for seven PCB congeners

IUPAC No.	[*Mackay et al.*, 1992] range	[*Mackay et al.,* 1992] calculated, recommended value	[*Finizio et al.*, 1997]	[*Dunnivant et al.,* 1992] calculated value*
28	20.27 – 33.0	-	-	28.58
52	2.53 – 160	47.59	47.59	31.92
101	7.09 – 217	35.48	35.48	24.55
118	-	-	-	12.56
138	2.13 – 69.0	-	10.84	13.00
153	2.33 – 224	42.9	18.24	16.48
180	1.013 – 102	-	-	10.74

* - values chosen for modelling

As seen from table B4 the range of Henry constant values presented in the handbook by *D.Mackay et al.* [1992] is very wide. For three congeners (52, 101 and 153) recommended values are given in [*Mackay et al.,* 1992]. The same values are presented later in the article by *A.Finizio et al.* [1997]. The only exception is Henry constant for PCB-153 which value presented in the above mentioned paper is more than twice lower than that recommended by *D.Mackay* [1992]. The constants for PCB-52, 101, 138 and 153 from [*Dunnivant et al.,* 1992] which are absent in the handbook by *D.Mackay* are comparable with values presented in the paper [*Finizio et al.,* 1997]. In addition data on three remained congeners are also given in this paper. These very values have been chosen for simulation calculations.

In order to describe PCBs behavior in the environment it is necessary to determine temperature dependencies of Henry constant. The dependence can be expressed by equation:

$$\log H = \log H_{298} + \frac{\Delta H_W}{2.303R}\left(\frac{1}{T_0} - \frac{1}{T}\right) \qquad \text{(B1)}$$

where H_{298} is Henry constant (Pa×m^3/mol) at 25^0C (298K);
ΔH_W is the enthalpy of volatilization from water, kJ/mol;
R is the universal gas constant, 8.314×10^{-3} kJ/mol K;
T is the absolute temperature, K.

Measured values of ΔH_W for two congeners (PCB-28 and PCB-52) and PCB homologous groups with the number of chlorine atoms from three to seven are summarized in the paper [*Wania,* 1997] and presented in table B5.

On the basis of eq.(B1) temperature dependence of Henry constant can be expressed in form:

$$\log H = -A/T\,(K) + B \qquad \text{(B2)}$$

where $A = \Delta H_W/2.303R$;
$B = \log H_{298} + \Delta H_W/2.303R(298)$.

Table B5. Measured values of ΔH_W for a number of PCB congeners and homologous groups

Congeners and homologue groups	ΔH_W, kJ/mol	Reference cited from [*Wania*, 1997]
PCB-28	50	[*ten Hulscher et al*., 1992]
PCB-52	52	[*ten Hulscher et al*., 1992]
Trichlorobiphenyls	61.8	[*Burkhard et al*., 1985]
Tetrachlorobiphenyls	64.7	[*Burkhard et al*., 1985]
Pentachlorobiphenyls	67.2	[*Burkhard et al*., 1985]
Hexachlorobyphenyls	69.4	[*Burkhard et al*., 1985]
Heptachlorobiphenyls	71.3	[*Burkhard et al*., 1985]

Using ΔH_W values from table B5 and Henry constants at 25^0C from table B4 the following temperature dependencies of Henry constants were determined (table B6):

Table B6. Coefficients of Henry constant (Pa m^3/mol) temperature dependencies (B.2) for seven PCB congeners

IUPAC No.	Chlorine atom position	*A*	*B*
28	2,4,4’	3227 [*Burkhard et al*., 1985] 2611 [*ten Hulscher et al*., 1992]	12.28 10.22
52	2,2’,5,5’	3379 [*Burkhard et al*., 1985] 2716 [*ten Hulscher et al*., 1992]	12.84 10.62
101	2,2’,4,5,5’	3510 [*Burkhard et al*., 1985]	13.17
118	2,3’,4,4’,5	3510 [*Burkhard et al*., 1985]	12.88
138	2,2’,3,4,4’,5’	3625 [*Burkhard et al*., 1985]	13.27
153	2,2’,4,4’,5,5’	3625 [*Burkhard et al*., 1985]	13.38
180	2,2’,3,4,4’,5,5’	3724 [*Burkhard et al*., 1985]	13.53

The comparison of Henry constant values for PCB-28 and 52 calculated on the basis of the data of *L.P.Burkhard et al.* [1985] and *Th.E.M. ten Hulscher et al.* [1992] at different ambient temperature values are presented in table B7.

Table B7. Henry constants (Pa m^3/mol) for PCB-28 and 52 at different temperatures calculated from data of *L.P.Burkhard et al.* [1985] and *Th.E.M. ten Hulscher et al.* [1992]

Reference	PCB-28				PCB-52			
	0^0C	10^0C	20^0C	25^0C	0^0C	10^0C	20^0C	25^0C
[*Burkhard et al*., 1985]	2.88	7.54	18.46	28.58	2.90	7.94	20.30	31.92
[*ten Hulscher et al*., 1992]	4.53	9.86	20.36	28.58	4.69	10.54	22.41	31.92

The data of table B7 show that Henry constant values calculated on the basis of *Th.E.M. ten Hulscher* values for 0^0C are about 1.5 time higher than those obtained by *L.P.Burkhard* data [*ten Hulscher et al.* 1992]. This discrepancy decreases with temperature increase and at the temperature of 25^0C Henry constant values coincide. For modelling purposes temperature dependencies determined by *L.P.Burkhard's* data were used (for PCB-28: $\log H = -3227/T(K) + 12.28$; for PCB-52: $\log H = -3379/T(K) + 12.84$) [*Burkhard et al.* 1985].

B.2.3. Temperature dependence of octanol-air partition coefficient

Temperature dependencies of octanol-air partition coefficients for 15 PCBs were determined *by T.Harner and T.F. Bidleman* [1996] for temperature range from -10^0 to $+ 30^0$C in the form:

$$\log K_{OA} = A/T(K) - B. \qquad \text{(B3)}$$

Five of them are from the list of congeners chosen above for modelling. For the rest (PCB-28 and 52) the following estimate was made. First using data of table B2 the saturated vapor pressure of subcooled liquid at 20^0C (293K) was calculated. Then using the regression equation derived by *T.Harner and T.F.Bidleman* [1996] octanol-air partition coefficient at 20^0C was estimated.

For congeners without chlorine atom and for mono-ortho congeners (PCB-28):

$$\log K_{OA} = (-1.268) \log p^0_L + 6.135, \qquad r^2 = 0.995 \qquad \text{(B4)}$$

For multi-ortho congeners (PCB-52):

$$\log K_{OA} = (-1.015) \log p^0_L + 6.490, \qquad r^2 = 0.997 \qquad \text{(B5)}$$

For trichlorobiphenyls in [*Harner and Bidleman,* 1996] the experimental dependence was estimated for PCB-29 only. For this reason coefficient A for PCB-28 was taken to be equal to the corresponding coefficient for PCB-29 (3792).

Among five tetrachlorobiphenyls for which temperature dependencies of K_{OA} were estimated by *T.Harner and T.F.Bidleman* [1996] only PCB-49 has the configuration similar to that of PCB-52 (two chlorine atoms in ortho position) and close values of p^0_L and consequently of

K_{OA} at 20^0C. For this reason the coefficient A for PCB-52 was assumed to be equal to the corresponding coefficient for PCB-49 (3981).

Coefficient B was calculated by formula:

$$B = A/293 - \log K_{OA}^{293}, \quad \text{(B6)}$$

where K_{OA}^{293} is the octanol-air partition coefficient at 20^0C (293K).

The dependencies determined experimentally and estimated are presented in table B8.

Table B8. Octanol-air partition coefficient dependence on temperature for seven PCB congeners: $\log K_{OA} = A/T(K) - B$

IUPAC No.	Chlorine atom positions	A	B	Reference
28	2,4,4’	3792	4.63	Estimate (see text)
52	2,2’,5,5’	3981	5.02	Estimate (see text)
101	2,2’,4,5,5’	3841	3.82	[*Harner and Bidleman,* 1996]
118	2,3’,4,4’,5	4693	5.92	[*Harner and Bidleman,* 1996]
138	2,2’,3,4,4’,5’	4584	5.57	[*Harner and Bidleman,* 1996]
153	2,2’,4,4’,5,5’	4695	6.02	[*Harner and Bidleman,* 1996]
180	2,2’,3,4,4’,5,5’	4535	4.70	[*Harner and Bidleman,* 1996]

Octanol-air partition coefficients at 25^0C determined on the basis of these dependencies are given in table B9.

Table B9. Octanol-air partition coefficients at 25^0C for seven PCBs

IUPAC No.	Chlorine atom positions	$\log K_{OA}$
28	2,4,4’	8.09
52	2,2’,5,5’	8.34
101	2,2’,4,5,5’	9.07
118	2,3’,4,4’,5	9.83
138	2,2’,3,4,4’,5’	9.81
153	2,2’,4,4’,5,5’	9.74
180	2,2’,3,4,4’,5,5’	10.52

According to table B9 K_{OA} value increases with the increase of PCB chlorination degree. Besides within the homologue group K_{OA} value for PCB-118 (mono-ortho congener) is higher than for PCB-101 (congener with two chlorine atoms in ortho-position).

B.2.4. Molecular diffusion coefficients

In order to describe POP air-soil exchange process it is necessary to know molecular diffusion coefficients for air and water. Molecular diffusion coefficient of an organic compound in air (D_A, cm^2/s) can be estimated by formula [*Schwarzenbach et al.,* 1993]:

$$D_A = 10^{-3} \cdot \frac{T^{1.75}\left[(1/M_{air}) + (1/M)\right]^{1/2}}{p\left[\overline{V}_{air}^{1/3} + \overline{V}_m^{1/3}\right]^2} \qquad \text{(B7)}$$

where T is the absolute temperature, 298 K;
M_{air} is the mean molecular air mass, ~29 g/mol;
M is the molecular mass of an organic substance, g/mol;
p is the pressure, 1 atm;
$\overline{V}_{air}$ is the mean molecular volume of gases in air, ~20.1 cm^3/mol;
$\overline{V}_{\mathrm{m}}$ is the organic matter molecular volume, cm^3/mol.

The values of molecular masses and molar volumes for seven PCB congeners taken from the handbook [*Mackay et al.,* 1992] are given in table B10.

Table B10. Molecular masses (g/mol) and molar volumes (cm^3/mol) for seven PCB congeners [*Mackay et al.,* 1992]

IUPAC No.	Chlorine atom positions	M, g/mol	$\overline{V}$, cm^3/mol
28	2,4,4’	257.5	247.3
52	2,2’,5,5’	292	268.2
101	2,2’,4,5,5’	326.4	289.1
118	2,3’,4,4’,5	326.4	289.1
138	2,2’,3,4,4’,5’	360.9	310
153	2,2’,4,4’,5,5’	360.9	310
180	2,2’,3,4,4’,5,5’	395.3	330.9

Using eq.(B7) diffusion coefficient D_A was determined for PCB-153. It is equal to 4.58×10^{-6} cm^2/s.

Diffusion coefficients for the rest of congeners were estimated by the following formula:

$$\frac{D_A}{D_A^{153}} \cong \left[\frac{M^{153}}{M}\right]^{1/2} \qquad \text{(B8)}$$

where D_A^{153} is the molecular diffusion coefficient of PCB-153 in air;
D_A is the molecular diffusion coefficient of a given PCB congener in air;
M^{153} is the molecular mass of PCB-153, g/mol;
M is the molecular mass of a given PCB congener.

The obtained values of molecular diffusion coefficients in air are given in table B11.

Table B11. Molecular diffusion coefficients in air at 25^0C of PCB seven congeners, D_A, m^2/s

IUPAC No.	Chlorine atom positions	D_A, m^2/s
28	2,4,4’	5.42×10^{-6}
52	2,2’,5,5’	5.09×10^{-6}
101	2,2’,4,5,5’	4.82×10^{-6}
118	2,3’,4,4’,5	4.82×10^{-6}
138	2,2’,3,4,4’,5’	4.58×10^{-6}
153	2,2’,4,4’,5,5’	4.58×10^{-6}
180	2,2’,3,4,4’,5,5’	4.38×10^{-6}

For the determination of molecular diffusion coefficients for organic substances in water (D_W, cm^2/s) the following ratio [*Schwarzenbach et al.,* 1993] can be used:

$$D_W = \frac{13.26 \times 10^{-5}}{\mu^{1.14} \cdot (\overline{V}_m)^{0.589}} \qquad \text{(B9)}$$

where μ is the solution viscosity in centipoise at a certain temperature is taken to be equal to water viscosity, 0.894 cps at 298K,
$\overline{V}_m$ is the mean molecular volume of a substance, cm^3/mol.

Using eq.(B9) molecular diffusion coefficient for PCB-153 was estimated as 5.14×10^{-10} m^2/s.

Diffusion coefficients of the rest congeners were estimated by the following formula:

$$\frac{D_W}{D_W^{153}} \cong \left[\frac{M^{153}}{M}\right]^{1/2}, \qquad \text{(B10)}$$

where D_W^{153} is the molecular diffusion coefficient of PCB-153 in water;
D_W is the molecular diffusion coefficient of a given PCB congener in water;
M^{153} is the molecular mass of PCB-153, g/mol;
M is the molecular mass of a given PCB congener.

D_W values obtained are presented in table B12.

Table B12. Molecular diffusion coefficients of seven PCB congeners in water at 25^0C, D_W, m^2/s

IUPAC No.	Chlorine atom positions	D_W, m^2/s
28	2,4,4’	6.09×10^{-10}
52	2,2’,5,5’	5.71×10^{-10}
101	2,2’,4,5,5’	5.40×10^{-10}
118	2,3’,4,4’,5	5.40×10^{-10}
138	2,2’,3,4,4’,5’	5.14×10^{-10}
153	2,2’,4,4’,5,5’	5.14×10^{-10}
180	2,2’,3,4,4’,5,5’	4.91×10^{-10}

Data of tables B11 and B12 show that the molecular diffusion coefficients both in air and water decrease with the increase of chlorination degree.

B.2.5. Gas/particle partitioning in the atmosphere

PCB partitioning between the gas and particulate phase in the atmosphere independent of the sorption mechanism is characterized quantitatively by partition coefficient K_P ($m^3/\mu g$):

$$K_P = \frac{C_P}{C_G \cdot TSP}, \qquad \text{(B11)}$$

where C_P is PCB concentration bound with aerosol particles, ng/m^3,
C_G is PCB concentration in the gas phase, ng/m^3,
TSP is the concentration of total suspended particulate matter in air, $\mu g/m^3$.

According to Junge-Pankow model the basic mechanism of POP sorption is adsorption on the particle surface. The fraction of adsorbed substance (ϕ) can be determined by equation [*Junge,* 1977; *Pankow,* 1987]:

$$\phi = c\theta / (p^0_L + c\theta) \qquad \text{(B12)}$$

where θ is the specific area of aerosol particles, m^2/m^3,
c is the constant equal to 0.17 Pa m [*Junge*, 1977].

Fractions of PCB adsorbed on particles calculated for the background aerosol ($\theta = 1.5\times10^{-4}$ m^2/m^3) from eq.(B12) and the data of table B2 are given in table B13.

Table B13. PCB fractions adsorbed on atmospheric aerosol particles at different temperatures, %

IUPAC No.	Chlorine atom positions	$\phi \times 100$, %			
		-10^0C	0^0C	10^0C	25^0C
28	2,4,4’	5	1	0.4	0.1
52	2,2’,5,5’	11	3	1	0.2
101	2,2’,4,5,5’	44	15	5	0.8
118	2,3’,4,4’,5	72	37	13	2
138	2,2’,3,4,4’,5’	88	60	26	5
153	2,2’,4,4’,5,5’	84	53	21	4
180	2,2’,3,4,4’,5,5’	97	88	61	16

As evident from table B13 fractions of PCBs bound with particles increase with the increase of chlorination degree. Moreover, for all congeners the extent of adsorption increases with temperature decrease.

R.L.Falconer et al. [1995] using the Junge-Pankow model estimated the fraction of PCB bound with particles for urban aerosol ($\theta = 1.1\times10^{-3}$ m^2/m^3). It was shown that in each homologue group mono-ortho-congeners and especially non-ortho congeners have lower vapour pressure and consequently they are sorbed to a greater extent on aerosol particles. As seen from table B13 the extent of PCB-118 (mono-ortho pentachlorobiphenyl) adsorption is higher than of PCB-101 (pentachlorobiphenyl with two chlorine atoms in ortho-position). Field experiments carried out in Chicago in February 1988 and June 1989 confirmed this tendency. At the same time the comparison of calculated and observed data indicated the overestimation of sorption values obtained by *Junge-Pankow* model. The same results were obtained by *T.Harner and T.F.Bidleman* in Chicago experiments made in February-March 1995 [*Harner and Bidleman,* 1998].

According to the adsorption model gas/particle partition coefficient is connected with saturated vapour pressure of subcooled liquid through the following relationship:

$$\log K_P = m \log p^0_L + b \qquad \text{(B13)}$$

where m and b are constants depending on a substance class.

R.L.Falconer et al. [1995] showed that partition coefficient K_P of non-ortho congeners is higher than relevant coefficients of multi-ortho congeners at equal p^0_L values.

In accordance with an alternative absorption model by *J.F. Pankow* ([*Harner and Bidleman,* 1998] and references therein) aerosol particles are covered with organic film which absorbs POP from the air. *T.Harner and T.F.Bidleman* [1998] give an equation linking gas/particle partition coefficient and octanol-air partition coefficient assuming that values of POP activity coefficients in octanol and organic matter coincide and the molecular mass of the organic matter is equal to the organic mass of octanol:

$$\log K_P = \log K_{OA} + \log f_{OM} - 11.91 \qquad \text{(B14)}$$

where f_{OM} is the fraction of organic matter of aerosol particles absorbing gaseous POP (for urban aerosol $f_{OM} = 0.1 - 0.2$).

T.Harner and T.Bidleman [1998] demonstrated that under urban conditions the absorption model describes gas/particle partitioning in the atmosphere better than the previous model. The calculated data agree with observations. For congeners with equal K_{OA} values and with different number of atoms in ortho-position the difference in K_P values is insignificant.

T.Harner and T.F.Bidleman [1998] give empirical dependence of $\log K_P$ on $\log K_{OA}$ obtained on the basis of the experiments carried out in Chicago in February-March 1995:

$$\log K_P = 0.654 \cdot \log K_{OA} - 9.183; \qquad r^2 = 0.876, \qquad n = 33 \qquad \text{(B15)}$$

Since PCB absorption is a basic mechanism of sorption only under urban conditions with relatively high content of organic matter, in our calculations we used the adsorption the Junge-Pankow model.

B.2.6. PCB sorption by soil and bottom sediments

PCB sorption by soils and bottom sediments is characterized quantitatively by organic carbon-water partition coefficient (K_{OC}, m^3/kg).

K_{OC} is usually estimated by the value of octanol-water partition coefficient. Values of octanol-water partition coefficient are presented in table B14.

Table B14. Octanol-water partition coefficients (log K_{OW}) for seven PCBs

IUPAC No	[*Hawker and Connel*, 1988]	[*Mackay et al*., 1992], recommended value
28	5.67	5.8
52	5.84	6.1
101	6.38	6.4
118	6.74	-
138	6.83	-
153	6.92	6.9
180	7.36	-

Table B15 gives octanol-water partition coefficients for seven PCBs chosen for modelling purposes. K_{OW} values recommended by *D.Mackay et al.* [1992] were used for PCB-28, 52, 101 and 153. For PCB-118, 138 and 180 values from earlier work [*Hawker and Connel,* 1988] were taken.

Table B15. Octanol-water partition coefficients for seven PCBs chosen for modelling

IUPAC No.	log K_{OW}
28	5.8
52	6.1
101	6.4
118	6.74 [*Hawker and Connel.,* 1988]
138	6.83 [*Hawker and Connel.,* 1988]
153	6.9
180	7.36 [*Hawker and Connel.,* 1988]

Organic carbon-water partition coefficients were calculated by the following relation:

$$K_{OC} = 0.41\ K_{OW} \qquad \text{[Karikhoff, 1981]} \qquad \text{(B16)}$$

K_{OC} values for seven PCBs are shown in table B16.

Table B16. Organic carbon-water partition coefficients for seven PCB congeners

IUPAC No.	log K_{OC}, dm^3/kg	K_{OC}, m^3/kg
28	5.41	259
52	5.71	516
101	6.01	1030
118	6.35	2253
138	6.44	2772
153	6.51	3257
180	6.97	9393

As seen from table B16 PCBs sorption by soils and bottom sediments increases with the increase of chlorine atoms number in the molecule.

B.2.7. PCB dry deposition

The process of PCB dry deposition is considered to be an important mechanism of PCB scavenging from the atmosphere ([*Holsen et al.,* 1991; *Offenberg and Baker,* 1997] and references therein).

The total flux of PCB dry deposition on a smooth surrogate surface can be expressed by the equation [*Holsen et al.,* 1991]:

$$F_D = V_{DG}C_G + V_{DF}C_F + V_{DC}C_C, \qquad \text{(B17)}$$

where
- V_{DG} is the dry deposition velocity of gaseous PCBs on the smooth surrogate surface;
- C_G is the gaseous PCB concentration;
- V_{DF} is the dry deposition velocity of PCBs bound with fine particles on the smooth surrogate surface;
- C_F is the concentration of PCBs bound with fine particles;
- V_{DC} is the dry deposition velocity of PCBs bound with coarse particles on the smooth surrogate surface;
- C_C is the concentration of PCB bound with coarse particles.

Concentrations of PCBs in the gas phase and PCBs bound with fine and coarse particles (with aerodynamic diameter exceeding 6.5 μm) were measured by *T.M.Holsen et al*. [1991] in Chicago in June-July 1990. The concentration of gaseous PCBs (C_G) was 10.4 ng/m^3, the concentration of PCB bound with fine particles (C_F) - 3.2 ng/m^3 and bound with coarse particles C_C - 0.9 ng/m^3. The observed total flux of PCBs dry deposition on the smooth surrogate surface (F_D) was equal to 6.04 $\mu g/m^2$/day. V_{DG} and V_{DF} values published in literature [*Holsen et al.,* 1991] are 0.01 - 0.1 and 0.1 - 0.5 cm/s. Then from eq. (B17) the velocity of dry deposition of PCBs bound with coarse particles on the smooth surrogate surface was 4.8 - 7.3 cm/s. These values are in a good agreement with value 5.1 cm/s calculated for mass median diameter (MMD) of aerosol particles equal to 26.8 μm measured in Chicago experiment.

Using eq.(B17) in [*Holsen et al.,* 1991] it was shown that the input of dry deposition to the total flux is: for gaseous PCBs - 1.5 - 15%, for PCBs bound with fine particles - 4.6 - 23% and for PCBs bound with coarse particles - 62 - 94%. Such a great contribution of PCBs bound with coarse particles can be explained by their much higher deposition velocities. At the same time the overall velocity of PCBs dry deposition calculated as the ratio of the total flux F_D (6.04 μg/m^2/day) to the total concentration (C_G +C_F + C_C = 14.5 ng/m^3) is 0.5 cm/s due to higher concentrations of gaseous PCBs. This value is in line with range 0.04-3 cm/s obtained in [*Eisenreich et al.,* 1981]. For the calculation of the total dry deposition flux the authors of the paper recommend to use the value of PCBs dry deposition velocity equal to 0.1 - 0.5 cm/s. The comparison of the total deposition flux measured in Chicago with the value for the rural area [*Eisenreich et al.,* 1981] calculated by *T.M.Holsen et al.* indicated that the PCB flux in urban area is three orders of magnitude higher than that in rural areas.

Thus on the basis of the data [*Holsen et al.,* 1991] mean velocity of PCBs dry deposition is 0.5 cm/s. In urban areas 75% of the total dry deposition is conditioned by PCBs bound with coarse particles (>6.5 μm). These data are valid only for a smooth surrogate surface and values of the flux and dry deposition on the actual surface should be further studied.

B.2.8. PCB wet deposition

Wet deposition is another important mechanism of PCB scavenging from the atmosphere. Total dimensionless ratio W_T is determined by equation:

$$W_T = W_G(1 - \phi) + W_P\phi, \qquad \text{(B18)}$$

where W_G is the washout ratio of the gas phase;
W_P is the washout ratio of PCB bound with aerosol particles;
ϕ is the PCB fraction bound with aerosol particles.

Due to sufficiently high values of Henry constants the efficiency of gaseous PCB washout with precipitation is relatively low. Washout ratios W_G determined as inverse values to dimensionless Henry constant (RT/H) at 25^{0}C are of the order of 10^1 -10^2. Washout ratios of PCB scavenging with rain (W_P) for particle-bound PCB are essentially higher. Experimental data [*Franz and Eisenreich,* 1998] show that W_P values are in the range of 10^3 - 10^5 at mean value about 4×10^4. This paper also summarizes various published data indicating that W_P for PCB scavenging with rain is 10^2 - 10^6.

Experimental data demonstrated that the efficiency of PCB washout with snow is higher than with rain [*Franz and Eisenreich,* 1998]. W_P mean value for washout with snow is 3×10^5 and the input of the fraction bound with aerosol particles is estimated as 88%. *T.Franz and S.J.Eisenreich* [1998] give also a regression equation for the estimation of the washout ratio for PCB scavenging with snow (W_T):

$$\log W_T = 0.71(\pm 0.08)\log\phi + 5.34(\pm 0.08); \qquad r^2 = 0.73, \qquad p < 0.05, \qquad \text{(B19)}$$

where ϕ is PCB fraction bound with aerosol particles.

B.2.9. PCB degradation in the environment

Atmosphere

Data of *E.S.C.Kwok et al.* [1995] show that the basic mechanism of PCB degradation in the atmosphere is the reaction with hydroxyl radical and that all other mechanisms can be neglected. Hence the degradation constant for the atmosphere can be calculated by equation:

$$k^*_{OH} = k_{OH}\,[OH] \qquad \text{(B20)}$$

where k^*_{OH} is the constant of a pseudo-first order, s^{-1};
k_{OH} is the rate constant of PCB reaction with hydroxyl radical, cm^3/molecule/s;
[OH] is the air concentration of hydroxyl radical, molecule/cm^3.

At the latitude of 45^0N mean diurnal concentration of hydroxyl radical in the surface layer of 2 km depth is 2×10^6 molecule/cm^3 in summer, 0.8×10^6 molecule/cm^3 in spring and autumn and 0.09×10^6 molecule/cm^3 in winter at mean annual concentration 0.8×10^6 molecule/cm^3 [*Yu Lu and Khall*, 1991]. Values of k_{OH} for homologous groups with 3-6 chlorine atoms were estimated by *E.S.C.Kwok et al.* [1995]. Mean seasonal and annual values of k^*_{OH} calculated on the basis of these data are given in table B17.

Table B17. k^*_{OH} values for PCB homologous groups

Number of chlorine atoms	$k_{OH} \times 10^{12}$ cm^3/molecule/s		k^*_{OH}, s^{-1}			
	range	mean	summer	spring/autumn	winter	Annual mean
3 (PCB-28)	1.0 - 2.1	1.6	3.2×10^{-6}	1.3×10^{-6}	1.4×10^{-7}	1.3×10^{-6}
4 (PCB -52)	0.36 - 1.7	1.0	2.0×10^{-6}	8.0×10^{-7}	9.0×10^{-8}	8.0×10^{-7}
5 (PCB -101,118)	0.3 - 0.9	0.6	1.2×10^{-6}	4.8×10^{-7}	5.4×10^{-8}	4.8×10^{-7}
6 (PCB -138,153)	0.16 - 0.5	0.3	6.0×10^{-7}	2.4×10^{-7}	2.7×10^{-8}	2.4×10^{-7}

Values of gaseous PCB half-lives in the atmosphere are presented in table B18:

Table B18. Gaseous PCB half-lives in the atmosphere, h

Number of chlorine atoms	Half-lives in the atmosphere, h			
	summer	spring/autumn	winter	annual mean
3 (PCB -28)	60	148	1375	148
4 (PCB -52)	96	241	2139	241
5 (PCB -101,118)	160	401	3566	401
6 (PCB -138,153)	321	802	7131	802

Bearing in mind that the degradation of organic matter bound with particles is much slower than in the gas phase, the effective constant of PCB degradation rate in the atmosphere can be calculated in the following way:

$$k_d = (1 - \phi)\, k^*_{OH,} \qquad \text{(B21)}$$

where ϕ is PCB fraction bound with particles.

In the handbook [*Mackay et al.,* 1992] the half-life of PCB-180 in the atmosphere is estimated as 5500 hours (about 8 months). Therefore k_{EF} for PCB-180 is 3.5×10^{-8} s^{-1}.

Natural waters

D.Mackay et al. [1992] consider that the half-life of trichlorobiphenyls in natural waters is 17000 hours (about 2 years), tetra-, penta-, hexa- and heptachlorobiphenyls - 55000 hours (about 6 years).

Soils and bottom sediments

According to the expert estimate of *D.Mackay et al*. [1992] the half-life of PCBs with the number of chlorine atoms from three to seven in soils and bottom sediments is 55000 hours (about 6 years).

Vegetation

PCB degradation constants in vegetation were determined by the method described in chapter 1 on the basis of experimental data obtained in [*Thomas et al*., 1998]:

Table B19. Ratio of PCB concentrations in air and vegetable lipids

IUPAC No.	C_V/C_A (25^0C)	K_{OA} (25^0C)	$K_{OA}/(C_V/C_A)$
28	3.5×10^8	5.7×10^8	1.6
52	3.9×10^8	1.3×10^9	3.3
101	8.0×10^8	6.2×10^9	7.8
118	1.5×10^9	4.8×10^{10}	32
138	2.0×10^9	4.2×10^{10}	21
153	1.2×10^9	3.2×10^{10}	27
180	3.0×10^9	1.7×10^{11}	57

Values of these constants are presented in the following table.

Table B20. Degradation rates in vegetation for seven PCB congeners

IUPAC No.	k_{dV}, h^{-1}	$t_{1/2}$, h
28	9.7×10^{-7}	198
52	1.7×10^{-6}	116
101	2.8×10^{-6}	69
118	4.2×10^{-6}	46
138	2.6×10^{-6}	73
153	4.2×10^{-6}	46
180	2.3×10^{-6}	83

ANNEX C

Physical-chemical properties of PAH

Polycyclic aromatic compounds (polycyclic hydrocarbons) - PAH are high-molecular compounds in which benzene ring is the main structural element. The simplest PAH are naphthalene and biphenyl.

The connection of benzene rings to naphthalene is possible:

- first, by linear annelation - acen series (anthracene, tetracene, pentacene);
- second, by angular annelation - phen series (phenanthrene, tetraphene, pentaphene etc.).

The structure of acens and phens can be combined and repeated in more condensed molecules. Complication of biphenyl molecule can be due to annelation both of six-membered (benzene) rings and five-membered rings. Compounds consisting of only six-membered rings form several series - biphenyl, perylene, pyrene and anthanthrene. The combination of five- and six-membered rings forms two series of compounds - fluorene and fluoranthene. Besides different lateral substitutes: alkyl- and aryl - radicals, functional groups and cycles with heterocyclic atoms can be added to the benzene core. Thus hundreds of substances with different physical-chemical and biological properties can be referred to polycyclic aromatic hydrocarbons. Many PAH meet the requirements imposed to persistent organic pollutants. However, their carcinogenity is of a particular interest. International Agency on Cancer Research (IACR) in the 80-s began the publication of a series of monographs dedicated to "evaluation carcinogenic risk of chemical compounds for man". Among 628 substances considered by experts of IACR, 50 compounds belonged to PAH. As a consequence 14 PAH potentially dangerous for man were selected. They are benzo[a]anthracene, benzo[a]pyrene, benzo[b]fluoranthene, benzo[k]fluoranthene, benzo[j]fluoranthene, dibenzo[a,h]anthracene, dibenzo[a,h]acridine, dibenzo[a,j]acridine, dibenzo[a,e]pyrene, dibenzo[a,h]pyrene, dibenzo[a,i]pyrene, indeno[1,2,3-cd]pyrene, 5-methylchrysene.

For the control of the environment pollution in different countries and different time specialists suggested lists of priority PAH. For example, for the atmosphere of background regions 16 PAH [*Rovinsky et al*., 1988] were selected, for the evaluation of emission in Europe under ESQUAD project 6 Borneff PAH [*van den Hout*, 1994] were selected. While compiling priority lists in addition to the hazard of these compounds to man and biota a possibility to employ observation data for the evaluation of anthropogenic load and revealing the contribution of various sources to pollution levels were considered. Four PAH-indicators (benzo[a]pyrene, benzo[b]fluoranthene, benzo[k]fluoranthene and indeno[1,2,3-cd]pyrene) were listed in the Protocol on persistent organic pollutants under UN ECE Convention on Long-Range Transboundary Air Pollution of 1979.

C.1. *Selection of priority PAH for modelling*

The selection of PAH for transboundary modelling was based on the available priority lists and on the level of knowledge of their physical-chemical properties. For comprehension of partitioning between gas and aerosol phase and the atmosphere-underlying surface exchange processes it was necessary to include a number of species with the widest range of properties defining their behaviour in the environment.

Based on the above discussed principles PAH list includes 10 compounds: phenanthrene, anthracene, pyrene, fluoranthene, benzo[a]anthracene, benzo[a]pyrene, benzo[e]pyrene, benzo[b]fluoranthene, benzo[k]fluoranthene and indeno [1,2,3-cd]pyrene. It should be mentioned that according to [*Axenfeld et al*., 1991] these ten compounds give about 80% of PAH emissions.

The structure, composition and some properties of these compounds are presented in table C1. First comes the name of PAH according to IUPAC nomenclature. The first four compounds have not high molecular mass and occur in the atmosphere mostly in the gas state. It is conditioned by high saturated vapour pressure of subcooled liquid, see table C2. The last three compounds as high-molecular ones and occur in the atmosphere predominately associated with particles, others represent intermediate cases. Due to low saturated vapour pressure of subcooled liquid - 4.12×10^{-6} Pa [*Mackay et al.,* 1992] benzo[k]fluoranthene is present in the atmosphere practically only in the aerosol phase and the gas phase can be neglected. For benzo[b]fluoranthene physical-chemical properties available in literature are not sufficient for modelling. However, its structure similar to benzo[k]fluoranthene gives the reason to suppose that it will behave in a similar way. According to [*Baart et al*., 1995] indeno[1,2,3-cd]pyrene is also concentrated on particles. Therefore these three PAH are omitted in the following discussion of physical-chemical properties used in calculations of gas exchange between soil and vegetation.

For numerical modelling benzo[a]pyrene was chosen because the greatest number of data for this substances on emissions, measurements and physical-chemical properties are available. In future it is planned to model and analyse polyaromatic compounds listed above.

Table C1. Structure, composition and some properties of selected PAH

Compound	Structural formula	Empirical formula	Molec. mass	Carcinogenic activity*
Phenanthrene	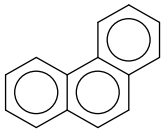	$C_{14}H_{10}$	178.2	—
Anthracene	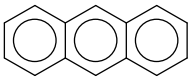	$C_{14}H_{10}$	178.2	±
Pyrene	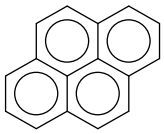	$C_{16}H_{10}$	202.3	—
Fluoranthene	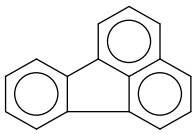	$C_{16}H_{10}$	202.3	—
Benzo[a]anthracene	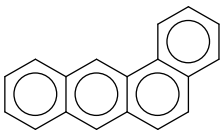	$C_{18}H_{22}$	228.3	+
Benzo[a]pyrene	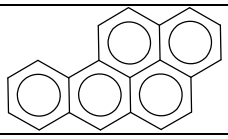	$C_{20}H_{12}$	252.3	+++
Benzo[e]pyrene	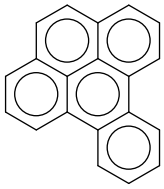	$C_{20}H_{12}$	252.3	—
Benzo[b]fluoranthene	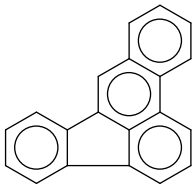	$C_{20}H_{12}$	252.3	++
Benzo[k]fluoranthene	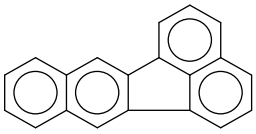	$C_{20}H_{12}$	252.3	—
Indeno[1,2,3–cd]pyrene	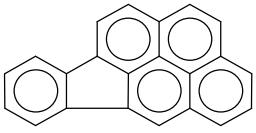	$C_{22}H_{12}$	276	+

* — - not carcinogen, ± - doubtful carcinogen, + -weak carcinogen, ++ - carcinogen, +++ - strong carcinogen.

C.2. *Physical-chemical properties*

C.2.1. PAH physical-chemical properties at 25^0C

PAH physical-chemical properties at 25^0C taken from [*Mackay et al.*, 1992] are given in table C2. Further they are used as basic data for estimating appropriate temperature dependencies.

Table C2. PAH physical-chemical properties at 25^0C [*Mackay et al.*, 1992]

PAH	T_m	Solubility, mol/m^3		Vapour pressure, Pa		log K_{OW}	H^{**}, Pa·m^3/mol	logK_{OA} ***
	^0C	S_S	S_L	p^0_S	p^0_L			
Phenanthrene	101	6.173×10^{-3}	34.847×10^{-3}	0.02	0.113	4.57	3.24	7.45
Anthracene	216.2	2.53×10^{-3}	19.65×10^{-3}	0.001	0.0778	4.54	3.96	7.34
Pyrene	156	6.52×10^{-4}	12.89×10^{-3}	0.6×10^{-3}	0.0119	5.18	0.92	8.61
Fluoranthene	111	1.186×10^{-3}	8.41×10^{-3}	1.23×10^{-3}	8.72×10^{-3}	5.22	1.037	8.60
B[a]A****	160	4.82×10^{-5}	1.045×10^{-3}	2.8×10^{-5}	6.06×10^{-4}	5.91	0.581	9.53
B[a]P****	175	1.51×10^{-5}	4.59×10^{-4}	7.0×10^{-7}	2.13×10^{-5}	6.04	0.046	10.77
B[e]P****	178	1.59×10^{-5}	5.17×10^{-4}	7.4×10^{-7}	2.41×10^{-5}	6.04*	0.020	10.77

* log K_{OW} for B[a]P

** $H = p^0_S/S_S = p^0_L/S_L$

*** $K_{OA} = K_{OW}\,RT/H$

**** B[a]A -benzo[a]anthracene; B[a]P - benzo[a]pyrene; B[e]P - benzo[e]pyrene

Here S_S and S_L are solubilities in solid and liquid states, respectively

C.2.2. Dependence of saturated vapour pressure on temperature

Dependencies of subcooled liquid vapour pressure on PAH temperature in the form log $p^0_L = -A/T + B$ were determined earlier [*Hincley et al.*, 1990]. Coefficients of this dependence are presented in table C3.

Table C3. Coefficients of subcooled liquid vapour pressure dependence on PAH temperature in the form log $p^0_L = -A/T + B$ [*Hincley et al.*, 1990]

PAH	*A*	*B*
Phenanthrene	3716	11.46
Anthracene	3642	11.18
Pyrene	4104	11.92
Fluoranthene	4040	11.35
B[a]A	4742	12.63
B[a]P	4989	11.59
B[e]P	4803	11.11

C.2.3. Dependence of Henry constant on temperature

Like in the case of PCB Henry constant dependence on temperature is presented in the form $\log H = -A/T + B$ where A and B are constant coefficients. At known enthalpies of aggregate transitions A can be calculated in the following way:

$$A = (\Delta H_v - \Delta H_s^e)/2.3R = \Delta H_v/2.3R - \Delta H_s^e/2.3R, \qquad \text{(C1)}$$

where ΔH_v and ΔH_s^e are enthalpies of evaporation and solubility, respectively, for the liquid phase;
R is the gas constant.

In the case of PAH being in solid state at standard conditions values ΔH_v and ΔH_s^e characterize aggregate transitions of the subcooled liquids. Value $\Delta H_v/2.3R$ is equal to coefficient A of temperature dependence of subcooled liquid vapour pressure (see above "*Dependence of saturated vapour pressure on temperature*"). Enthalpy of subcooled liquid solubility is calculated by subtraction of enthalpy of fusion ΔH_m from enthalpy of solid matter solubility ΔH_s: $\Delta H_s^e = \Delta H_s - \Delta H_m$. Then using formula (C1) we determine coefficient A and if Henry coefficient at 25^0C is known, it is possible to calculate values of coefficient B ($B = \log H\ (25^0\text{C}) - A/298$).

Temperature dependencies of Henry constants for PAH obtained in such a way are presented in table C4. These values were obtained using values of coefficient A from table C3 and values $H(25^0\text{C})$ from table C2. Values of enthalpy of solubility were taken from [*May et al.*, 1983], enthalpies of fusion were calculated by formula $\Delta H_m = \Delta S_m T_m$, where T_m - temperature of melting point in K (table C2) and ΔS_m - PAH entropy of fusion is taken from [*Hincley et al*., 1990].

Table C4. Coefficients of Henry constant dependencies on temperature of PAH as $\log H$ (Pa m^3/mol) $= -A/T + B$

PAH	*A*	*B*
Phenanthrene	2749	9.74
Anthracene	2601	9.33
Pyrene	3157	10.56
Fluoranthene	2644	8.89
B[a]A	3147	10.32
B[a]P	3263	9.61
B[e]P	3263	9.25

The dependencies presented in table C4 refer to fresh (distilled) water. Estimates of Henry constant temperature dependencies of benzo[a]pyrene for sea water was obtained earlier [*Vozhzennikov et al.*, 1997]:

$$\log H\ (\text{Pa m}^3/\text{mol}) = 7.67 - 2634/T. \qquad \text{(C2)}$$

For other PAH the estimate of Henry constant for sea water can be obtained by the following empirical formula connecting a substance solubility in sea water with its solubility in distilled water [*Schwarzenbach et al.*, 1993]:

$$\log S = \log S^s + K^s C_s, \qquad \text{(C3)}$$

where S and S^s are solubilities in distilled and salted water respectively, M/l;
C_s is the salt content, M/l;
K^s is salting out constant, l/M.

Since $\log H^s \approx \log p^0 - \log S^s$, and $\log H = \log p^0 - \log S$, where H^s - Henry constant for salted water and vapour pressure and solubility, refer to the same state of a substance, then we have:

$$\log H^s = \log H + K^s C_s, \qquad \text{(C4)}$$

where H^s and H are prescribed in one and the same units.

In normal sea water $C_s \approx 0.5$ M/l, mean value from literature data on K^s for phenanthrene is 0.29 l/M, anthracene - 0.30 l/M, for pyrene - 0.31 l/M [*Schwarzenbach et al.*, 1993]. For the rest of PAH sufficiently reasonable value of K^s is obviously 0.3 l/M.

C.2.4. Dependence of octanol-air partition coefficient on temperature

Octanol-air partition coefficient K_{OA} is equal to the ratio of equilibrium volumetric substance concentration in octanol (C_O, g/l) and in air (C_A, g/l). Experimentally determined values of K_{OA} are known only for a limited set of species mainly for PCB [*Harner et al.*, 1995; *Harner and Bidleman*, 1996]. For the rest of substances they can be estimated by eq.(A6) (Annex A). K_{OA} values for PAH at 25^0C obtained by this formula are given in table C2. Coefficient A of temperature dependence K_{OA} in form $\log K_{OA} = A/T - B$ can be calculated in the same way as a corresponding coefficient of Henry constant temperature dependence:

$$A = -(\Delta H_{so}^e - \Delta H_v)/2.3R, \qquad \text{(C5)}$$

where ΔH_{so}^e is the solubility enthalpy in octanol of a substance in the liquid state.

Values ΔH_{so}^e for PAH were not found in literature. It is known, however, that dissolution enthalpy of liquid nonpolar organic substances in organic solvents is not high, for example, for PCB values ΔH_{so}^e vary from -9.08 to 18.5 kJ/mol and on the average is 7% of ΔH_v [*Harner and Bidleman*, 1996]. Therefore for hydrophobic substances $A \approx \Delta H_v/2.3R$, i.e temperature dependence coefficient at $1/T$ for K_{OA} can be considered to be approximately equal to the temperature dependence of subcooled liquid vapour pressure. Using this assumption and values K_{OA} at 25^0C presented in table C2, we obtain K_{OA} temperature dependence coefficients (table C5).

Table C5. Coefficients of octanol-air partition coefficient dependencies on temperature for PAH in form $\log K_{OA} = A/T - B$

PAH	*A*	*B*
Phenanthrene	3716	5.02
Anthracene	3642	4.88
Pyrene	4104	5.16
Fluoranthene	4040	4.96
B[a]A	4742	6.38
B[a]P	4989	5.97
B[e]P	4803	4.99

As it was mentioned above, eq.(A6) (Annex A) used for calculations of values K_{OA} at 25^0C is an approximate one since $K_{OA} = C_O / C_A$ and $K_{OW}\, RT/H = (C_O^w C_W)/(C_W^o C_A)$, where C_O^w, C_W and C_W^o - equilibrium volumetric concentrations of a substance in octanol saturated by water, in pure water and in water saturated by octanol respectively. Solubility of hydrophobic substances which PAH refer to at octanol saturation by water is changed insignificantly whereas their solubility in water at its saturation by octanol increases as much as several times [*Schwarzenbach et al*., 1993]. Due to this fact value $K_{OW}\, RT/H$ is usually several times lower than real K_{OA}, for example, for PCB and *p,p*'-DDT in 1.6 - 7.4 times. Assuming that for PAH the ratio of calculated values K_{OA} to real ones is somewhere in the middle of this range, i.e. it is equal to 4.5, it is possible to correct dependencies given in table C5 by magnifying coefficient *B* by log4.5 = 0.65.

C.2.5. Molecular diffusion coefficients

Molecular diffusion coefficients of benzo[a]pyrene in air and water computed by formulas (B7) and (B9) from Annex B are equal to 5×10^{-6} and 5.65×10^{-10} m^2/s. Using these values molecular diffusion coefficients for other compounds can be calculated by formulas similar to (B8) and (B9). The required molar volumes and molar masses are presented in the following table:

Table C6. PAH molar volumes and molar masses [*Mackay et al.*, 1992]

PAH	*M*, g/mol	V_m
Phenanthrene	178.2	199
Anthracene	178.2	197
Pyrene	202.3	214
Fluoranthene	202.3	217
B[a]A	228.3	248
B[a]P	252.3	263
B[e]P	252.3	-

Calculated molecular diffusion coefficients for air and water are summarized in table C7.

Table C7. Molecular diffusion coefficients

PAH	D_A, m^2/s	D_W, m^2/s
Phenanthrene	5.95×10^{-6}	6.73×10^{-10}
Anthracene	5.95×10^{-6}	6.73×10^{-10}
Pyrene	5.58×10^{-6}	6.31×10^{-10}
Fluoranthene	5.58×10^{-6}	6.31×10^{-10}
B[a]A	5.26×10^{-6}	5.95×10^{-10}
B[a]P	5×10^{-6}	5.66×10^{-10}
B[e]P	5×10^{-6}	5.66×10^{-10}

C.2.6. Gas/particle partitioning of PAH in the atmosphere

Aerosol particles/air partitioning of PAH is characterized quantitatively by partitioning coefficient K_P ($m^3/\mu g$):

$$K_P = C_P/(C_G \cdot (TSP)), \qquad \text{(C6)}$$

where C_P is the substance concentration bound with aerosol particles, ng/m^3;
C_G is the concentration of gaseous matter, ng/m^3;
TSP is the air content of aerosol particles, $\mu g/m^3$.

In earlier works K_P temperature dependence was presented as $\log K_P = A + B/T$ where A and B are constants for a given substance. In the recent years the temperature effect on K_P is usually described through substance properties dependent on it - vapour pressure of subcooled liquid and octanol-water partition coefficient:

$$\log K_P = m_r \times \log p^0_L + b_r, \qquad \text{(C7)}$$
$$\log K_P = m \times \log K_{OA} + b, \qquad \text{(C8)}$$

where m, b, m_r and b_r are constants determined for a considered class of substances.

T.Harner and T.F.Bidleman [1998] on the example of PCB showed that K_{OA} is a better predictor for K_P compared to p^0_L since it characterizes not only substance volatility but also its absorption by the organic matter of aerosol particles. Unfortunately correlation of K_P with K_{OA} was obtained only for urban air in Chicago on evidence of a small number of measurements.

$$\log K_P = 8.29 \times \log K_{OA} - 10.263; \qquad r^2 = 0.999, \qquad n = 4 \qquad \text{(C9)}$$

At present, therefore, it is preferable to use dependencies of K_P on p^0_L. Some of such dependencies are given in table C8.

Table C8. Coefficients of particle/air partition dependence on p^0_L for PAH in the form $\log K_P = m_r \times \log p^0_L + b_r$

Location of sampling	m_r	b_r	Reference
Rural area	-0.649 ± 0.209	-4.79 ± 1.19*	[*Gustafson and Dickhut*, 1997]
Rural area	-1.00	-5.47	[*Cotham and Bidleman*, 1995]
Suburb	-0.966 ± 0.137	-7.6 ± 1.1*	[*Gustafson and Dickhut*, 1997]
City	-0.745	-4.666	[*Harner and Bidleman*, 1998]
City	-1.03 ± 0.19	-8.0 ± 1.2*	[*Gustafson and Dickhut*, 1997]
City	-0.694	-5.18	[*Cotham and Bidleman*, 1995]
Industrial area	-1.04 ± 0.17	-7.4 ± 1.3*	[*Gustafson and Dickhut*, 1997]

* Coefficients b_r given in [*Gustafson and Dickhut*, 1997] are cut down by log760 = 2.88 to convert the pressure prescribed in mm of mercury column to Pascal.

C.2.7. PAH sorption by soils and bottom sediments

Like in the case of PCB, PAH sorption by soils and bottom sediments is characterized quantitatively by organic carbon-water partition coefficient (K_{OC}, m^3/kg).

K_{OC} was estimated using the value of octanol-water partition coefficient. Values of octanol-water partition coefficients recommended by *D.Mackay et al.* [1992] are presented in table C9.

Table C9. Octanol-water partition coefficients for PAH

PAH	log K_{OW}
Phenanthrene	4.57
Anthracene	4.54
Pyrene	5.18
Fluoranthene	5.22
B[a]A	5.91
B[a]P	6.04

Organic carbon-water partition coefficients were calculated by formula (B16) of Annex B. Calculated K_{OC} values for PAH are presented in table C10.

Table C10. Organic carbon-water partition coefficients of PAH

PAH	log K_{OC}, dm^3/kg	K_{OC}, m^3/kg
Phenanthrene	4.18	15.2
Anthracene	4.15	14.2
Pyrene	4.79	62.1
Fluoranthene	4.83	68.0
B[a]A	5.52	333
B[a]P	5.65	500

C.2.8. PAH wet deposition

Washout ratios by rain W_P of PAH bound with atmospheric aerosol are in the range of 10^3 to 2×10^5 [*Bidleman*, 1988]. For winter months typical values W_P range from 10^3 to 10^4 whereas for summer they are about 10^5 [*Ligocki et al*., 1985a; *Herrmann*, 1987]. Similar values were obtained from the calculation made on the basis of PAH concentrations in air and rain water in the background regions cited in [*Rovinsky et al*., 1988; *McVeety and Hites*, 1988; *Dickhut and Gustafson*, 1995; *Poster and Baker*, 1996].

Washout ratios W_G of gaseous PAH as evidenced by data of [*Ligocki et al*., 1985b] are quite satisfactory predicted by Henry's law. The maximum theoretical value W_G corresponds to B[e]P - $W_G \approx 10^5$, the minimum one - to phenanthrene and anthracene - $W_G \approx 10^3$. Apparently the input of washout of PAH on particles and of gaseous PAH are comparable within an order of magnitude (at the same time it is necessary to take into account the gas phase (fraction).

C.2.9. PAH degradation in the environment

Atmosphere

Gaseous PAH is decomposed in the atmosphere due to direct photolysis and reactions with active components present and first of all with hydroxyl radical ($OH^{\bullet}$). Consequently the effective constant of PAH degradation rate should be calculated as a sum of rate constants of these two processes:

$$k_d = k_p + k^*_{OH}, \qquad \text{(C10)}$$

where k^*_{OH} is the rate constant of pseudo-first order of PAH reaction with hydroxyl radical, s^{-1},
$k^*_{OH} = k_{OH}[OH]$;
k_{OH} is the rate constant of PAH interaction with hydroxyl radical, cm^3/molecule/s;
[OH] is hydroxyl radical air concentration, molecule/cm^3;
k_p is the rate constant of direct photolysis, s^{-1};
k_d is the total constant of degradation rate caused by due to all mechanisms, s^{-1}.

At temperate latitudes mean annual concentration of hydroxyl radical in the surface layer of 2 km thickness is about 10^6 molecules/cm^3 [*Yu Lu and Khall*, 1991]. Rate constants of the interaction with hydroxyl radical at 25^0C are equal to 3.2×10^{-11} cm^3/molecule/s for phenanthrene, to 1.3×10^{-10} cm^3/molecule/s for anthracene [*Bierman et al*., 1985]. The link of ionization potential of molecule with reaction rate constants is of an inverse dependence [*Bierman et al*., 1985]. Thus for phenanthrene mean annual value $k^*_{OH} = 3.2 \times 10^{-5}$ s^{-1} and the half-life of its gaseous fraction due to the reaction with $OH^{\bullet}$ is 6 hours. For anthracene $k^*_{OH} = 1.3\times10^{-5}$ s^{-1} and the half-life - about 1 hour.

Since no reliable experimental data on rates of direct photolysis of gaseous PAH in the atmosphere are available, in modelling of transport processes it seems reasonable to confine ourselves with degradation only due to the reaction with hydroxyl radical and to take overall

rate constants of degradation to be equal to k^*_{OH}. Since degradation rate of organic substances sorbed on aerosol particles is much lower than that of gaseous ones, then to obtain effective rate constant of PAH degradation in the atmosphere it is necessary to multiply k^*_{OH} by the fraction of the gas phase.

The following data on PAH half-life periods (including both gas and particulate phase) were recommended by *D.Mackay et al*. [1992] (see table C11).

Table C11. PAH half-lives in air, h

Compound	$t_{1/2}$, h	Reference
Phenanthrene	55	[*Mackay et al*., 1992]
Anthracene	55	
Pyrene	170	
Fluoranthene	170	
B[a]A	170	
B[a]P	170	
B[k]F	170	
I[1,2,3-cd]P	170	[*Baart et al*., 1995]

Natural waters

Degradation of PAH in natural waters may be conditioned by reaction with hydroxyl radical and UV-radiation effect.

Value of degradation rate constant k_{OH} for PAH in fresh water due to the reaction with hydroxyl radical is 10^{-6} s^{-1} [according to *Haag and Yao*, 1992; *Skurlatov et al.*, 1996; *Stamm et al*., 1991] (half-life $t_{1/2}$ - 8 days), in sea water half-life according to this reaction is several hundreds of days.

Direct photolysis rate constants in surface natural waters estimated by [*Zepp and Schlotzhauer*, 1979] are presented in table C12.

Table C12. Rate constants and half-lives for direct photolysis of PAH in summer noon in latitude 40^0N [*Zepp and Schlotzhauer*, 1979]

PAH	k_p, s^{-1}	$t_{1/2}$, h
Phenanthrene	2.3×10^{-5}	8.4
Anthracene	2.6×10^{-4}	0.75
Pyrene	2.8×10^{-4}	0.68
Fluoranthene	9.2×10^{-6}	21
B[a]A	3.3×10^{-4}	0.59
B[a]P	3.6×10^{-4}	0.54

It is evident that even in fresh water the predominating mechanism of PAH degradation is direct photolysis, i.e. $k_d \approx k_p$. In winter values k_p for B[a]A and B[a]P are lower in 2.7 and 2.2

times respectively [*Mill et al*., 1981] corresponding approximately to the decrease of solar radiation during winter period.

Half-lives recommended by *D.Mackay et al*. [1992] for PAH in natural waters are given in table C13.

Table C13. PAH half-lives in natural waters [*Mackay et al*., 1992]

Compound	$t_{1/2}$, h
Phenanthrene	550
Anthracene	550
Pyrene	1700
Fluoranthene	1700
B[a]A	1700
B[a]P	1700
B[k]F	1700

Soils and bottom sediments

Available data on PAH degradation rate in soils are rather contradictory. On the basis of experimental data on B[a]P obtained mainly in background regions its half-life in such regions is approximately 2 years [*Kolbow et al*., 1986; *Mackay and Paterson*, 1991]. In areas with elevated pollution, for instance, on the territory of an oil refinery plant the half-life can be appreciably shorter - from 5 to 60 days [*Shilina et al*., 1980; *Tonkopiy et al.*, 1979; *Shabad*, 1980].

Data of PAH degradation constants for soil recommended in [*Mackay et al*., 1992] are presented in the following table.

Table C14. PAH half-lives in soil [*Mackay et al*., 1992]

Compound	$t_{1/2}$, h
Phenanthrene	5500
Anthracene	5500
Pyrene	17000
Fluoranthene	17000
B[a]A	17000
B[a]P	17000
B[k]F	17000

ANNEX D

Physical-chemical properties of selected furans and dioxins

Polychlorinated dibenzo-*p*-dioxins/furans (PCDD/F) are toxic organic pollutants of great environmental interest. They are characterized by their ability to be transported over long distance and by high bioaffinity. PCDD/Fs are included in the Protocol on persistent organic pollutants under UN ECE Convention on Long-Range Transboundary Air Pollution of 1979.

D.1. *Selection of PCDD/F congeners for modelling*

Before consideration physical-chemical properties of PCDD/Fs and namely individual 2,3,7,8 - substituted congeners selected for the transboundary transport modelling due to their substantial contribution in to mixture toxicity and as reference compounds in various emission sources, it is necessary to make some general remarks.

The majority of PCDD/F are crystal species which melting point increases with the increase of the number of chlorine atoms in the molecule. On the contrary their solubility in water decreases with the increase of clorine atoms in molecule. High toxicity of some PCDD/Fs isomers and difficulties in substance preparation of required purity resulted in:

a) physical-chemical properties (constants) of the majority of compounds have not been determined by traditional experimental methods;

b) published data on physical-chemical properties of PCDD/Fs were mainly obtained by indirect methods such as gas chromography.

c) calculated values obtained by many authors are based on various approximations and assumptions and can be subjected to critical analysis.

In modelling of pollutant transport from emission sources a broad spectrum of physical-chemical properties and constants is used. In this review we discuss some physical-chemical properties and partition coefficients of polychlorinated dioxins and furans in the environment. More complete analysis of a wider spectrum of constants will be made in future.

The list of compounds selected for modelling contains six congeners from two homologous groups of furans: 1,2,3,7,8 - PeCDF; 2,3,4,7,8 - PeCDF; 1,2,3,4,7,8 - HxCDF; 1,2,3,6,7,8 - HxCDF; 1,2,3,7,8,9 - HxCDF; 2,3,4,6,7,8 - HxCDF; and one congener from the group of pentachlorodibenzo-p-dioxins - 1,2,3,7,8 - PeCDD.

Structure, brutto-formula and some properties of the listed congeners are presented in table D1. In this review basic physical-chemical properties of these very congeners will be outlined and discussed. Validation of the selection of the mentioned congeners will be given in the next report dedicated to the analysis of the composition of emissions from main source groups.

Table D1. Structure, composition and some properties of selected congeners PCDD/F

Compound	Structural formula	Brutto formulae	Molec. mass	Toxicity equivalent factor Teq
1,2,3,7,8-Cl_5dibenzofuran 1,2,3,7,8 - PeCDF	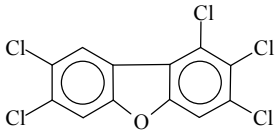	$C_{12}H_3Cl_5O$	340.42	0.05
2,3,4,7,8-Cl_5 dibenzofuran 2,3,4,7,8 - PeCDF	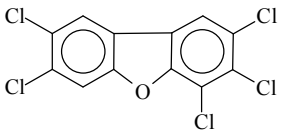	$C_{12}H_3Cl_5O$	340.42	0.5
1,2,3,4,7,8-Cl_6 dibenzofuran 1,2,3,4,7,8 -HxCDF	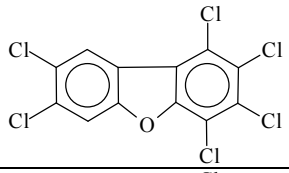	$C_{12}H_2Cl_6O$	374.86	0.1
1,2,3,6,7,8-Cl_6 dibenzofuran 1,2,3,6,7,8 -HxCDF	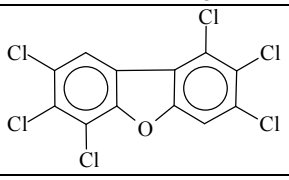	$C_{12}H_2Cl_6O$	374.86	0.1
1,2,3,7,8,9-Cl_6 dibenzofuran 1,2,3,7,8,9 -HxCDF	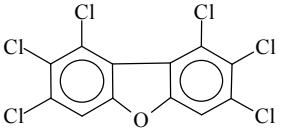	$C_{12}H_2Cl_6O$	374.86	0.1
2,3,4,6,7,8-Cl_6 dibenzofuran 2,3,4,6,7,8 -HxCDF	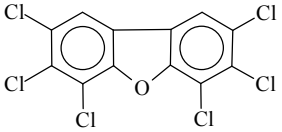	$C_{12}H_2Cl_6O$	374.86	0.1
1,2,3,7,8-Cl_5 dibenzo-p-dioxin 1,2,3,7,8 -PeCDD	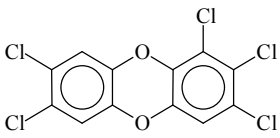	$C_{12}H_3Cl_5O_2$	356.41	0.5

D.2. *Physical-chemical properties*

D.2.1. *Temperatures of melting and boiling points*

Melting point (T_m)

Melting point of a crystal substance is one of its key constants. Melting point of selected dioxins determined by different investigators are presented in table D2.

For isomers of one homologous group with equal molecular mass the substitution positions of chlorine atoms in a molecule is the most important. For example, different in chlorine atom position of chlorine atoms 2,3,4,7,8-PeCDF and 1,2,3,7,8-PeCDF results in the difference of melting points almost as much as 30K. For three congeners HxCDF the difference is somewhat lower and is around of 6-8K. Data of *D.Mackay* [*Mackay et al*., 1992] most frequently used in model calculations unfortunately are limited by one selected congener from group PeCDF and by one selected congener from group HxCDF. For 1,2,3,7,8-PeCDD physical-chemical properties are not available.

Table D2. Melting points of selected PCDD/F isomers

Compound	Melting point, K				
	[*Fedorov,* 1993]	[*Rordorf*, 1989]		[*Chrostowski and Foster,* 1996]	[*Mackay et al.,* 1992]
		*	**		
1,2,3,7,8 – PeCDF	500	498	500	498	-
2,3,4,7,8 – PeCDF	469.5	469	469.5	469	469, 469.5
1,2,3,4,7,8 – HxCDF	499.5	498.5	499.5	502***	498.5, 499.5
1,2,3,6,7,8 – HxCDF	507	505	507		-
1,2,3,7,8,9 – HxCDF	-	-	-		-
2,3,4,6,7,8 – HxCDF	-	512	513		-
1,2,3,7,8 – PeCDD	514	513	514	513	-

* – calculated by *B.Rordorf* [*Rordorf*,1989]

** – is given by *B.Rordorf* from literature data

*** – one value for all substituted congeners in homologous group

Boiling point (T_b)

Boiling point of the selected species is not determined experimentally. For the first time *B.Rordorf* calculated them by the following equation:

$$T_b = 283 + 42.0\,X - 1.73 \cdot X^2 \pm 15, \text{ K}, \qquad \text{(D1)}$$

where T_b is the boiling point, K;

X is the number of chlorine atoms.

Using certain dependencies [*Govers*, 1993; *Govers et al.*, 1995; *Govers and Krop*, 1998] and data obtained by the authors on thermodynamic constants of selected congeners we calculated boiling point of the selected compounds. First of all, some thermodynamic constants of these substances were determined.

ΔH_v is the vaporisation enthalpy, kcal/mol;

V_0 is the molar liquid volume at temperature 25°C, cm^3/mol;

δ_o is the solubility parameter of *Scatchard-Hildebrand*, $(cal/cm^3)^{1/2}$.

Calculated parameter values of the selected compounds are presented in table D3.

Table D3. Parameters for calculations of boiling temperature

Compound	ΔH_v, kcal/mol	V_0, cm^3/mol	δ_0, $(cal/cm^3)^{1/2}$
1,2,3,7,8 – PeCDF	22.777	202.98	10.454
2,3,4,7,8 – PeCDF	22.724	203.22	10.435
1,2,3,4,7,8 – HxCDF	23.385	213.46	10.333
1,2,3,6,7,8 – HxCDF	23.470	213.96	10.340
1,2,3,7,8,9 – HxCDF	24.512	213.87	10.575
2,3,4,6,7,8 – HxCDF	23.599	210.45	10.455
1,2,3,7,8 – PeCDD	23.690	207.88	10.540

The comparison of our calculation results with the data of *B.Rordorf* is presented in table D4.

Table D4. Boiling point of selected PCDD/F isomers

Compound	Boiling temperature, K	
	[*Rordorf*, 1989] Calculated	Estimates Calculated by *Hildebrand* equation and ΔH_v by [*Govers et al.*, 1995]
1,2,3,7,8 – PeCDF	737.85	687.15
2,3,4,7,8 – PeCDF	737.85	694.35
1,2,3,4,7,8 – HxCDF	760.85	700.55
1,2,3,6,7,8 – HxCDF	760.85	698.95
1,2,3,7,8,9 – HxCDF	-	720.55
2,3,4,6,7,8 – HxCDF	760.85	703.05
1,2,3,7,8 – PeCDD	737.85	704.85

As seen from table D4, results of *B.Rordorf* [1989] exceed our data and the compounds with equal degree of chlorination have equal boiling points. In the latter case, results by *B.Rordord* seems to be suspicious for compounds with difference in molecular masses as much as 16 units (mol. oxygen mass) as it is in the case of pentachloro-p-dioxin and pentafuran with substitution in positions 1, 2, 3, 7, 8.

The calculations, presented here, give a possibility:

- to obtain the value of T_b for 1,2,3,7,8,9 - HxCDF;
- to indicate differences in boiling temperatures of congeners with an equal number of chlorine atoms but with substitution in different positions;
- to confirm the dependence of melting and boiling point on molecular mass. For instance, according to our calculations 1,2,3,7,8 - PeCDF has larger molecular mass and higher melting and boiling point than 1,2,3,7,8-PeCDD.

Thus the dependencies suggested by [*Govers*, 1993; *Govers et al.*, 1995; *Govers and Krop*, 1998] for calculations of thermodynamic constants on the basis of retention characteristics allow us to obtain more adequate results.

D.2.2. Enthalpies of aggregative transitions

Phase transfer enthalpy was calculated by *B.Rordorf* [1989] by the correlation method. As points of support *B.Rordorf* used experimentally determined values of boiling point, saturated vapour pressure, sublimation enthalpy and entropy for ten polychlorodibenzo-p-dioxins and four polychlorodibenzofurans, the majority of which were low chlorinated congeners (from mono to tetra), and for octachlorodibenzo-p-dioxin and octachlorodibenzofuran.

Our estimates were made on the basis of data and dependencies [*Govers*, 1993; *Govers et al.*, 1995; *Govers and Krop*, 1998] using the retention indices for these particular compounds.

Enthalpies of aggregative transitions calculated by *B.Rordorf* [1989] and in this report are presented in table D5.

Table D5. Enthalpies of aggregative transitions

Compound	Enthalpies of aggregative transitions (ΔH), kJ/mol			
	Sublimation, ΔH_S	Fusion, $\Delta H_m(T_m)$	Vaporization, $\Delta H_v(T_m)$	
	[*Rordorf*, 1989]			This report
1,2,3,7,8 – PeCDF	128.978	42.2	83.8	95.4
2,3,4,7,8 – PeCDF	130.430	42.2	85.8	95.2
1,2,3,4,7,8 – HxCDF	137.393	48.1	86.5	97.9
1,2,3,6,7,8 – HxCDF	137.083	48.1	86.1	98.3
1,2,3,7,8,9 – HxCDF	-	-	-	102.5

2,3,4,6,7,8 – HxCDF	136.794	48.1	85.7	98.8
1,2,3,7,8 – PeCDD	134.062	42.2	88.7	99.2

The differences obtained in enthalpy of evaporation reflect differences in methods used for calculations.

D.2.3. Vapour pressure of solid substance

Saturated vapour pressure of PCDD/F compounds is characterized by extremely low values. Saturated vapour pressure values of selected compounds at 25^0C for the solid state are given in table D6.

Table D6. Saturated vapour pressure values of selected compounds (literature data)

Compound	Vapour pressure values of selected compounds at 25 °C, p^0_S, Pa			
	[*Fedorov*, 1993]	[*Chrostowski and Foster*, 1996]	[*Rordorf*, 1989]	[*Mackay at al.*, 1992]
1,2,3,7,8 – PeCDF	3.3×10^{-7}	5.65×10^{-8}	2.3×10^{-7}	-
2,3,4,7,8 – PeCDF	4.7×10^{-7}	8.1×10^{-8}	3.5×10^{-7}	3.5×10^{-7}
1,2,3,4,7,8 – HxCDF	3.4×10^{-8}	$5.98\times10^{-9*}$	3.2×10^{-8}	3.2×10^{-8}
1,2,3,6,7,8 – HxCDF	3.9×10^{-8}		2.9×10^{-8}	3.5×10^{-8}
1,2,3,7,8,9 – HxCDF	-		-	
2,3,4,6,7,8 – HxCDF	-		2.6×10^{-8}	
1,2,3,7,8 – PeCDD	7.7×10^{-8}	1.25×10^{-8}	5.8×10^{-8}	

* - one value for all 2,3,7,8 - substituted congeners in homologous group

D.2.4. Temperature dependence of vapour pressure of solid substance

For calculations of temperature dependence of saturated vapour pressure of a solid substance *A.Bulgakov and D.Ioannisian* [1998] used known expression:

$$\ln p^0{}_S = \frac{\Delta S_S T - \Delta H_S}{RT} \quad , \tag{D2}$$

where ΔS_S is the sublimation entropy, J/mol·K;
ΔH_S is the sublimation enthalpy, J/mol;
R is the universal gas constant equal to 8.314 J/mol·K;
T is the temperature, K.

In spite of the fact that sublimation entropy and enthalpy values are not constant within a wide range of temperatures in the environment, their temperature dependencies can be neglected and eq.(D2) can be transformed to the form:

$$\log p^0{}_S = - A/T + B, \tag{D3}$$

Values of coefficients *A* and *B* obtained for 2,3,7,8 - substituted PCDF congeners [*Bulgakov and Ionissian*, 1998] based on thermodynamic constants [*Rordorf,* 1989] are shown in table D7.

Table D7. Coefficients of temperature dependencies of vapour pressure of solid substances for the selected compounds in the form (D3)

Compound	*A*	*B*
1,2,3,7,8 – PeCDF	-6737	15.98
2,3,4,7,8 – PeCDF	-6813	16.40
1,2,3,4,7,8 – HxCDF	-7177	16.56
1,2,3,6,7,8 – HxCDF	-7161	16.45
1,2,3,7,8,9 – HxCDF	-7161	16.47
2,3,4,6,7,8 – HxCDF	-7146	16.40
1,2,3,7,8 – PeCDD	-7003	16.25

D.2.5. Saturated vapour pressure of subcooled liquid

Saturated vapour pressure of subcooled liquid at 25^0C for selected compounds was calculated by different authors and the results are presented in table D8.

Table D8. Saturated vapour pressure of subcooled liquid from literature data

Compound	p^0_L (25 ^{0}C), Pa				
	[*Mackay, et al.,* 1992]	[*Eitzer and Hites*]		[*Chrostowski and Foster,* 1996]	[*Govers and Krop,* 1998]
		1991	1989a		
1,2,3,7,8 – PeCDF	-	3.63E-5	3.25E-5	7.36E-6	6.17E-5
2,3,4,7,8 – PeCDF	1.72E-5	2.17E-5	2.42E-5	5.35E-6	5.5E-5
1,2,3,4,7,8 – HxCDF	3.08E-6	8.07E-6*	7.83E-6	8.56E-7**	1.38E-5
1,2,3,6,7,8 – HxCDF	3.61E-6		7.32E-6		1.2E-5
1,2,3,7,8,9 – HxCDF	-	4.97E-6*	4.26E-6		2.2E-6
2,3,4,6,7,8 – HxCDF	-		5.81E-6		7.6E-6
1,2,3,7,8 – PeCDD	-	1.74E-5	2.10E-5	2.32E-6	1.2E-5

* - one value for two congeners;
** - one value for four congeners.

The difference in p^0_L values obtained by different authors reflects:

1. differences in methods at obtaining data for calculations;

2. differences in calculation methods and thermodynamic constants used and first of all it refers to entropy and enthalpy of substance transition to the vapour phase from the solid state and from the state of subcooled liquid.

Most complete data set at saturated vapour pressure over subcoled liquid is given in [*Eitzer and Hites,* 1989a; *Govers et al.,* 1998]. For calculations they used Kovats retention indices, determined by the method of gas chromatography. Calculations *P.Chrostowski and S.Foster* [1996] were based on data, obtained by correlation method of *B.Rordorf* [1989]. Results by *H.Govers and H.Krop* [1998] seem to be most reliable, since calculations of thermodynamic characteristics and partitioning constants of compounds were based on highly reproducible retention indices (Kovats indices) measured on the stationary phases of different polarity and provided with good statistics. Chromotographyc data were subjected to multiparametric regression and correlation analyses, which forms the basis of SOFA (Solubility parametrs for Fate Analysis) model. These data are preferable also since the calculation model considers orientation of sustituets and their mutual impact in molecule.

D.2.6. Temperature dependence of saturated vapour pressure of subcooled liquid

The dependence of saturated pressure on temperature (if a substance is in the state of subcooled liquid) can be described by the following equation:

$$\ln p_L^0 = \ln p_S^0 + \frac{\Delta S_m \left(\frac{T_m}{T} - 1 \right)}{R}, \qquad \text{(D4)}$$

where p^0_L is the saturated vapour pressure over subcooled liquid, Pa;
p^0_S is the saturated vapour pressure over solid substance, Pa;
ΔS_m is the entropy of fusion, kJ/mol·K;
T_m is the melting point, K;
R is the universal gas constant equal to 8.314 kJ/mol·K;
T is the temperature, K.

In a simplified form of temperature dependence p^0_L can be represented by the following equation:

$$\log p_L^0 = -\frac{A}{T} + B, \qquad \text{(D5)}$$

where A and B are the dimensionless coefficients.

Coefficients A and B for 2,3,7,8 - substituted congeners of PCDD/F were determined by *A.Bulgakov and D.Ioannisian* [1998]. Values A and B for the selected compounds are presented in table D9.

Table D9. Coefficient values of temperature dependence of saturated vapour pressure over subcooled liquid for the selected compound in the form (D5)

Compound	*A*	*B*
1,2,3,7,8 – PeCDF	- 4504	11.54
2,3,4,7,8 – PeCDF	- 4607	11.70
1,2,3,4,7,8 – HxCDF	- 4655	11.54
1,2,3,6,7,8 – HxCDF	- 4645	11.49
1,2,3,7,8,9 – HxCDF	- 4643	11.51
2,3,4,6,7,8 – HxCDF	- 4629	11.49
1,2,3,7,8 – PeCDD	- 4778	11.90

D.2.7. Solubility in water

Practically all polychlorinated organic compounds are poorly soluble in water. Solubility of substances from PCDD/F family is about 10^{-5}-10^{-11} mol/l. Solubility of the selected congeners in solid state at 25^0Cis presented in table D10.

Table D10. Solubility of the selected compounds in the solid state at 25^0C, literature data

Compound	Solubility in water S_S, mol/l		
	[*Friesen et al.,* 1990]	[*Mackay et al.*, 1992]	[*Ruelle and Kesselring*, 1997]
1,2,3,7,8 – PeCDF	-	-	-
2,3,4,7,8 – PeCDF	6.92E-10	6.93E-10	4.37E-10
1,2,3,4,7,8 – HxCDF	2.2E-11	2.2E-11	3.02E-11
1,2,3,6,7,8 – HxCDF	4.72E-11	4.72E-11	2.57E-11
1,2,3,7,8,9 – HxCDF	-	-	-
2,3,4,6,7,8 – HxCDF	-	-	-
1,2,3,7,8 – PeCDD	-	-	-

Solubility of a substance being in the state of subcooled liquid cannot be determined experimentally. Table D11 presents values S_L of the selected compounds taken from *H.Govers and H.Krop* [1998].

Table D11. Solubility of the selected compounds in the state of subcooled liquid

Compound	Solubility in water $S_{L,}$ mol/l
1,2,3,7,8 – PeCDF	3.16E-08
2,3,4,7,8 – PeCDF	2.09E-08
1,2,3,4,7,8 – HxCDF	7.08E-09
1,2,3,6,7,8 – HxCDF	6.03E-10
1,2,3,7,8,9 – HxCDF	2.29E-09
2,3,4,6,7,8 – HxCDF	4.17E-09
1,2,3,7,8 – PeCDD	7.76E-09

For S_L calculation the following equation can be used:

$$\ln S_L \approx \ln S_S + \frac{\Delta S_m \left(\frac{T_m}{T} - 1 \right)}{R}, \qquad \text{(D6)}$$

where S_S is the solubility in water of solid matter, mol/l;
ΔS_m is the entropy of fusion, kJ/mol·K;
T_m is the melting temperature, K;
T is the temperature, K.

Since in equations (D4) and (D6) the second components fully coincide, partitioning between air and water phase is determined by the equality of relationships $p^0_L / S_L = p^0_S / S_S$ which is called dimensional Henry constant (Pa m^3/mol).

D.2.8. Henry constant

Henry constant is a value characterizing the relationship of concentrations in the gas and liquid phase under equilibrium conditions.

Calculated values of Henry constant for the selected compounds at 25^0C are given in table D12.

Table D12. Henry constant value at 25^0C from literature data

Compound	Henry constant (H), Pa·m^3/mol.		
	[*Govers and Krop,* 1998]	[*Chrostowski and Foster,* 1996]	[*Mackay et al.* 1992]
1,2,3,7,8 – PeCDF	1.91	2.1	-
2,3,4,7,8 – PeCDF	2.57	1.5	5.05
1,2,3,4,7,8 – HxCDF	1.91	-	1.45
1,2,3,6,7,8 – HxCDF	1.91	2.25	7.4
1,2,3,7,8,9 – HxCDF	9.55	-	-
2,3,4,6,7,8 – HxCDF	1.78	-	-
1,2,3,7,8 – PeCDD	-	1.42	-

* - one value on all 2,3,7,8 - substituted congeners in homologous group

D.2.9. Temperature dependence of Henry constant

Henry constant value can be calculated by equation:

$$\log H = \log p^0_S - \log \Delta S_m, \quad \text{(D7)}$$

where p^0_S is the saturated vapour pressure of solid matter, Pa;
ΔS_m is the entropy of fusion, kJ/mol·K.

Usually it is transformed to the form:

$$\log H = -\frac{A}{T} + B, \quad \text{(D8)}$$

where coefficient A is determined from equation:

$$A = - \Delta H_v / 2.3 \cdot R + \Delta H_{wl} / 2.3 \cdot R, \quad \text{(D9)}$$

where ΔH_v is the enthalpy vaporization of subcooled liquid, kJ/mol;
ΔH_{wl} is the solubility enthalpy of liquid substance determined as a difference of solid matter solubility enthalpy and solid matter melting enthalpy ($\Delta H_{ws} - \Delta H_m$), kJ/mol;
ΔH_{ws} is the solid substance solubility enthalpy, kJ/mol;
ΔH_m is the solid substance melting enthalpy, kJ/mol;

then coefficient B is found:

$$B = \log H\,(25\ ^\circ\text{C}) - A/298 \quad \text{(D10)}$$

Calculation of the coefficient for 2,3,7,8 - substituted PCDD/F in equation (D8) has been made by *A.Bulgakov and D.Ioannisian* [1998] on the basis of data on aggregative transitions and Henry constant from [*Rordorf,* 1989; *Mackay et al.*, 1992; *Doucette and Andren,* 1988]. The obtained values A and B for selected compounds are given in table D13.

Table D13. Coefficients of temperature dependence of Henry constant for the selected compounds in the form (B8)

Compound	*A*	*B*
1,2,3,7,8 – PeCDF	4392	14.11
2,3,4,7,8 – PeCDF	4468	14.69
1,2,3,4,7,8 – HxCDF	4832	16.35
1,2,3,6,7,8 – HxCDF	4816	15.91
1,2,3,7,8,9 – HxCDF	4816	16.00
2,3,4,6,7,8 – HxCDF	4801	15.93
1,2,3,7,8 – PeCDD	4422	15.32

Table D14 contains thermodynamic characteristics of the selected compounds for calculation coefficients *A* and *B* made in this review. Values of solubility enthalpy were estimated on the basis of values ΔH_{ws} presented in [*Doucette and Andren*, 1988] for dichlorodibenzo - and oktachlorodibenzofuran. The values of coefficients of the Henry constant temperature dependence calculated on the basis of these data are presented in Table D15.

The comparison of two calculation series show, that data of different authors used for calculations of temperature dependence of physical-chemical constants give different results. Therefore while modelling the behaviour of these compounds, their fluxes onto the underlying surface due to wet deposition can be overestimated or underestimated.

Table D14. Values of aggregative transition enthalpy and Henry constant at 25°C selected for calculations of temperature dependence of Henry constant

Compounds	ΔH_m, kJ/mol [*Rordorf,* 1989]	ΔH_{ws}, kJ/mol estimates	ΔH_v, kJ/mol estimates	log *H* [*Govers and Krop*, 1998]
1,2,3,7,8 – PeCDF	42.4*	45*	95.16	- 2.72
2,3,4,7,8 – PeCDF			95.38	- 2.59
1,2,3,4,7,8 – HxCDF	48.1**	50**	98.3	- 2.72*
1,2,3,6,7,8 – HxCDF			97.9	
1,2,3,7,8,9 – HxCDF			102.7	- 3.02
2,3,4,6,7,8 – HxCDF			98.8	- 2.75
1,2,3,7,8 – PeCDD	42.4	47.5***	99.2	- 2.84

* - one value for two congeners;

** - one value for four congeners.

*** - [*Frisen and Webster*, 1990] for 1,2,3,4,7 - PeCDD.

Table D15. Coefficients of temperature dependence of Henry constants of selected compounds in the form (B8)

Compounds	*A*	*B*
1,2,3,7,8 – PeCDF	4844	13.58
2,3,4,7,8 – PeCDF	4854	13.71
1,2,3,4,7,8 – HxCDF	5041	14.18
1,2,3,6,7,8 – HxCDF	5021	14.08
1,2,3,7,8,9 – HxCDF	5271	14.68
2,3,4,6,7,8 – HxCDF	5071	14.25
1,2,3,7,8 – PeCDD	4923	13.66

D.2.10. Air-water partition coefficient and washout ratio

Partition coefficient between air and water - K_{AW} is a dimensionless value of Henry constant determined from the formula:

$$K_{AW} = \frac{H}{RT}, \qquad \text{(D11)}$$

where H is Henry constant, Pa m^3/mol;
T is the temperature, K;
R is the universal gas constant, R = 8.134 J/mol K.

The inverse value to K_{AW} is called washout ratio W_G of compound present in the atmosphere in gas phase. It is found from equation:

$$W_G = R \cdot T/H \qquad \text{(D12)}$$

Calculated values W_G at T = 298.13 K using Henry constant obtained by different authors are given in table D16.

Table D16. Washout ratios for the selected compounds

Compound	Values W_G (estimates)			Experimental data for W_G	
	[*Mackay et al.*, 1992]	[*Chrostowski and Foster,* 1996]	[*Govers and Krop*, 1998]	[*Eitzer and Hites,* 1989b]	[*Koester and Hites,* 1992]
1,2,3,7,8 – PeCDF	-	11800	1298	9300*	14000*
2,3,4,7,8 – PeCDF	4909	16525	964		
1,2,3,4,7,8 – HxCDF	1705	11017*	1298	8600*	10000*
1,2,3,6,7,8 – HxCDF	3345		1298		
1,2,3,7,8,9 – HxCDF	-		2596		
2,3,4,6,7,8 – HxCDF	-		1393		
1,2,3,7,8 – PeCDD	-	17456	1675	6300*	13000*

* - values presented correspond to all the homologous group

B.Eitzer and R.Hites [1989b] and *C.Koester and A.Hites* [1992] determined values W_G using concentrations of PCDD/F homologous groups in the soluble form and associated with particles in rain drops obtained experimentally in two US cities.

Calculated values of W_G using Henry constant from [*Govers and Krop*, 1998; *Mackay et al.*, 1992] are approximately by an order of magnitude lower than those calculated on the basis of experimental data.

Although, Henry constant for homologous group PCDD/F selected for modelling differs slightly. Only W_G estimate made for this review in magnitude of Henry constant published in [*Chrostowski and Foster*, 1996] is very close to experimental data.

D.2.11. Octanol-water partition coefficient K_{OW}

Partition coefficient octanol-water characterizes partitioning of a substance between water and organic phase represented by n-octanol ($C_8H_{16}OH$) as a surrogate of lipid media.

Coefficient K_{OW} can be either calculated or determined experimentally. The values of K_{OW} (dimensionless) published in original papers are presented in table D17.

Values of logK_{OW} for the selected compounds are within rather narrow range 6.6 - 7.7 and experimental and calculated data fit in this range.

Table D17. Values log K_{ow} for the selected compounds from literature data

Compound	log K_{OW}					
	Calculated value				Experimental	
	[*Fedorov*, 1993]	[*Crostowski and Foster,* 1996]	[*Govers and Krop*, 1998]	[*Mackay et al.,* 1992]	[*Shiu et al.*, 1988]	[*Sijm et al.*, 1989]
1,2,3,7,8 – PeCDF	-	6.5	6.9	-	-	6.79
2,3,4,7,8 – PeCDF	-	6.92	6.5	6.5	6.92	7.11
1,2,3,4,7,8 – HxCDF	-	7.0 *	7.53	7.0		
1,2,3,6,7,8 – HxCDF	-		7.57			
1,2,3,7,8,9 – HxCDF	-		7.76			
2,3,4,6,7,8 – HxCDF	-		7.65			
1,2,3,7,8 – PeCDD	6.64	7.4	7.5	-		6.64

* - for the whole homologous group HxCDF

D.2.12. Organic carbon-water partition coefficient, K_{OC}

Coefficient K_{OC} characterizes partitioning of a substance between soil organic carbon or bottom sediments and water and can be determined from the relationship obtained in [*Karikhoff et al.*, 1979; *Karikhoff*, 1981]:

$$K_{OC} = 0.41\ K_{OW} \qquad \text{(D13)}$$

K_{OC} values calculated for the selected compounds on the basis of data [*Govers and Krop*, 1998] are given in table D18.

Table D18. K_{OC} estimates for the selected compounds

Compound	$K_{OW,}$ [*Govers and Krop*, 1998]	$K_{OC,}$ dm^3/kg
1,2,3,7,8 – PeCDF	9.77E+6	4.0E+3
2,3,4,7,8 – PeCDF	12.88E+6	5.3E+3
1,2,3,4,7,8 – HxCDF	3.39E+7	1.39E+4
1,2,3,6,7,8 – HxCDF	3.72E+7	1.53E+4
1,2,3,7,8,9 – HxCDF	5.75E+7	2.36E+4
2,3,4,6,7,8 – HxCDF	4.47E+7	1.83E+4
1,2,3,7,8 – PeCDD	3.16E+6	1.3E+3

D.2.13. PCDD/F gas/particle partitioning in the atmosphere

Many organic compounds due to their properties can occur in the environment in two phases as gas and aerosol. Polychlorinated dibenzo-p-dioxins and polychlorinated furans are no exception.

Distribution of the substance in gas/particle system can be quantitatively estimated as a ratio of concentrations in gaseous and in aerosol phase.

In spite of the fact that commonly used methods of PCDD/F determination presume sampling of gas and aerosol phase the majority of authors confine themselves by the total content. There are not many studies dedicated to partitioning of homologous group of PCDD/F between vapour and aerosol. There are even less data on 2,3,7,8-substituted congeners. In this context most interesting is the analysis of results of air pollution in Central Europe presented in [*Hippelein et al.,* 1996; *Horstmann and McLachlan,* 1998]. The comparison of experimental data on PCDD/F concentration partitioning between vapours and particles obtained by these authors are outlined in table D19.

As seen from table D19 values C_G/C_P vary in a wide range even at close temperatures. C_G/C_P values for selected congeners determined in experiments [*Hippelein et al.,* 1996], were compared with estimates obtained in [*Chrostowski and Foster*, 1996] – «experiment» and «calculation», table D20.

As seen from table D20 the difference between calculated and measured values is very high and for the majority of selected congeners is about two orders of magnitude. When experimentally obtained values of C_G/C_P are used two types of errors can be introduced due to sampling conditions.

First, at the prolonged sampling under the conditions of rather high ambient temperatures (summer time) aerosol component concentration on the filter, can decrease due to secondary revolatilization from aerosol surface, and substance concentration in vapours can increase.
Second, together with the true vapour phase the sorbent can accumulate ultra fine particles capable to penetrate through pores of the filter material. This discrepancies however of errors is impossible to be explained.

Table D19. The ratio of concentrations of the selected homologous groups and 2,3,7,8 - substituted congeners in vapours and particles

Homolog group, Compound	Ratio of concentrations in vapours and on particles (C_G/C_P)			
	[*Eitzer and Hites,* 1989a]	[*Hippelein et al.*, 1996]	[*Müller et al.* 1998]	[*Horstmann and McLachlan,* 1998]
PeCDF	1.7	2.45	10.6	1.8
1,2,3,7,8 – PeCDF	1.83	2.04	-	1.57
2,3,4,7,8 – PeCDF	1.01	1.56	-	1.04
HxCDF	0.39	1.0	2.6	0.58
1,2,3,6,7,8 – HxCDF	0.35	0.75	-	0.58
1,2,3,4,7,8 – HxCDF	0.35	0.67	-	0.61
1,2,3,7,8,9 – HxCDF	0.17	0.67	-	0.61
2,3,4,6,7,8 – HxCDF	0.12	0.56	-	0.31
PeCDD	2.0	2.7	100% vapor	1.6
1,2,3,7,8 – PeCDD	0.8	1.5		0.99
Temperature, ^oC	25	20	~25	warm season
TSP, μg/m^3	*	34	*	*

* data on the atmospheric content of solid particles are not presented by the authors

Table D20. Comparison of C_G/C_P values obtained experimentally and by calculations

Homolog group, compound	Ratio in vapours and on particles (C_G/C_P)	
	Experiment	Calculation
PeCDF	2.7	-
1,2,3,7,8 - PeCDF	2.85	0.048
2,3,4,7,8 - PeCDF	1.78	0.036
HxCDF	1.0	-
1,2,3,6,7,8 - HxCDF	0.85	0.0058
1,2,3,4,7,8 - HxCDF	1.0	0.0058
1,2,3,7,8,9 - HxCDF	1.0	0.0058
2,3,4,6,7,8 - HxCDF	0.54	0.0058
PeCDD	2.7	0.015
1,2,3,7,8 - PeCDD	1.7	
Temperature, ^0C	17	17
TSP, μg/m^3	33	54

Gas/particles partitioning is first of all affected by air temperature. As it was shown, log G/P ratio has very good correlation (r = 0.96) with saturated vapour pressure and can be calculated by equation [*Eitzer and Hites,* 1989a]:

$$\log (C_G/C_P) = \log p^0_L + a_{0,} \qquad \text{(D14)}$$

where a_0 is the constant depending on measurement unit p^0_L;
p^0_L is the subcooled liguid, Pa.

Since p^0_L value is a function of temperature, the ratio C_G/C_P should have temperature dependence.

Besides temperature gas/particles relationship is affected by the content of particulate matter in the atmosphere.

High sorption properties of dioxins and furans are confirmed by considerably high values of absorption heat 11-32 kcal/mol [*Eitzer and Hites*, 1989a].

Eq.(D15) describes temperature dependence of substance partitioning between vapours and particles with regard for the concentration of solid particulate matter:

$$\log [C_G (TSP) / C_P] = a'_0 + a_1/T, \quad \text{(D15)}$$

where TSP is the total concentration of solid particulate matter (aerosol), μg/m^3;
a'_0 and a_1 are coefficients determined experimentally.

The inverse value of $C_G(TSP)/C_P$ is called the partition coefficient K_P and it has the dimension m^3/μg and can be calculated from the formula:

$$K_P = C_P/(C_G\, TSP) \quad \text{(D16)}$$

Using results from [*Hippelein et al.*, 1996] we calculated K_P values for different temperatures, table D21.

Table D21. K_P coefficient variation versus temperature

Homolog group, Compound	Partition coefficient K_P, m^3/μg			
	0 °C	2.4 °C	12 °C	20 °C
PeCDF	0.418	0.157	0.0273	0.0121
1,2,3,7,8 - PeCDF	0.319	0.216	0.0361	0.0144
2,3,4,7,8 - PeCDF	0.686	0.289	0.0619	0.0188
HxCDF	1.884	0.755	0.118	0.0294
1,2,3,6,7,8 - HxCDF	2.8229	1.12	0.244	0.0390
1,2,3,4,7,8 - HxCDF	1.932	1.214	0.223	0.044
1,2,3,7,8,9 - HxCDF	1.932	1.214	0.223	0.044
2,3,4,6,7,8 - HxCDF	1.026	0.889	0.244	0.0529
PeCDD	0.374	0.237	0.0333	0.0170
1,2,3,7,8 – PeCDD	0.666	0.464	0.0774	0.0197
TSP, μg/m^3	35	31	30	34

On the basis of estimates presented it is possible to draw the following conclusions:

1. for all homologous groups and selected congeners K_P value decreases with temperature increase;
2. K_P values calculated for the whole group and 2,3,7,8-substituted congeners of this group can differ appreciably;
3. K_P values for groups PeCDD and PeCDF are close but for the group of dioxins they are always higher.

Substance partitioning between "vapours-particles" phases can be quantitatively characterized by the fraction of substances adsorbed on particles ϕ using the following equations:

$$\phi = c\theta / (p^0_L + c\theta), \qquad \text{(D17)}$$

where c is the constant equal to 0.17, Pa·m [*Junge*, 1977];
θ is the specific surface of aerosol particles, m^2/m^3;
p^0_L is the supersaturated vapour pressure of subcooled liquid, Pa.

For background regions θ is equal to 1.5×10^{-4} m^2/m^3 from [*Whitby*, 1978]. Table D22 presents ϕ values determined experimentally and estimates obtained with p^0_L values from literature data. ϕ values calculated on the basis of p^0_L [*Govers and Krop*, 1998] demonstrate the best correlation with experimental data with exception for ϕ for 2,3,4,6,7,8-HxCDF.

Table D22. Fraction of selected **PeCDD/F** congeners sorbed on particles

Homolog group, Compound	Substance fraction associated with particles (ϕ)						
	Experiment				Estimate of different values p^0_L		
	[*Müller et al.* 1998]	[*Eitzer and Hites*, 1989a]	[*Hippelein et al.*, 1996]	[*Horstmann, McLachlan*, 1998]	[*Govers et al.*, 1998]	[*Bulgakov and Ioannisian*, 1998]	[*Mackay et al.*,1992]
PeCDF	0.086	0.37	0.29	0.36	-	-	-
1,2,3,7,8- PeCDF	-	0.35	0.33	0.39	0.29	0.087	-
2,3,4,7,8- PeCDF	-	0.50	0.39	0.49	0.32	0.125	0.60
HxCDF	0.24	0.73	0.50	0.64	-	-	-
1,2,3,6,7,8-HxCDF	-	0.74	0.57	0.63	0.65	0.23	0.86
1,2,3,4,7,8-HxCDF	-	0.74	0.60	0.62	0.68	0.23	0.89
1,2,3,7,8,9-HxCDF	-	0.86	0.60	0.62	0.53	0.23	-
2,3,4,6,7,8-HxCDF	-	0.89	0.64	0.77	0.25	0.22	-
PeCDD	0	0.33	0.37	0.38	-	-	-
1,2,3,7,8 – PeCDD		0.56	0.40	0.50	0.63	0.27	-
Temperature, ^{0}C	~25	25	20	warm season	25	25	25

D.2.14. Removal of dioxins and furans from the atmosphere with dry and wet depositions

Cleansing of the atmosphere takes place due to wet and dry deposition of pollutants on particles and from the gas phase. Depending on physical-chemical properties of pollutants these processes can be more or less significant. As it was shown by *J.Schroeder et al*. [1997] for dioxins and furans wet deposition is most important, see table D23.

Table D23. Deposition from the atmosphere of the selected homologous groups [*Schroeder et al.,* 1997]

Homolog group	Fraction of different deposition types, %			
	Wet	Dry		
		Aerosol phase		Gas phase
		>2.9 μm	< 2.9 μm	
PeCDF	68	13	6	13
HxCDF	77	13	6	4
PeCDD	73	12	6	9

Washout ratio of the selected compounds in the gas phase is considered above in section (air-water partition coefficient K_{AW}).

Deposition from the atmosphere of substances sorbed on particles are characterized quantitatively by washout coefficient W_P. W_P values obtained in experiments [*Eitzer and Hites*, 1989b] for the selected groups of dioxins and furans are shown in table D24.

Table D24. Washout ratio of substances sorbed on particles

Homologous group	Washout ratio, W_P
PeCDF	18 000
HxCDF	10 000
PeCDD	18 000

Total washout ratio is usually designated by W and calculated from equation:

$$W_T = W_P \phi + W_G (1 - \phi),$$

(D18)

where ϕ is the substance fraction associated with aerosol;
W_P is the washout ratio of a substance associated with aerosols;
W_G is the washout ratio of the vapour phase.

Value W_T of PCDD/F homologous groups ranges from 15000 to 150000. W_T of the selected furans does not exceed 20000 and PeCDD is equal to 30000.

Dry deposition is composed by dry deposition of particles and dry deposition of substances in the gas phase. In dry deposition process temperature is an important factor - dry deposition can increase with temperature increase. Another important factor influencing dry deposition velocity is the content of particulates. The joint impact of these two factors was observed in the experiment, see table D25.

In the process of dry deposition three simultaneous processes can take place - particle sedimentation, coalescence and diffusion. The role of these processes is different for different underlying surfaces. From viewpoint of specialists at dry deposition on forest vegetation diffusion processes will be more intensive.

Dry deposition velocities of all PCDD/F on water surface for the gas phase and particles were estimated in [*McLachlan*, 1998] to be equal to 0.003 m/s.

Table D25. Dry deposition velocities of particles [*Koester and Hites*, 1992]

Homolog group	Dry deposition velocities of particles, cm/s	Deposition conditions
PeCDF	0.064	t = 17 °C, TSP = 50 μg/m^3
	0.090	t = 26 °C, TSP = 80 μg/m^3
HxCDF	0.12	t = 17 °C, TSP = 50 μg/m^3
	0.086	t = 26 °C, TSP = 80 μg/m^3
	0.023	-
PeCDD	0.015	t = 17 °C, TSP = 50 μg/m^3
	0.34	t = 26 °C, TSP = 80 μg/m^3

D.2.15. Behaviour of substances in the atmosphere. Chemical interaction of dioxins and furans with active components of the atmosphere

Species being in the gas phase entering the troposphere (the upper layer of the atmosphere) can be transformed due to reactions with radicals and under the impact of ultra-violet radiation.

Radical reactions

Chlorinated dioxins and furans are chemically inert. Up till now investigators focused their attention on their interaction with radicals: OH, NO_3 and O_3. In studies of reaction kinetic rate constants of compounds similar by structure to PCDD/F were determined (see table D26 where data of [*Kwok et al*., 1994] are presented).

Extremely low values of dibenzo-p-dioxin and dibenzofuran rate constants of reactions with ozone and radical NO_3 make it possible to ignore degradation of chlorinated dibenzo-p-dioxins and furans in the atmosphere due to their reactions with ozone and radical NO_3 since reactivity of chlorinated compounds is even less than that of non-chlorinated ones.

Table D26. Rate constants of reactions and calculated life-time in the atmosphere of dibenzo-p-dioxin and dibenzofuran with basic radicals and ozone (at room temperature)

Rate constants of reactions, cm/molec./s	Dibenzo-p-dioxin	Dibenzofuran
k_{OH}	1.48×10^{-11}	3.9×10^{-12}
k_{NO3}	3.9×10^{-27} $[NO_2]$	$< 7 \times 10^{-30}$ $[NO_2]$
k_{O3}	$< 5 \times 10^{-20}$	$< 8 \times 10^{-20}$
Calculated life-time in troposphere, days		
OH^-	1.0	3.7
NO_3^-	> 4.9	> 7
O_3	> 330	> 205

Rate constants of gaseous PCDD/F decomposition due to interaction with OH were theoretically predicted by *R.Atkinson* even in 1991 for a great number of individual compounds. Reasoning from these calculated values and the following relationship:

$$k^*_{OH} = k_{OH} \cdot [OH], \qquad \text{(D19)}$$

where k^*_{OH} is the reaction rate constant of the pseudo-first order, s^{-1};
k_{OH} is the reaction rate constant with hydroxyl radical, m^3/molec/s;
[OH] is the hydroxyl-radical concentration in air, molec/cm^3.

we obtained rate constants of reactions with hydroxyl-radical for selected compounds from PCDD/F family for different seasons, see table D27. In doing so we considered OH concentration for different seasons. For example, for the territory located at 45^0N we used values of OH [*Yu Lu and Khall*, 1991] equal to:

- summer – 2×10^6 molec/cm^3;
- spring and autumn – 0.8×10^6 molec/cm^3;
- winter – 0.09×10^6 molec/cm^3;
- mean annual – 0.8×10^6 molec/cm^3.

Table D27. Reaction rates of selected gas phase dioxins and furans with hydroxyl-radical for different seasons

Compound	k_{OH}, cm^3/molec/s [*Atkinson*, 1991]	k_{OH}^*, s^{-1}			
		summer	autumn/ spring	winter	mean annual
1,2,3,7,8 – PeCDF	2.5E-12	5.00E-06	2.00E-06	2.25E-07	2.00E-06
2,3,4,7,8 – PeCDF	1.8E-12	3.60E-06	1.44E-06	1.62E-07	1.44E-06
1,2,3,4,7,8 – HxCDF	1.6E-12	3.20E-06	1.28E-06	1.44E-07	1.28E-06
1,2,3,6,7,8 – HxCDF	1.6E-12	3.20E-06	1.28E-06	1.44E-07	1.28E-06

1,2,3,7,8,9 – HxCDF	1.8E-12	3.60E-06	1.44E-06	1.62E-07	1.44E-06
2,3,4,6,7,8 – HxCDF	7.4E-13	1.48E-06	5.92E-07	6.66E-08	5.92E-07
1,2,3,7,8 – PeCDD	6.5E-12	1.30E-05	5.20E-06	5.85E-07	5.20E-06

Photolytic decomposition of PCDD/F in the atmosphere

Photolysis of chlorinated dibenzo-p-dioxins and furans occurring in the atmosphere in the gas state was not confirmed experimentally. Therefore in modelling of the atmospheric transport this processes can be neglected.

Particles of different genesis associated with highly chlorinated compounds can reach the upper layers of the atmosphere. In this case there arises a necessity to estimate photolic degradation of the substance on particles. *K.G.Koester and R.Hites*, [1992] carried out a series of model experiments and used as particles-carriers both clean silica gel artificially covered with a mixture of dioxins and furans of a known composition and several samples of flying ash with established content of dioxins and furans [*Koester and Hites*, 1992]. As a result time of half-life for some dioxins and furans with 4, 5, 6 and 8 chlorine atoms in the molecule was obtained.

In the case of sorption on silica gel time of half-life of chlorinated dioxins of four homologous groups (from tetra to octa) are shorter than that of chlorinated dioxins and ranges from 3 to 14 hours. Half-life time of chlorinated dioxins belonging to the same homologous group varied in the experiment from 88 to 270 hours.

However, clean silica gel cannot be an adequate surrogate of atmospheric aerosol. In case of PCDD/F sorption by particles of flying ash no concentration reduction under the impact of UV-radiation is observed. Lack of reliable experimental data on photolic degradation rate and atmospheric particle compositions prevents from the consideration of photolic decomposition process in modelling of the long-range transport of the selected compounds.

D.2.16. Degradation rates of PCDD/F in different natural compartments

Degradation rates of species in different natural compartments are characterized quantitatively by the time (periods) of their half-life.

Degradation in the atmosphere

The atmospheric half-life of the selected compounds from PCDD/F family were estimated on the basis of rates of reactions with hydroxyl-radical. The obtained values are presented in table D28.

The handbook by *D.Mackay et al.* [1992] recommends to use value 550 hours in estimating the life-time of compounds from dioxin and furan family for 2,3,7,8-substituted PeCDD, PeCDF.

Table D28. Half-lives of the selected compounds in the atmosphere

Compound	Half-life in the atmosphere, h			
	summer	autumn/spring	winter	mean annual
1,2,3,7,8 – PeCDF	38.50	96.25	855.56	96.25
2,3,4,7,8 – PeCDF	53.47	133.68	1188.27	133.68
1,2,3,4,7,8 – HxCDF	60.16	150.39	1336.81	150.39
1,2,3,6,7,8 – HxCDF	60.16	150.39	1336.81	150.39
1,2,3,7,8,9 – HxCDF	53.47	133.68	1188.27	133.68
2,3,4,6,7,8 – HxCDF	130.07	325.17	2890.39	325.17
1,2,3,7,8 – PeCDD	14.81	37.02	329.06	37.02

Degradtion in the surface waters

Stability of polychlorinated dibenzo-p-dioxins and furans in surface waters is discussed reasonably in detail in the review by *A.A.Bulgakov and D.A.Ioannisian* [1998]. Like in the of atmosphere these stable substances are degraded mainly due to reaction with hydroxyl-radical. Rate constants of the reaction with OH - radical for penta- and hexa - chlorinated dioxins and furans is estimated by the authors as 4×10^9 l/molec×s.

Half-life of these species in water is 550 hours for 2,3,7,8-substituted PeCDD and PeCDF and 1700 hours for HxCDF [*Mackay et al*., 1992].

Degradation in soil and bottom sediments

Highly chlorinated dibenzo-p-dioxins and furans are very stable in such environmental compartments as soil and bottom sediments. For example, as a result of investigations of soil pollution caused by the accident in the region of Sevezo city, the half-life of 2,3,7,8-TCDD was estimated to be not less than 10 years.

Expert estimates of degradation rates of the selected groups of PCDD/F in soil and bottom sediments [*Mackay et al.*, 1992] are presented in table D29.

Table D29. Half-lives of selected PCDD/F in soils and bottom sediments

Environmental compartment	Half-lives of selected homologous groups		
	2,3,4,7,8 – PeCDF	1,2,3,4,7 - PeCDD	1,2,3,6,7,8 – HxCDF
Soil	10.000- 30.000 17.000 about 2 year	10.000- 30.000 17.000 about 2 year	10.000- 30.000 17.000 about 2 year
Bottom sediments	>30.000 55.888	>30.000 55.888	>30.000 55.888

	about 6 year	about 6 year	about 6 year

ANNEX E

Annual and monthly statistics for POPs

E1. *Annual statistics for POPs in precipitation*

DE 1 WESTERLAND GERMANY
January 1996 - December 1996

Component	W. Mean	Min	Max	Num bel	Num day	Samp flag	QA flag
Precipitation	-	0	87.6	3	12	M	
Benzo[a]pyrene	3.88	0	18	1	12	M	

DE 9 ZINGST GERMANY
January 1996 - December 1996

Component	W. Mean	Min	Max	Num bel	Num day	Samp flag	QA flag
Precipitation	-	0	76.6	1	12	M	
Benzo[a]pyrene	8.4	0	66	1	12	M	
PCB_101	0.03	0	0.6	1	12	M	9
PCB_118	0.07	0	0.07	1	12	M	9
PCB_138	0.07	0	0.78	1	12	M	9
PCB_149	0.03	0	0.03	1	12	M	9
PCB_153	0.07	0	0.4	1	12	M	9
PCB_177	0.07	0	0.07	1	12	M	9
PCB_18	0.07	0	0.07	1	12	M	9
PCB_180	0.07	0	0.07	1	12	M	9
PCB_26	0.01	0	0.01	1	12	M	9
PCB_28	0.01	0	0.01	1	12	M	9
PCB_44	0.07	0	0.07	1	12	M	9
PCB_52	0.07	0	0.07	1	12	M	9

DE0009R ZINGST GERMANY

January 1997 - December 1997

Component	W. Mean	Min	Max	Num bel	Num day	Samp flag	QA flag
PCB_101	0.336	0	1.3	7	12	M	
PCB_118	0.081	0	0.3	11	12	M	
PCB_138	0.457	0	3.8	7	12	M	
PCB_153	0.428	0	3.1	7	12	M	
PCB_180	0.931	0	8	6	12	M	
PCB_28	0.01	0	0.01	12	12	M	
PCB_52	0.371	0	3	8	12	M	
Sum_PCB	2.239	0	7.15	8	11	M	
Benzo[a]pyrene	6.259	0	33	2	12	M	
Precipitation	-	0	87.8	10	12	M	

FI96 PALLAS FINLAND

January 1996 - December 1996

Component	Mean ng/m^2 day	Min	Max	Num bel	Num day	Samp flag	QA flag
PCB_101	0.3	0.09	0.77	0	11	1W	8
PCB_118	0.14	0.04	0.35	0	11	1W	8
PCB_138	0.5	0.11	1.73	0	11	1W	8
PCB_153	0.48	0.12	1.72	0	11	1W	8
PCB_180	0.38	0.09	1.47	0	11	1W	8
PCB_28	0.42	0.23	0.89	0	11	1W	8
PCB_52	0.2	0	0.32	1	11	1W	8
Precipitation	-	0	11	1	12	1W	
Benzo[a]pyrene	2.2	0	8	8	10	1W	8

IE0002R TURLOUGH HILL IRELAND

January 1997 - December 1997

Component	W. Mean	Min	Max	Num bel	Num day	Samp flag	QA flag
PCB_101	0.803	0.5	3.5	12	12	M	1
PCB_118	0.803	0.5	3.5	12	12	M	1
PCB_138	0.803	0.5	3.5	12	12	M	1
PCB_153	0.803	0.5	3.5	12	12	M	1
PCB_180	0.803	0.5	3.5	12	12	M	1
PCB_52	0.803	0.5	3.5	12	12	M	1
Benzo[a]pyrene	-	32.1	358.6	0	12	M	

IS91 STORHOFDI ICELAND

January 1996 - December 1996

Component	W. Mean	Min	Max	Num bel	Num day	Samp flag	QA flag
PCB_101	0.04	0	0.37	4	24	W2	
PCB_105	0.02	0	0.13	11	24	W2	
PCB_118	0.04	0	0.16	6	24	W2	
PCB_138	0.06	0	0.73	9	24	W2	
PCB_153	0.07	0	0.63	4	24	W2	
PCB_156	0.01	0	0.07	11	24	W2	
PCB_180	0.04	0	0.37	4	24	W2	
PCB_28	0.16	0	1.99	8	24	W2	
PCB_31	0.16	0	2.09	11	24	W2	
PCB_52	0.06	0	0.51	4	24	W2	
Precipitation	-	4	122	0	24	W2	

IS0091R STORHOFDI ICELAND

January 1997 - December 1997

Component	W. Mean	Min	Max	Num bel	Num day	Samp flag	QA flag
PCB_101	0.008	0	0.08	13	24	W2	
PCB_105	0.002	0	0.02	21	24	W2	
PCB_118	0.008	0	0.06	13	24	W2	
PCB_138	0.008	0	0.06	13	24	W2	
PCB_153	0.011	0	0.06	14	24	W2	
PCB_156	0.005	0	0.08	17	24	W2	
PCB_180	0.011	0	0.06	10	24	W2	
PCB_28	0.185	0	2.54	11	24	W2	
PCB_31	0.151	0	1.92	12	24	W2	
PCB_52	0.05	0	0.81	12	24	W2	
Precipitation off	-	7	149	0	24	W2	

SE 2 RORVIK SWEDEN

January 1996 - December 1996

Component	Mean Ng/m2 day	Min	Max	Num bel	Num day	Samp flag	QA flag
PCB_101	0.14	0	0.27	1	12	W1	8
PCB_118	0.07	0	0.14	2	12	W1	8
PCB_138	0.29	0.13	0.6	0	12	W1	8
PCB_153	0.25	0	0.49	1	12	W1	8
PCB_180	0.23	0.09	0.53	0	12	W1	8
PCB_28	0.46	0.25	0.85	0	12	W1	8
PCB_52	0.27	0.15	0.48	0	12	W1	8
Precipitation	-	0	36.1	3	12	W1	
benzo_a_pyrene	10.58	2	27	3	12	W1	8

E2. *Annual statistics for POPs in air*

CZ0003R KOSETICE CZECH REPUBLIC

January 1997 - December 1997

Component	Arit mean	Arit sd	Geom mean	Geom sd	Min	50%	Max	Num bel	Num samp	Samp flag	QA flag
PCB_101	22.873	14.724	14.73	3.682	0.5	23	79	5	51	W	
PCB_118	3.725	2.532	2.828	2.308	0.5	3	13	6	51	W	
PCB_138	32.539	23.165	22.342	3.149	0.5	25.5	112	3	51	W	
PCB_153	40.637	22.327	29.559	3.167	0.5	39	101	3	51	W	
PCB_180	25.48	22.654	16.403	3.147	0.5	16.5	117	3	51	W	
PCB_28	24.814	15.74	16.831	3.334	0.5	23.5	84	3	51	W	
PCB_52	19.833	12.994	12.787	3.664	0.5	19	72	5	51	W	
Benzo[a]pyrene	0.642	1.99	0.084	8.387	0.005	0.055	13.77	10	51	W	

CZ0003R KOSETICE CZECH REPUBLIC

January 1996 - December 1996

Component	Arit mean	Arit sd	Geom mean	Geom sd	Min	50%	Max	Num bel	Num samp	Samp flag	QA flag
Benzo_a_pyrene	0.054	0.084	0.025	3.23	0.005	0.019	0.332	0	31	W	

FI0096R PALLAS FINLAND

January 1996 - December 1996

Component	Arit mean	Arit sd	Geom mean	Geom sd	Min	50%	Max	Num bel	Num samp	Samp flag	QA flag
PCB_101	1.529	0.816	1.359	1.646	0.628	1.189	3.335	0	12	W1	
PCB_118	0.519	0.278	0.456	1.702	0.199	0.422	1.057	0	12	W1	
PCB_138	1.432	1.252	1.042	2.323	0.322	1.112	4.711	0	12	W1	
PCB_153	1.523	1.389	1.115	2.261	0.388	1.231	5.301	0	12	W1	
PCB_180	0.872	0.647	0.601	2.748	0.131	0.873	2.21	0	12	W1	
PCB_28	3.169	0.854	3.066	1.308	2.126	2.782	4.729	0	12	W1	
PCB_52	1.919	0.896	1.766	1.505	1.061	1.614	4.007	0	12	W1	
Benzo_a_pyrene	0.015	0.014	0.011	2.25	0.004	0.007	0.053	0	12	W1	

IS0091R STORHOFDI ICELAND

January 1996 - December 1996

Component	Arit mean	Arit sd	Geom mean	Geom sd	Min	50%	Max	Num bel	Num samp	Samp flag	QA flag
PCB_101	0.992	1.702	0.621	3.08	0	0.4	7.7	10	24	W2	
PCB_105	0.383	0.685	0.934	1.473	0	0	2.9	15	24	W2	
PCB_118	0.998	2.193	0.592	4.061	0	0.1	9.7	16	24	W2	
PCB_138	1.329	2.486	0.985	3.213	0	0.1	10.6	13	24	W2	
PCB_153	1.767	3.367	0.862	3.862	0	0.4	14.9	11	24	W2	
PCB_156	0.091	0.193	0.554	2.284	0	0	0.8	20	23	W2	
PCB_180	0.721	1.106	0.757	2.606	0	0.1	3.8	12	24	W2	
PCB_28	5.063	5.287	3.524	2.2	0	3.9	22.9	2	24	W2	
PCB_31	3.417	6.084	2.033	2.475	0	1.1	25.4	10	24	W2	
PCB_52	2.09	2.073	1.472	2.487	0	1.4	8	2	24	W2	

IS0091R STORHOFDI ICELAND

January 1997 - December 1997

Component	Arit mean	Arit sd	Geom mean	Geom sd	Min	50%	Max	Num bel	Num samp	Samp flag	QA flag
PCB_101	0.297	0.432	0.873	1.493	0	0	1.07	15	24	W2	
PCB_105	0.045	0.117	0.786	1.731	0	0	0.45	20	24	W2	
PCB_118	0.2	0.305	0.616	1.865	0	0	1.2	13	24	W2	
PCB_138	0.268	0.38	0.662	1.73	0	0	1.5	12	24	W2	
PCB_153	0.267	0.407	0.588	1.87	0	0.11	1.8	11	24	W2	
PCB_156	0.006	0.029	0.921	1.481	0	0	0.14	23	24	W2	
PCB_180	0.103	0.165	0.584	1.924	0	0	0.6	15	24	W2	
PCB_28	1.955	2.645	1.814	1.882	0	0	9	13	24	W2	
PCB_31	2.093	2.473	1.92	1.869	0	0	6.9	12	24	W2	
PCB_52	0.887	1.057	1.332	1.339	0	0	3.14	13	24	W2	

NO0042G SPITZBERGEN NORWAY

January 1996 - December 1996

Component	Arit mean	Arit sd	Geom mean	Geom sd	Min	50%	Max	Num bel	Num samp	Samp flag	QA flag
PCB_101	4.928	6.493	2.279	3.474	0.37	1.54	29.12	0	48	D2	3
PCB_105	1.229	1.658	0.576	3.976	0.01	0.54	8	1	48	D2	3
PCB_118	2.417	3.266	1.053	4.231	0.01	0.67	18.07	1	48	D2	3
PCB_138	1.343	1.539	0.814	2.743	0.12	0.65	7.19	0	48	D2	3
PCB_153	2.285	2.894	1.274	2.954	0.17	1.13	12.89	0	48	D2	3
PCB_156	0.089	0.153	0.035	4.17	0.005	0.04	0.84	18	48	D2	3
PCB_180	0.74	1.676	0.182	5.512	0.005	0.18	7.85	6	48	D2	3
PCB_28	69.783	109.787	34.089	3.094	3.26	24.35	499.51	0	48	D2	3
PCB_31	62.153	96.052	31.339	3.009	2.94	24	426.72	0	48	D2	3
PCB_52	19.615	37.133	8.378	3.245	1.32	5.71	219.68	0	48	D2	3
Benzo[a]pyrene	0.006	0.024	0.134	9.649	0	0.001	0.146	24	38	D2	

SE0002R RORVIK SWEDEN

January 1996 - December 1996

Component	Arit mean	Arit sd	Geom mean	Geom sd	Min	50%	Max	Num bel	Num samp	Samp flag	QA flag
PCB_101	3.529	2.216	3.025	1.786	1.061	3.037	9.299	0	11	W1	
PCB_118	1.113	0.628	0.98	1.685	0.423	0.979	2.702	0	11	W1	
PCB_138	1.954	1.099	1.75	1.602	0.833	1.512	4.886	0	11	W1	
PCB_153	2.149	1.243	1.904	1.649	0.833	1.698	5.422	0	11	W1	
PCB_180	0.768	0.327	0.712	1.491	0.397	0.607	1.518	0	11	W1	
PCB_28	5.272	1.868	5.03	1.361	3.027	4.529	9.905	0	11	W1	
PCB_52	4.166	2.343	3.699	1.65	1.616	3.865	10.324	0	11	W1	
Benzo[a]pyrene	0.094	0.099	0.046	4.297	0.003	0.044	0.275	0	11	W1	

NO0042G SPITZBERGEN NORWAY

January 1997 - December 1997

Component	Arit mean	Arit sd	Geom mean	Geom sd	Min	50%	Max	Num bel	Num samp	Samp flag	QA flag
PCB_101	1.759	2.31	1.072	2.549	0.06	0.91	9.97	0	52	D2	3
PCB_105	0.314	0.301	0.209	2.555	0.01	0.19	1.11	0	52	D2	3
PCB_114	0.031	0.035	0.019	2.641	0.005	0.02	0.15	14	52	D2	3
PCB_118	0.742	0.761	0.513	2.262	0.1	0.41	3.27	0	52	D2	3
PCB_123	0.025	0.029	0.015	2.651	0.005	0.01	0.12	15	52	D2	3
PCB_128	0.107	0.089	0.077	2.323	0.01	0.06	0.39	0	52	D2	3
PCB_138	0.517	0.42	0.385	2.213	0.04	0.37	2.06	0	52	D2	
PCB_141	0.124	0.101	0.091	2.304	0.005	0.08	0.41	1	52	D2	3
PCB_149	0.648	0.606	0.46	2.338	0.02	0.39	2.74	0	52	D2	3
PCB_153	0.702	0.596	0.528	2.123	0.09	0.42	2.91	0	52	D2	
PCB_156	0.047	0.04	0.034	2.336	0.005	0.03	0.17	2	52	D2	3
PCB_157	0.011	0.007	0.009	1.702	0.005	0.01	0.04	20	52	D2	3
PCB_167	0.026	0.022	0.019	2.184	0.005	0.02	0.11	4	52	D2	3
PCB_170	0.072	0.064	0.05	2.464	0.005	0.06	0.31	2	52	D2	3
PCB_18	67.297	124.716	39.707	2.624	1.12	35.07	898.11	0	52	D2	3
PCB_180	0.193	0.163	0.138	2.37	0.01	0.16	0.92	1	52	D2	
PCB_183	0.074	0.053	0.056	2.315	0.005	0.06	0.22	2	33	D2	3
PCB_187	0.138	0.096	0.106	2.219	0.005	0.1	0.37	1	52	D2	3
PCB_189	0.006	0.004	0.006	1.47	0.005	0.005	0.03	49	52	D2	3
PCB_206	0.009	0.011	0.006	1.832	0.005	0.005	0.05	48	52	D2	3
PCB_209	0.013	0.014	0.009	2.239	0.005	0.005	0.05	41	52	D2	3
PCB_28	45.933	80.166	24.628	3.013	0.41	22.49	543.66	0	52	D2	3
PCB_31	43.404	76.225	23.609	2.941	0.45	21.14	521.39	0	52	D2	3
PCB_33	39.826	71.706	20.14	3.111	0.37	18.02	461.89	0	52	D2	3
PCB_37	10.11	19.616	4.058	3.528	0.17	4.04	93.18	0	52	D2	3
PCB_47	7.121	13.317	3.68	2.88	0.1	3.23	82.85	0	52	D2	3
PCB_52	10.375	17.88	5.866	2.631	0.33	5	113.67	0	52	D2	3
PCB_66	8.621	16.161	3.575	3.373	0.2	3.14	76.99	0	52	D2	3
PCB_74	4.109	7.761	1.77	3.254	0.08	1.56	36.2	0	52	D2	3
PCB_99	0.754	0.984	0.47	2.448	0.04	0.37	4.52	0	52	D2	3
Benzo[a]pyrene	0.015	0.036	0.07	8.88	0	0.001	0.205	27	51	D2	3

E3. *Monthly mean values on data for POPs in air*

		Year	Jan	Feb	Mar	Apr	May	Jun	Jul	Aug	Sep	Oct	Nov	Dec	QA
CZ3R	PCB_101	1997	23.9	3.375	23	35	27.75	28.5	37	32.25	22.25	7.1	14.5	15	
CZ3R	PCB_118	1997	0.8	1.875	4	5.6	4.5	5.5	6.6	5	3.75	1.7	2.75	2.333	
CZ3R	PCB_138	1997	34.1	8.125	22.25	46.8	32.75	54	66.8	41	26.5	10.9	20.5	15.333	
CZ3R	PCB_153	1997	48.7	8.375	27.5	51.8	35.75	51.75	68	45.25	34.5	25.9	43.5	38	
CZ3R	PCB_180	1997	43.1	5.125	15	38.6	20.5	36.5	55.6	27	14	7.1	16.25	13.333	
CZ3R	PCB_28	1997	23.7	6.625	25.5	35.8	31	34.5	36.8	35.25	25.5	8.9	17.25	12.333	
CZ3R	PCB_52	1997	15.7	13.125	23.25	29.6	25.25	21.125	23.3	27.5	20	7.1	16	16	
CZ3R	Benzo[a]pyrene	1996	0.233	0.076	0.053	0.036	0.013	0.011	0.011	0.012	-	-	-	-	
FI96R	PCB_101	1996	3.335	1.663	1.189	1.12	1.201	1.824	2.73	1.915	1.029	0.923	0.787	0.628	
FI96R	PCB_118	1996	1.057	0.72	0.42	0.422	0.458	0.553	0.988	0.559	0.313	0.315	0.219	0.199	
FI96R	PCB_138	1996	4.711	2.75	1.359	1.266	1.076	1.56	1.786	1.112	0.478	0.372	0.322	0.386	
FI96R	PCB_153	1996	5.301	2.889	1.445	1.271	1.082	1.663	1.631	1.231	0.533	0.447	0.388	0.393	
FI96R	PCB_180	1996	2.21	1.357	0.913	0.873	0.918	1.348	1.457	0.705	0.234	0.134	0.131	0.179	
FI96R	PCB_28	1996	3.63	3.177	2.748	2.126	2.211	2.782	4.729	3.863	2.592	2.254	4.223	3.697	
FI96R	PCB_52	1996	2.046	1.614	1.393	1.404	1.62	2.635	4.007	3.123	1.682	1.258	1.188	1.061	
FI96R	Benzo[a]pyrene	1996	0.007	0.053	0.021	0.007	0.015	0.007	0.004	0.011	0.027	0.006	0.004	0.021	
IS91R	PCB_101	1996	0.053	0.85	6.006	0.918	0.439	1	0.706	0.597	0.25	0.266	0.45	0.34	
IS91R	PCB_101	1997	0	0	0.075	0.982	0.935	0.793	0.024	0	0	0	0.49	0.189	
IS91R	PCB_105	1996	0.2	0.621	2.174	0.62	0.242	0.4	0.339	0	0	0	0	0	
IS91R	PCB_105	1997	0.015	0	0	0	0	0	0.135	0.005	0	0	0.163	0.189	
IS91R	PCB_118	1996	0.2	1.914	7.039	1.152	0.245	0.75	0.581	0.045	0.05	0.003	0.025	0.03	
IS91R	PCB_118	1997	0.027	0.255	0.585	0.523	0.3	0.077	0	0	0	0	0.327	0.189	
IS91R	PCB_138	1996	0.653	2.221	8.374	1.513	0.484	1.3	0.871	0.406	0	0	0.025	0.09	
IS91R	PCB_138	1997	0.027	0.315	0.79	0.816	0.411	0.39	0.242	0.014	0	0	0.163	0	
IS91R	PCB_153	1996	0.62	3.29	11.029	2.067	0.387	1.5	1.116	0.639	0.05	0.121	0.075	0.36	
IS91R	PCB_153	1997	0.052	0.215	0.915	0.7	0.304	0.388	0.16	0.009	0	0	0.327	0	
IS91R	PCB_156	1996	0.05	0.207	0.606	0.047	0.048	0.05	0.048	0	0	0	0	0	
IS91R	PCB_156	1997	0	0	0	0	0	0	0.063	0	0	0	0	0	
IS91R	PCB_180	1996	1.923	1.321	3.042	0.43	0.435	0.6	0.548	0.077	0.25	0.016	0	0.06	
IS91R	PCB_180	1997	0.006	0.155	0.26	0.343	0.119	0.068	0.076	0.005	0	0	0.163	0	
IS91R	PCB_28	1996	3.763	3.141	19.852	3.54	4.926	8.45	5.11	2.023	3.2	1.7	2.65	3.1	
IS91R	PCB_28	1997	2.701	3.2	4.043	5.879	3.464	3.578	0.051	0	0	0	0	0	
IS91R	PCB_31	1996	4.1	1.397	21.384	0	0	0	0.258	2.335	3.3	2.165	3	3.56	
IS91R	PCB_31	1997	3.43	2.83	3.578	5.506	4.18	5.12	0.157	0	0	0	0	0	
IS91R	PCB_52	1996	3.533	2.279	7.274	1.593	1.139	1.8	0.706	0.561	1.45	1.419	1.65	1.82	
IS91R	PCB_52	1997	1.576	1.525	0.142	2.426	1.709	1.69	0.051	0	0	0	1.465	0	
NO42G	PCB_138	1996	0.316	0.418	0.61	2.082	1.414	3.352	3.276	1.516	0.707	0.416	0.481	1.013	3
NO42G	PCB_101	1996	1.397	1.154	0.92	13.248	15.102	11.413	5.864	1.627	0.903	0.714	0.988	1.515	3
NO42G	PCB_101	1997	0.44	0.8	0.759	2.814	1.425	2.418	1.121	1.984	4.727	1.508	1.195	1.12	3
NO42G	PCB_105	1996	0.136	0.084	0.21	1.017	1.318	2.165	3.794	1.497	0.653	0.336	2.17	0.587	3
NO42G	PCB_105	1997	0.082	0.16	0.151	0.376	0.313	0.593	0.363	0.302	0.608	0.224	0.28	0.197	3
NO42G	PCB_114	1997	0.005	0.011	0.02	0.038	0.03	0.067	0.022	0.035	0.065	0.028	0.029	0.015	3
NO42G	PCB_118	1996	0.409	0.247	0.62	3.258	3.712	6.235	8.154	2.377	0.917	0.44	0.392	0.5	3
NO42G	PCB_118	1997	0.204	0.37	0.429	0.857	0.635	1.337	0.551	0.842	1.548	0.666	0.725	0.517	3
NO42G	PCB_123	1997	0.021	0.008	0.009	0.03	0.02	0.04	0.019	0.029	0.051	0.023	0.026	0.012	3
NO42G	PCB_128	1997	0.038	0.065	0.089	0.104	0.1	0.213	0.216	0.088	0.132	0.042	0.062	0.097	3
NO42G	PCB_138	1997	0.216	0.375	0.62	0.571	0.536	1.102	0.726	0.37	0.585	0.254	0.33	0.467	3
NO42G	PCB_141	1997	0.04	0.072	0.051	0.148	0.132	0.233	0.17	0.111	0.175	0.086	0.108	0.127	3
NO42G	PCB_149	1997	0.198	0.333	0.301	0.896	0.619	0.995	0.558	0.692	1.183	0.554	0.663	0.623	3
NO42G	PCB_153	1996	0.441	0.917	0.9	4.5	2.138	5.95	4.78	1.98	0.86	0.506	1.66	2.003	3

		Year	Jan	Feb	Mar	Apr	May	Jun	Jul	Aug	Sep	Oct	Nov	Dec	QA
NO42G	PCB_153	1997	0.334	0.502	1.013	0.836	0.716	1.51	0.708	0.509	0.775	0.394	0.498	0.577	3
NO42G	PCB_156	1996	0.006	0.017	0.04	0.244	0.055	0.255	0.14	0.091	0.035	0.032	0.03	0.109	3
NO42G	PCB_156	1997	0.02	0.032	0.054	0.044	0.04	0.105	0.085	0.041	0.055	0.012	0.02	0.047	3
NO42G	PCB_157	1997	0.005	0.009	0.014	0.01	0.009	0.02	0.017	0.009	0.011	0.006	0.009	0.012	3
NO42G	PCB_167	1997	0.011	0.018	0.039	0.026	0.025	0.058	0.038	0.021	0.02	0.012	0.011	0.018	3
NO42G	PCB_170	1997	0.022	0.06	0.11	0.064	0.053	0.1	0.121	0.064	0.095	0.022	0.037	0.103	3
NO42G	PCB_18	1997	21.016	21.16	37.761	237.986	62.892	97.145	121.451	38.142	80.927	21.556	18.44	43.373	3
NO42G	PCB_180	1996	0.053	0.139	0.16	2.086	0.194	1.985	0.402	0.289	0.15	0.14	1.385	1.861	3
NO42G	PCB_180	1997	0.079	0.16	0.319	0.182	0.158	0.31	0.339	0.169	0.192	0.072	0.091	0.207	3
NO42G	PCB_183	1997	-	-	-	-	0.053	0.127	0.127	0.06	0.068	0.036	0.043	0.06	3
NO42G	PCB_187	1997	0.048	0.085	0.126	0.149	0.144	0.24	0.243	0.121	0.142	0.078	0.108	0.123	3
NO42G	PCB_189	1997	0.01	0.005	0.009	0.005	0.005	0.008	0.007	0.005	0.005	0.005	0.005	0.007	3
NO42G	PCB_206	1997	0.006	0.006	0.009	0.005	0.005	0.019	0.013	0.011	0.005	0.005	0.005	0.005	3
NO42G	PCB_209	1997	0.016	0.024	0.013	0.006	0.005	0.017	0.013	0.011	0.006	0.014	0.016	0.012	3
NO42G	PCB_28	1996	18.71	18.45	12.88	285.997	205.478	27.903	59.558	50.233	34.537	18.302	15.53	33.798	3
NO42G	PCB_28	1997	10.586	10.862	21.689	139.856	41.72	64.312	63.203	34.881	94.985	14.856	11.932	24.527	3
NO42G	PCB_31	1996	16.723	16.594	11.59	253.302	175.418	25.043	53.677	46.263	32.22	17.614	15.372	33.852	3
NO42G	PCB_31	1997	10.648	11.205	21.493	134.363	39.072	60.658	59.967	32.126	87.162	13.534	10.96	23.183	3
NO42G	PCB_33	1997	8.74	9.53	17.723	118.223	34.827	54.823	50.642	32.184	93.982	10.476	9.238	18.99	3
NO42G	PCB_37	1997	1.186	2.115	2.843	22.234	7.249	11.62	8.042	11.986	37.018	4.288	1.895	2.4	3
NO42G	PCB_47	1997	1.834	2.635	3.146	21.328	6.007	8.468	6.736	5.521	19.747	2.414	1.72	3.06	3
NO42G	PCB_52	1996	5.458	4.582	3.59	93.542	60.302	7.072	12.637	10.972	6.83	3.712	3.73	7.138	3
NO42G	PCB_52	1997	2.938	4.517	4.933	29.602	8.645	13.208	10.797	8.374	25.72	3.71	2.85	5.157	3
NO42G	PCB_66	1997	0.932	2.173	1.999	14.571	5.327	8.148	5.26	11.662	34.983	6.758	3.12	1.79	3
NO42G	PCB_74	1997	0.548	1.14	1.159	8.527	2.753	4.02	2.767	5.02	15.918	2.46	1.115	0.95	3
NO42G	PCB_99	1997	0.198	0.39	0.419	1.138	0.605	1.043	0.452	0.879	2.023	0.624	0.51	0.37	3
NO42G	Benzo[a]pyrene	1996	0.074	0.009	0.004	0.001	0.001	0.001	0	0	0.001	0.003	0.003	0.006	3
NO42G	Benzo[a]pyrene	1997	0.098	0.043	0.007	0.001	0	0.001	0	0.001	0	0.001	0.002	0.01	3
SE2R	PCB_101	1996	1.061	1.687	1.864	4.683	2.992	3.082	4.277	9.299	3.557	3.828	2.487	-	
SE2R	PCB_118	1996	0.423	0.573	0.602	1.422	0.827	1.13	1.313	2.702	1.266	1.231	0.751	-	
SE2R	PCB_138	1996	0.833	1.529	1.082	2.592	1.494	1.398	1.995	4.886	2.266	1.97	1.449	-	
SE2R	PCB_153	1996	0.833	1.631	1.258	2.83	1.765	1.248	2.238	5.422	2.381	2.479	1.559	-	
SE2R	PCB_180	1996	0.534	0.841	0.584	1.027	0.565	0.397	0.47	1.518	0.905	0.976	0.629	-	
SE2R	PCB_28	1996	3.027	4.544	4.468	7.497	4.514	4.402	4.414	9.905	5.083	5.239	4.894	-	
SE2R	PCB_52	1996	1.616	2.194	2.287	5.439	3.15	4.05	4.271	10.324	4.376	4.444	3.68	-	
SE2R	Benzo[a]pyrene	1996	0.275	0.148	0.266	0.034	0.008	0.003	0.016	0.023	0.054	0.091	0.12	-	

E4. *Monthly mean values on data for POPs in precipitation*

		Year	Jan	Feb	Mar	Apr	May	Jun	Jul	Aug	Sep	Oct	Nov	Dec	QA
DE0001R	Precipitation	1996	0	13.6	5	2.4	32.5	9.3	32.1	58.4	31.1	36.1	92.1	12.2	
DE0001R	Benzo[a]pyrene	1996	-	9.49	3.51	0.29	3.91	7.6	2	2.3	0.67	2.3	5.2	18	
DE0009R	PCB_101	1996	-	0.03	0.03	0.03	0.03	0.6	0.03	0.03	0.03	0.03	0.03	0.03	9
DE0009R	PCB_101	1997	-	0.03	0.74	0.03	0.7	0.44	1.3	0.2	0.03	0.03	0.03	0.03	
DE0009R	PCB_118	1996	-	0.07	0.07	0.07	0.07	0.07	0.07	0.07	0.07	0.07	0.07	0.07	9
DE0009R	PCB_118	1997	-	0.07	0.07	0.3	0.07	0.07	0.07	0.07	0.07	0.07	0.07	0.07	
DE0009R	PCB_138	1996	-	0.07	0.07	0.07	0.07	0.78	0.07	0.07	0.07	0.07	0.07	0.07	9
DE0009R	PCB_138	1997	-	0.07	0.07	0.07	0.18	0.07	0.49	0.32	0.07	0.07	3.8	0.52	
DE0009R	PCB_149	1996	-	0.03	0.03	0.03	0.03	0.03	0.03	0.03	0.03	0.03	0.03	0.03	9
DE0009R	PCB_153	1996	-	0.07	0.07	0.07	0.07	0.4	0.07	0.07	0.07	0.07	0.07	0.07	9
DE0009R	PCB_153	1997	-	0.07	0.07	0.07	0.26	0.07	0.07	0.6	0.07	0.24	3.1	0.36	
DE0009R	PCB_177	1996	-	0.07	0.07	0.07	0.07	0.07	0.07	0.07	0.07	0.07	0.07	0.07	9
DE0009R	PCB_18	1996	-	0.07	0.07	0.07	0.07	0.07	0.07	0.07	0.07	0.07	0.07	0.07	9
DE0009R	PCB_180	1996	-	0.07	0.07	0.07	0.07	0.07	0.07	0.07	0.07	0.07	0.07	0.07	9
DE0009R	PCB_180	1997	-	0.07	0.07	0.07	0.07	1.1	8	1.7	1.2	0.59	0.07	1.2	
DE0009R	PCB_26	1996	-	0.01	0.01	0.01	0.01	0.01	0.01	0.01	0.01	0.01	0.01	0.01	9
DE0009R	PCB_28	1996	-	0.01	0.01	0.01	0.01	0.01	0.01	0.01	0.01	0.01	0.01	0.01	9
DE0009R	PCB_28	1997	-	0.01	0.01	0.01	0.01	0.01	0.01	0.01	0.01	0.01	0.01	0.01	
DE0009R	PCB_44	1996	-	0.07	0.07	0.07	0.07	0.07	0.07	0.07	0.07	0.07	0.07	0.07	9
DE0009R	PCB_52	1996	-	0.07	0.07	0.07	0.07	0.07	0.07	0.07	0.07	0.07	0.07	0.07	9
DE0009R	PCB_52	1997	-	0.07	0.41	0.43	0.07	0.15	0.07	0.07	0.07	0.07	0.07	3	
DE0009R	Precipitation	1996	0.6	22.5	8.2	18.8	62.3	39.7	32.2	57.7	27.8	34	90.2	15.8	
DE0009R	Precipitation	1997	0	32.7	27.2	19.8	87.8	35.9	19.4	31.1	36.5	45.6	30.6	34.6	
DE0009R	Sum_PCB	1997	-	0.39	1.44	0.98	1.36	1.91	-	2.97	1.52	1.08	7.15	5.19	
DE0009R	SummePCB	1996	-	0.6	0.6	0.6	0.6	2.3	0.32	0.6	0.6	0.6	0.6	0.6	9
DE0009R	Benzo[a]pyrene	1996	-	8.4	12	3	0.67	0.67	1.5	4	2	4.3	9.9	66	
DE0009R	Benzo[a]pyrene	1997	-	3.1	2.6	6.8	5.2	1.8	0.67	6.4	1.1	4	33	6.9	
FI0096R	Precipitation	1996	0	4	0.3	8	1.5	6	1.1	7.5	1	2.8	11	5	
FI0096R	PCB_101	1996	-	0.11	0.18	0.09	0.14	0.3	0.12	0.55	0.6	0.32	0.09	-	
FI0096R	PCB_118	1996	-	0.04	0.06	0.04	0.04	0.18	0.04	0.23	0.24	0.23	0.08	-	
FI0096R	PCB_138	1996	-	0.11	0.19	0.12	0.18	0.33	0.15	0.98	1.23	0.32	0.15	-	
FI0096R	PCB_153	1996	-	0.12	0.18	0.13	0.19	0.31	0.18	0.89	1.12	0.3	0.12	-	
FI0096R	PCB_180	1996	-	0.09	0.13	0.09	0.13	0.16	0.14	0.73	0.96	0.2	0.09	-	
FI0096R	PCB_28	1996	-	0.25	0.55	0.23	0.31	0.3	0.34	0.41	0.3	0.89	0.79	-	
FI0096R	PCB_52	1996	-	0.12	0.32	0.18	0.2	0.2	0	0.24	0.21	0.3	0.27	-	
FI0096R	Benzo[a]pyrene	1996	-	1	1	0	2	0	1	8	-	7	1	-	
IE0002R	PCB_101	1997	3.5	0.5	3.5	2	1	0.5	1	0.5	2	1	0.5	0.5	1
IE0002R	PCB_118	1997	3.5	0.5	3.5	2	1	0.5	1	0.5	2	1	0.5	0.5	1
IE0002R	PCB_138	1997	3.5	0.5	3.5	2	1	0.5	1	0.5	2	1	0.5	0.5	1
IE0002R	PCB_153	1997	3.5	0.5	3.5	2	1	0.5	1	0.5	2	1	0.5	0.5	1
IE0002R	PCB_180	1997	3.5	0.5	3.5	2	1	0.5	1	0.5	2	1	0.5	0.5	1
IE0002R	PCB_52	1997	3.5	0.5	3.5	2	1	0.5	1	0.5	2	1	0.5	0.5	1
IE0002R	Precipitation	1997	41.7	214.2	32.1	37	104.4	209	56.2	193.3	57.7	133.8	358.6	244.7	
IS0091R	PCB_101	1996	0.058	0.14	0.063	0.057	0.06	0.078	0.043	0.014	0	0.066	0.016	0.011	
IS0091R	PCB_101	1997	0.018	0.01	0.01	0.013	0.013	0	0	0	0	0.007	0	0.013	
IS0091R	PCB_105	1996	0.028	0.06	0.025	0.038	0.04	0.031	0.021	0	0	0	0	0	
IS0091R	PCB_105	1997	0	0	0	0	0	0	0	0	0	0.01	0	0.008	
IS0091R	PCB_118	1996	0.065	0.16	0.044	0.04	0.04	0.06	0.035	0.014	0	0.038	0.006	0.007	
IS0091R	PCB_118	1997	0.022	0.02	0.016	0.013	0.014	0.019	0	0	0	0.003	0	0	

		Year	Jan	Feb	Mar	Apr	May	Jun	Jul	Aug	Sep	Oct	Nov	Dec	QA
IS0091R	PCB_138	1996	0.13	0.19	0.088	0.131	0.16	0.118	0.054	0	0	0.019	0	0	
IS0091R	PCB_138	1997	0.026	0.01	0.014	0.013	0.017	0.016	0	0	0	0.005	0	0	
IS0091R	PCB_153	1996	0.139	0.18	0.084	0.117	0.14	0.129	0.07	0.02	0	0.034	0.025	0.004	
IS0091R	PCB_153	1997	0.04	0	0.02	0.012	0.017	0.008	0	0	0	0.005	0	0.004	
IS0091R	PCB_156	1996	0.015	0.02	0.013	0.011	0.02	0.031	0.021	0	0	0	0	0	
IS0091R	PCB_156	1997	0	0	0.02	0.025	0.02	0	0	0	0.007	0.002	0	0	
IS0091R	PCB_180	1996	0.053	0.1	0.054	0.098	0.23	0.062	0.039	0.015	0.004	0.013	0.006	0	
IS0091R	PCB_180	1997	0.022	0.02	0.02	0.026	0.013	0.012	0	0	0	0.013	0	0.013	
IS0091R	PCB_28	1996	0.042	0	0.048	0	0.35	0.103	0.081	0	0.012	0.08	1.287	0.568	
IS0091R	PCB_28	1997	0.407	0.04	0.054	0.107	0.192	0	0.195	0	0	0.232	0	0.525	
IS0091R	PCB_31	1996	0.011	0	0	0	0.44	0.092	0.063	0	0.024	0.086	1.35	0.622	
IS0091R	PCB_31	1997	0.414	0.01	0.036	0.099	0.145	0	0.167	0	0	0.176	0	0.352	
IS0091R	PCB_52	1996	0.028	0.03	0.077	0.017	0.15	0.044	0.034	0.005	0.008	0.098	0.331	0.155	
IS0091R	PCB_52	1997	0.105	0.03	0.012	0.028	0.066	0.041	0.056	0	0	0.074	0	0.114	
IS0091R	Precipitation off	1996	83.891	61	87.337	48.148	33	51.337	83.42	65.138	105.1	86.987	52.657	42.103	
IS0091R	Precipitation off	1997	77.041	41	84.16	43.961	34.226	27.513	57.248	60.417	76.784	136.744	57.018	86.988	
SE0002F	Precipitation	1996	0	2.1	0	14.3	24.1	11.3	0	14.9	36.1	19.7	9.6	2.7	
SE0002F	PCB_101	1996	-	0.27	-	0.19	0.07	0.06	-	0.1	0.24	0.19	0.11	0.1	
SE0002F	PCB_118	1996	-	0.08	-	0.11	0.07	0	-	0.07	0.1	0.07	0.07	0.07	
SE0002F	PCB_138	1996	-	0.43	-	0.37	0.19	0.21	-	0.21	0.6	0.32	0.23	0.2	
SE0002F	PCB_153	1996	-	0.42	-	0.34	0.18	0.15	-	0.19	0.49	0.33	0.25	0.23	
SE0002F	PCB_180	1996	-	0.31	-	0.26	0.13	0.16	-	0.09	0.53	0.36	0.24	0.13	
SE0002F	PCB_28	1996	-	0.43	-	0.49	0.32	0.32	-	0.85	0.25	0.7	0.53	0.36	
SE0002F	PCB_52	1996	-	0.28	-	0.15	0.39	0.33	-	0.25	0.21	0.26	0.33	0.17	
SE0002R	Benzo[a]pyrene	1996	-	18	-	6	3	8	-	11	15	27	13	8	

References

Atkinson R. [1991] Atmospheric lifetimes of dibenzo-p-dioxins and dibenzofurans. *The science of the Total Environment*, v.104, pp.17-33.

Axenfeld F., Münch J. and J.M.Pacyna [1991] Belastung von Nord- und Ostsee durch ökologisch gefährliche Stoffe am Beispiel atmosphärischer Quecksilberkomponenten. Teilprojekt: Europäische Test-Emissionensdatenbasis von Quecksilber-Komponenten für Modellrechnungen. Dornir, Report 104 02 726, p.99.

Baart A.C., Berdowski J.J.M., van Jaarsveld J.A. and K.J.Wulffraat [1995] Calculation of atmospheric deposition of contaminants on the North Sea. TNO-MEP - R 95/138, Delft, The Netherlands.

Bacci E., Cerejeira M.J., Gaggi C., Chemello G., Calamari D. and M.Vihgi [1990a] Bioconcentration of organic chemical vapours in plant leaves: The Azalea model. *Chemosphere*, v.21, pp.525-535.

Bacci E., Calamari D., Gaggi C. and M.Vihgi [1990b] Bioconcentration of organic chemical vapours in plant leaves: Experimental measurements and correlation. *Environ. Sci. Technol.*, v.24, pp.885-889.

Bacci E., Cerejeira M.J., Gaggi C., Chemello G., Calamari D. and M. Vihgi [1992] *Bull. Environ. Contam. Toxicol.*, v.48, pp.8-17.

Baldocchi D.D., Hicks B.B. and P.Camara [1987] A Canopy stomatal resistance model for gaseous deposition to vegetated surfaces. *Atmos.Environ.*, v.21, №1, pp.91-101.

Berdowski, J.J.M., J. Baas , J.P.J. Bloos, A.J.H. Visschedijk and P.Y.J.Zandveld [1997] The European emission inventory of heavy metals and persistent organic pollutants for 1990. TNO Institute of Environmental Sciences, Energy Research and Process Innovation, UBA-FB report 104 02 672/03, Apeldoorn, p.239.

Berg T. and A.-G.Hjellbrekke [1998] Heavy metals and POPs within the ECE region. Supplementary data for 1989-1996. Kjeller, Norwegian Institute for Air Research (NILU EMEP/CCC-Report 7/98).

Bidleman T.F. [1988] Atmospheric processes. *Environ. Sci. Technol.*, v.22, pp.361-367.

Bierman H.W., Leod H.M., Atkinson R., Winer A.M. and J.N.Pitts [1985] Kinetics of the gas-phase reactions of the hydroxyl radical with narhtalene, phenantrene and anthracene. *Environ.Sci.Technol.*, v.19, pp.244-248.

Boström C. E. and R.-H.Tuija [1997], Airborne Pollution Load to the Baltic Sea 1991 – 1995, *Balt. Sea Environ*. Proc., No69.

Bulgakov A.A. and D.A.Ioannisian [1998] Review of physical – chemical properties of polychlorinated dibenzo-p-dioxins (PCDDs) and dibenzofurans (PCDFs) in respect to their longe-range transport in the atmosphere. pp.5-31.

Burkhard L.P., Armstrong D.E. and A.W.Andren [1985] Henry's law constants for the polychlorinated biphenyls. *Environ. Sci. Technol*., v.19, pp.590-596.

Chrostowski P.C. and S.A.Foster [1996] A methodology for assessing congener-specific partitioning and plant uptake of dioxins and dioxin-like compound. *Chemosphere*, v.32, pp.11, 2285-2304.

Coleman P. J., Lee R. G. M., Alcock R. E. and K.C.Jones [1997] Observations on PAH, PCB, and PCDD/F trends in UK. Urban air. *Environ. Sci. Technol.*, v.31, pp.2120-2124.

Cotham W. E. and T.F.Bidleman [1995] Polycyclic aromatic hydrocarbons and polychlorinated biphenils in air at an urban and a rural site near Lake Michigan. *Environ. Sci. Technol.*, v.29, pp.2782-2789.

Dickhut R.M. and K.E.Gustafson [1995] Atmospheric washout of polycyclic aromatic hydrocarbons in the Southern Chesapeake Bay region. *Environ.Sci.Technol.*, v.29, pp.1518-1525.

Gustafson K.E. and R.M.Dickhut [1997] Particle/gas concnetrations and distributions of PAHs in the atmosphere of Southern Chesapeake Bay. *Environ.Sci.Technol.*, v.31, 140-147.

Doucette W.J. and A.W.Andren [1988] Aqueous solubility of selected biphenyl, furan and dioxin congeners. *Chemosphere,* v.17, No2, pp.243-252.

Dunnivant F.M., Elzerman A.W., Jurs P.C. and M.N.Hansen [1992] Quantitative structure-property relationships for aqueous solubilities and Henry's law constants of polychlorinated biphenyls. *Environ. Sci. Technol.,* v.26, pp.1567-1573.

Duyzer J. H. and R.F.van Oss [1997] Determination of deposition parameters of a number of persistent organic pollutants by laboratory experiments. TNO-Report TNO-MEP-R97/150.

Eisenreich S.J., Looney B.B. and J.D.Thornton [1981] Airborne organic contaminants in the Great Lakes ecosystem. *Environ.Sci.Technol.*, v.15, pp.30-38.

Eitzer B. D. and R.Hites [1989a] Polychlorinated dibenzo-p-dioxins and dibenzofurans in the atmosphere of Bloomington, Indiana. *Environ. Sci. Technol.,* v.23, No11, pp.1389-1395.

Eitzer B.D. and R.A.Hites [1989b] Atmospheric transport and deposition of polychlorinated dibenzo-p-dioxins and dibenzofurans. *Environ. Sci. Tecnol.*, v.23, No11, pp.1396-1401.

Eitzer B.D. and R.A. Hites [1991] Vapor pressure of chlorinated dioxins and dibenzofurans. The science of the total environment, v. 104, pp. 9 -15.

ECMWF [1994]. The Description of the ECMWF/WCRP Level III-A Global Atmospheric. Data Archive. ECMWF Operations Department Shinfield Park, Reading.

EMEP/CORINAIR [1996] Atmospheric Emission Inventory Guidebook - First Edition (ed. by G. McInnes). European Environment Agency, Copenhagen.

Falconer R.L. and T.F.Bidleman [1994] Vapor pressures and predicted particle/gas distributions of polychlorinated biphenyl congeners as functions of temperature and ortho-chlorine substitution. *Atmos. Environ.*, v.28, pp.547-554.

Falconer R.L., Bidleman T.F. and W.E.Cotham [1995] Preferential sorption of non- and mono-ortho polychlorinated biphenyls to urban aerosols. *Environ. Sci. Technol.*, v.29, pp.1666-1673.

Fedorov L.F.[1993] Dioxins as a fundamental factor of technogenic pollution of nature. *Ecological Chemistry*, № 3, pp.169-187. (In Russian)

Finizio A., Mackay D., Bidleman T. and T.Harner [1997] Octanol-air partition coefficient as a predictor of partitioning of semi-volatile organic chemicals to aerosols. *Atmos. Environ*. v.31, pp.2289-2296.

Franz T. and S.J.Eisenreich [1998] Snow scavenging of polychlorinated biphenyls and polycyclic aromatic hydrocarbons in Minnesota. *Environ. Sci.*, v.32, N.12, pp.1771-1778.

Friesen K. J and G.R.B.Webster. [1990] Temperature dependence of the aqueous solubilities of highly chlorinated dibenzo-p-dioxins. *Environ. Sci. Technol*., v.24, N.1, pp.97-101.

Friesen K.J., Vilk J. and D.C.G.Muir [1990] Aqueous solubilities of selected 2,3,7,8 – substituted polychlorinated dibenzofurans (PCDFs). *Chemosphere*, v.20, No1-2, pp.27-32.

Govers H. A.J. and H.B.Krop [1998] Partition constants of chlorinated dibenzofurans and dibenzo-p-dioxins. *Chemosphere*, v.37, No9-12, pp.2139-2152.

Govers H.A.J. [1993] Calculation of partition constants for a series of organic compounds via a novel solubility-parameter-based Method. *Chem. Soc. Faraday Trans.*, v.89, N.20, pp.3751-3759.

Govers H.A.J., Frans W.M., van der Wielen and K.Olie [1995] Derivation of solubility parametrs of chlorinated dibenzofurans and dibenzo[p]dioxins from gas chromatographic retention parameters via SOFA. *Chromagraphy A*, v.715, pp.267-278.

Haag W.G. and C.C.D.Yao [1992] Rate constants for reaction of hydrocyl radicals with several drinking water contaminants. *Environ. Sci. Technol.*, v.26, pp.1005-1013.

Halsall C.J., Lee R.G.M., Coleman P.J., Burnett V., Harding-Jones P. and K.C.Jones [1995] PCB in UK Urban Air. *Environ.Sci.Technol.*, v.29, pp.2368-2376.

Harner T. and T.F.Bidleman [1996] Measurements of octanol-air partition coefficients for polychlorinated biphenyls. *Chem. Eng. Data*, v.41, pp.895-899.

Harner T. and T.F.Bidleman [1998] Octanol-air partition coefficient for describing particle/gas partitioning of aromatic compounds in urban air. *Environ. Sci. Technol.*, v.32, pp.1494-1502.

Harner T., Mackay D. and K.C. Jones [1995] Model of the long-term exchange of PCBs between soil and the atmosphere in the southern UK. *Environ. Sci. Technol.*, v.29, pp.1200-1209.

Hauk H., Umiauf G. and M.S.McLachlan [1994] Uptake of gaseous DDE in spruce needles. *Environ. Sci. Technol*., v.28, pp.2372-2379.

Hawker D.W. and D.W.Connel [1988] Octanol-water partition coefficients of polychlorinated biphenyl congeners. *Environ. Sci. Technol.*, v.22, pp.382-387.

Herrman R. [1987] Environmental transfer of some organic micropollutants. In: Schulze E.-D., Zwolfer H (Eds), Ecological Studies, v. 61, Springer, Verlag, Berlin, Heidelberg, pp.68-99.

Hincley D.A., Bidleman T.F. and W.T. Foreman [1990] Determination of vapor pressures for non-polar and semi-polar organic compounds from gas chromatographic retention data. *Chem. Eng. Data*, v.35(3), pp.232-237.

Hippelein M., Kaupp H., Dorr G., McLachlan M. and O.Hutzinger [1996] Baseline contamination assessment for a new resource recovery facility in Germany. Part II: atmospheric concentrations of PCDD/F. *Chemosphere*, v.32, №8, pp.1605-1616.

Holsen T.M., K.E.Noll, L.Shi-Ping and W.Lee [1991] Dry Deposition of Polychlorinated Biphenyls in Urban Areas. *Environ. Sci. Technol.,* v.25, pp.1075-1081.

Horstmann M. and M. S. McLachlan [1998] Atmospheric deposition of semivolatile organic compounds to two forest canopies, *Atmos. Environ.*, v.32, pp. 1799 - 1809.

Jacobs C.M.J. and W.A.J. van Pul [1996] Long-range atmospheric transport of persistent organic pollutants, I: Description of surface-Atmosphere exchange modules and implementation in EUROS. National Institute of Public Health and the Environment, Bilthoven, The Netherlands. Report No.722401013.

Junge C.E. [1977] Basic considerations about trace constituent in the atmosphere is related to the fate of global pollutant. In: Fate of pollutants in the air and water environment. Part I, I.H. Suffet (ed.) (Advanced in *Environ. Sci. Technol*., v.8), Wiley-Interscience, New York.

Karikhoff S. W., Brown D.S. and T.A. Scott [1979] Sorption of hydrophobic pollutants on natural waters. *Water Res*. v.13, pp.241-248.

Karikhoff S.W. [1981] Semiempirical estimation of sorption of hydrophobic pollutants on natural sediments and soils. *Chemosphere*, v. 10, pp. 833-846.

Kerler F. and J. Schönherr [1988] Permeation of lipophilic chemicals across plant cuticules: prediction from partitioning coefficient and molar volume. *Arch. Environ. Contam. Toxicol*., v. 17, pp. 7-12.

Koester C.J. and Hites A. [1992] Wet and dry deposition of chlorinated dioxins and furans. *Environ. Sci. Technol.*, v. 26, N.7, pp. 1375 - 1382.

Kolbow D., Hikoshi H., Tutill C., Frank C. W., Wiersma G.B., Crokett A.B. and R.D. Schonbrod [1986] Kinetic analysis: Benzo(a)pyrene in southeastern Ohio. *Environ. Monit. Assess*., v.6, pp. 231-257.

Kömp P. and M.S. McLachlan [1997a] Influence of temperature on the plant/air partitioning of semivolatile organic compounds. *Environ. Sci. Technol.*, v.31, 886 - 890.

Kömp P. and M.S. McLachlan [1997b] Interspecies variability of the plant/air partitioning of polychlorinated biphenyls. *Environ. Sci. Technol.*, v.31, 2944 - 2948.

Kwok E.S.C., Atkinson R. and J.Arey [1995] Rate constants for the gas-phase reactions of the OH radical with dichlorobiphenyls, 1-chlorodibenzo-p-dioxin, 1,2-dimethoxybenzene, and diphenyl ether: estimation of OH radical reaction rate constants for PCBs, PCDDs, and PCDFs. *Environ. Sci. Technol.*, v.29, No.6, pp.1591-1598.

Ligocki M.P., Lueberger C. and J.F.Pankow [1985a] Trace organic compound in rain. II. Gas scavenging of neutral organic compounds. *Atmos.Environ.*, v.19, pp.1609-1617.

Ligocki M.P., Lueberger C. and J.F.Pankow [1985b] Trace organic compound in rain. III. Particle scavenging of neutral organic compounds. *Atmos.Environ.*, v.19, pp.1619-1626.

Lohmann R. and Jones K.C. [1998] Dioxins and furans in air and deposition: A review of levels, behaviour and processes. *The science of the Total Environment*, v.219, pp.53-81

Lükewille A., ed. [1998] EMEP Expert Meeting on Measurements of Persistent Organic Pollutants (POP) in Air and Precipitation. Kjeller, Norwegian Institute for Air Research (NILU EMEP/CCC-Report 8/98).

MacCrady J.K. and S.P. Maggard [1993] Uptake and photodegradation of 2,3,7,8- tetrachlorodibenzo-p-dioxinsorbed to grass foliage. *Environ. Sci. Technol.*, v.27, pp. 343 - 350.

Mackay D. and S.Paterson [1991] Evaluating the fate of organic chemicals: a level III fugacity model. *Environ. Sci. Technol*, v.25, pp. 427-436.

Mackay D., Shiu W.Y. and K.C.Ma. [1992] Illustrated handbook of physical-chemical properties and environmental fate for organic chemicals. CRC Press. Boca Raton, FL., vol. II.

May W.E., Wasik S.P., Miller M.M., Tewari Y.B., Brown-Thomas J.M. and R.N.Goldberg [1983] Solution thermodynamics of some slightly soluble hydrocarbons in water. *Chem. Eng. Data*, v.28, pp. 197 - 200

McLachlan M.S. [1998] Basic considerations and practical experience in the development of methods to measure atmospheric deposition of persistent organic pollutants. Kjeller, Norwegian Institute for Air Research (NILU EMEP/CCC-Report 8/98).

McLachlan M.S., Welsch-Pausch K. and J.Tolls [1995] Field validation of a model of uptake of gaseous SOC in Lolium multiflorum (Rye grass). *Environ. Sci. Technol.*, v.29, pp. 1998-2004.

McVeety B.D. and R.A. Hites [1988] Atmospheric deposition of policyclic aromatic hydrocarbons to water surfaces: a mass balance approach. *Environ. Sci. Technol.*, v. 22, pp. 511-536.

Mill T., Mabey W.R., Lan B.Y. and A. Baraze A. [1981] Photolysis of polycyclic aromatic hydrocarbons in water. *Chemosphere*, v.10, pp. 1281-1290.

Müller J.F., Hawker D.W. and D.W. Connell [1994] Calculation of bioconcentration factor of persistent hydrophobic compounds in the air/vegetation system. *Chemosphere*, v.20(4), pp.623-640.

Müller J.F., McLachlan M.S., Hawker D.W. and D.W. Connell [1998] Polychlorinated dibenzodioxins and polychlorinated dibenzofurans in the atmospheric environment of Brisbane, Australia. *Clean air*, v.32, N.3, pp.27-31.

Offenberg J.H. and J.E.Baker [1997] Polychlorinated biphenyls in Chicago precipitation: enhanced wet deposition to near-shore Lake Michigan. *Environ. Sci. Technol.*, v.31, pp.1534-1538.

Pankow J.F. [1987] Review and comparative analysis of the theories on partitioning between the gas and aerosol particulate phases in the atmosphere. *Atmos. Environ.*, v.21, pp.2275-2283.

Paterson S., Mackay D. and C. McFarlane [1994] A model of ogranic chemical uptake by plants from soil and the atmosphere. *Env. Sci. Technol.*, v.28, No. 13, pp.2259-2266.

Paterson S., Mackay D., Bacci E. and D. Calamari [1991] Correlation of the equilibrium and kinetics of leaf-air exchange of hydrofobic organic pollutants. *Environ. Sci. Technol*., v.25, pp.866 - 871.

Paterson S., Mackay D., Tam D. and W.Y. Shiu [1990] Uptake of organic chemicals by plants: review of processes, correlations and models. *Chemosphere*, v.21, pp.297-331.

Pekar M. [1996] Regional models LPMOD and ASIMD. Algorithms, parametrization and results of application to Pb and Cd in Europe scale for 1990 MSC-E Report 9/96, September.

Pekar M., Gusev A., Pavlova N., Strukov B., Erdman L., Ilyin I. and S.Dutchak [1998] Long-range transport of selected POPs. Development of transport models for lindane, polychlorinated biphenyls, benzo(a)pyrene. EMEP/MSC-E Report 2/98, Part I.

Poster D.L. and J.E. Baker [1996] Influence of submicron particles on hydrophobic organic contaminants in precipitation. II. Concentrations and distribution of polyciclic aromatic hydrocarbons and chlorinated biphenyls rain water. *Environ. Sci. Technol.* v.30, pp.349-354.

Price C.E. [1983] A review of the factors influencing the penetration of pesticides through plant leaves. In: Cutler D.F., Alvin K.L., Price C.E. (eds) The plannt cuticule. Linnaeus Society Symp. Series, No.10, Academic press, New York, pp.237-252.

Riederer M. [1990] Estimating partitioning and transport of organic chemicals in the follage/atmosphere system: discussion of a fugacity-based model. *Environ. Sci. and Technol,* v.24, No. 6, pp.829- 837.

Rordorf B. F. [1989] Prediction of vapor pressures, boiling points and enthalpies for twenty-nine halogenated dibenzo-p-dioxins and fifty-five dibenzofurans by a vapor pressure correlation method. *Chemosphere,* v. 18, N. 1-6, pp. 783-788.

Rovinsky F.Ya., Teplitzkaia T.A. and T.A.Alekseeva [1988] Background monitoring of PAH. L., Hydrometeoizdat (in Russian).

Ruelle P. and U.W.Kesselring [1997] Aqueous solubility prediction of environmentally important chemicals from the mobile order thermodynamics. *Chemosphere,* v.34, N. 2, pp. 275-298.

Schroeder J., Welch- Pausch K. and M.McLachlan [1997] Measurement of atmospheric deposition of polychlorinated dibenzo-p-dioxins and dibenzofurans. *Atmospheric Environment*, v.31, N.18, pp.2983 – 2989.

Schulz D.E., G.Petrick and J.C. Duinker [1989] Complete characterization of polychlorinated biphenyl congeners in commercial Aroclor and Clophen mixtures by multidimensional gas chromatography-electron capture detection. *Environ. Sci. Technol.*, v. 23, No. 7.

Schwarzenbach R.P., Gschwend P.M. and D.M. Imboden [1993] Environmental organic chemistry. John Wiley&Sons Inc., New York.

Shabad L.M. [1980] Chemical cancerogens (PAH) entering to the atmosphere and their circulation in the environment. In: Complex global monitoring of pollutions in the environment. International symposium proceedings, Riga, pp. 231-239, (In Russian).

Shilina A.I., Vaneeva L.V. and A.V. Zhuravleva [1980] Benzo[a]pyrene life-time in the soil at its application with soil dust particles. In: Pollutions migration in soils and boundary media. II Allunion Meeting Proceedings, Obninsk, pp. 100-105, (in Russian).

Shiu W.Y., Doucette W., Gobas F.A.P.C., Andren A. and D.Mackay [1988] Physical-chemical properties of chlorinated dibenzo-p-dioxins. *Environ. Sci. Technol.*, v. 22, N. 6, pp. 651-658.

Shtamm E.V., Purmal A.P. and Yu.I. Skurlatov [1991] The role of hydrogen peroxide in the nature environment. Uspekhi Khimii, v.60, issue 11, pp.2373-2411, (In Russian).

Sijm D.T.H.M., Wever H., de Vries P.J. and A.Opperhuizen [1989] Octan-1-ol/ water partition coefficients of polychlorinated dibenzo-p-dioxins and dibenzofurans: experimental values determined with a stirring method. *Chemosphere,* v.19, N.1-6, pp.263-266.

Simonich S.L. and R.A. Hites [1994] Importance of vegetation in removing polyciclyc aromatic hydrocarbons from the atmosphere. *Nature*, v.370, pp.49-51.

Skurlatov Yu.I., Duka G.G. and A.Misiti [1996] Introduction to ecological chemistry. Moscow. High school.

Strand A. and O. Hov [1996] A model Strategy for the Simulation of Chlorinated Hydrocarbon Distribution in the Global Environment. *Water, Air and Soil Pollution*, v.86, pp.283-316.

ten Hulscher Th.E.M., van der Velde L.E. and W.A. Bruggeman [1992] Temperature Dependence of Henry's Law Constants for Selected Chlorobenzenes, Polychlorinated Biphenyls and Polycyclic Aromatic Hydrocarbons. *Environ. Toxicol. Chem.*, v.11, pp.1595-1603.

Thomas G., Sweetman A. J., Ockenden W. A., Mackay D. and K.C. Jones [1998] Air-pasture transfer of PCBs. *Environ. Sci. Technol*., v.32, pp. 930 - 942.

Tolls J. and M.S. McLachlan [1994] Partitioning of semi-volatile organic compounds between air and Lolium Multiflorum (welsch ray grass). *Environ. Sci. Technol.*, v.28, pp. 159 - 166

Tonkopiy N.I., Shestopalova G.E. and V.Ya. Rozanova [1979] Some facts determining benzo[a]pyrene degradation in soils. In: Carcenogenic substances in the environment. M., pp. 65-68. (In Russian).

van den Hout ed. [1994] The impact of atmospheric deposition of non-acidifying pollutants on the Quality of European forest soils and the North sea, Main report of the ESQUAD project, RIVM rep.722401003, IMW-TNO rep.R93/329.

Vozhzennikov O.I., Bulgakov A.A., Popov V.E., Lukoyanov N.F., Naidenov A.V. Burkov A.J. Kutnyakov J.V. and V.G.Hzirnov [1997] Review of migration and transformation parameters of selected POPs, EMEP/MSC-E Report 3/97.

Wania F. [1997] Modelling sea-air exchange of persistent organic pollutants: focus on temperature and other seasonal parameters. In: sea-air exchange: processes and modelling. Ed. by J.M.Pacyna, D.Broman and E.Lipiatou 1998, pp.161-190

Wania F. and D. Mackay [1996] Tracking the distribution of persistent organic pollutants. *Environ. Sci. Technol*., v.30, No.9, pp.390A-396A.

Whitby K.T. [1978] The physical characteristics of sulphur aerosols. *Atm. Environ.*, v.12, pp.135-195.

Yu Lu and M.A.K. Khall [1991] Tropospheric OH: model calculation of spacial, temporal and secular variations. Chemosphere, v.23, pp.397-444.

Zepp R.G. and P.F.Schlotzhauer [1979] Photoreactivity of selected aromatic hydrocarbons in water. In: Polynuclear Hydrocarbons, T.W.Jones and T.Leber, Eds., Ann Arbor Science, Ann Arbor, MI.

Notations

c	constant dependent on thermodynamic parameters of the adsorption process and on properties of aerosol particle surface in the Junge law;
C_A	concentrations in air, mol/m^3;
C_G	gaseous pollutant concentration, ng/m^3;
C_P	concentration of a pollutant bound with particulate matter, ng/m^3;
C_V	concentrations in vegetation, mol/m^3;
C_W	concentration in water, mol/m^3;
D_A	molecular diffusion coefficient for air, m^2/s;
d_{SR}	fugitive conduction between the leaf surface layer and internal leaf reservoir normalized to fresh leaf area, mol/Pa/h/m^3;
D_W	molecular diffusion coefficient for water, m^2/s;
H	Henry constant, Pa m^3/mol;
k_{OH}	reaction rate constant with hydroxyl radical, m^3/molec/s;
k^*_{OH}	reaction rate constant of the pseudo-first order, s^{-1};
k_1	uptake rate, s^{-1};
k_2	clearance rate, s^{-1};
k_{AV}	mass transfer coefficient through leaf-air interface, s^{-1};
K_{AW}	air/water partition coefficient;
K_{CW}	cuticle-water partition coefficient;
k_d	degradation rate, s^{-1};
K_H	dimensionless Henry constant;
K_{iA}	partition coefficient in the system (component *i*)/air;
K_{OA}	octanol-air partition coefficient;
K_{OC}	organic carbon-water partition coefficient, m^3/kg;
K_{OW}	octanol-water partition coefficient;
K_P	gas-particle partition coefficient, m^3/μg;
k_{SR}	mass transfer coefficient between the leaf surface layer and internal reservoir of a leaf, m/s;
k_v	volatilization rate, s^{-1};
K_{VA}	bioconcentration factor;

K_{WA} water/air partition coefficient;

L volumetric fraction of lipids in a leaf;

M molar mass, g/mol;

M_{air} mean molecular air mass;

P cuticle permeability coefficient, cm/s;

p^0_L saturated vapour pressure over subcooled liquid, Pa;

p^0_S saturated vapour pressure over solid substance, Pa;

R universal gas-constant, J/mol K;

R_b the sum of resistances of laminar and turbulent atmospheric layers, s/m;

R_C cuticle resistance, s/m;

R_L leaf surface resistance, s/m;

R_S stomatal resistance, s/m;

R_T the total resistance to air/vegetation exchange, s/m;

S_L solubility of liquid state, mol/l;

S_S solubility of solid state, mol/l;

T_b boiling temperature, K;

T_m melting point, K;

TSP total concentration of solid particulate matter (aerosol), $\mu g/m^3$;

V_d deposition velocity, cm/s;

v_i leaf volume fraction accounted for component i;

V_m molar volume, cm^3/mol;

W_G washout ratio of the vapour phase;

W_P washout ratio for the aerosol phase;

W_T washout ratio for PCB scavenging;

Z_A fugitive capacity of air, $mol/Pa/m^3$;

Z_L is fugitive capacity of leaf lipid component, $mol/Pa/m^3$;

θ specific surface of aerosol particles, m^2/m^3;

ϕ fraction bound with aerosol particles;

ΔH_m fusion enthalpy, kJ/mol;

ΔH_S sublimation enthalpy, J/mol;

ΔH_s^e enthalpy of solubility for the liquid phase, kJ/mol;

ΔH_{so}^e solubility enthalpy in octanol of a substance in the liquid state, kJ/mol;

ΔH_v vaporisation enthalpy for the liquid phase, kJ/mol;

ΔH_W enthalpy of volatilization from water, kJ/mol;

ΔS_m fusion entropy, kJ/mol·K;

ΔS_S sublimation entropy, J/mol·K;

[OH] hydroxyl-radical concentration in air, $molec/cm^3$